Novel insights into the clinical heterogeneity and treatment of chronic lymphocytic leukaemia

Marwan Cheng Kuang Kwok

BSc (Hons) *Lond*, MB ChB *Leeds*, MRCP (UK)

A thesis submitted to the
University of Birmingham for the degree of
DOCTOR OF PHILOSOPHY

Institute of Cancer and Genomic Sciences
College of Medical and Dental Sciences
University of Birmingham
October 2017

ABSTRACT

Chronic lymphocytic leukaemia (CLL) is characterised by marked disease heterogeneity and is currently incurable. While clinical outcome has improved with chemoimmunotherapy, B cell receptor (BCR) signalling inhibitors and Bcl-2 inhibitors, some patients, particularly those with poor-risk features such as *TP53* or *ATM* defects, eventually relapse from these agents and die from CLL. Hence, the development of new CLL treatment approaches is still needed. This thesis presents work undertaken to discover novel biological and therapeutic insights through the characterisation of patients with spontaneous CLL regression, the evaluation of ATR inhibition as a therapeutic strategy, and the assessment of the impact of post-treatment minimal residual disease (MRD) in CLL.

Spontaneous regression occurs in less than 2% of CLL cases and the features that underpin this rare event remain largely unknown. The first part of this thesis describes an investigation into the features of 19 individuals who underwent spontaneous CLL regression. CLL tumours that have undergone spontaneous regression express somatically mutated immunoglobulin genes, demonstrate short telomeres and a phenotype of clonal anergy with unresponsiveness to both IgM and IgD BCR stimulation. Other phenotypic features include reduced CD49d and ROR1 expression, and increased FasR expression. This profile suggests a model in which the CLL clone undergoes an initial period of proliferation which subsequently subside into a state of anergy and low proliferation. Genomic analysis revealed that spontaneous regression can occur in the presence of genomic alterations including *TP53* mutations. These findings identify spontaneous CLL regression as a unique subset of CLL and support the use of BCR signalling inhibition for the treatment of CLL.

TP53 and ataxia telangiectasia mutated (*ATM*) defects are associated with genomic instability and chemoresistance in CLL, and therapies capable of providing durable remissions in refractory *TP53* or *ATM* defective CLL are limited. The second part of this

thesis describes a study investigating ataxia telangiectasia and Rad3 related (ATR) inhibition as a synthetically lethal strategy to target CLL cells with *TP53* or *ATM* defects, using a highly-specific ATR inhibitor AZD6738. Irrespective of *TP53* or *ATM* status, induction of CLL cell proliferation upregulated ATR protein, which then became activated in response to replication stress. In *TP53* or *ATM* defective CLL cells, inhibition of ATR signalling led to an accumulation of unrepaired DNA damage, which was carried through into mitosis due to defective cell cycle checkpoints, resulting in cell death by mitotic catastrophe. Consequently, ATR inhibition was selectively cytotoxic to both *TP53* and *ATM* defective CLL cell lines and primary cells. This was confirmed *in vivo* using primary xenograft models of *TP53* or *ATM* defective CLL, where treatment with ATR inhibitor resulted in decreased tumour load and reduction in the proportion of CLL cells with such defects. Moreover, ATR inhibition sensitised *TP53* or *ATM* defective primary CLL cells to chemotherapy and ibrutinib. These findings suggest that ATR is a promising therapeutic target for *TP53* or *ATM* defective CLL that warrants clinical investigation.

The long-term prognostic value of MRD status in therapeutic settings other than frontline chemoimmunotherapy is unclear. The final part of this thesis presents a retrospective analysis of all patients from a single institution who achieved at least a partial response with various therapies between 1996 and 2007, and received a bone marrow MRD assessment at the end of treatment. MRD negativity correlated with both progression-free survival (PFS) and overall survival (OS) independent of the type and line of treatment, as well as known prognostic factors including adverse cytogenetics. The greatest impact of achieving MRD negativity was seen in patients receiving frontline treatment, with 10-year PFS of 65% vs 10% and 10-year OS of 70% vs 30% for MRD-negative vs positive patients. These results demonstrate the long-term benefit of achieving MRD negativity regardless of the therapeutic setting and treatment modality, and support its use as a prognostic marker for long-term PFS and as a potential therapeutic goal in CLL.

ACKNOWLEDGEMENT

The work described in this thesis was supported by a clinical research training fellowship awarded by Leukaemia & Lymphoma Research (Bloodwise) tenured from 2014 to 2017. Preliminary work leading to this fellowship was undertaken through a National Institute for Health Research academic clinical fellowship. This work was performed both at the University of Birmingham Institute of Cancer and Genomic Sciences and at the Haematological Malignancy Diagnostic Service laboratory in Leeds, and I would like to express my gratitude to the staff for their generosity and willingness to accommodate myself and my research projects at their respective institutions.

In particular, I would like to thank my primary supervisor Prof. Tatjana Stankovic and co-supervisor Prof. Peter Hillmen for their excellent mentorship and support at every stage of my research and academic training over the years, and for the freedom and encouragement they have provided me to explore my own ideas within and beyond the confines of their expertise. Enormous thanks also goes to Dr Angelo Agathanggelou and Dr Andy Rawstron for sharing their incredible scientific knowledge and expertise, for their help with technical trouble-shooting, and for the wide-ranging scientific discussions we had, which on occasions continued into the middle of the night!

I would also like to thank Prof. Paul Moss and Dr Guy Pratt for their help with navigating the ethical approval process and for their constructive comments from time to time; to Dr Nicholas Davies, Dr Ceri Oldreive, Dr Eva Petermann, Dr Andrew Beggs, Prof Malcolm Taylor, Dr Paul Evans, Prof. Duncan Baird and Dr Francesco Forconi for their scientific advice, discussion and/or collaboration; to Dr Anshita Goel, Dr Archana Sharma-Oates and Prof. Jean-Baptiste Cazier for providing bioinformatics analysis; to Mr Edward Smith, Dr Surita Dalal and Ms Naheema Gordon for their technical support; to Dr Shankara

Paneesha and Dr Paul Moreton for their help with patient recruitment at their respective hospitals; and to all patients who donated blood samples for the studies described herein.

I am also indebted to the training received at the EHA-ASH Translational Research Training in Hematology (TRTH) programme, for which I was a participant in the 2015 class. I would like to thank particularly the Group 2 faculty: Dr Cynthia Dunbar (Bethesda), Dr Ulrich Jäger (Vienna), Dr Ami Bhatt (Stanford), Dr Ruud Delwel (Amsterdam) and Dr Donna Neuberg (Boston) for their constructive advice on my work.

Finally, I would like to thank Prof. Junia Melo (now in Adelaide) and Dr Charles Chuah (now in Singapore) for sparking my interest in leukaemia research some 12 years ago, while I was a second-year medical student, through a summer stint in their laboratory.

All work presented in the thesis was performed by myself unless otherwise specified in the methods and/or results chapters.

PUBLICATIONS

Key publications

1. Kwok M, Davies N, Agathanggelou A, Smith E, Oldreive C, Petermann E, Stewart G, Brown J, Lau A, Pratt G, Parry H, Taylor M, Moss P, Hillmen P, Stankovic T. ATR inhibition induces synthetic lethality and overcomes chemoresistance in *TP53* or *ATM* defective chronic lymphocytic leukemia cells. *Blood.* 2016; 127:582-595 (PMID: 26563132)

2. Kwok M, Rawstron AC, Varghese A, Evans PAS, O'Connor SJM, Doughty C, Newton DK, Moreton P, Hillmen P. Minimal residual disease is an independent predictor for 10-year survival in CLL. *Blood.* 2016; 128:2770-2773 (PMID: 27697770)

Manuscript in preparation

1. Kwok M, Rawstron AC, Agathanggelou A, Goel A, Oldreive C, Jones R, Drennan S, Sharma-Oates A, Evans P, Smith E, Mao J, Beaumont J, Rai J, Hamada M, Dalal S, Gordon N, Davies N, Parry H, Beggs A, Munir T, Moreton P, Paneesha S, Pratt G, Taylor M, Forconi F, Baird D, Cazier J-B, Moss P, Hillmen P, Stankovic T. Features and potential mechanisms underpinning spontaneous disease regression in chronic lymphocytic leukemia.

Contributing publications

1. Davies NJ, Kwok M, Gould C, Oldreive CE, Mao J, Parry H, Smith E, Agathanggelou A, Pratt G, Taylor AMR, Moss P, Griffiths M, Stankovic T. Dynamic changes in clonal cytogenetic architecture during progression of chronic lymphocytic leukemia in patients and patient-derived murine xenografts. *Oncotarget*. 2017; 8:44749-44760 (PMID: 28496009)

2. Agathanggelou A, Smith E, Davies NJ, Kwok M, Zlatanou A, Oldreive CE, Mao J, Da Costa D, Yadollahi S, Perry T, Kearns P, Skowronska A, Yates E, Parry H, Hillmen P, Reverdy C, Delansorne R, Paneesha S, Pratt G, Moss P, Taylor AMR, Stewart GS, Stankovic T. USP7 inhibition alters homologous recombination repair and

targets CLL cells independent of ATM/p53 functional status. *Blood.* 2017; 130:156-166 (PMID: 28495793)

Review / Book Chapter

1. Kwok M, Stankovic T. Targeting the ATR signaling pathway to overcome chemoresistance in cancer. In Johnson DE (ed), *Targeting Cell Survival Pathways to Enhance Response to Chemotherapy*. 2017; Elsevier Publishing Company (in press)

Conference Papers

1. Kwok M, Rawstron AC, Varghese A, Evans PAS, O'Connor SJM, Doughty C, Newton DK, Moreton P, Hillmen P. Minimal residual disease is an independent predictor for progression-free and overall survival in chronic lymphocytic leukaemia. *Lancet.* 2014;383:S66

2. Kwok M, Davies N, Agathanggelou A, Smith E, Petermann E, Yates E, Brown J, Lau A, Stankovic T. ATR Inhibition Exacerbates Replication Stress in TP53 or ATM Deficient CLL Cells and Enhances Sensitivity to Chemotherapy and Targeted Therapy. *Blood (ASH Annual Meeting Abstracts)*. 2014 Dec 6; 124(21): Abstract 3340.

3. Agathanggelou A, Skowronska A, Davies N, Kwok M, Clokie S, Griffiths M, Taylor A, Stankovic T. CLL Progression Is Associated with Increased Clonal Diversity and Replication Stress. *Blood (ASH Annual Meeting Abstracts)*. 2014 Dec 6; 124(21): Abstract 1977.

4. Kwok M, Davies N, Agathanggelou A, Smith E, Petermann E, Yates E, Brown J, Lau A, Stankovic T. Synthetic lethality in chronic lymphocytic leukaemia with DNA damage response defects by targeting the ATR pathway. *Lancet*. 2015 Feb 26; 385:S58. (PMID: 26312880)

5. Oldreive C, Davies N, Skowronska A, Kwok M, Pratt G, Moss P, Griffiths MJ, Clokie S, Taylor AMR, Stankovic T. Kinetics of CLL Subclonal Architecture: Spontaneous Disease Progression or Treatment-Induced Selection? *Blood (ASH Annual Meeting Abstracts)*. 2015 Dec 3; 126(23): Abstract 167.

PRIZES AND AWARDS

Prizes and awards obtained in relation to the work described in this thesis are listed below:

2014	Bloodwise Clinical Research Training Fellowship
2014	American Society of Hematology Abstract Achievement Award
2015	EHA-ASH Translational Research Training in Hematology (TRTH)
2016	UK Chronic Lymphocytic Leukaemia (UKCLL) Forum, Hamblin Prize
2017	Royal College of Pathologists Specialty Research Medal

TABLE OF CONTENTS

CHAPTER 1

INTRODUCTION

CHAPTER 2

PATIENTS, MATERIALS & METHODS

CHAPTER 3

FEATURES AND MECHANISMS UNDERPINNING SPONTANEOUS DISEASE REGRESSION IN CLL

CHAPTER 4

PRE-CLINICAL EFFICACY AND MECHANISM OF ATR INHIBITION IN CLL

CHAPTER 5

LONG-TERM PROGNOSTIC SIGNIFICANCE OF MINIMAL RESIDUAL DISEASE IN CLL

CHAPTER 6

CONCLUSION

LIST OF FIGURES

LIST OF TABLES

LIST OF ABBREVIATIONS

4HC	4-hydroperoxycyclophosphamide
9-1-1	RAD9-RAD1-HUS1 complex
95% CI	95% confidence interval
AID	activation-induced deaminase
ALC	absolute lymphocyte count
ALT	alternative lengthening of telomeres
ANOVA	analysis of variance
APOBEC	apolipoprotein B mRNA editing catalytic subunit
APS	ammonium persulphate
ARID1A	AT-rich interaction domain 1A
ASO	allele-specific oligonucleotide
ATP	adenosine triphosphate
ATR	ataxia telangiectasia and Rad3 related
ATRIP	ATR-interacting protein
BCR	B cell receptor
BLM	Bloom syndrome protein
BLNK	adaptor protein B-cell linker
BRCA	breast cancer type 1 susceptibility protein
BSA	bovine serum albumin
BTK	Bruton tyrosine kinase
BWA	Burrows-Wheeler Aligner
CD40L	CD40 ligand
CDR3	complementarity-determining region 3
CFSE	carboxyflourescein succinindyl ester
CI	drug combination index
CLL	chronic lymphocytic leukaemia
Cmax	maximal plasma concentrations
CML	chronic myeloid leukaemia
CNA	copy number aberrations
cnLOH	copy-neutral loss of heterozygosity
COSMIC	Catalogue of Somatic Mutations in Cancer
CR	complete response
CRi	CR with incomplete marrow recovery
Ct	cycle threshold
DAPI	4',6-diamidino-2-phenylindole
ddNTP	dideoxynucleotides
DDR	DNA damage response
DFCI	Dana Farber Cancer Institute
DLBCL	diffuse large B-cell lymphoma
DMEM	Dulbecco's Modified Eagle's Medium
DMSO	dimethylsulphoxide
DNA-PK	DNA-dependent protein kinase
DSB	DNA double-strand break
EC_{50}	Drug dose producing 50% cell killing

ECL	chemiluminescence
EDTA	ethylenediaminetetraacetic acid
ELISA	enzyme-linked immunosorbent assay
ETAA1	Ewing's tumor-associated antigen 1
FANCM	Fanconi anaemia complementation group M protein
FBS	foetal bovine serum
FC	fludarabine and cyclophosphamide
FCMR	FCR plus mitoxantrone
FCR	fludarabine, cyclophosphamide and rituximab
FISH	fluorescent in situ hybridisation
FOXO	forkhead box O
FSC	forward scatter
FSC-A	FSC-area
FSC-H	FSC-height
GATK	Genome Analysis Tool Kit
GlyCAM-1	glycosylation dependent cell adhesion molecule 1
HLA	histocompatibility leukocyte antigen
HR	hazard ratio
HRR	homologous recombination repair
HU	hydroxyurea
ICGC	International Cancer Genome Consortium
IGH	immunoglobulin heavy chain
IGHV	immunoglobulin heavy chain variable region
indel	small insertions and deletions
IP3	inositol-1,4,5-triphosphate
IR	ionising radiation
IWCLL	International Workshop on CLL
Jnk	c-Jun N-terminal kinase
LAIR1	leucocyte associated immunoglobulin like receptor 1
mAb	monoclonal antibodies
MACS	magnetic-activated cell sorting
MAdCAM-1	mucosal vascular addressin cell adhesion molecule 1
MBL	monoclonal B cell lymphocytosis
M-CLL	CLL with mutated IGHV
MDM2	mouse double minute 2 homologue
MDR	minimally deleted region
MEK	mitogen activated protein kinase kinase
MHC	major histocompatibility complex
MRD	minimal residual disease
MRN	MRE11-RAD50-NBS1 complex
mRNA	messenger RNA
mTOR	mechanistic target of rapamycin
NBS1	nibrin
NFAT	nuclear factor of activated T cells
NGS	next generation sequencing
NHEJ	non-homologous end joining
NHS	National Health Service (UK)
NOG	NOD/Shi-scid/IL-2Rγ

nPR	nodular PR
OS	overall survival
PARP	poly (ADP-ribose) polymerase
PBMC	peripheral blood mononuclear cell
PBS	phosphate-buffered saline
PCR	polymerase-chain reaction
PD-L1	programmed death-ligand 1
PECAM-1	platelet endothelial cell adhesion molecule 1
PFS	progression-free survival
pH3	phosphohistone H3 ser-10
PI3K	phosphoinositide 3-kinase
PIKK	phosphoinositide 3-kinase related kinase
PKC	protein kinase C
PLCγ2	phospholipase C-γ2
PR	partial response
Rb	retinoblastoma
REC	research ethics committee
RIC	reduced intensity conditioning
RPA	Replication protein A
RS	Richter syndrome
SCT	haematopoietic stem cell transplantation
SDS	sodium dodecyl sulphate
SHIP1	SH2 domain inositol 5-phosphatase 1
SHM	somatic hypermutation
SHP-1	SH2-containing tyrosine phosphatase-1
sIgD	surface IgD
sIgM	surface IgM
SMC1	structural maintenance of chromosomes protein 1
SNP	single nucleotide polymorphism
SNV	single nucleotide variants
SSC	side scatter
ssDNA	single-stranded DNA
Syk	spleen tyrosine kinase
TCR	T cell receptor
TEMED	tetramethylethylenediamine
TFS	treatment-free survival
TLR	toll-like receptor
TOPBP1	topoisomerase 2-binding protein 1
TRAP	telomeric repeat amplification protocol
TTFT	time to first treatment
U-CLL	CLL with unmutated IGHV
UTB	urea/Tris buffer
VCAM-1	vascular cell adhesion protein 1
VEP	variant effect predictor
VAF	variant allelic fraction
VLA-4	very late antigen-4
WES	whole exome sequencing
WGS	whole genome sequencing
WRN	Werner syndrome ATP-dependent helicase

CHAPTER 1

INTRODUCTION

1.1. Chronic Lymphocytic Leukaemia

1.1.1. Epidemiological features

Chronic lymphocytic leukaemia (CLL) is a clonal lymphoproliferative disorder of mature B lymphocytes (Chiorazzi et al., 2005; Fabbri and Dalla-Favera, 2016). As the most common haematological malignancy in the Western world, CLL has an incidence of 3,515 cases in the United Kingdom in 2011, contributing to 37% of all new cases of leukaemia diagnosed that year (Cancer Research UK). The aetiology of CLL, like many other haematological malignancies, is not clearly defined, although a combination of genetic and environmental factors are likely to be involved. Up to 10% of CLL cases have a familial association, suggesting a strong genetic role in the pathogenesis of this disease (Slager et al., 2013).

CLL has a predilection for elderly individuals with the median age of diagnosis being around 70 and the majority of patients diagnosed between 60 to 80 years of age. It is uncommon in individuals aged 40 or below, with incidence rising with increasing age beyond the 45-49 year age group. CLL is more prevalent in males, with a male:female ratio of approximately 2:1. For reasons as yet unclear, CLL is most common among Caucasians, less prevalent in Afro-Caribbean or South Asian populations, and rare in East Asia. It has been postulated that a combination of genetic susceptibility and immune predisposition may potentially account for such a difference, with a lower incidence in Asian populations of single nucleotide polymorphisms (SNP) within gene susceptibility loci associated with CLL, and substantial differences in immunoglobulin heavy chain (*IGHV*) gene usage in these populations compared to Caucasians (Yang et al., 2015).

1.1.2 Clinical Features

CLL is a clinically heterogeneous disease with clinical course varying greatly among patients. The majority of patients are referred with incidental findings of unexplained lymphocytosis. Others may present with lymphadenopathy and/or hepatosplenomegaly due to infiltration of CLL cells in these lymphoreticular organs. Patients with more progressive disease might experience B-symptoms, characterised by night sweats, fever and weight loss. Infiltration of bone marrow with malignant lymphocytes would result in bone marrow failure with consequential development of anaemia, thrombocytopenia (leading to haemorrhage or bruising) and/or neutropenia (leading to enhanced susceptibility to infection). Finally, autoimmune haemolytic anaemia, or less commonly, thrombocytopenia, is also a feature of CLL. Whereas many individuals experience an indolent course for many years without the need for treatment, others have a rapidly progressive course with poor response to therapy.

Diagnosis of CLL relies on examination of the peripheral blood film, which typically reveals the accumulation of small, round lymphocytes with scant cytoplasm and the presence of smear cells. The diagnosis is then confirmed by assessment of the peripheral blood immunophenotype using multiparameter flow cytometry. In CLL, this would reveal a monoclonal (light-chain restricted) population of CD19, CD5 and CD23 positive cells, with low expression of CD20 and CD79b, and negativity for FMC7 and CD10 (Rawstron et al., 2017). In accordance with the International Workshop on CLL (IWCLL) guidelines, a diagnosis of CLL mandates the presence of at least 5×10^9 lymphocytes per litre in the peripheral blood, together with the appropriate immunophenotype and evidence of clonality established by flow cytometry (Hallek et al., 2008).

1.1.3. Natural history and clinical heterogeneity of CLL

It is now recognised that CLL is invariably preceded by monoclonal B cell lymphocytosis (MBL), defined as the asymptomatic expansion of a monoclonal B lymphocyte population to a maximum of 5 x 10^9 B cells/L in the peripheral blood (Landgren et al., 2009). The prevalence of MBL is estimated to be in the range of 3-5% among the general population aged 50 years or above, and rises with increasing age. The prevalence of MBL is also substantially higher among first-degree relatives of patients with familial or sporadic CLL (Strati and Shanafelt, 2015).

In a previous study I contributed to where we monitored a cohort of 185 individuals with CLL-phenotype MBL, we discovered that the risk of progressive lymphocytosis was dependent on the presentation B cell count. Progressive lymphocytosis was unlikely in subjects having a presentation B lymphocyte count below 1.9 x 10^9/L, and much more commonly among those with >4 x 10^9 B cells/L, where the 5-year risk was >30%. The risk of progression to CLL in individuals with MBL presenting with lymphocytosis was estimated to be 1-2% per year (Rawstron et al., 2008). Further studies led to segregation of MBL cases into distinct low count (<0.5 x 10^9 B cells/L) and high count (0.5-5 x 10^9 B cells/L) groups, where progression from low-count MBL to CLL is very unusual (Strati and Shanafelt, 2015). High-count MBL, on the other hand, display the full spectrum of cytogenetic aberrations seen in CLL, and more recently has been shown to harbour mutations commonly found in CLL. Moreover, subclonal expansion of CLL driver mutations was found in a proportion of high-count MBL cases, indicating evolution from MBL into CLL (Barrio et al., 2017).

Among patients who progress from MBL to CLL, the subsequent clinical course is heterogeneous. The majority of patients with CLL display an indolent disease course, characterised by blood lymphocyte counts that remain largely unchanged (**Figure 1.1A**) or increasing slowly over time (**Figure 1.1B**). These individuals are often asymptomatic, and typically do not require treatment. Many of these individuals lead a normal life expectancy,

Figure 1.1

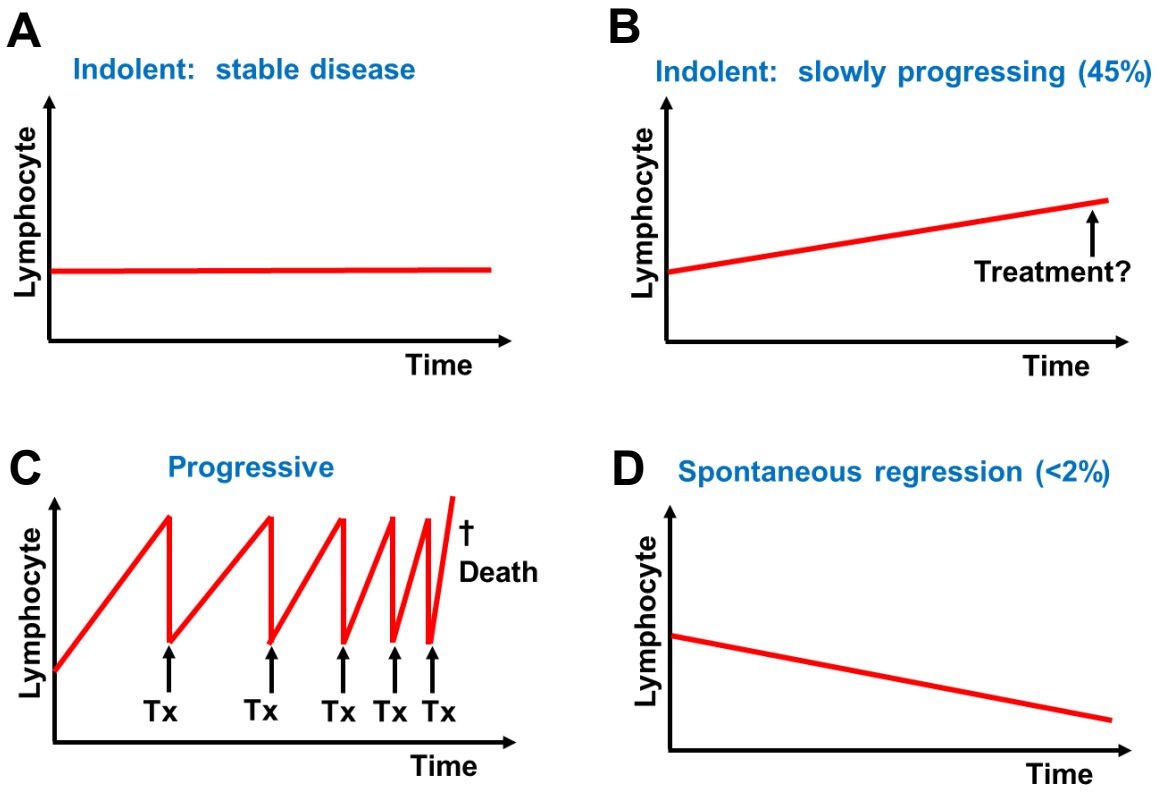

The clinical heterogeneity of CLL. The majority of patients with CLL have stable (A) or slowly progressing (B) disease that does not require treatment at diagnosis. A substantial minority have relapse/refractory disease (C). Spontaneous CLL regression (D) occurs very rarely. The percentages quoted are rough estimates of the proportion of within each category based on patients followed up at Queen Elizabeth Hospital Birmingham. Tx; treatment.

and eventually succumb to other acute illnesses or co-morbidities. On the other hand, a substantial proportion of patients develop progressive CLL. This is characterised by rapidly rising peripheral blood lymphocyte count, typically doubling within 6 months or less, together with features such as progressive B-symptoms and/or adenopathy, and the development of cytopenias resulting from bone marrow infiltration. These patients typically require imminent treatment. While most respond to first-line therapies, many eventually relapse. Those who relapse proceed to second-line treatments, but the durability of remission often decreases with each additional treatment. Most of these patients eventually die from a CLL-related cause, either from CLL itself, from its complications such as infections exacerbated by disease-related immunosuppression, or from treatment-related toxicities (**Figure 1.1C**). Very rarely, patients with CLL undergo spontaneous disease regression, characterised by a sustained reduction or resolution of lymphocytosis and adenopathy over time without treatment (**Figure 1.1D**). Spontaneous disease regression is estimated to occur in less than 1-2% of patients with CLL.

This clinical heterogeneity of CLL is reflected in the clinical staging systems devised by Kanti Rai in 1975 and Jacques-Louis Binet in 1981 which remain in routine use today (Binet et al., 1981; Rai et al., 1975). In the Rai staging system, patients are categorised into 5 stages (0 to IV) of increasing risk of disease progression. Differentiation into the 5 stages are based on the presence, or otherwise, of lymphadenopathy (stage I) and splenomegaly (stage II), as well as anaemia (stage III) and thrombocytopenia (stage IV), with stage 0 characterised by the absence of any of these features The Binet staging system utilises a similar criteria. Patients are classified into three stages (A, B and C) of worsening prognosis, according to the extent of adenopathy and the presence or absence of cytopenias. Stage A and B patients have adenopathy involving <3 or ≥3 anatomical areas, respectively, and no cytopenias, whereas those with stage C disease have anaemia and/or thrombocytopenia. At the time of publication, the median overall survival (OS) was not reached at 10 years of follow up for stage A patients, and 7 years and 2 years respectively

for those in stage B and C. Although survival figures have vastly improved over the ensuing years, the differences in outcomes of these patients serve as a reminder of the disease heterogeneity of CLL.

Finally, disease transformation from CLL to an aggressive lymphoma, known as Richter syndrome (RS), is a recognised sequelae of CLL, and occurs in 5-10% of CLL patients. The majority of these patients transform to diffuse large B-cell lymphoma (DLBCL), although occasionally patients can transform into Hodgkin's lymphoma. DLBCL arising in this context can either be clonally related to the pre-existing CLL, or unrelated (de novo). Patients progressing to Richter's syndrome with clonally-related DLBCL transformations have universally poor prognosis, with a median survival of 8-14 months (Parikh et al., 2014). Despite recent therapeutic advances in CLL, effective treatment options for this category of patients are currently limited.

1.2. The Biological Basis of Disease Heterogeneity in CLL

1.2.1. An overview of CLL pathogenesis

1.2.1.1. CLL cellular origin and pathogenesis

Healthy B cells originate from pluripotent haematopoietic stem cells, which differentiate into committed common lymphoid progenitors and thence into pro-B cells. In the bone marrow, pro-B cells develop through the pre-B cell stage into immature B cells. During this developmental process, pro-B cells undergo recombination of specific gene segments encoding the immunoglobulin variable regions. For instance, within the gene locus encoding the immunoglobulin heavy chain, this involves recombining a V_H, a D_H and a J_H segment from multiple V_H, D_H and J_H segments to enable generation of B cell receptors (BCR) of diverse specificities (i.e. V(D)J recombination). Immature B cells with BCR that recognise foreign antigens are positively selected, whereas self reactive B cells undergo receptor editing, or are eliminated through clonal deletion. Immature B cells subsequently exit the bone marrow into the peripheral blood, initially as transitional (naïve) B cells expressing both IgM and IgD (Cooper, 2015).

Following exposure to antigen, naïve B cells become activated, migrate to lymph nodes, and mature to become follicular or marginal zone B cells. The generation of memory and antibody-producing plasma cells from follicular B cells occur through a T-cell and germinal centre dependent pathway. Upon receiving co-stimulatory signals from antigen-activated T cells, B cells proliferate and differentiate into memory cells and plasma cells of different isotypes. A substantial proportion of these B cells enter germinal centres within lymph nodes where they undergo somatic hypermutation (SHM) of their immunoglobulin variable region genes to enable further BCR diversification. Upon an additional T-cell

mediated selection process known as affinity maturation, selected B cell clones with the highest antigenic affinity undergo differentiation into memory and plasma cells. On the other hand, memory cells and plasma cells are generated from marginal zone B cells through an alternative pathway that is independent of germinal centre reaction and interaction with T cells (De Silva and Klein, 2015; Kurosaki et al., 2015).

Analysis of genes encoding the immunoglobulin heavy chain variable region (*IGHV*) in CLL cells revealed that in some patients the *IGHV* genes have undergone SHM, whereas in others they have not (Damle et al., 1999; Fais et al., 1998; Hamblin et al., 1999). This indicates that in patients with hypermutated *IGHV* (M-CLL), the likely normal counterpart to the CLL cell would be a post-germinal centre B cell, whereas in patients with unmutated *IGHV* (U-CLL), this would be a pre-germinal centre B cell. In an attempt to identify the cellular origin of CLL cells, studies were conducted to compare the gene expression profiles of patients with M-CLL and U-CLL against those of different normal human B cell subsets. The gene expression profiles of M-CLL and U-CLL were found to be largely similar, and displayed the highest similarity to memory B cells (Klein et al., 2001; Rosenwald et al., 2001). A subsequent gene expression study showed that both M-CLL and U-CLL are likely to be derived from normal mature CD5+ B cells (Seifert et al., 2012). On the other hand, work comparing the methylomes of CLL cells with healthy B cell subsets indicates that M-CLL and U-CLL are epigenetically distinct, with methylome of M-CLL and U-CLL being related to memory B cells and naïve B cells respectively (Kulis et al., 2012). Thus, the exact cellular derivation of CLL remains contentious, with M-CLL likely originating from germinal centre dependent memory B cells, and U-CLL either from naïve B cells or germinal centre independent memory B cells.

Whereas CLL is seen as a malignancy of mature B cells (either memory or naïve) based on shared immunophenotypes, gene expression profiles and methylomes as outlined above, evidence from two recent studies have provided speculation that the CLL initiating event could occur much earlier in the B cell developmental process, possibly at the level of

the haematopoietic stem cell. In one study, CD34+ haematopoietic stem cells were isolated from the bone marrow of patients with CLL, and then engrafted into immunodeficient mice. These xenografts displayed increased B lymphoid haematopoiesis, eventually developing into a condition akin to MBL. This was characterised by B cell monoclonality or oligoclonality, CD5 expression, *IGHV* SHM and the usage of V_H, D_H and J_H gene segment combinations commonly seen in high-count MBL and CLL, but distinct from that of the original CLL clone from which these xenografts were derived (Kikushige et al., 2011). Although no CLL-associated cytogenetic abnormality was detected in the CD34+ haematopoietic stem cell compartment in these CLL patients, a second study utilising deep targeted next generation sequencing (NGS) demonstrated that mutations present in the CLL clone were also present in CD34+ cells, albeit at a much lower mutant allelic frequency (Damm et al., 2014).

These observations suggest that CLL pathogenesis could begin early during lymphoid development. However, the subsequent development of MBL and the progression from MBL to CLL is contingent on the acquisition of the various cancer hallmarks, particularly that of apoptotic resistance and enhanced proliferation of the malignant lymphoid cells (Hanahan and Weinberg, 2011). In CLL, a large body of evidence suggests that this is dependent on several factors: (1) antigen-driven BCR signalling; (2) the interaction of CLL cells with different components of the microenvironment; and (3) the progressive accumulation of genetic lesions (**Figure 2**). The nature of BCR signalling (section 1.2.2), microenvironmental interactions (section 1.2.3) and genetic aberrations (section 1.2.4) not only influence the development of CLL but also dictate its subsequent clinical course, and account for the enormous disease heterogeneity that is characteristic of this malignancy.

1.2.1.2. CLL as a disease of failed apoptosis

Historically, CLL is viewed as a pathological accumulation of non-proliferative B-lymphocytes due a failure to undergo apoptosis. Apoptosis is mediated through either the

Figure 1.2

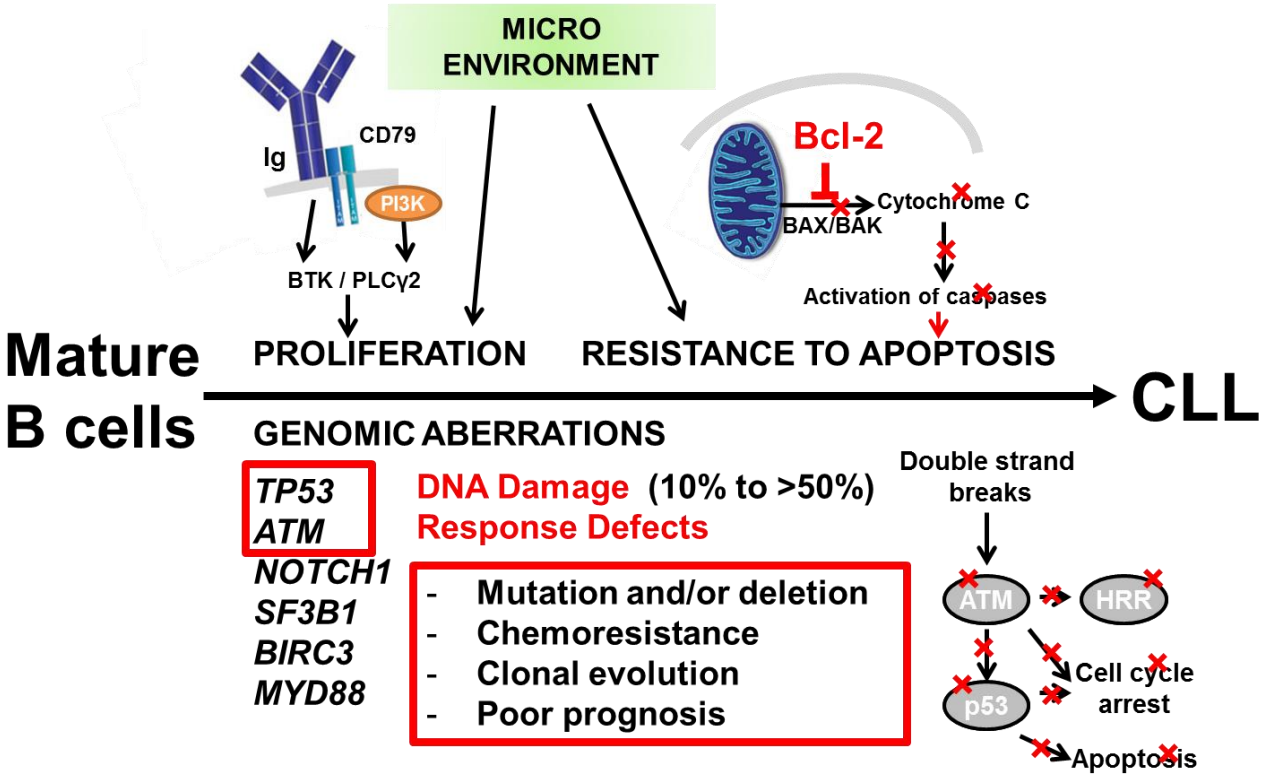

Drivers of CLL pathogenesis and progression. The determinants of CLL pathogenesis and subsequent disease progression are summarised in this schematic diagram. These include BCR signalling, overexpression of anti-apoptotic proteins (e.g. Bcl-2), microenvironmental interactions and genomic aberrations (e.g. *TP53* or *ATM* defects).

extrinsic pathway or the intrinsic pathway, both resulting in caspase activation which leads to cell death. The extrinsic pathway is activated through the binding of death ligands (e.g. Fas ligand, TRAIL and TNFα) to their respective cell surface receptors (i.e. Fas/CD95, TRAIL receptor/DR4 and TNFα receptor), leading to caspase activation. The intrinsic pathway, on the other hand, is regulated through antiapoptotic proteins (e.g. Bcl-2, Bcl-XL and Mcl-1) and proapoptotic proteins (e.g. Bim, Bid and Puma). Proapoptotic proteins are activated in the presence of cellular stress such as DNA damage. Once activated, proapoptotic proteins bind to and inactivate antiapoptotic proteins, the latter of which constrain the activity of two essential mediators of the intrinsic apoptotic pathway: Bax and Bak. The balance between the activity of antiapoptotic and proapoptotic proteins determines the outcome of this apoptotic pathway. When a threshold of proapoptotic activity is exceeded, Bax and Bak together induce the permeabilisation of mitochondrial membrane, allowing efflux of cytochrome c from the mitochondria to the cytoplasm. Cytochrome c in turn triggers a cascade of caspase activation (Taylor et al., 2008).

Indeed, a high level of Bcl-2 expression, relative to normal B cells, is a characteristic of most CLL cells (Faderl et al., 2002). The mechanism through which Bcl-2 is overexpressed in CLL cells, however, has not been thoroughly elucidated. An early study of the methylation status of *BCL2* showed widespread demethylation of both copies of the *BCL2* gene in 20 cases of CLL, indicating that epigenetic derepression of *BCL2* could contribute to an overexpression of the Bcl-2 protein in CLL cells (Hanada et al., 1993). In addition, there have been suggestions that Bcl-2 overexpression might be due to the loss of the microRNA miR15a/16-1. In two-thirds of CLL cases, miR15a/16-1 expression has been shown to be downregulated due to a deletion of chromosome 13q14.2 where miR15a/16-1 is located (discussed in section 1.2.4.3), or to an inactivating mutation of miR15a/16-1 (Calin et al., 2002; Calin et al., 2005). MicroRNAs are small non-coding RNA molecules that post-transcriptionally regulate gene expression by binding to and silencing specific mRNAs. In human megakaryocytic cell lines, transfection of miR15a/16-1 was shown to suppress Bcl-2

levels, suggesting the reverse could possibly occur in CLL cells, leading to apoptotic resistance (Cimmino et al., 2005).

In addition to Bcl-2 overexpression, recent studies have shown that Mcl-1 can also be overexpressed in CLL (Awan et al., 2009; Pepper et al., 2008). Furthermore, the acquisition of inactivating *TP53* mutations provides yet another means through which CLL cells can evade apoptosis (Zenz et al., 2010a). Nuclear p53 transcriptionally activates proapoptotic proteins and represses antiapoptotic proteins in response to DNA damage. Cytoplasmic p53 also induces Bax/Bak activation and suppresses Bcl-2 and Bcl-XL activity (Amaral et al., 2010). Thus, the loss of p53 function enables CLL cells to continue to survive despite acquisition of deleterious and genomically destabilising DNA lesions. Finally, CLL cells engage in BCR signalling (section 1.2.2) and interact with accessory cells in the microenvironment (section 1.2.3), both of which play an important role in supporting CLL cell survival.

1.2.1.3. CLL as a proliferative malignancy

To view CLL merely as a disease arising from the accumulation of lymphocytes that have failed apoptosis, however, ignores the substantial level of CLL proliferative activity seen in many patients with this condition, as well as the importance of CLL proliferation in shaping their clinical course. The proliferative activity of CLL is most vividly captured by *in vivo* isotope labelling studies. In an important study by Messmer and colleagues, patients with CLL were given daily deuterated water, allowing incorporation of deuterium into newly synthesised DNA within dividing cells, which can then be measured through regular blood sampling. In a cohort of 19 CLL patients, CLL cells were found be born at a rate of 0.11% to 1.76% per day. The highest birth rates were found among patients with progressive CLL, particularly those who have been treated previously (Messmer et al., 2005). Subsequent *in vivo* isotope labelling studies in a larger cohort of recently diagnosed CLL patients confirmed

the association between higher proliferation rate and disease progression, as evidenced by a shorter time to first treatment (TTFT). Additionally, higher proliferation rates were associated with U-CLL, as well as with other adverse prognostic markers such as CD38 and ZAP-70 positivity, and adverse cytogenetics (e.g. del(11q)) (Murphy et al., 2017).

These *in vivo* isotope labelling studies also captured the rates of CLL cell death, reflecting a natural process of cell turnover (Messmer et al., 2005). It is likely that the balance between CLL cell proliferation and cell death dictates the absolute disease burden at any one time, as well as the clinical course of each individual patient with CLL. CLL cell proliferation is driven by BCR signalling and a number of other important cellular pathways. These drivers of CLL proliferation will be discussed in subsequent sections. In addition, two biomarkers, namely telomere length and CD38 expression, may reflect, respectively, the proliferation history and the proliferation potential of CLL cells.

Telomere length. The early proliferation history of individual patients' CLL cells may be deciphered from analyses of telomere length. Telomeres are protective structures found within either ends of each chromosome. They are progressively shortened with each cell division owing to the end-replication problem of DNA polymerase. When telomeres are shortened beyond a threshold, cells undergo senescence or apoptosis. CLL cells, like other tumour cells, are able to overcome replicative senescence by expressing telomerase, an enzyme that extends telomere length by adding hexameric TTAGGG repeats to telomere ends. In CLL, short telomeres and high telomerase expression or activity predict for disease progression and a more aggressive clinical course. Moreover, short telomeres and high telomerase activity have been associated with U-CLL and adverse cytogenetics across several studies (Damle et al., 2004; Rampazzo et al., 2012; Roos et al., 2008; Terrin et al., 2007). Although telomerase activity may allow CLL cells with short telomeres to continue to replicate, further shortening of telomeres beyond the threshold for replicative senescence leads to a loss of the protective effects of telomeres, leading to DNA double-strand breaks (DSBs) and telomeric fusions, and giving rise to genomic instability (Lin et al., 2010).

CD38 expression. CD38 is a transmembrane glycoprotein that binds platelet endothelial cell adhesion molecule 1 (PECAM-1; CD31). It has multiple cellular functions, supporting the cell-cell interactions that are essential for the activation, survival and migration of immune cells (Brachtl et al., 2014). CD38 is perhaps the most established and widely used CLL prognostic marker in clinical practice. Studies have consistently shown that CD38 positivity in ≥20% or ≥30% of CLL cells is associated with inferior prognosis (Del Poeta et al., 2001; Hamblin et al., 2002; Ibrahim et al., 2001). However, CD38 may also be viewed as a marker of proliferative potential in CLL. The CD38 positive fraction within a CLL clone is enriched for proliferating cells that are Ki-67 positive, and exhibit higher telomerase activity compared to the CD38 negative fraction (Damle et al., 2007). Furthermore, in an *in vivo* deuterium labelling study, the CD38 positive CLL fraction was shown to contain a greater proportion of deuterium labelled cells. Since the deuterium labelled CLL cells represent newly divided cells during the labelling period, this indicates that the CD38 positive CLL fraction had a higher proliferation rate compared to their CD38 negative counterpart (Calissano et al., 2009).

1.2.1.4. CLL as a disease of immune dysfunction

CLL as a disease is also characterised by a state of impaired immunity (Forconi and Moss, 2015). T cell dysfunction, in particular, has been extensively investigated. The development of CLL is often accompanied by an increase in T cell numbers, particularly an expansion of CD8+ T cells, resulting in an inversion of the CD4:CD8 ratio (CD4:CD8 < 1) in some patients (Christopoulos et al., 2011). Within each of the CD4+ and CD8+ T cell compartments, the preferential expansion of antigen-experienced memory T cells over naïve T cells leads to a skewing of the T cell subset distribution towards memory cells (Hofbauer et al., 2011; Nunes et al., 2012; Tinhofer et al., 2009; Walton et al., 2010).

Both CD4+ and CD8+ T cells have been shown to exhibit features of T cell exhaustion. Exhausted T cells can be identified by the surface expression of T cell exhaustion markers such as PD-1, CD160 and CD244, and display impaired proliferation. In the case of exhausted CD8+ T cells, impaired cytotoxic activity is also apparent due to defective granzyme localisation to the immunological synapse (Riches et al., 2013). Moreover, the formation of immunological synapse is impaired due to defective actin polymerisation, resulting in curtailed recruitment of key regulatory proteins to the synapse required for effective cytotoxic (in case of CD8+ T cells) or co-stimulatory (in case of CD4+ T cells) activity (Ramsay et al., 2008). CLL cells may exert a direct inhibitory effect on autologous T cells, leading to their functional impairment. This is evidenced by changes in the gene expression profile in healthy T cells, upon co-culturing with CLL cells, to that seen in T cells derived from CLL patients (Gorgun et al., 2005). This inhibitory effect on T cells is also evidenced from the observation that defects in the formation of immunological synapse are seen in healthy T cells upon exposure to CLL cells (Ramsay et al., 2008). Finally, studies have been conducted to sequence T cell receptors (TCR) from CLL patients. These studies revealed restriction in the TCR repertoire among CLL patients compared to healthy individuals, and evidence of TCR oligoclonality in these patients (Vardi et al., 2016; Vardi et al., 2017). This suggests the possibility of an antigen-driven selection process for specific TCR, similar in nature to the selection of stereotyped BCR by antigens in CLL (to be discussed in section 1.2.2.2).

Natural killer (NK) cell numbers are also increased in CLL, and like T cells, functional defects are evident (Huergo-Zapico et al., 2014; Parry et al., 2016). On the other hand, healthy B cell numbers, and possibly also function, is markedly suppressed in CLL. This is reflected by hypogammaglobinaemia involving one or more of the three immunoglobulin classes (IgG, IgA and IgM) which a frequent occurrence in CLL patients, and contributes to an increased susceptibility to infections (Rozman et al., 1988). Finally, there is also evidence pointing to defects in the activity of neutrophils and other components

of the innate immune system such as the complement system (Kontoyiannis et al., 2013; Schlesinger et al., 1996). Together, these defects result in a state of impaired immunity in patients with CLL. Given the increasingly recognised roles of the immune system in countering tumour growth, as well as infection, it is likely that these immune defects play a role in the pathogenesis and progression of CLL.

1.2.2. B cell receptor signalling

1.2.2.1. The BCR signalling pathway

Several pieces of experimental evidence have underscored the central importance of B cell receptor (BCR) signalling in the pathogenesis of CLL. Firstly, through V(D)J recombination, receptor editing and SHM, the human body is physiologically capable of producing a diverse BCR repertoire (of up to 2×10^{12} unique specificities) (Langerak et al., 2012). It would therefore be uncommon to find any two B lymphocyte clones carrying identical BCR in a healthy individual. However, up to one-third of CLL patients exhibit stereotyped BCR usage, whereby specific combinations of *IGHV* genes are utilised at much higher frequencies than expected. Patients whose CLL BCR belonging to one of the stereotyped BCR subsets would have very similar BCR specificities. This implicates a role for the recognition of antigens by BCR, and the resultant selection of the B lymphocyte carrying the corresponding BCR specificity, in the pathogenesis of CLL (Messmer et al., 2004; Widhopf et al., 2004). Secondly, patients with CLL belonging to different stereotyped BCR subsets can have markedly different clinical course (Murray et al., 2008). Likewise, there is a marked difference in the prognosis of patients with U-CLL and M-CLL, providing further evidence for an antigen-driven process in the development and progression of CLL (Hamblin et al., 1999). Finally, BCR signalling inhibitors such as ibrutinib, idelalisib and acalabrutinib have shown clinical efficacy both within and outside clinical trials, further

highlighting the importance of BCR signalling in CLL pathogenesis (Byrd et al., 2013; Furman et al., 2014).

BCR signalling is initiated by the binding of an antigen to the BCR expressed on the B lymphocyte cell surface. In CLL, these antigens are usually either autoantigens or foreign antigens, such as bacterial and viral antigens (Hoogeboom et al., 2013; Rosen et al., 2010; Steininger et al., 2012), although CLL has also shown capacity for antigen-independent autonomous BCR signalling (Duhren-von Minden et al., 2012). The BCR is a transmembrane complex composed of a membrane immunoglobulin attached to two proteins, CD79a and CD79b. Upon binding of an antigen to the membrane immunoglobulin, the following events occur in chronological order in a *positive* signalling event (Stevenson et al., 2011; Woyach et al., 2012):

First, a BCR signalosome is formed which is required for signal initiation (**Figure 1.3A**). This begins with the phosphorylation of the intracellular portion of CD79a and CD79b by the kinase Lyn. This results in the recruitment of other proteins, including spleen tyrosine kinase (Syk), Bruton tyrosine kinase (BTK), phospholipase C-γ2 (PLCγ2) and the adaptor protein B-cell linker (BLNK), to CD79a and CD79b in order to form a complex known as the BCR signalosome. Syk mediates the dual phosphorylation of CD79a and CD79b required for positive BCR signal transduction. BLNK, on the other hand, provides a scaffold onto which other proteins, notably BTK and PLCγ2, bind to and exert their effect. The binding of antigens to the BCR also results in the aggregation of these BCR on the cell membrane, resulting in the formation of microclusters known as lipid rafts.

Second, the signal is propagated from the BCR signalosome through BTK, PLCγ2* and *PI3K (**Figure 1.3A-B**). Once the BCR signalosome is formed, BTK and PLCγ2 become activated through phosphorylation. BTK can self-phosphorylate, and can also be phosphorylated by Syk and Lyn. On the other hand, PLCγ2 is phosphorylated by BTK and Syk. PLCγ2, once phosphorylated, exerts its action through two pathways, the protein

Figure 1.3

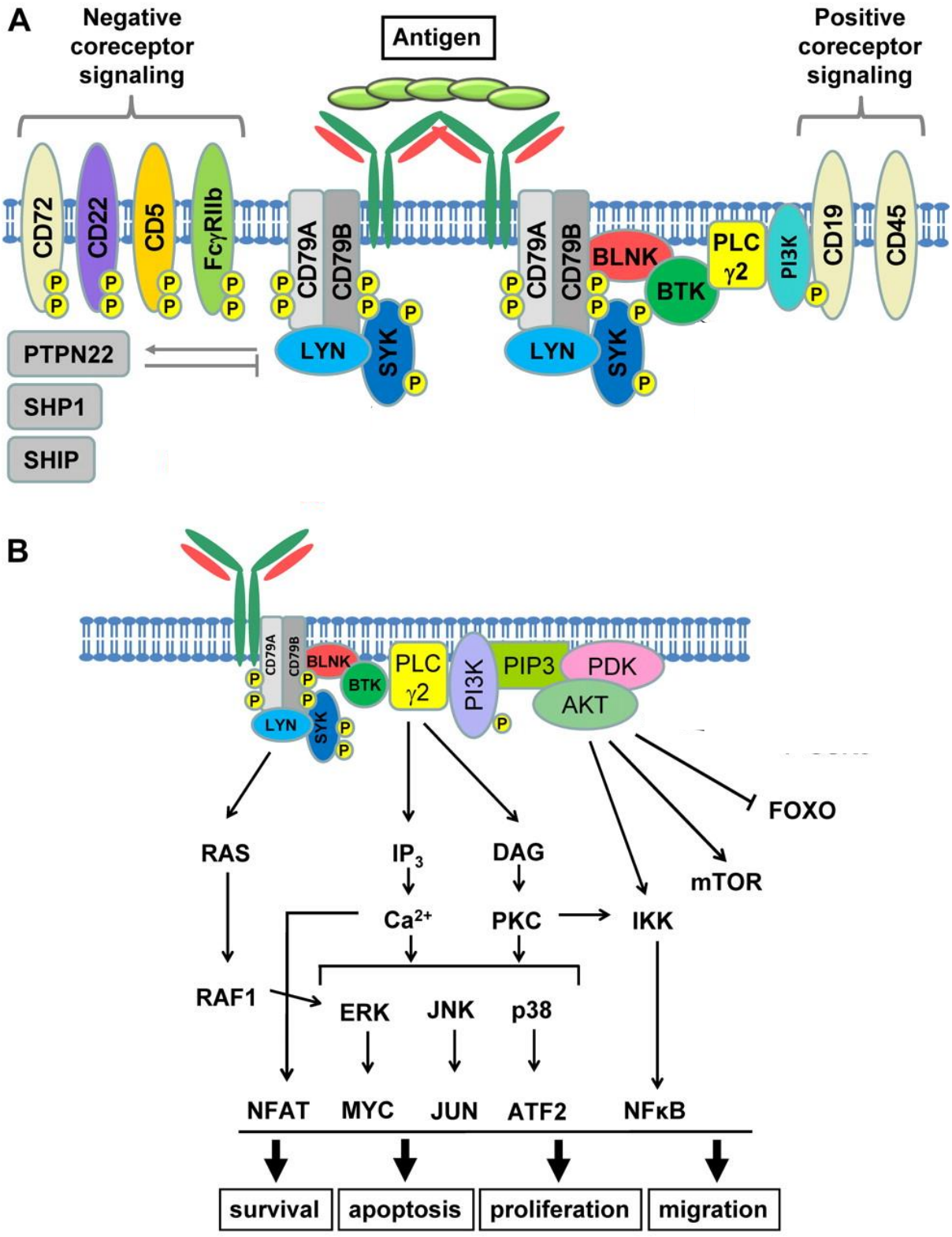

B cell receptor signalling in CLL. Reproduced with minor modifications from Stevenson *et al* (2011). B-cell receptor signaling in chronic lymphocytic leukemia. Blood. *118*, 4313-4320.

kinase C (PKC) pathway and the inositol-1,4,5-triphosphate (IP3) pathway, the latter of which mediates calcium flux from the endoplasmic reticulum. Phosphoinositide 3-kinase (PI3K), although not part of the initial signalosome, is subsequently recruited and phosphorylated by Lyn. Upon binding to the positive BCR co-receptor CD19, phosphorylated PI3K mediates downstream signalling through the PI3K/Akt pathway.

Third, signalling through downstream pathways leads to modulation of transcriptional activity to enhance cell survival and proliferation (**Figure 1.3B**). Signalling through the PKC pathway, and calcium flux, lead to phosphorylation and activation of intermediates such as Erk, c-Jun N-terminal kinase (Jnk) and p38. These intermediates in turn activates the transcription factors Myc, Jun and AFT2 respectively. In addition, calcium flux directly activates the transcription factor nuclear factor of activated T cells (NFAT). Furthermore, signalling through the PKC and Akt pathways results in phosphorylation and subsequent proteasomal degradation of the NF-κB inhibitory molecule I-κB. This activates NF-κB and allows its translocation to the nucleus where it performs its transcriptional modulatory activities. Akt also activates other growth pathways such as mechanistic target of rapamycin (mTOR) and inhibits proapoptotic proteins such as Forkhead Box O (FOXO). Finally, Lyn can signal through the Ras/Raf pathway, leading to Erk and Myc activation. Therefore, positive BCR signalling converges onto a number of transcription factors which modulates transcriptional activity to promote cell survival, migration and proliferation. In CLL, these activities occur within CLL cells, and are required for disease maintenance and progression.

Positive signalling through the BCR also results in downstream effects beyond transcriptional modulation (Spaargaren et al., 2003). In particular, positive BCR signalling has been shown to modulate integrin activity through “inside-out” integrin signalling. For instance, the activation of CD49d through “inside-out” signalling requires the activation specifically of Lyn, Syk, PI3K, BTK, IP3-mediated calcium release and PKC. Moreover, the promotion of B cell migration by chemokines such as CXCL12, which binds to the cell

surface receptor CXCR4, is also dependent on BCR signalling pathways. Subsequent to the engagement of CXCR4 by CXCL12, integrin-mediated migration of B cells is dependent on the activation of BTK and PLCγ2 in an “outside-in” signalling process (de Gorter et al., 2007). Thus, in these ways, positive BCR signalling and pathways regulating cell adhesion and trafficking are tightly coupled, and together promote the homing of CLL cells to lymph nodes where proliferation takes place. Finally, BCR signalling also appears to modulate the expression of the antiapoptotic protein Mcl-1. In CLL cells, BCR signalling triggered by immobilised anti-IgM, but not soluble anti-IgM, was shown to increase the level of Mcl-1 expression and protect CLL cells from chemotherapy-induced (but not spontaneous) apoptosis (Petlickovski et al., 2005).

With few exceptions, CLL cells express IgM and IgD BCR of the same specificity on their cell surface, albeit at different densities in different patients. The few exceptions to this are in CLL cells with class-switched BCR, which express IgG (Potter et al., 2006). Positive signalling events are largely identical whether occurring through IgM or IgD BCR, but the end result might differ. IgM stimulation promotes CLL cell cycle progression and proliferation, with limited effect on cell survival (Guarini et al., 2008). IgD stimulation, in contrast, has been shown to enhance CLL cell survival, but does not induce proliferation (Zupo et al., 2000). The latter has been attributed, in part, to significantly lower levels of Myc induction following IgD BCR signalling, in comparison with IgM BCR signalling (Krysov et al., 2012). However, a recent study has suggested the contrary: that IgM but not IgD signalling promotes CLL cell survival. This study also showed that IgM stimulation, in comparison to IgD stimulation, led to more prolonged downstream activation resulting in enhanced levels of chemokine secretion (Ten Hacken et al., 2016). Overall, the functional roles and relative contribution of IgM and IgD BCR signalling in CLL pathogenesis remain incompletely understood.

1.2.2.2. CLL anergy and negative regulation of BCR signalling

Anergy, in B lymphocytes, refers to a state of unresponsiveness to BCR stimulation. In healthy B cells, this occurs following chronic antigenic stimulation of BCR in the absence of a co-stimulatory signal from antigen-activated T cells. Physiologically, anergy exists as a mechanism through which autoreactive lymphocytes that have evaded clonal deletion during their developmental process are silenced in the peripheral circulation. Studies have shown that B cell anergy is a dynamic and reversible process, and that maintenance of anergy requires constant BCR occupancy and signalling. Indeed, BCR occupancy must exceed a threshold in order for anergy to occur, whereas removal of the occupying antigens results in recovery of response to BCR stimulation within minutes (Gauld et al., 2005). Mechanistically, anergy occurs as a consequence of signalling through a *negative* BCR signalling pathway (**Figure 1.3A**). This regulatory pathway is mediated by negative transmembrane co-receptors, such as FcγRIIb, CD5, CD22, CD72 and leucocyte associated immunoglobulin like receptor 1 (LAIR1) (Perbellini et al., 2014; Stevenson et al., 2011; Woyach et al., 2012). These inhibitory co-receptors may be activated through co-ligation with BCR and subsequent phosphorylation by Lyn. Once activated, these co-receptors recruit a number of downstream phosphatases, notably SH2 domain inositol 5-phosphatase 1 (SHIP1) and/or SH2-containing tyrosine phosphatase-1 (SHP-1). SHIP1 and SHP-1 inhibit *positive* BCR signalling in different ways. SHIP1 has been shown to suppress the PI3K pathway (Getahun et al., 2016). SHP-1, on the other hand, dephosphorylates several proteins involved in positive BCR signalling, including Syk (Adachi et al., 2001). The maintenance of B cell anergy necessitates continuous inhibitory signalling through both SHIP1 and SHP-1 pathways (Getahun et al., 2016).

CLL cells are variably stimulated and anergised *in vivo*. Anergic CLL cells are unresponsive to BCR stimulation. More specifically, anergic CLL cells display a lack of responsiveness to IgM BCR crosslinking by anti-IgM antibodies. CLL cells that fail to respond to IgM receptor stimulation often, but not always, retain responsiveness to IgD

receptor stimulation (Lanham et al., 2003). Anergic CLL cells downregulate cell surface IgM expression, but spontaneous recovery of surface IgM expression and responsiveness can become apparent following incubation of these cells *in vitro* in media deplete of antigen (Mockridge et al., 2007). The latter observation substantiates the notion that chronic antigenic stimulation is required for the maintenance of anergy, and that IgM BCR endocytosis following antigenic stimulation may account for the low surface IgM expression in anergic CLL cells. Other features displayed by anergic CLL cells include constitutive phosphorylation of Erk as well as mitogen activated protein kinase kinase (MEK) that is upstream of Erk, and increased basal NFAT activation (Muzio et al., 2008).

1.2.2.3. Determinants of the heterogeneity of BCR signalling responses in CLL

There is substantial heterogeneity of BCR signalling activity among patients with CLL. In addition, within an individual patient, there can be considerable intraclonal variability in the signalling capacity of CLL cells, with some cells exhibiting features of anergy, and others displaying much higher propensity for positive BCR signalling (Coelho et al., 2013). Inter-patient variability in BCR signalling is a recognised contributor to the clinical heterogeneity of CLL. The factors influencing BCR signalling capacity and their clinical impact will be discussed here:

IGHV mutational status. As alluded to previously in section 1.2.1.1., M-CLL and U-CLL may reflect different B cell maturation stages during which differentiation arrest and malignant transformation to CLL occurs. This results in differences in *IGHV* SHM that can be detected upon *IGHV* gene sequencing using DNA extracted from CLL cells. A convention is generally adopted whereby CLL *IGHV* sequences of <98% homology to germline *IGHV* sequences denotes U-CLL, whereas ≥98% homology to germline sequences represents M-CLL (Rosenquist et al., 2017). Clinically, *IGHV* mutational status identifies two subgroups of CLL patients with different prognosis: M-CLL which is usually associated with more indolent

disease, and therefore good prognosis; and U-CLL which is associated with a more aggressive clinical course, and hence poorer prognosis (Damle et al., 1999; Hamblin et al., 1999). Subsequent studies have revealed that U-CLL cases are generally responsive to IgM BCR ligation. On the other hand, many, but not all, M-CLL patients display features of anergy to varying degrees. They generally possess lower CLL surface IgM expression, and reduced responsiveness to BCR stimulation compared to U-CLL cases (Lanham et al., 2003; Mockridge et al., 2007).

IGHV stereotypy. BCR belonging to a particular stereotyped subset have three features in common. Firstly, with few exceptions, they must have the same *IGHV* mutational status. Secondly, the *IGHV* gene used must be phylogenetically related, as evidenced by belonging to the same clan, with *IGHV1/5/7* genes forming clan 1, *IGHV2/4/6* genes clan 2 and the *IGHV3* gene clan 3. Finally, they must have similar complementarity-determining region 3 (CDR3): the sequence located at the junction between the recombined V_H, D_H and J_H gene segments responsible for the unique specificity of the BCR (Agathangelidis et al., 2012; Bystry et al., 2015). In CLL, 19 major stereotyped subsets have been identified. Four of these subsets are particularly well characterised. Subset 1 contains U-CLL cases utilising *IGHV1/5/7*, *IGHD6-19* and *IGHJ4*, and has a 13 amino acid CDR3 sequence. Subset 2 cases utilise *IGHV3-21* and *IGHJ6*, with a CDR3 of 9 amino acids, and can either be M-CLL or U-CLL. Subset 4 consists of M-CLL cases with *IGHV4-34/IGHD5-18/IGHJ6* and a CDR3 of 20 amino acid, while subset 8 comprises U-CLL cases with *IGHV4-39/IGHD6-13/IGHJ5* and a CDR3 of 19 amino acids (Stamatopoulos et al., 2017). Subsets 1, 2 and 8 are associated with an aggressive clinical course, with subset 8 being additionally linked to a high risk of transformation to RS. Subset 4 CLL cases, on the contrary, display a very indolent clinical course (Baliakas et al., 2014). The variation in clinical behaviour among these stereotyped subsets may be explained, in part, by differences in BCR signalling responses. Subsets 1 and 8 CLL cells respond strongly to BCR stimuli, especially subset 8 cases which exhibit a distinct avidity to a broad range of antigens (Del Giudice et al., 2014;

Gounari et al., 2015). In contrast, subset 4 CLL cells manifest features of B cell anergy (Gounari et al., 2015).

ZAP-70 expression. ZAP-70, alongside *IGHV* mutational status, is one of the more commonly used prognostic biomarkers in CLL. ZAP-70 is primarily involved in TCR signalling by acting as a signalling intermediate, with a role similar to that of Syk in BCR signalling. ZAP-70 is not ordinarily expressed in healthy B cells. However, it is variably expressed in a proportion of CLL cases. ZAP-70 expression is associated with U-CLL, with ZAP-70 positive CLL cells displaying enhanced BCR signalling upon IgM ligation, as evidenced by higher levels of Syk and PLCγ2 phosphorylation, as well as calcium flux, in comparison to ZAP-70 negative cells (Chen et al., 2005; Chen et al., 2002). Recently, evidence has emerged that the Toll-like receptor (TLR) signalling pathway also activates Syk, and collaborates with the BCR signalling pathway in driving CLL proliferation. However, TLR-mediated Syk activation in CLL cells is highly dependent on ZAP-70 (Wagner et al., 2016). This may provide an explanation for the enhanced BCR signalling activity in ZAP-70 positive CLL cells. As such, ZAP-70 positivity, using 20% positive cells as cut-off, was shown to confer more rapid CLL progression and poorer OS (Crespo et al., 2003).

1.2.3. Microenvironmental interactions

1.2.3.1. CLL cell homing and trafficking

CLL cells betray a dependence on the tumour microenvironment. This is evident from prolonged *in vitro* culture of these cells without stromal support, which inevitably results in cell death. Within the *in vivo* tumour microenvironment, CLL cells interact with a number of other cell types. These include mesenchymal stromal cells, monocyte-derived nurse-like cells, follicular dendritic cells and T cells. These accessory cells are located mostly within lymphoid tissues such as the lymph nodes and bone marrow, and provide prosurvival and

proliferative signals to CLL cells. Together, they form a niche within which CLL cells are protected from apoptosis, and support CLL cell growth and proliferation (Burger, 2011). Positive BCR signalling in CLL cells, for instance, occurs almost exclusively in proliferation centres within lymph nodes, and to a much lesser extent in the bone marrow (Herishanu et al., 2011).

However, not all CLL cells reside in these niches. Instead, the vast majority are circulating within the peripheral blood. CLL cells in the peripheral blood are mostly quiescent, and are less protected from cell death. The difference in the characteristic of CLL cells within the lymphoid tissue and peripheral blood compartments is apparent from the gene expression differences of CLL cells obtained from these two sites. CLL cells resident within lymph nodes have higher expression of genes associated with BCR positive signalling, including Myc and NF-κB activation, which promote cell survival and proliferation (Herishanu et al., 2011). Hence, *in vivo*, there is a constant traffic of CLL cells between proliferation niches and the peripheral blood. CLL cells move into lymph nodes to receive survival signals and to proliferate, following which they exit into the peripheral circulation, to return at a later time.

Such a process of CLL cell trafficking is essential for the development and progression of CLL, and is facilitated by a number of pathways and microenvironmental interactions. The most important among these are interactions between chemokines and chemokine receptors, and those between adhesion molecules and their ligands. These interactions will be explained in more detail below:

Chemokine-chemokine receptor interactions. CLL cells express on their cell surface multiple chemokine receptors, including CXCR4, CXCR5, CCR6 and CCR7 (Durig et al., 2001). CXCR4 and CXCR5 are both expressed at a high level on CLL cells, whereas the expression of CCR6 is intermediate and more variable. CXCR4 binds CXCL12, a chemokine that is produced by various cell types including nurse-like cells and bone marrow

mesenchymal stromal cells within lymphoid tissues. The CXCR4-CXCL12 interaction confers a prosurvival effect on CLL cells, and allows peripheral blood CLL cells to migrate along a CXCL12 chemokine gradient towards, and, through the endothelium, into these lymphoid tissues (Burger et al., 2000; Mohle et al., 1999). CXCL12 binding to CXCR4 is also likely to play a role in retaining CLL cells within lymph nodes. This can be inferred from an *in vivo* isotope labelling study which shows that CLL cells with delayed exit from lymph nodes possess higher levels of CXCR4 expression (Calissano et al., 2009). Nevertheless, CXCR4 is downregulated following BCR ligation, allowing newly proliferated CLL cells to exit from lymph nodes into the circulation (Vlad et al., 2009). Thus, the CLL population that has recently divided can be identified by its low level of CXCR4 expression. Over time, these cells recover CXCR4, permitting eventual re-entry into lymph nodes (Calissano et al., 2011; Coelho et al., 2013), as illustrated in **Figure 1.4**. CXCR5 has also been shown to be important in the homing of CLL cells into lymph nodes through binding to the chemokine CXCL13, which is secreted by nurse-like cells (Burkle et al., 2007). In comparison with CXCR4 and CXCR5, the role of CCR6 in CLL has been less extensively studied. However, its ligand, CCL20, is highly expressed in lymph nodes, thus supporting a potential role for CLL cell homing (Rossi et al., 1997). Interestingly, like CXCR4, the expression of CCR6 on B lymphocytes and CXCR5 on CLL cells is also markedly reduced following BCR engagement (Krzysiek et al., 2000; Saint-Georges et al., 2016). Finally, CCR7 is also high expressed on CLL cells and may also play a role in cell homing (Till et al., 2002).

Adhesion molecules. Transendothelial migration requires CLL cells to adhere to and roll on the vascular endothelium. This is facilitated by adhesion molecules expressed on the CLL cell surface. Two of the functionally most important adhesion molecules in CLL are CD49d and CD62L. CD49d is an α4 integrin that associates with CD29, a β1 integrin, to form a heterodimer known as very late antigen-4 (VLA-4). CD49d binds to vascular cell adhesion protein 1 (VCAM-1), expressed on the surface of endothelial cells and bone marrow stromal cells, as well as fibronectin within the extracellular matrix

Figure 1.4

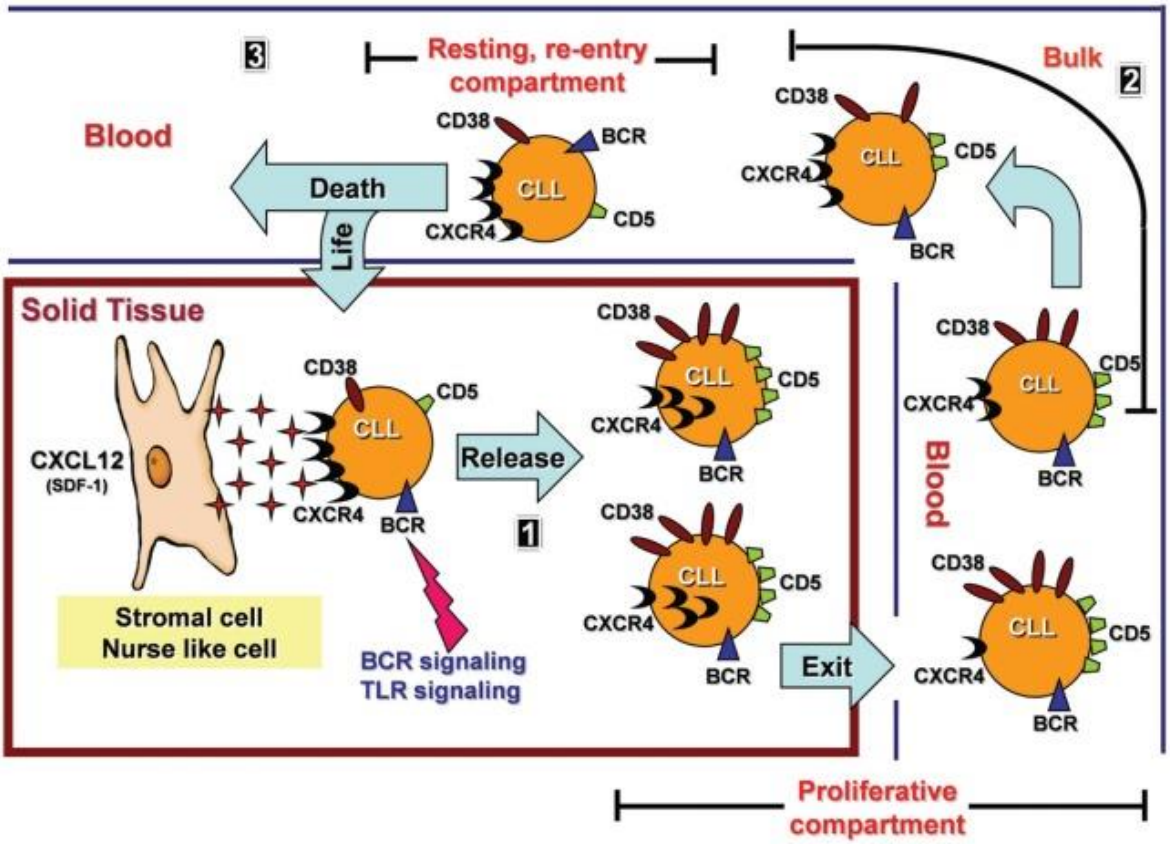

Trafficking of CLL cells between the proliferative and peripheral blood compartments. CLL cells traffic continuously between the proliferative compartment in the lymph nodes and the peripheral blood circulation. (1) Newly proliferated CLL cells downregulate CXCR4 expression to allow their exit from the lymph nodes into the peripheral circulation. They also have high CD38 and CD5 expression. (2) Over time, these CLL cells recover CXCR4 expression and downregulate CD38 and CD5 expression. (3) Circulating CLL cells with high CXCR4 expression home to the lymph nodes along the CXCL12 chemokine gradient where they re-enter the proliferative compartment for further proliferation. Reproduced from Calissano *et al* (2011). Intraclonal Complexity in Chronic Lymphocytic Leukemia: Fractions Enriched in Recently Born/Divided and Older/Quiescent Cells. Mol Med. *17*, 1374-1382.

(Brachtl et al., 2014). CD49d was shown to be crucial for the transendothelial migration of CLL cells across a CXCL12 chemokine gradient, and blocking CD49d inhibited this (Till et al., 2005). The importance of CD49d for CLL cell trafficking into lymph nodes was demonstrated by a positive association between CD49d expression levels and lymphadenopathy (Till et al., 2002). CD49d was also shown to facilitate homing of CLL cells to the bone marrow (Brachtl et al., 2011). Clinically, patients with ≥30% CLL cells expressing CD49d had poorer OS and treatment-free survival (TFS) in a meta-analysis of published studies, supported by a validation cohort (Bulian et al., 2014). On the other hand, CD62L, also known as L-selectin, is a member of the selectin family of adhesion molecules. CD62L binds to such ligands as CD34, glycosylation dependent cell adhesion molecule 1 (GlyCAM-1) and mucosal vascular addressin cell adhesion molecule 1 (MAdCAM-1) expressed on endothelial cell surface to facilitate CLL entry into lymph nodes. Low CD62L expression has been linked to an impaired transendothelial migration of CLL cells, and CD62L inhibition may result in cell death (Burgess et al., 2013; Gu et al., 2001). Similar to CXCR4, BCR triggering can also result in the downregulation of CD62L expression to facilitate the exit of recently proliferated CLL cells from lymph nodes (Vlad et al., 2009).

1.2.3.2. CLL interactions with T cells

Co-stimulatory signals from CD4+ T helper cells are indispensable for the differentiation and proliferation of healthy B lymphocytes in response to antigenic stimulation. Conversely, the failure to receive a co-stimulatory signal upon BCR ligation results in B cell anergy (section 1.2.2.2). In healthy B lymphocytes, BCR activation is usually followed by the internalisation of the BCR-bound antigen and its presentation on class II major histocompatibility complexes (MHC). Simultaneously, two co-stimulatory molecules, CD80 and CD86, are upregulated on the B lymphocyte. Presentation of the MHC-bound antigen to a CD4+ T cell, facilitated by a co-stimulatory signal mediated through the binding

of CD80/CD86 on the B lymphocyte to CD28 on the T cell, leads to activation of that T cell. The activated CD4+ T cell then reciprocates by activating the B lymphocyte. This is facilitated by the upregulation of CD40L on the T cell, which binds CD40 that is constitutively expressed on the B lymphocyte, to create a second co-stimulatory signal. The activated T cell also releases multiple cytokines that support the proliferation of the B lymphocyte.

In CLL cells, although *in vitro* ligation of BCR by anti-IgM triggers modulation of transcription in favour of enhanced proliferation (Guarini et al., 2008), the actual increase in proliferation was modest in the absence of co-stimulation (Balakrishnan et al., 2015). In contrast, a high level of CLL cell proliferation was seen in patient lymph nodes (Herishanu et al., 2011). This indicates that additional signals are required for CLL proliferation *in vivo* in addition to BCR activation. Indeed, CLL cells were demonstrated to be capable of presenting antigens to autologous CD4+ T cells or allogenic T cells with the same histocompatibility leukocyte antigen (HLA) restriction, and that these T cells in turn induced the activation and proliferation of CLL cells (Os et al., 2013). Further evidence of a requirement for T cell co-stimulatory signals emerged from primary CLL xenotransplantation studies on immune deficient murine models. Transplanted human CLL cells do not engraft in mice in the absence of T cells. However, when autologous CD34+ haematopoietic progenitor cells were co-transplanted with CLL cells, which differentiated *in vivo* into T cells, the transplanted CLL cells were able to engraft and proliferate in mice (Bagnara et al., 2011). Similarly, co-transplantation of human CLL cells into mice, alongside autologous T cells that were activated *ex vivo*, enabled engraftment and proliferation of the CLL clone (Patten et al., 2015). Finally, CLL cells proliferated robustly *in vitro* upon co-culturing with CD40L expressing cells, especially in the presence of cytokines such as IL-21 or IL-4, further substantiating the role of co-stimulatory signals in CLL proliferation (Balakrishnan et al., 2015; Pascutti et al., 2013).

1.2.4. Genomic aberrations

1.2.4.1. Spectrum of copy number aberrations in CLL

Like all other malignancies, genomic aberrations contribute to the pathogenesis and subsequent development of CLL. However, unlike other malignancies such as chronic myeloid leukaemia (CML), there is no recognised initiating lesion in CLL responsible for its malignant transformation. Rather, genomic aberrations in CLL tend to accumulate throughout the natural history of the disease. The combination of acquired lesions and the sequence of acquisition of these lesions differ from one patient to another, helping to shape the unique clinical course of each individual.

Cytogenetic analysis of CLL began in the late 1980s and continued into the 1990s, culminating in the Döhner hierarchical classification system of cytogenetic lesions that is still in use today (Dohner et al., 2000). Among the cytogenetic abnormalities in CLL, del(13q14) is the most prevalent, and is present in approximately 55% of individuals with the condition. This is followed by del(11q22-23), trisomy 12, del(17p) and del(6q15-21), reported in 18%, 16%, 7% and 6% respectively of the Döhner cohort. Of note, the Döhner cohort comprised predominantly of treatment naïve CLL patients. Among relapsed/refractory patients, the frequencies of del(11q), trisomy 12 and del(17p) would generally be higher, reflecting the functional impact of these lesions on disease biology. When the clinical impact of these lesions was considered, del(13q14) as the sole abnormality conferred the best prognosis, followed by no abnormality. Trisomy 12 appeared next, and conferred intermediate risk. Del(11q) then followed, with del(17p) being associated with the worst TFS and OS outcomes (Dohner et al., 2000).

Our knowledge of copy number aberrations (CNAs) in CLL has expanded in the ensuing years, due to newer technologies such as single nucleotide polymorphism (SNP) arrays and next generation sequencing (NGS). SNP arrays utilise a library of probes complementary to different possible allelic variations within each genomic region. This

allows determination of copy number and the allelic composition within each genomic locus from which the presence of CNAs could be inferred (see section 2.5.1 for further detail) (Nowak et al., 2009). Unlike FISH, SNP arrays permit a comprehensive analysis of CNAs across the entire genome. Such an unbiased genome-wide discovery of CNAs can also be achieved through whole genome sequencing (WGS) or whole exome sequencing (WES), although CNA analysis from WES data is limited by coverage of only the coding regions which comprise a small fraction of the genome.

Application of these technologies on large patient cohorts has provided insight into the spectrum of CNAs in CLL. Firstly, the range of recurrent CNAs in CLL is small, with only 9 CNAs found at a frequency of >3% by WGS in a cohort of 452 individuals with stable or progressive CLL. These are del(13q14), trisomy 12, del(11q), del(14q), amp(2p), del(17p), del(18p), del(6q) and amp(8q) (Puente et al., 2015). In another study of 538 mainly progressive individuals by WES, only del(13q14), trisomy 12, del(11q), del(17p), del(6q), amp(2p) and del(8p) was found in >3% of the cohort (Landau et al., 2015) (**Figure 1.5**). Secondly, whereas some CNAs are predominantly clonal, for example del(13q14) and trisomy 12, others such as del(11p) and del(17p) may be present only in a fraction of CLL cells within an individual, and therefore subclonal (Landau et al., 2015). Clonal lesions are likely to have arisen early during CLL development, whereas subclonal lesions may have been acquired during subsequent disease evolution (Landau et al., 2013).

1.2.4.2. Spectrum of driver mutations in CLL

In addition to structural DNA lesions such as CNAs, gene mutations constitute a major source of genomic aberrations in CLL. Studies have found that a proportion of CLL cases carry mutational signatures consistent with apolipoprotein B mRNA editing catalytic subunit (APOBEC) activity (Alexandrov et al., 2013; Kasar et al., 2015). APOBEC proteins are cytidine deaminases that generate targeted DNA damage. Activation-induced

Figure 1.5

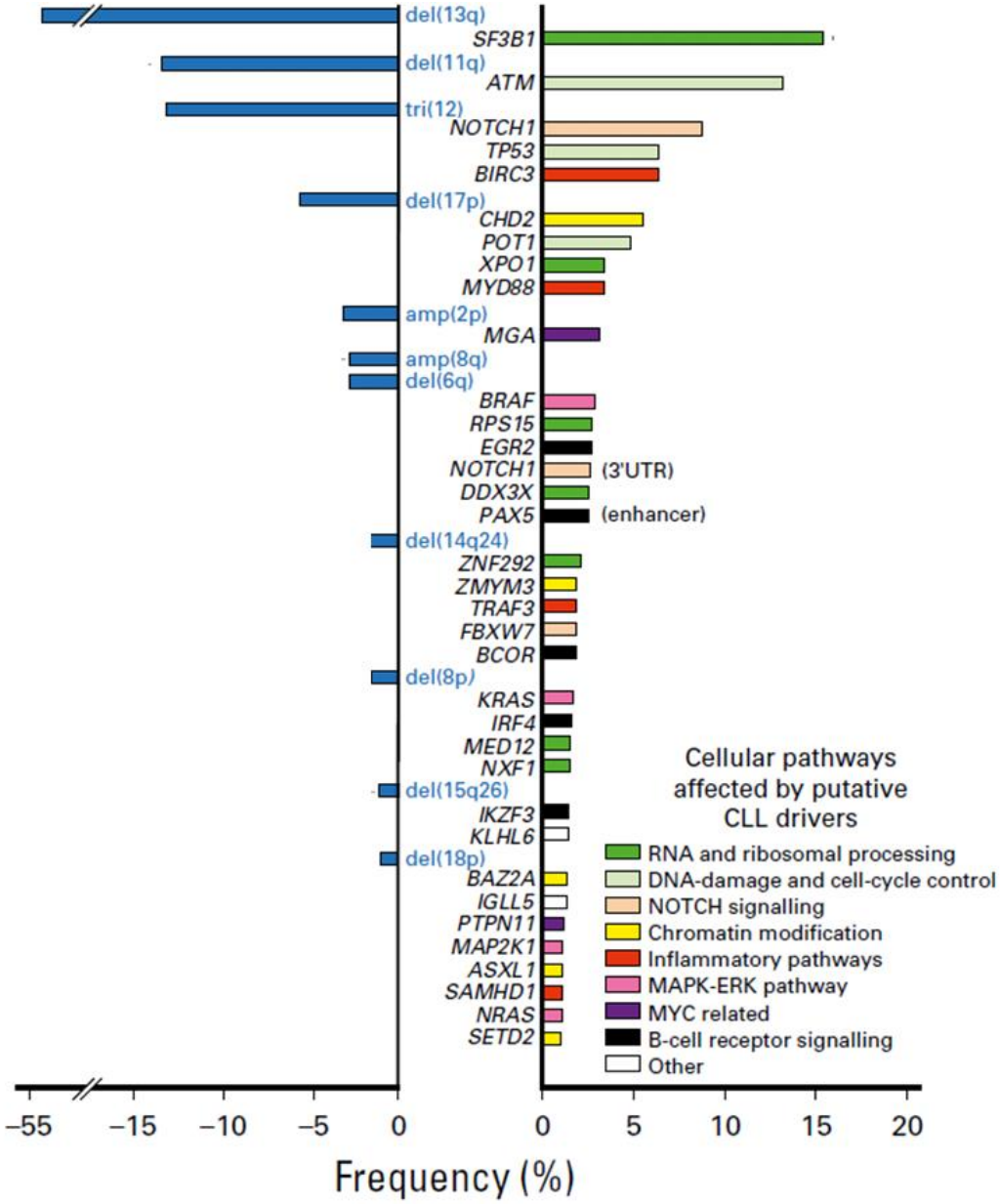

The genomic landscape of CLL. Copy number aberrations are displayed on the left and putative driver mutations are displayed on the right. Reproduced with minor modifications from Wu *et al* (2017). Clinical Implications of Novel Genomic Discoveries in Chronic Lymphocytic Leukemia. J Clin Oncol. *35*, 984-995.

deaminase (AID) is an APOBEC protein that is involved in the SHM process within germinal centres during B cell development (Patten et al., 2012). Therefore, it is plausible that some of the gene mutations may arise, in part, from AID activity during the development of CLL.

Numerous WES and WGS studies have been carried out over the past decade to comprehensively catalogue somatic mutations in CLL, including single nucleotide variants (SNVs) and small insertions and deletions (indels). Effort has also been made within these studies to identify putative genomic drivers: recurrent genes mutations that are likely functional significance and confer growth advantage on CLL cells. Two of the largest such studies are the Spanish International Cancer Genome Consortium (ICGC) study and the Dana Farber Cancer Institute (DFCI) study on patients from the German CLL study group CLL8 trial (Landau et al., 2015; Puente et al., 2015). Combining data from these two studies (n=990), a total of 75 significantly mutated genes were found, of which 28 were common to both studies (**Figure 1.5**). The most frequently mutated genes are *SF3B1*, *ATM*, *NOTCH1*, *TP53, BIRC3*, *CHD2*, *POT1, XPO1* and *MYD88.* These genes are involved in a wide range of cellular processes including DNA damage response (DDR), cell cycle regulation, RNA processing, NOTCH signalling as well as other growth and inflammatory signalling pathways (Lazarian et al., 2017). Thus, through acquiring a spectrum of genetic mutations, CLL cells are able to co-opt diverse cellular functions to enhance their own survival and proliferation.

The following section will discuss the functional and clinical consequences of a select few of the most frequent and significant genomic aberrations in CLL.

1.2.4.3. Functional significance of genomic aberrations in CLL

13q14 deletion. Del(13q14) is the single most frequent genomic event in CLL. The majority of 13q deletions in CLL involve a minimally deleted region (MDR) on 13q14.2 which contains the *DLEU2* gene. *DLEU2* encodes for a long non-coding RNA with unknown

function. However, located within an intron of *DLEU2* is the miR15a/16-1 cluster, discussed earlier in section 1.2.1.2. In an important study by Klein and colleagues, deletion of the 13q14 MDR or of miR15a/16-1 itself led to the development of CLL in mice. Moreover, deletion of miR15a/16-1 resulted in enhanced proliferation of murine B cells. In human CLL cells with del(13q14), re-expression of miR15a/16-1 led to a downregulation of genes essential for cell cycle progression, and suppressed CLL cell proliferation (Klein et al., 2010). The importance of the miR15a/16-1 cluster in controlling cell proliferation is confirmed in another study employing a human megakaryocytic cell line, wherein transfection of miR15a/16-1 resulted in downregulation of cell cycle genes (Calin et al., 2008).

As discussed in section 1.2.1.2, experiments on these megakaryocytic cells also suggested a potential role for miR15a/16-1 in regulating Bcl-2 expression (Calin et al., 2008; Cimmino et al., 2005). However, this could not be validated in two other studies, including in CLL primary cells, where no correlation was observed between miR15a/16-1 and Bcl-2 expression levels (Fulci et al., 2007; Linsley et al., 2007). In the study by Klein *et al*, only modest effect on Bcl-2 expression was observed upon re-introduction of miR15a/16-1 in del(13q14) CLL cells (Klein et al., 2010). Finally, it is important to note that in many cases of del(13q14), the deletion encompasses other genes that surround the MDR, including known tumour suppressors such as the retinoblastoma (Rb) gene, and other putative tumour suppressors such as *DLEU7* and *RNASEH2B*. Although del(13q14) CLL as a group is associated with a better prognosis, larger deletions that extend beyond the MDR are linked to the development of more aggressive CLL in murine models (Lia et al., 2012). This correlated with comparatively poorer clinical outcomes in patients with a larger del(13q14) compared to those with a smaller del(13q14) (Ouillette et al., 2011; Parker et al., 2011).

17p deletion and TP53 mutation. The *TP53* gene is located within 17p13, and encodes for the transcription factor p53 which plays a crucial tumour suppressor role in regulating cell cycle arrest (see section 1.4.1) and apoptosis (see section 1.2.1.2) in response to DNA damage, thereby contributing to the maintenance of genome integrity

(Bieging et al., 2014). Like many other malignancies, the majority of *TP53* lesions in CLL are loss-of-function mutations or deletions, acquired by CLL cells as a means to promote survival and unperturbed proliferation. Del(17p) occurs in 8-10% of untreated CLL cases, but is enriched in patients relapsing from cytotoxic chemotherapy, affecting 40-50% of these individuals (Pospisilova et al., 2012). Over 80% of CLL patients with del(17p) have an inactivating mutation in their remaining *TP53* allele. On the other hand, a smaller proportion of patients (about 5% of an untreated CLL cohort) have monoallelic or biallelic *TP53* mutation in the absence of del(17p) (Malcikova et al., 2009). Many of these are missense mutations, with the majority occurring within exons 5-8 of the *TP53* gene, which encodes for the DNA binding domain of p53. These mutations may cause conformational change in p53 or disrupt its binding to DNA, thus hampering the transcriptional regulation of p53 target genes (Marinelli et al., 2013; Zenz et al., 2008; Zenz et al., 2010c). A minority of *TP53* missense mutations, in contrast, may have gain-of-function effects, possibly through the transactivation of other transcription factors such as NF-κB (Trbusek et al., 2011).

Patients with monoallelic *TP53* aberrations have poor prognosis, and display chemorefractoriness (Zenz et al., 2008). However, biallelic *TP53* inactivating lesions carry even poorer prognosis compared to del(17p) alone since the latter might possess some residual DDR activity whereas the former would not (Malcikova et al., 2009; Zenz et al., 2010a). The observation that >80% of del(17p) patients acquire concomitant *TP53* mutation could be explained by a selective effect, whereby biallelic *TP53* inactivated CLL cells with survival and proliferative advantage are selected in favour of those with monoallelic *TP53* loss (Malcikova et al., 2009).

11q deletion and ATM mutation. The *ATM* gene encodes for ataxia telangiectasia mutated (ATM) which is another important component of the DDR. ATM is a protein kinase that is activated in response to DSBs, and mediates repair of these breaks through homologous recombination. It also plays a role in cell cycle regulation and the induction of apoptosis through activating p53, which is downstream of ATM (Marechal and

Zou, 2013; Shiloh and Ziv, 2013). The ATM gene is located on chromosome 11q22-23, and similar to *TP53*, *ATM* may be disrupted through inactivating mutations or deletions. Unlike the *TP53* gene, however, the *ATM* gene spans more than 60 exons, and mutations within *ATM* are distributed throughout these exons, with no mutation hotspot (Stankovic and Skowronska, 2014). Previous work undertaken by our group provided demonstration that DDR is impaired in CLL cells with *ATM* mutation. This was demonstrated through reduced or absent phosphorylation of ATM and ATM downstream targets such as structural maintenance of chromosomes protein 1 (SMC1), nibrin (NBS1) and p53 upon exposure to ionising radiation (IR), which induces DSBs. In addition, the loss of ATM function was marked by a failure to induce apoptosis in response to DNA damaging agents (Austen et al., 2005).

CLL patients with the loss of one *ATM* allele through del(11q) may subsequently acquire an inactivating mutation in the remaining *ATM* allele. Indeed, 35-50% of del(11q) patients also harbour an *ATM* mutation (Austen et al., 2007; Skowronska et al., 2012). Whereas residual ATM activity is typically seen in individuals with del(11q) alone, complete functional inactivation of ATM occurs in those with biallelic loss. Complete inactivation of ATM is also observed in individuals with a dominant negative *ATM* mutation in the absence of del(11q), whereby the mutant ATM inhibits the activity of the functional ATM derived from the wild-type *ATM* allele (Austen et al., 2005). Consequently, patients with complete functional loss of ATM display particularly adverse prognosis (Austen et al., 2007). This was demonstrated within the UK CLL4 trial where patients were treated with chemotherapy-based regimens. Compared to patients with a sole del(17p) defect, those with del(11q) alone comparatively better progression-free survival (PFS) and OS, while those with del(11q) and an *ATM* mutation had inferior PFS and OS (Skowronska et al., 2012).

BIRC3 mutation. Deletions of 11q can be of variable sizes, and larger deletions may disrupt other genes within 11q including *BIRC3*. *BIRC3* is deleted in up to 80% of patients with del(11q), and BIRC3 deletion may co-occur with up to 40% of patients with an

ATM mutation (Rose-Zerilli et al., 2014). Functionally, *BIRC3* negatively regulates MAP3K14, an activator of NF-kB signalling. Thus, in CLL cases where *BIRC3* is mutated, NF-kB signalling is rendered constitutionally active. The clinical importance of this gene is corroborated by the inferior outcome demonstrated in CLL patients with a *BIRC3* mutation, where the adverse impact of *BIRC3* mutations on OS and TFS was found to be similar to that of *TP53* mutations (Rossi et al., 2012a; Rossi et al., 2013). In patients with del(11q) who possess both *ATM* or *BIRC3* mutations, however, *ATM* mutation but not *BIRC3* mutation confers additional adverse prognosis over and above that associated with monoallelic del(11q) (Rose-Zerilli et al., 2014).

SF3B1 mutation. The *SF3B1* gene encodes for core components of the spliceosome, a protein complex essential for removing introns from messenger RNA (mRNA) precursors in a process known as splicing. Mutations of the *SF3B1* gene occur in up to 15% of previously untreated CLL patients, and are associated with adverse prognosis (Rossi et al., 2013). Interestingly, *SF3B1* mutations frequently occur with del(11q) or *ATM* mutations, and that del(11q) patients carrying an *SF3B1* mutation have poorer outcomes compared to those with del(11q) alone (Jeromin et al., 2014; Wang et al., 2011). This suggests the possibility that *SF3B1* might act synergistically with *ATM*. Although ATM kinase activity remains normal in CLL patients with sole *SF3B1* mutation, transcriptional and apoptotic response to DNA damaging agents is impaired, implicating a potential role of *SF3B1* in DDR (Te Raa et al., 2015). More recently, a transcriptomic analysis comparing *SF3B1* wild-type and mutant CLL cells indicates that multiple pathways could be deregulated by *SF3B1* mutations, including DDR, telomere maintenance and Notch signalling (Wang et al., 2016).

NOTCH1 mutation. The *NOTCH1* gene encodes for a transmembrane receptor that mediates a signalling cascade leading to the transcriptional activation of genes essential for cell survival, apoptotic resistance and proliferation (Lobry et al., 2011). *NOTCH1* mutations, occurring in about 10% of CLL patients, lead to impaired degradation of the

receptor and constitutional activation of the Notch signalling pathway. Like *SF3B1* mutations, *NOTCH1* mutations confers adverse prognosis (Baliakas et al., 2015; Rossi et al., 2012b).

1.2.5. Spontaneous disease regression in CLL

In the above sections, the important enablers of CLL development and progression have been discussed. BCR signalling activity, microenvironmental interactions and genomic aberrations converge to drive CLL cell proliferation and apoptotic resistance, facilitated by a state of impaired tumour immunity. However, the nature of the BCR signalling activity, microenvironmental interactions and genomic aberrations is inevitably different in different individuals, as is the balance between CLL cell proliferation and cell death. Variation in these processes across patients underlies the enormous disease heterogeneity seen in CLL, and account for the patients' disparate clinical course, with some progressing rapidly and others much more slowly or not at all. Indeed, a multitude of prognostic biomarkers have been discovered to predict the likely clinical outcome of individual CLL patients (**Table 1.1**).

Of particular interest is a group of patients whose CLL decreases or disappears over time without treatment. Spontaneous tumour regression, manifested by a reduction or disappearance of the malignant clone without treatment, is an intriguing phenomenon. Although uncommon, spontaneous disease regression has been described in solid tumours such as neuroblastoma (Brodeur and Bagatell, 2014; Diede, 2014). Among haematological malignancies, spontaneous disease regression was reported in acute myeloid leukaemia (Daccache et al., 2007; Paul et al., 1994), chronic myeloid leukaemia (Musashi et al., 1997), myeloma and lymphoma (Kaufmann et al., 1995; Puig et al., 2009), as well as in CLL (Del Giudice et al., 2009; Herishanu et al., 2012; Nakhla et al., 2013; Thomas et al., 2002). In some cases, spontaneous tumour regression was linked to infections, blood transfusions or second malignancies that can be associated with a pro-inflammatory state (Paul et al., 1994; Schmidt et al., 1995). Alternatively, spontaneous regression has been variously attributed to

Table 1.1. Prognostic factors in chronic lymphocytic leukaemia.

Established prognostic factors	
Clinical stage	(Binet et al., 1981; Rai et al., 1975)
CD38	(Del Poeta et al., 2001; Hamblin et al., 2002; Ibrahim et al., 2001)
ZAP-70	(Crespo et al., 2003)
***IGHV* mutational status**	(Damle et al., 1999; Hamblin et al., 1999)
Cytogenetics (17p-, 11q-, 12+, 13q-)	(Dohner et al., 2000)
***TP53* mutations**	(Malcikova et al., 2009; Zenz et al., 2010a; Zenz et al., 2008)

Novel prognostic factors	
CD49d	(Bulian et al., 2014)
ROR1	(Cui et al., 2016)
Telomere length	(Damle et al., 2004; Rampazzo et al., 2012; Roos et al., 2008)
***IGHV* stereotypy**	(Baliakas et al., 2014)
Complex karyotype	(Herling et al., 2016; Thompson et al., 2015)
Putative driver mutations (e.g. *ATM*, *SF3B1, NOTCH1, BIRC3, NFKBIE*)	(Landau et al., 2015; Mansouri et al., 2015; Rossi et al., 2013; Skowronska et al., 2012; Stilgenbauer et al., 2014)
MRD negativity	Table 1.2 & Chapter 5

Established prognostic factors refer to those that are widely used in clinical practice, whereas novel prognostic factors are those that have been reported recently and not yet widely used in routine practice. MRD; minimal residual disease.

the spontaneous apoptosis of malignant cells and clonal evolution in a case of mantle cell lymphoma (Kaufmann et al., 1995), and neurotrophin deprivation, epigenetic changes, telomere shortening and cellular senescence in neuroblastoma (Brodeur and Bagatell, 2014).

In CLL, spontaneous disease regression is indicated by a sustained reduction or resolution of lymphocytosis, adenopathy, cytopenias and disease-related symptoms, in the absence of treatment or other plausible clinical explanations (Del Giudice et al., 2009; Thomas et al., 2002). Spontaneous disease regression is estimated to occur in 1-2% of CLL patients. A single case of spontaneous CLL regression resulting in absent minimal residual disease has been reported (Herishanu et al., 2012). However, in the majority of cases residual CLL cells remain detectable in the peripheral blood by flow cytometry despite clinical disease remission (Del Giudice et al., 2009; Nakhla et al., 2013; Thomas et al., 2002). There are few studies in the literature on CLL spontaneous regression. They comprise entirely of single case reports or small case series, with limited laboratory correlates. To date, there are two published series containing more than five cases.

The first series is a collection of 10 cases from a UK group (Thomas et al., 2002). In these patients, spontaneous CLL regression occurred over a course of two to 20 years, with the highest lymphocyte count ranging from 5.7 x 10^9/L to 124 x 10^9/L, falling to 1.2 x 10^9/L to 27 x 10^9/L at the time of study. This was accompanied by a reduction or disappearance of adenopathy without treatment. Interesting, two of the patients had trisomy 12 on cytogenetic analysis. However, no other biological studies were carried out.

The second series consists of 9 cases from an Italian group (Del Giudice et al., 2009). In these patients, spontaneous regression occurred over a median of 9 years (range 3-24 years), with a reduction of lymphocytosis to below 4 x 10^9/L and resolution of adenopathy. No evident clinical conditions, autoimmune disease, drug intake or viral infections were able to account for the disease regression. In all 9 cases, CD38 and ZAP-70 expression were negative. In addition, of the 7 cases where *IGHV* sequencing was

performed, all were *IGHV* mutated, with the use of *IGVH3* genes in 6 of 7 cases. Furthermore, a microarray analysis was carried out on the residual CLL population, comparing 4 of these individuals against 12 others with stable or progressive disease. A diverse range of genes were found to be differentially expressed among the spontaneous regressors in comparison with non-regressing CLL patients, including those involved in signal transduction, RNA metabolism, transcriptional regulation, lipid metabolism, apoptosis and cell cycle regulation. No clear mechanism of spontaneous regression was found, although a number of potential contributors, such as BCR signalling and immune control, were suggested.

In summary, with the exception of the two individuals with trisomy 12 from the UK series, all other previously reported individuals with spontaneous CLL regression had good risk biological features. However, few published studies on CLL spontaneous regression are available, reflecting the rarity of this event. Within the few published studies, biological characterisation has been limited in scope, and the mechanism of spontaneous regression remains elusive.

1.3. Current therapeutic approaches in CLL

1.3.1. Chemotherapy-based treatment approaches

1.3.1.1. Chemotherapy-based treatments in CLL (Figure 1.6)

Therapeutic options for CLL have historically been rather limited. Alkylating agents such as chlorambucil was the primary agent used for CLL in the 1970s and 1980s. While substantial cytoreduction and symptomatic relief was afforded by chlorambucil, complete remissions were uncommon. The purine analogue fludarabine was introduced in the 1990s, and its use, either alone or in combination with cyclophosphamide, led to higher remission rates (Catovsky et al., 2007; Rai et al., 2000).

The addition of monoclonal antibodies (mAb) to chemotherapy represents the first major therapeutic advance in CLL. The monoclonal antibody rituximab targets CD20, which is expressed on CLL cells at low levels. Upon binding to CD20, rituximab mediates cell death by direct signalling through CD20, or by activating complement and other immune cells (Weiner, 2010). In the multicentre phase III randomised study of the German CLL group CLL8 trial comparing fludarabine and cyclophosphamide (FC) versus fludarabine, cyclophosphamide and rituximab (FCR) where 817 patients were randomly assigned to either groups, FCR demonstrated superiority compared to FC (Hallek et al., 2010). Cytogenetic subgroup analyses in the study showed that the addition of rituximab resulted in better outcomes in del(11q) but not del(17p) CLL. Moreover, extended follow-up revealed long-term treatment-free remission among a proportion of M-CLL patients following FCR (Thompson et al., 2016). Currently, chemoimmunotherapy remains a standard CLL treatment in the frontline setting.

Figure 1.6

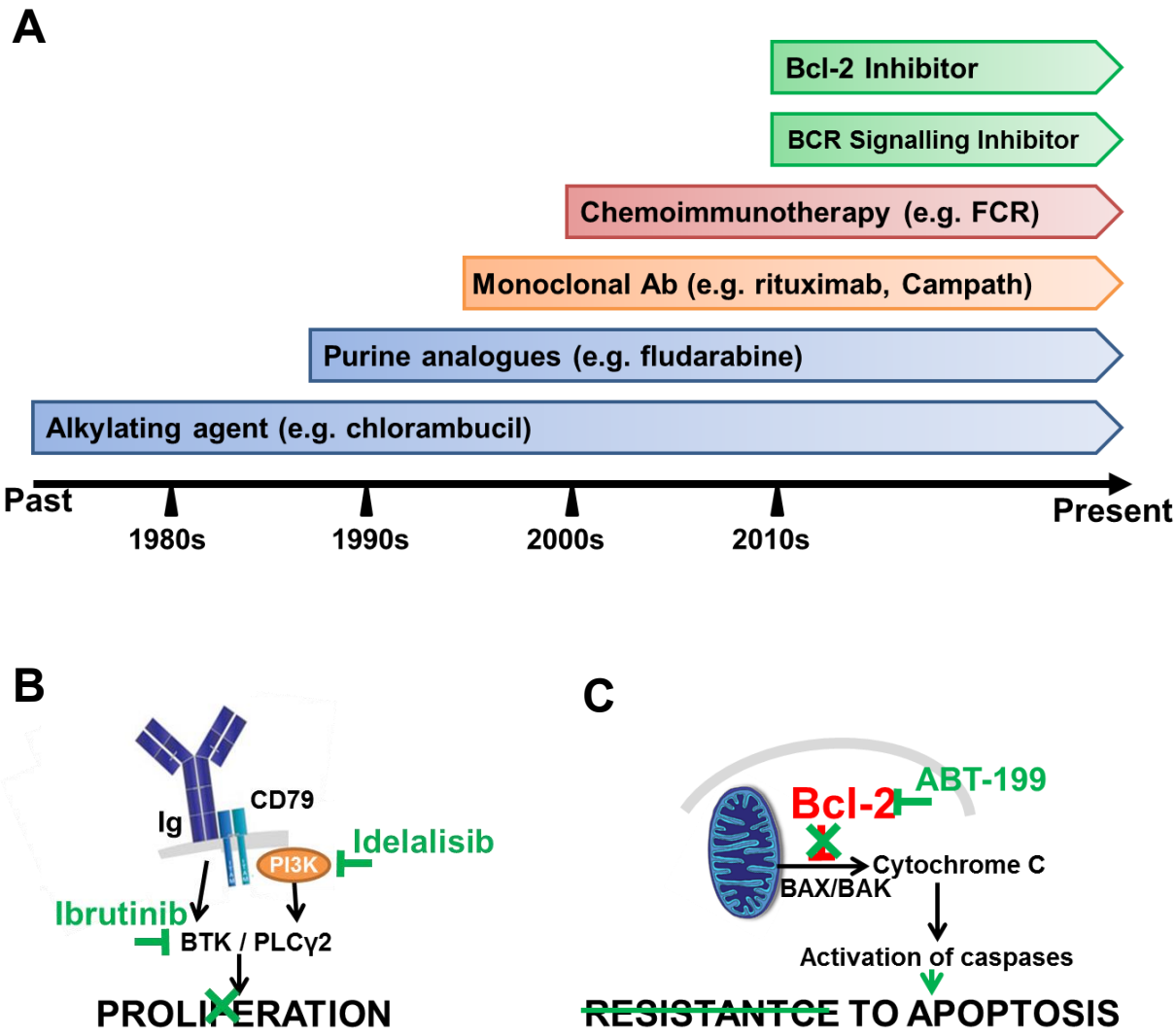

Current treatment approaches in CLL. (A) Timeline summarising the major historical advances in CLL treatment. (B) Mechanism of action of the BCR signalling inhibitors ibrutinib and idelalisib. (C) Mechanism of action of the Bcl-2 inhibitor venetoclax (ABT-199). Ab. Antibody; Ig, immunoglobulin.

1.3.1.2. Limitations of chemotherapy-based CLL treatments

Despite the effectiveness of chemoimmunotherapy in a substantial proportion of CLL patients, major problems exist. These relate to toxicity, long-term effects and chemoresistance. The myelosuppressive effects of FCR are well described, and are not always well-tolerated, especially in older or frailer individuals (Hallek et al., 2010). In addition, secondary malignancies such as myelodysplastic syndrome and acute myeloid leukaemia may subsequently arise from previous treatment with chemoimmunotherapy (Tam et al., 2008).

Clonal evolution is an important mechanism driving disease progression in cancer, and may be spontaneous, accelerated by treatment or treatment-induced (Davies et al., 2017). The idea of therapy-driven clonal expansion was supported by the observation, in paired pre-treatment and post-treatment samples, that the allelic fraction of subclonal driver mutations may increase over time during the course of treatment, eventually becoming clonal. Of note, not all treated cases result in clonal evolution, with some patients maintaining clonal equilibrium. However, clonal evolution predicts for shorter PFS and TFS (Landau et al., 2013). In patients receiving chemotherapy-based treatments, chemoresistance and disease relapse coincides with an expansion of *TP53* mutant subclones. Moreover, the presence of detectable *TP53* mutations at the time of FCR treatment, even within a small fraction of CLL cells, confers adverse treatment outcome (Landau et al., 2015; Rossi et al., 2014). While FCR-based treatments do not appear to specifically select for *ATM* mutations or deletions, del(11q) as well as del(17p) are frequent in relapsed cases, possibly reflecting their underlying genomic instability through the loss of DDR function (Tam et al., 2014).

1.3.2. Chemotherapy-free treatment approaches

1.3.2.1. Chemotherapy-free treatments in CLL (Figure 1.6)

The problems with chemotherapy with respect to toxicity and chemoresistance have propelled the development of novel chemotherapy-free CLL treatments. The clinical discovery and translation of small molecule inhibitors targeting BCR signalling and Bcl-2 represent the second major therapeutic advance in CLL.

Ibrutinib and acalabrutinib are inhibitors of BTK. Idelalisib, on the other hand, inhibits the p110δ isoform of PI3K, one of the two PI3K isoforms utilised by B cells. Clinical trials have confirmed the efficacy of ibrutinib in relapsed/refractory CLL. Consistent with its p53-independent mechanism of action, administration of ibrutinib in heavily pre-treated del(17p) CLL patients yielded comparable response rates to those with no detectable del(17p) (Byrd et al., 2013). Moreover, the PFS outcome with ibrutinib was superior to that of the CD20 mAb ofatumamab, as well as to historical PFS data on the CD52 mAb alemtuzumab, the latter of which has hitherto been the standard treatment for del(17p) CLL (Burger et al., 2014; Byrd et al., 2014; Pettitt et al., 2012). Likewise, acalabrutinib and idelalisib have respectively shown efficacy in relapsed/refractory CLL (Byrd et al., 2016).

Venetoclax is a selective inhibitor of Bcl-2. In patients with relapsed/refractory CLL, venetoclax treatment produced an overall response rate of 79%, and a complete response (CR) rate of 20%. Consistent with its p53-independent activity, response rates did not differ substantially between patients with del(17p) and those without (Roberts et al., 2016).

1.3.2.2. Limitations of current chemotherapy-free CLL treatments

Despite the excitement surrounding these novel small molecule inhibitors, and their remarkable efficacy in poor-risk CLL compared to existing therapies, these agents are not

without their limitations. Firstly, while myelosuppression is less common in patients treated with BCR signalling inhibitors and Bcl-2 inhibitors, each of these inhibitors has its own unique toxicity profile that may make them unsuitable for certain patients. For instance, ibrutinib may be associated with cardiovascular toxicity and a bleeding risk in some individuals. Idelalisib, on the other hand, may cause colitis, pneumonitis and hepatotoxicity (Lampson et al., 2016). Indeed, several clinical trials of idelalisib have recently been terminated because of drug-related adverse events. Secondly, these treatments are not curative. In particular, BCR signalling inhibitors do not produce deep remissions, and CRs are uncommon (Byrd et al., 2013; Byrd et al., 2016). As a result, patients are generally on long term treatment with these drugs, with associated cost and patient compliance implications. Finally, therapeutic resistance to these inhibitors is an important and growing concern.

Notwithstanding the high ibrutinib response rates in del(17p) patients, patients on ibrutinib harbouring del(17p) or del(11q) in their CLL clone have inferior PFS compared to individuals without these cytogenetic aberrations. Indeed, a 3-year follow-up study of patients on ibrutinib treatment shows that only 48% of del(17p) patients and 74% of del(11q) patients remained in remission at 30 months, compared to 87% of those without del(17p) or del(11q) (Byrd et al., 2015). Most patients relapse from ibrutinib with a *BTK* or *PLCγ2* mutation, while others undergo clonal evolution and acquire other genomic aberrations. In addition, a small group of patients experience transformation to RS while on ibrutinib. The majority of these patients were found to carry del(17p), del(11q) and/or a complex karyotype (Burger et al., 2016; Maddocks et al., 2015; Woyach et al., 2014a). In addition, complex karyotype predicted for an increased risk of clinical progression while on venetoclax (Anderson et al., 2017).

These observations may reflect a heightened level of genomic instability within the CLL cells from relapsing patients, as a result of DDR impairment from a loss of functional p53 or ATM. This could be exacerbated by the use of BCR signalling inhibitors. Indeed, it

has recently been shown that BCR signalling inhibitors, particularly PI3K inhibitors such as idelalisib, increase genomic instability in B lymphocytes by upregulating their expression of AID. This consequently results in increased SHM and chromosomal translocation frequency, both within the *IGH* gene locus, and in other parts of the genome that could be due to off-target effects of AID (Compagno et al., 2017). Patients relapsing from BCR signalling inhibitors have limited salvage options and poor clinical outcome, with a median survival of 3.1 months following discontinuation of ibrutinib as reported recently (Jain et al., 2015). For all the above reasons, additional CLL treatment strategies and therapeutic combinations are still needed.

1.4. The ATR pathway as a novel therapeutic target

1.4.1. The DNA damage response

The DDR is an essential cellular mechanism for the maintenance of genome integrity. This is accomplished through a network of intricately connected pathways, resulting in a dichotomous outcome: either repair and resolution of the incipient DNA lesion, or apoptotic cell death, depending on the nature and severity of the afflicting lesion.

ATM and ataxia telangiectasia and Rad3 related (ATR) are the two master regulators of DDR. ATM and ATR respond to different types of DNA lesions. ATM is a member of the phosphoinositide 3-kinase related kinase (PIKK) family of proteins. ATM responds primarily to DNA DSBs that can arise from physiological processes such as meiotic recombination and V(D)J recombination, or from exogenous genotoxic agents such as IR. The ATM signalling pathway (**Figure 1.7**) is initiated by docking of the MRE11-RAD50-NBS1 (MRN) complex to the DSB which stabilises DSB ends. ATM is then recruited to the MRN complex. At the MRN complex, ATM autophosphorylates, leading to its conversion from an inactive dimer form to active monomers. Activated ATM in turn phosphorylates a large number of substrates. Among these is the histone H2AX, yielding γH2AX. The phosphorylated histone γH2AX provides a platform for the recruitment and activation of downstream molecules. These include BRCA1 and 53BP1. They commit cells to homologous recombination repair (HRR) and non-homologous end joining (NHEJ) respectively, which are the two main pathways for DSB repair (Awasthi et al., 2016; Cremona and Behrens, 2014).

Cell cycle regulation is also an important ATM function. The cell cycle is divided into four sequential phases: G1, S, G2 and M. During the S phase DNA synthesis occurs, and within the M phase cells undergo mitosis. These two phases are separated by gap phases

Figure 1.7

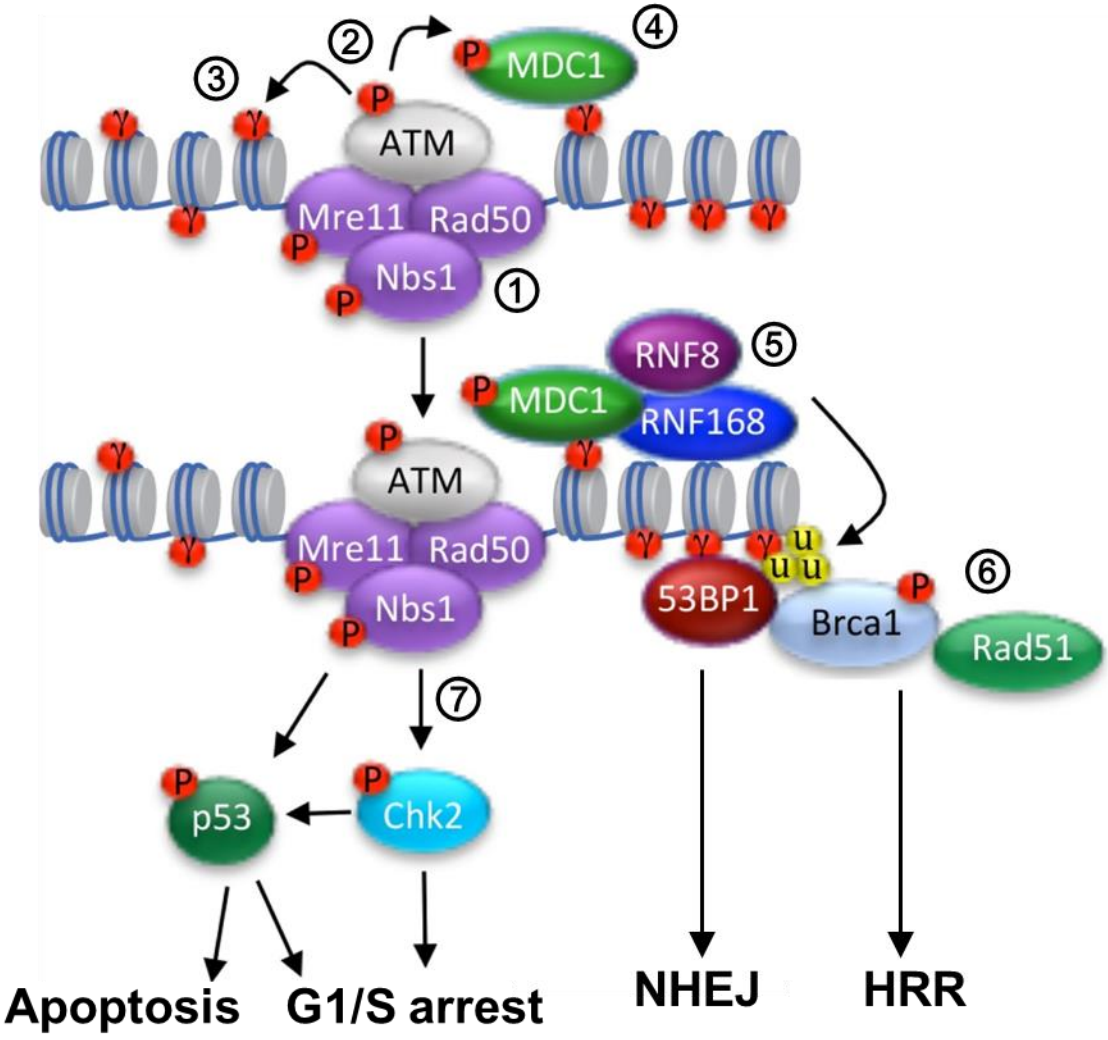

The ATM signalling pathway. (1) The MRE11-RAD50-NBS1 (MRN) complex is recruited to the site of the DSB which stabilises DSB ends. (2) ATM is recruited to the MRN complex and is activated by autophosphorylation and dimerisation. (3) ATM phosphorylates the histones H2AX to form γH2AX. (4) MDC1 binds to γH2AX. (5) MDC1 recruits the ubiquitin ligases RNF8 and RNF168, which ubiquitylates γH2AX and promotes the recruitment of 53BP1 and BRCA1. (6) BRCA1 mediates homologous recombination repair (HRR) whereas 53BP1 mediates non-homologous end joining (NHEJ). (7) ATM also mediates G1/S cell cycle arrest and apoptosis by activating Chk2 and p53. Reproduced with modifications from Anacker & Moody (2017). Modulation of the DNA damage response during the life cycle of human papillomaviruses. Virus Res. *231*, 41-49.

(G1 and G2), which allow additional time for cell growth and to ensure conditions are suitable for commencing DNA replication or mitosis. There are two major checkpoints that control cell cycle progression: the G1/S checkpoint that regulates cell cycle entry and the initiation of DNA replication, and the G2/M checkpoint that regulates entry into mitosis.

ATM controls principally the G1/S checkpoint through its downstream effector Chk2 and the transcription factor p53. Firstly, ATM upregulates and activates p53. The latter is achieved by directly phosphorylating p53 and by promoting the proteasomal degradation of mouse double minute 2 homologue (MDM2), a negative regulator of p53. Active p53 induces the expression of p21, which suppresses the activity of the cyclin dependent kinase Cdk2 required for entry into S phase, leading to G1/S cell cycle arrest. Secondly, ATM phosphorylates and activates Chk2. In turn, Chk2 activates p53 and inhibits the phosphatase Cdc25A essential for Cdk2 activation. This results in G1/S cell cycle arrest. Hence, ATM induces G1/S arrest through both p53 dependent and independent mechanisms, allowing time for DNA repair (Abraham, 2001). However, in cells with irreparable DNA damage, ATM signalling promotes their apoptosis through its activation of p53 (section 1.2.1.2).

ATR is also a PIKK. However, in contrast to ATM, ATR has wide-ranging roles in the regulation of DNA replication and response to single-stranded DNA (ssDNA) perturbations during this process (Cimprich and Cortez, 2008). In addition, similar to ATM and p53, ATR also plays an important role in cell cycle regulation. The following sections will describe the functions of ATR and the ATR signalling pathway, and illustrate how targeting this pathway could potentially be useful in treating cancers including CLL, particularly in those with *TP53* or *ATM* defects.

1.4.2. Functional roles of ATR and the ATR signalling cascades

1.4.2.1. Regulation of DNA replication initiation

DNA replication (**Figure 1.8A**) begins with the unwinding of the DNA double helix. This process is mediated by DNA helicase, which separates the two DNA strands as it moves along the DNA double helix. The position at which the DNA double helix first opens up is known as the replication origin. Opening up of the DNA double helix exposes the two parental DNA strands, which act as templates for the synthesis of two daughter strands. Synthesis of the two daughter strands is catalysed by DNA polymerase, which recognises each nucleotide on the two parental strands, and pairs it with a complementary nucleotide to form the daughter strands. DNA strands can only be synthesised in one direction, from 5' to 3'. Therefore, while one of the daughter strands (5' to 3') can be synthesised continuously in the forward direction, the other daughter strand (3' to 5') has to be synthesised in the reverse direction to the overall direction of DNA synthesis. The 3' to 5' daughter strand is synthesised as short DNA fragments called Okazaki fragments that are then joined together. The localised region of DNA synthesis is called the replication fork, which moves along the parental DNA double helix, and in doing so elongating the two daughter strands. This movement is known as replication fork progression. From the replication origin, two replication forks are formed, progressing in the opposite direction from each other. Therefore, daughter strands are elongated in both directions from the replication origin (Frouin et al., 2003).

In human cells, replication origins can arise simultaneously at multiple sites throughout the genome. Multiple replication origins, about 14 on average, are replicated together in clusters called replication factories. An important function of ATR is its ability to protect replication forks by acting as a negative regulator of replication origin initiation. This limits the activation of new replication factories, thereby directing replication towards already active factories (Chen et al., 2015; Ge and Blow, 2010). Such negative regulation of

Figure 1.8

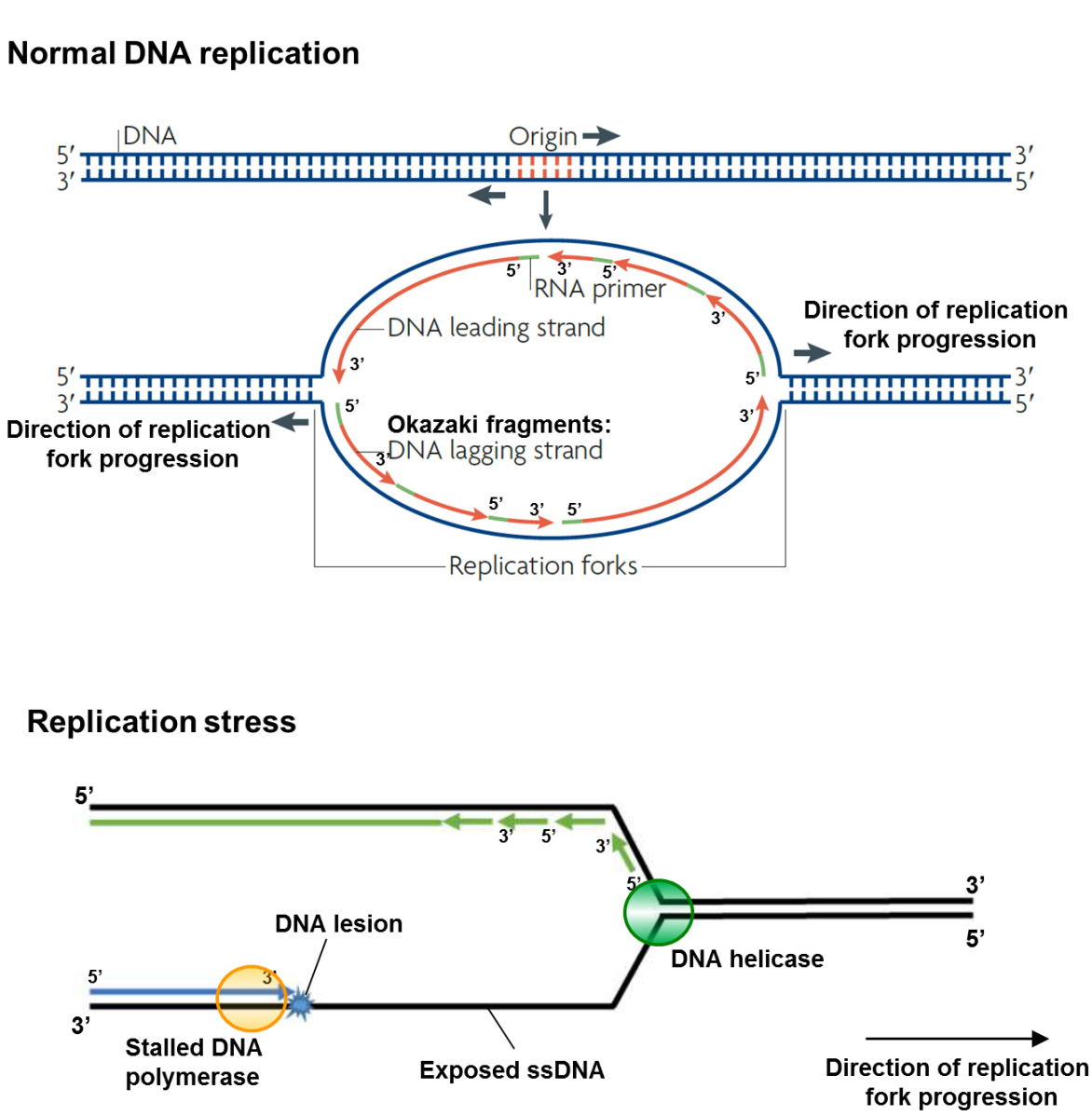

Normal and aberrant DNA replication. (A) Replication is initiated at replication origins and involves the opening of the DNA double helix (by DNA helicase) and the synthesis of daughter strands (by DNA polymerase). The leading strand is synthesised continuously in the forward direction, whereas the lagging strand is synthesised as Okazaki fragments that are joined together. From the replication origin, two replication forks are formed, travelling in the opposite direction from each other. **(B)** Replication stress occurs when replication fork progression is disrupted, e.g. due to a DNA lesion. Continued unwinding of the DNA double helix by DNA helicase, despite stalled DNA polymerase, leads to exposed ssDNA that is prone to breakage. Reproduced with modifications from Mechali (2010). Eukaryotic DNA replication origins: many choices for appropriate answers. Nat Rev Mol Cell Biol. *11*, 728-738, and from Gao *et al* (2017). Mechanisms of Post-Replication DNA Repair. Genes. *8*, 64.

replication initiation is important in preventing the depletion of cellular pools of nucleotides and replication proteins, which would otherwise result in replication fork breakage and genomic instability.

1.4.2.2. Maintenance of replication fork stability

During DNA replication, replication fork progression can slow or stall due to replication obstacles such as DNA damage. This may lead to continued unwinding of the DNA double helix despite stalled DNA polymerase. Consequently, long stretches of ssDNA within replication forks are exposed. Exposed ssDNA are prone to damage, resulting in replication fork breakage (**Figure 1.8B**). The ATR pathway functions to prevent this by protecting exposed ssDNA and repairing the replication obstacle that leads to the slowing or stalling of replication fork progression. Exposed ssDNA is rapidly coated with replication protein A (RPA), which stabilises the replication fork and protects ssDNA from deleterious degradation by cellular endonucleases (Marechal and Zou, 2015).

The ATR signalling cascade (**Figure 1.9A**) is initiated by the independent recruitment of two complexes to RPA coated ssDNA. The first of these is a heterodimer composed of ATR and the ATR-interacting protein (ATRIP). The second is the RAD9-RAD1-HUS1 (9-1-1) complex. At the exposed ssDNA, the ATR-ATRIP complex binds to RPA, and engages with the 9-1-1 complex. Further recruitment of topoisomerase 2-binding protein 1 (TOPBP1) or Ewing's tumor-associated antigen 1 (ETAA1) activates ATR by stimulating ATR kinase activity (Bass et al., 2016; Cotta-Ramusino et al., 2011; Haahr et al., 2016). Functionally active ATR in turn phosphorylates the downstream effector molecule Chk1, and other proteins including Werner syndrome ATP-dependent helicase (WRN), Bloom syndrome protein (BLM) and SMARCAL1 (Awasthi et al., 2016).

Through these proteins, ATR promotes replication fork stability and mediates replication restart in the event of fork stalling. This is achieved through fork reversal whereby

Figure 1.9

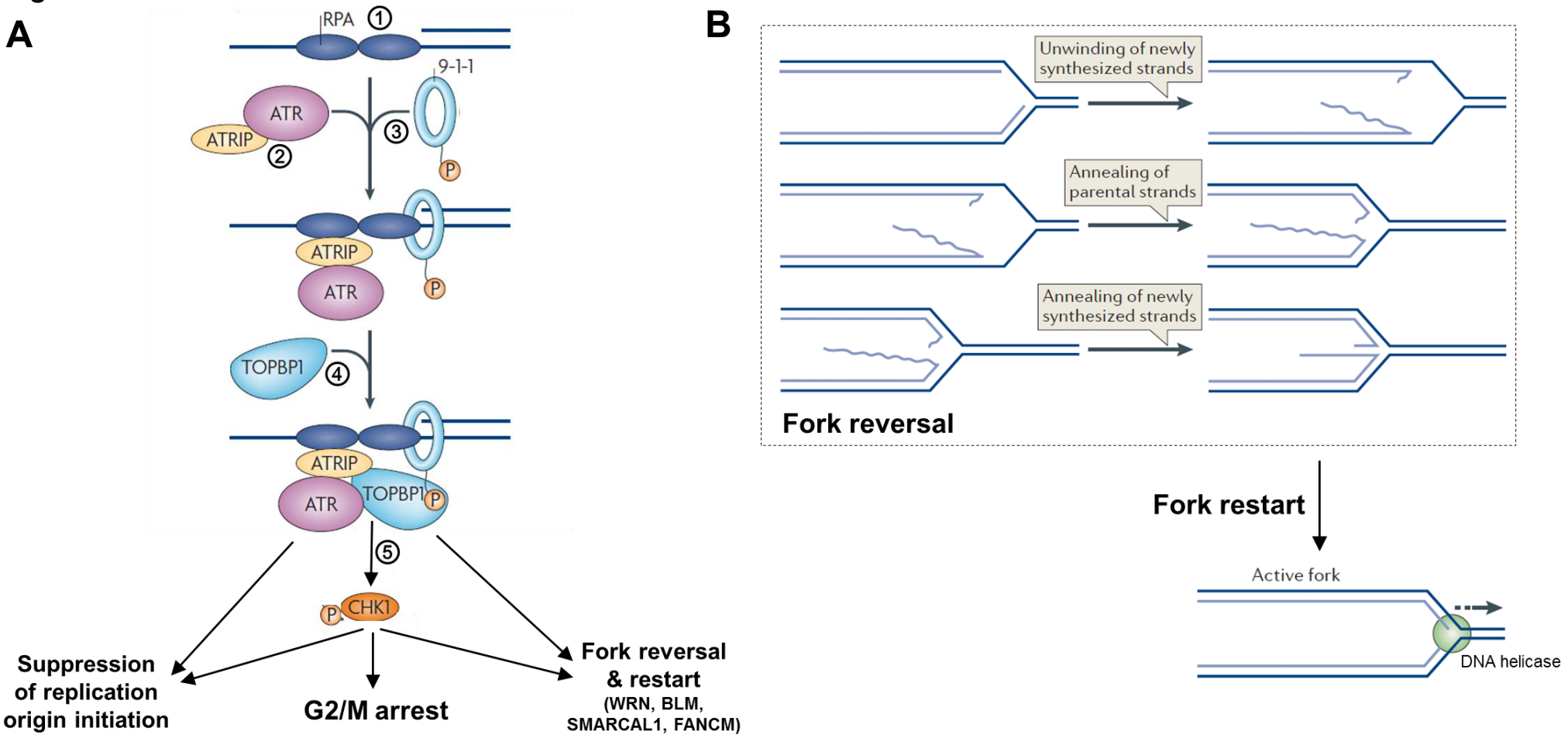

The ATR signalling pathway. **(A)** (1) Exposed ssDNA at the site of replication fork stalling is coated with RPA to stabilise the replication fork. (2) ATR/ATRIP binds RPA and (3) engages with the 9-1-1 complex. (4) ATR is activated by the recruitment of TOPBP1 or ETAA1 (not shown). (5) ATR phosphorylates Chk1, and ATR/Chk1 engages in the tripartite actions of suppression of replication origin initiation, G2/M cell cycle arrest, and fork reversal and restart. **(B)** Fork reversal involves unwinding of newly synthesised strands, and the sequential annealing of parental and daughter strands. Fork reversal is followed by fork restart. Reproduced with modifications from Cimprich & Cortez (2008). ATR: an essential regulator of genome integrity. Nat Rev Mol Cell Biol. *9*, 616-627, and from Neelsen & Lopes (2015). Replication fork reversal in eukaryotes: from dead end to dynamic response. Nat Rev Mol Cell Biol. *16*, 207-220.

stalled forks reverse their course, and through fork remodelling (Neelsen and Lopes, 2015). Helicases such as WRN and BLM, and translocases such as SMARCAL1 and the Fanconi anaemia complementation group M protein (FANCM) are thought to play a major role in this process (Berti and Vindigni, 2016). Fork reversal, remodelling and restart together ensure completion of DNA replication and prevent fork breakage (**Figure 1.9B**).

Proteins downstream of ATR also serve additional functions in facilitating fork repair, through suppression of new replication origin firing (BLM and FANCM), and protection of replication forks from breakage or degradation (WRN) (Berti and Vindigni, 2016). Furthermore, Chk1 diffuses throughout the nucleus to suppress new replication origin initiation (Petermann et al., 2010). Thus, the regulatory activities of ATR signalling are amplified and propagated globally throughout the cell nucleus in the event of replication fork stalling. This is crucial in curtailing further replication fork stalls, thereby conserving the supply of RPA for those replication forks that are already stalled and to ensure that an excess supply of RPA is maintained (Fragkos et al., 2015).

1.4.2.3. Regulation of cell cycle progression

Similar to ATM, ATR also participates in the regulation of cell cycle progression. However, in contrast to ATM which controls primarily the G1/S checkpoint, ATR controls principally the G2/M checkpoint through the activity of Chk1. Mechanistically, this involves inhibiting the phosphatase Cdc25C to prevent it from binding to Cdk1. Cdc25C removes inhibitory phosphorylation from Cdk1 that is a prerequisite for mitotic entry. In the presence of stalled replication forks, abolition of Cdk1 activity through Chk1-mediated phosphorylation of Cdc25C prevents premature entry of replicatively perturbed cells into mitosis, until replication stalling is rectified and genomic duplication is complete (Peng et al., 1997; Sorensen et al., 2003).

1.4.3. ATR as a cancer therapeutic target

1.4.3.1. Replication stress and DNA damage as consequences of ATR inhibition

When replication fork progression is disrupted, slowing or stalling of replication forks ensues. This results in replication stress, defined as a state of cellular stress which arises due to the presence of stalled replication forks and unreplicated DNA (Zeman and Cimprich, 2014). Replication stress may arise, for instance, from unrepaired DNA damage, which obstructs replication fork progression. Such DNA damage may be generated spontaneously during DNA metabolism, or by environmental genotoxic agents (Ciccia and Elledge, 2010). The ATR signalling pathway ameliorates replication stress through its tripartite role in the regulation of DNA replication initiation, the maintenance of replication fork stability, and cell cycle regulation, as outlined above. Conversely, inhibition of the ATR pathway is a potent inducer of replication stress.

A consequence of ATR inhibition is the excessive replication origin initiation in an unscheduled and uncontrolled manner. This occurs independently of any additional sources of replication stress, either endogenous or exogenous. Indeed, studies have shown that the number of active replication forks in cancer cells is increased when ATR is inhibited, in the absence of DNA damaging agents or other sources of replication stress (Couch et al., 2013). Excessive and uncontrolled replication origin initiation as a result of ATR inhibition depletes the cellular pool of essential replication factors such as nucleotides and replication proteins. This leads to a decrease in the rate of replication fork elongation and stalling of replication forks (Petermann et al., 2010; Toledo et al., 2013). This is evidenced by experiments in cancer cells showing rapid reduction in inter-origin distance indicating increased replication origin initiation, accompanied by reduction in replication fork progression rate, upon inhibition of ATR (Couch et al., 2013). These observations are consistent with the induction of replication stress.

Excessive and uncontrolled initiation of replication origin initiation also generates excessive amounts of ssDNA. Exposed ssDNA is normally coated with RPA. However, when ATR is inhibited, the excess of ssDNA exhausts the nuclear pool of RPA. Unprotected ssDNA is susceptible to fork breakage, thereby precipitating DNA damage (Toledo et al., 2013). Furthermore, ATR inhibition prevents proper regulation of SMARCAL1, the deregulated activities of which promotes excessive replication fork regression and fork collapse, resulting in DNA damage (Couch et al., 2013). Together, these mechanisms underpin the DNA damage caused by ATR inhibition.

1.4.3.2. Replication stress as a therapeutic vulnerability in cancer cells

An elevated level of replication stress is a defining feature of malignant cells. Although the precise mechanism underlying this remains unclear, it has been hypothesised that the accelerated consumption of RPA resulting from unchecked tumour proliferation, could be a contributing factor (Toledo et al., 2013). Other potential mechanisms, such as the deregulation of replication initiation, have also been postulated (Hills and Diffley, 2014; Macheret and Halazonetis, 2015). Given the high constitutive levels of cellular replication stress inherent in many tumours, it follows that they are likely to be particularly sensitive to replication stress overload instigated by inhibition of ATR.

Until recently, it has been assumed that ATR is physiologically indispensable and not amenable to therapeutic targeting (Brown and Baltimore, 2003). Indeed, human ATR mutations are uncommon, even in cancer. Among the few cancer types where ATR mutations have been reported, the acquisition of these mutations has been associated with tumour progression and poor clinical outcome (Zighelboim et al., 2009). Moreover, abrogation of the ATR gene is embryonically lethal, while its deletion in adult mice results in rapid aging and stem cell loss (de Klein et al., 2000; Ruzankina et al., 2007). In patients with Seckel syndrome in whom ATR signalling is defective due to hypomorphic germline mutation

of both ATR alleles, growth retardation, dwarfism, microcephaly and mental impairment are typical manifestations (Murga et al., 2009; O'Driscoll et al., 2003).

Nonetheless, whereas complete or near-complete abolition of ATR activity likely results in toxicity to healthy tissues, partial suppression of ATR activity was shown to be tolerable in healthy cells but not in tumour cells. In a study by Schoppy and colleagues, reduction of ATR in mice to 10% of normal levels, by deleting one ATR allele and replacing the other one with a Seckel allele, resulted in minimal adverse effect on healthy haematopoietic and intestinal tissues. In contrast, suppression of ATR to this level was adequate to severely restrict the growth of fibrosarcomas driven by H-Ras and p53 loss, as well as acute myeloid leukaemia driven by N-Ras and the MLL-ENL translocation (Gilad et al., 2010). Such a reduction of ATR level likewise prevented the development of Myc driven lymphomas and pancreatic tumours featuring high levels of replication stress (Murga et al., 2011). Therefore, healthy and tumour cells may demonstrate differential sensitivity to ATR inhibition, making it a potential cancer therapeutic strategy.

1.4.3.3. ATR pathway addiction and the concept of synthetic lethality

The substantial functional redundancy within cellular DDR pathways is widely recognised, wherein more than one pathway is capable of performing the same role. Physiologically this provides protection against disruption of normal DDR mechanisms, particularly in cancer where DDR genes are mutated with high frequency. However, when one pathway is disrupted, cells become heavily reliant on collateral pathways. Thus, where two independent pathways regulate an essential DDR process, the absence of one pathway is compatible with cell survival, while the absence of both results in cell death. This gives rise to an emerging therapeutic concept known as synthetic lethality, in which collaborating pathways are abolished to induce cytotoxicity (McLornan et al., 2014; Shaheen et al., 2011).

From the studies highlighted above, it is apparent that tumours with heightened levels of replication stress, such as those driven by Myc or Ras, are exquisitely sensitive to ATR inhibition. Understanding other circumstances under which tumour cells become addicted to ATR is essential to identifying further predictive biomarkers of sensitivity to ATR inhibition. There is evidence that such an addiction to ATR may occur in tumours with *TP53* or *ATM* functional loss.

1.4.3.4. Synthetic lethality with TP53 functional loss

The loss of the G1/S cell cycle checkpoint due to *TP53* functional loss imposes upon tumour cells a dependence on the G2/M cell cycle checkpoint controlled primarily through ATR via its downstream kinase Chk1. Consequently, ATR inhibition may have synthetically lethal properties in *TP53* deficient tumours.

Nghiem and colleagues provided one of the earliest evidence demonstrating hypersensitivity of G1/S checkpoint deficient cells to ATR loss. In this study, investigators observed that the osteosarcoma cell line U2OS in the absence of ATR function displayed premature chromatin condensation, in response to hydroxyurea or ultraviolet radiation induced replication stress. Premature chromatin condensation is indicative of mitotic catastrophe, a form of cell death occurring during mitosis due to the accumulation of catastrophic levels of DNA damage (Castedo et al., 2004). Moreover, repression of p53 function by overexpression of MDM2, a negative regulator of p53, markedly potentiated the lethal effect of ATR inhibition in these cells (Nghiem et al., 2001). These findings were recapitulated in a later study showing that a p53 deficient colorectal cell line rendered ATR deficient by replacing both wild-type ATR alleles with Seckel alleles, exhibited marked sensitivity to hydroxyurea or cisplatin induced replication stress. However, restoration of p53 function reduced its sensitivity to these agents (Sangster-Guity et al., 2011).

These *in vitro* studies were complemented by *in vivo* experiments, in which *ATR* knockout murine models were generated from *TP53* knockout mice. Mice with concomitant loss of both ATR and p53 displayed markedly reduced survival compared to those harbouring isolated loss of ATR. In addition, animals carrying a combined loss of ATR and p53, but not those with loss of ATR or p53 alone, exhibited high levels of DNA damage (Ruzankina et al., 2009). In a further study using xenotransplantation models of both p53 wild-type and p53 mutant triple-negative breast cancer, Chk1 inhibition potentiated chemotherapy-induced apoptosis in p53 mutant xenografts but not in the p53 wild-type counterparts. Combining Chk1 inhibition with the topoisomerase inhibitor irinotecan resulted in suppression of tumour growth and prolongation of survival in p53 mutant but not wild-type xenografts (Ma et al., 2012).

1.4.3.5. Synthetic lethality with ATM functional loss

ATR inhibition results in the induction of replication stress and DNA damage. In the absence of ATR, stalled forks and DNA damage are dependent on ATM for repair. Furthermore, as discussed earlier, ATM also plays an important role in cell cycle regulation. Thus, ATR may also be synthetically lethal with ATM functional loss.

Consistent with this, Reaper and colleagues showed that ATR inhibition was invariably cytotoxic to ATM defective tumour cell lines. Moreover, ATR inhibition was more profoundly synergistic with replication stress inducing genotoxic agents such as cisplatin and carboplatin, in tumour cell lines with ATM defects compared to those without, and in cells subjected to pharmacological inhibition of ATM compared to cells without ATM inhibition (Reaper et al., 2011).

1.4.3.6. Small molecule inhibitors of ATR

As mentioned in section 1.4.1, ATR is a PIKK. As a result of the atypical nature of PIKKs relative to other more conventional kinases, the design and development of selective ATR kinase inhibitors has not been straightforward. Early inhibitors of ATR were not specific. However, more recently, two drug companies have manufactured potent and highly specific ATR inhibitors. They are respectively VE-821 and its analogue VX-970 manufactured by Vertex Pharmaceuticals, as well as AZ20 and AZD6738 developed by AstraZeneca (Charrier et al., 2011; Foote et al., 2013). They are all ATP-competitive ATR kinase inhibitors.

AZ20 is a sulfoximine morpholinopyrimidine with potent and selective activity against the ATR kinase. It was generated through an AstraZeneca lead compound discovery and optimisation programme, which involved screening a compound library with structural similarity to PI3K and PIKK inhibitors, and modification of the identified lead compound (Foote et al., 2013). AZD6738 is a newly synthesised analogue of AZ20, with improved pharmacodynamic and pharmacokinetic properties, and is suitable for oral administration (Foote et al., 2015).

Both AZD6738 and VX-970 have now entered phase I/II clinical testing. However, most of these studies have been initiated recently, and no results have yet been reported. As of March 2017, 11 clinical trials on ATR inhibitors are ongoing for a range of malignancies. These studies examine the use of the ATR inhibitor either alone or in combination with a range of conventional and novel therapeutic agents, including cisplatin, carboplatin, gemcitabine, etoposide, irinotecan, the poly (ADP-ribose) polymerase (PARP) inhibitors olaparib and veliparib, and the programmed death-ligand 1 (PD-L1) immune checkpoint inhibitor durvalumab.

1.5. Minimal residual disease in CLL

1.5.1. The concept of post-treatment minimal residual disease

Post-treatment response assessment in CLL is made in accordance with the IWCLL 2008 response criteria, in which a CR, which denotes the complete normalisation of blood counts and the complete disappearance of symptoms and signs associated with the disease (Hallek et al., 2008), is recognised as the therapeutic end-point. However, residual CLL cells may still be present after treatment even though no clinically detectable disease remains. The residual CLL population remaining after treatment is known as minimal residual disease (MRD). The expansion of residual CLL cells may lead to eventual disease relapse with the duration of remission dependent on the depth of remission (i.e. the amount of residual CLL cells) and the rate of CLL repopulation (i.e. the CLL doubling time).

In some haematological malignancies, such as CML and acute lymphoblastic leukaemia (ALL), periodic monitoring of MRD has become a routine clinical practice. In these malignancies, as well as in others where MRD assays are available, the absence of detectable MRD is almost always associated with improved clinical outcome. MRD can therefore be used as a prognostic biomarker to predict the likelihood of disease relapse following treatment. MRD measurements are also increasingly being used to guide treatment. For instance, MRD levels at the end of induction therapy for ALL or AML may dictate the choice of the subsequent consolidation therapy (Ivey et al., 2016; Vora et al., 2014; Vora et al., 2013). On the other hand, patients with CML on tyrosine kinase inhibitors who no longer have molecularly detectable disease could potentially cease treatment (Mahon et al., 2016; Melo and Ross, 2011).

In CLL, MRD can now be detected, in the bone marrow or peripheral blood, to a sensitivity of one CLL cell in 10,000 leukocytes (10^{-4}) using multiparameter flow cytometry or

polymerase-chain reaction (PCR) based molecular methods. In addition, treatments are now available that can deplete CLL cells to a level below detection by these sensitive methods in some patients. However, MRD assays are not in routine clinical use in CLL, and have not thus far been used to guide management of CLL patients. The following sections will describe methodologies for detecting CLL MRD, as well as the current literature on the clinical value of MRD assessment in CLL.

1.5.2. Approaches for measuring MRD

1.5.2.1. Multiparameter flow cytometry

As discussed in section 1.1.2, flow cytometry enables a diagnosis of CLL to be made based on the unique phenotypic features that distinguish CLL cells from other blood cells, including healthy B lymphocytes. On the same basis, MRD can be measured by flow cytometric quantification of the cellular population with a CLL phenotype at the end of treatment. This is the most widely used approach for MRD analysis.

The earliest attempt to quantify MRD utilises traditional CLL phenotypic markers: CD19 and CD5, together with either κ or λ, depending on the light chain restriction of the CLL clone. However, the sensitivity of this method in distinguishing CLL cells from healthy B cells was low. In particular, while the proportion of healthy B cells expressing CD5 is generally <30%, CD5 expression may be present in up to 90% of healthy B cells in the regenerating blood after chemotherapy-containing treatments (Cabezudo et al., 1997). Moreover, a proportion of CLL cases may have an atypical phenotype with weak expression of CD5 (Romano et al., 2015). In an attempt to design a more sensitive flow cytometry based MRD assay, Rawstron and colleagues compared the sensitivity of different phenotypic markers in differentiating healthy and neoplastic B cells in patients with CLL (Rawstron et al., 2001). Within the peripheral blood, the marker that produces the greatest

degree of separation between healthy B cells and CLL cells was CD20, followed by CD79a/b and CD5. Compared to healthy B cells, CLL cells typically express low levels of CD20 and CD79a/b, and high levels of CD5. A four colour MRD flow cytometry assay was developed using the CD19/CD5/CD20/CD79b combination, which is capable of detecting CLL cells in the peripheral blood to a sensitivity of one CLL cell in 10,000 leukocytes.

Subsequent attempts have been made by the European Research Initiative in CLL to standardise a MRD flow cytometry panel for use across patients receiving different treatments, and to harmonise its use across different centres internationally (Rawstron et al., 2007). This is particularly important for patients who received treatments that incorporate rituximab, because CD20 could be downmodulated on CLL as well as healthy B cells by rituximab (Jilani et al., 2003). Together with the fact that an atypical CLL phenotype might include low CD5 and/or high CD79b expression, and that progenitor B cells do not express CD20 and CD79b, the CD19/CD5/CD20/CD79b combination alone might not be sufficient to sensitively detect MRD in all CLL patients.

Therefore, a large number of four-colour combinations of phenotypic markers were tested, and three of these showed the lowest inter-laboratory variability and false positive rate. These were combinations of CD19/CD5 with CD20/CD38, CD81/CD22 and CD43/CD79b respectively. These three 4-colour combinations formed the basis of the harmonised MRD panel (Rawstron et al., 2007). Further improvements include efforts to consolidate the three 4-colour tubes into two 6-colour tubes, and more recently, by eliminating redundant markers to further simplify the assay into a single-tube panel consisting of six markers (Rawstron et al., 2013; Rawstron et al., 2016). These six core markers are CD19, CD20, CD5, CD43, CD79b and CD81. The use of these 6 markers alone could readily differentiate CLL cells from healthy B cells in the majority of CLL patients treated with a range of different therapies. The inclusion of CD43 (high in CLL vs healthy B cells) could help differentiate CLL cells from healthy B cells in atypical CLL cases with low CD5 and/or high CD79b. In addition, the expression of CD5 and CD81 could together

distinguish CLL cells from progenitor B cells, because CD5 expression is low and CD81 expression is high in B cell progenitors, and vice versa in CLL cells. Analysis of the sensitivity of this single-tube 6-colour assay shows that a limit of detection of 1 CLL cell in 100,000 (10^{-5}) leukocytes could be reliably achieved with an acquisition of 2,000,000 events, and a limit of detection of 1 CLL cell in 10,000 leukocytes (10^{-4}) could be achieved with 200,000 events.

1.5.2.2. Quantitative PCR and high-throughout sequencing

MRD quantitation by multiparameter flow cytometry is relatively inexpensive and rapid. However, its sensitivity is currently limited to 10^{-4} to 10^{-5} CLL cells. On the other hand, PCR-based molecular methods could be more expensive and time-consuming, but they enable higher sensitivity of MRD detection to be achieved. Moreover, DNA samples could be stored and analysed retrospectively.

PCR-based methods generally exploit the unique *IGHV* CDR3 sequence of the CLL clone to distinguish it from healthy polyclonal B cells. One approach through which this can be achieved is by quantitative allele-specific oligonucleotide (ASO) PCR. In this method, the *IGHV* gene of the patient's CLL is first sequenced prior to the commencement of treatment. From the *IGHV* sequence, ASO primers corresponding to the unique CDR3 sequence of the CLL clone is then generated. After the end of treatment, MRD can be monitored by real-time quantitative PCR using these CLL-specific primers. The sensitivity of this methodology can reach up to 1 CLL cell in 1,000,000 leukocytes (10^{-6}) (Pfitzner et al., 2000; Voena et al., 1997).

More recently, deep sequencing of the *IGHV* gene has been used to replace quantitative PCR for MRD detection (Logan et al., 2013; Rawstron et al., 2016). Deep sequencing refers to an NGS approach where a targeted region of the genome is sequenced to a high coverage (i.e. >1000 times). This allows sequence variants to be

detected and the frequency of the variant quantified within a sample containing different cellular populations, such as a mixture of CLL cells and healthy B cells. Like the real-time quantitative PCR method, the *IGHV* gene of the patients' CLL cells is sequenced before treatment, but no subsequent design of CLL-specific primers is required. Detection of MRD following the end of treatment utilises deep *IGHV* sequencing with consensus primers, and the results obtained are then compared to the known *IGHV* sequence of the CLL clone. The difference between the *IGHV* sequences of the CLL cells and healthy B cells allow any residual CLL clone to be detected and quantified, to a sensitivity of 10^{-5} to 10^{-6}.

1.5.3. Clinical significance of MRD in CLL

1.5.3.1. Treatments capable of achieving MRD negativity

In CLL, the current requirement for MRD negativity is less than one CLL cell in 10,000 leukocytes (10^{-4}), as stipulated in the IWCLL 2008 guidelines (Hallek et al., 2008). Historically, the only CLL treatment capable of achieving sustained MRD negativity is haematopoietic stem cell transplantation (SCT) (Dreger et al., 2010; Moreno et al., 2006). However, the majority of patients requiring treatment for CLL are elderly, frail or have multiple co-morbidities. Despite the availability of reduced intensity conditioning (RIC) regimens for allogeneic SCT, transplant-related mortality remains substantial for this group of elderly individuals. The availability of chemoimmunotherapy has allowed MRD negativity to be achievable in a substantial proportion of CLL patients without having to undergo an allogeneic SCT. In the German CLL study group CLL8 trial comparing FCR vs FC discussed earlier in section 1.3.1.1, MRD negativity at the end of treatment was observed in the peripheral blood in 63% of patients who received FCR compared to 35% who received FC, and in the bone marrow in 44% of patients who received FCR vs 28% of FC-treated patients. Although FCR was superior to FC overall, patients who attained MRD negativity had similar clinical outcome regardless of whether they were treated to MRD negativity with

FC or FCR. The overall superiority of the FCR arm was due to a higher proportion of patients achieving MRD negativity with FCR compared to FC (Bottcher et al., 2012).

MRD negativity is also achievable with mAbs alone. For instance, a substantial proportion of patients (20%) achieved bone marrow MRD negativity with alemtuzumab in a historical clinical trial (Moreton et al., 2005). With regards to novel small molecule inhibitors, MRD negativity is uncommon with BCR signalling inhibitors. However, recent reports have shown that this is achievable with venetoclax, including among patients having adverse biological features such as *TP53* mutations (Eichhorst et al., 2015; Ma et al., 2015).

1.5.3.2. Prognostic impact of MRD

Numerous studies (**Table 1.2**) have assessed the prognostic significance of MRD in univariate analyses, in which the outcome of MRD-negative patients was compared directly to the outcome of MRD positive patients. The majority of these studies were conducted as part of a clinical trial evaluating the efficacy of a single (or occasionally two) therapeutic agent, either in the frontline or the relapsed/refractory setting. In these studies, attainment of MRD negativity was invariably associated with improved PFS and OS. For instance, in previously untreated patients receiving FC or FCR as part of the German CLL8 trial, PFS, with a 4 year follow-up, was 69, 41 and 15 months respectively for post-treatment MRD levels of $<10^{-4}$, $\geq10^{-4}$ to $\geq10^{-2}$ and $\geq10^{-2}$ (Bottcher et al., 2012). In patients treated with combined bendamustine and rituximab, this was not reached, 32 and 12 months respectively for the above MRD levels with a median follow-up of 2 years (Fischer et al., 2012). In relapsed/refractory patients receiving alemtuzumab, the TFS for MRD negative vs positive individuals was not reached vs 20 months, and the OS was not reached vs 41 months with a follow-up of 3 years (Moreton et al., 2005).

Nevertheless, univariate analyses alone do not provide insight as to whether improved clinical outcome is due to the attainment of MRD negativity, or whether MRD

Table 1.2. Previously published studies on the prognostic significance of MRD in CLL.

	Treatment	n	BM/ PB MRD	MRD assessment method	Median Follow-up (years)	PFS		OS	
						Univariate p value	Multivariate p value	Univariate p value	Multivariate p value
FRONTLINE SETTING									
(Bosch et al., 2008)	FCM	18	BM	Flow cytometry	2.5	n.s.	-	-	-
(Lamanna et al., 2009)	F → C → R (sequential)	23	PB / BM	ASO *IGHV* qPCR	5.0	0.007	-	-	-
(Maloum et al., 2009)	FC	33	PB	Flow cytometry	5.3	<0.001	-	n.s.	-
(Bottcher et al., 2012)	FC / FCR	254	PB	Flow cytometry	4.3	<0.001	<0.001	<0.001	<0.001
(Fischer et al., 2012)	BR	45	PB	Flow cytometry	2.3	<0.001	-	-	-
(Abrisqueta et al., 2013)	FCMR	63	BM	Flow cytometry	4.0	0.03	-	-	-
(Santacruz et al., 2014)	FC / FCR	255	PB	Flow cytometry	6.1	<0.001	<0.001	0.012	0.014
(Strati et al., 2014)	FCR	161	BM	Flow cytometry	2.3	<0.001	0.03	0.006	0.02
(Goede et al., 2014)	Obinutuzumab + chlorambucil	364	PB / BM	Flow cytometry	not provided	<0.001	-	-	-
(Thompson et al., 2016)	FCR	170	BM	ASO *IGHV* qPCR	12.8	<0.001	-	<0.001	-
RELAPSED/REFRACTORY SETTING									
(Wierda et al., 2005)	FCR	32	BM	ASO *IGHV* qPCR	1.7	n.s.	-	-	-
(Moreton et al., 2005)	Alemtuzumab	34	BM	Flow cytometry	3.0	<0.001	-	<0.001	-
(Pettitt et al., 2012)	Alemtuzumab + methylprednisolone	25	BM	Flow cytometry	not provided	0.009	-	-	-

F, fludarabine; C, cyclophosphamide; M, mitoxantrone; R, rituximab; B, bendamustine; BM, bone marrow; PB, peripheral blood; ASO; allele-specific oligonucleotide; PFS; progression-free survival; OS, overall survival. Adapted from Thompson & Weirda (2016). Eliminating minimal residual disease as a therapeutic end point: working toward cure for patients with CLL. Blood. *127*, 279-286. Modified and updated.

negativity is a surrogate for other factors that predict for favourable clinical outcome. Such an insight can be obtained from multivariate analyses, which take into consideration other prognostic factors that could also influence outcome. However, few studies have evaluated the impact of MRD within multivariate analyses. In the German CLL8 trial where such an analysis was performed, MRD negativity predicted for PFS and OS independently of clinical response, del(17p) and *IGHV* mutational status (Bottcher et al., 2012). On the other hand, the independent prognostic significance of MRD outside the frontline chemoimmunotherapy setting is unknown.

1.6. Aims

The work described in this thesis aims to generate novel insights into the mechanisms behind disease heterogeneity of CLL and improve its treatment. This is achieved by focusing on three unique groups of patients: (1) patients with an exceptionally good outcome, who have undergone spontaneous disease regression; (2) patients with an exceptionally poor outcome, whose CLL harbours *TP53* or *ATM* defects; and (3) patients with an exceptionally good response to treatment, who attained MRD negativity. The specific aims of each of the three components of this work are outlined below:

Features and mechanisms underpinning spontaneous disease regression in CLL (Chapter 3). The biological features and processes underpinning the natural history of patients with spontaneous CLL regression are unknown. My aim is to undertake a comprehensive phenotypic, functional and genomic study on these patients in order to answer three questions: (1) What are the key biological features of spontaneously regressed CLL? (2) What are the phenotypic changes during spontaneous CLL regression and the potential mechanism underpinning these changes? (3) What can we learn about the treatment of CLL from these patients?

Pre-clinical efficacy and mechanism of ATR inhibition in CLL (Chapter 4). Current therapeutic options for CLL, particularly for patients with *TP53* or *ATM* defects, remain inadequate. My aim is to undertake a pre-clinical evaluation of the ATR inhibitor AZD6738 in CLL in order to answer three questions: (1) What is the therapeutic efficacy of ATR inhibition in CLL, particularly in CLL with *TP53* or *ATM* defects? (2) What is the mechanism underlying the cytotoxic effects of ATR inhibition in CLL? (3) What is the effect of combining ATR inhibition with other CLL treatments?

Long-term independent prognostic significance of MRD in CLL (Chapter 5). The independent prognostic significance of MRD is unknown in CLL outside the frontline chemoimmunotherapy setting. My aim is to undertake a single-centre, retrospective analysis of patients who have received MRD assessments after their treatment for CLL, in order to answer two questions: (1) What is the long-term prognostic value of MRD in the frontline and relapsed/refractory settings respectively? (2) What is the independent prognostic significance of MRD in CLL?

CHAPTER 2

PATIENTS,
MATERIALS & METHODS

2.1. Clinical cohorts and CLL samples

2.1.1. Birmingham and Leeds CLL cohorts

The majority of samples used in the spontaneous CLL regression study (Chapter 3) and all samples used in the ATR inhibitor study (Chapter 4) were obtained from patients diagnosed with CLL at Queen Elizabeth Hospital Birmingham or at Birmingham Heartlands Hospital. The spontaneous CLL regression study also included the use of samples from patients diagnosed at St. James's University Hospital or Pinderfields General Hospital in Leeds, or from individuals enrolled within UK multicentre clinical trials. For the retrospective MRD study (Chapter 5), all patients enrolled were treated for CLL at St. James's University Hospital in Leeds or at associated hospitals in the Yorkshire region. All research involving patients was conducted in accordance with the Declaration of Helsinki, with full approval from the local National Health Service (NHS) research ethics committee (REC). These local CLL cohorts are described in more detail below:

Birmingham CLL cohort. Patients attending CLL clinic were consented for blood donation under the REC protocol 10/H1206/58 (West Midlands – Solihull Research Ethics Committee). A system has been in place for many years whereby blood samples were collected and archived during each clinic visit, resulting in a local biobank of CLL samples with different clinical and biological characteristics. These archived samples were used for the investigations described in the ATR inhibitor study. For the spontaneous CLL regression study, both fresh and archived samples were used, depending on the investigation.

Spontaneous CLL regression cohort. Patients with spontaneous CLL regression were identified from a review of (1) all patients with a diagnosis of CLL who have attended a haematology clinic at Queen Elizabeth Hospital Birmingham or Birmingham Heartlands Hospital for the past 5 years; and (2) all patients with CLL who have been enrolled in the

Leeds community outreach monitoring programme. The latter scheme allows patients with stable disease to be discharged from outpatient follow-up, with regular blood samples being sent by their general practitioner to the Haematological Malignancy Diagnostic Service (HMDS) laboratory in Leeds for monitoring. Patients identified as meeting the criteria for spontaneous disease regression were contacted and invited to attend an outpatient appointment where the research study was discussed in detail. Written consent was obtained from subjects who agreed to take part, and a blood sample was collected. An amendment of the REC protocol 10/H1206/58 was specifically made to allow patients who have been discharged from outpatient follow-up to be recalled, and to include Leeds as a participating centre.

Leeds MRD study cohort. This cohort includes all patients from Leeds and associated regional hospitals who have received an MRD assessment after completion of CLL treatment in the 12 year period from 1996 to 2007. These patients all received MRD assessments as part of the clinical trials they were enrolled in. Ethical approval for the respective trials includes approval for MRD assessments to be carried out and patients to be followed up.

2.1.2. Clinical trial cohorts

Within the CLL spontaneous regression study, a number of investigations involve comparison of spontaneous regression cases against progressive as well as indolent cases. All indolent cases were derived from the local Birmingham CLL cohort. Progressive samples, on the other hand, were taken from patients due to commence treatment as part of a UK clinical trial. These trials are described below:

IcICLLe trial. This is a phase II trial enrolling 40 patients onto ibrutinib, 20 of whom are treatment-naïve and 20 have previously been treated. As part of this study, extended

CLL immunophenotypic analysis was carried out on peripheral blood samples taken before and at regular intervals during treatment. The pre-treatment immunophenotypic data from the entire IcICLLe cohort was used for comparison against the immunophenotypic results from the spontaneous CLL regression cohort.

CLARITY trial. This is a phase II trial enrolling previously treated patients onto venetoclax plus ibrutinib. Because CLL Mcl-1 expression data was not available from the IcICLLe cohort, the pre-treatment Mcl-1 expression data from this cohort was used instead for comparison against the Mcl-1 expression results from the spontaneous regression cohort.

2.1.3. Sample preparation

Venous blood samples were collected into 9 ml vacutainer tubes coated with heparin or ethylenediaminetetraacetic acid (EDTA). They were either used directly for flow cytometry experiments, or processed to separate peripheral blood mononuclear cells (PBMCs) from other components within the blood sample.

Isolation of PBMCs from whole blood. The blood sample was first diluted in RPMI-1640 medium (Sigma) supplemented with 10% foetal bovine serum (FBS; Sigma), where 10 ml of the medium was added to every 20 ml of whole blood. Up to 30 ml of the diluted blood was then layered onto 10 ml of Lymphoprep solution (Axis-Shield) in a 50 ml Falcon tube. The tube was then centrifuged at 1700 rpm for 30 minutes with brake off. This procedure exploits the differential density of PBMCs relative to erythrocytes and granulocytes. Erythrocytes and granulocytes sediment through the Lymphoprep layer to the bottom of the Falcon tube, leaving the PBMCs to be collected at the interface between the uppermost plasma layer and the Lymphoprep layer at the end of centrifugation. The isolated

PBMCs were then washed twice in RPMI-1640 with 10% FBS, and counted using a haemocytometer (Kova).

Cell freezing and storage. Washed PBMCs were resuspended in a freezing medium containing 90% FBS and 10% dimethylsulphoxide (DMSO; Sigma), and transferred into 1.5 ml cryovials. Cryovials were then wrapped in cotton wool and placed in a container at -80°C to allow gradual cooling of the samples. The samples were subsequently transferred to be stored in liquid nitrogen.

Cell thawing and revival. To use archived samples stored in liquid nitrogen, samples were first thawed rapidly in a 37°C water bath. The thawed cells were then transferred to a universal tube and 10 ml of RPMI-1640 with 10% FBS was added dropwise to the cells. The supernatant was quickly removed after centrifugation to avoid prolonged exposure to DMSO which may be toxic for the cells.

2.1.4. Cell sorting

A number of investigations in the spontaneous CLL regression study required the use of isolated CD19+ CD5+ CLL cells. The isolation of these cells from PBMCs was carried out using a two-step magnetic-activated cell sorting (MACS) process. This involves first isolating CD19+ B lymphocytes by depleting all other cell types. The sorted CD19+ B lymphocyte population was then enriched for CD19+ CD5+ CLL cells by positive sorting for CD5+ cells.

Isolation of CD19+ B lymphocytes. CD19+ B lymphocytes were isolated from PBMCs using the human B-CLL cell isolation kit (Miltenyl Biotec). First, PBMCs were resuspended in MACS buffer containing phosphate-buffered saline (PBS), 0.5% bovine serum albumin (BSA) and 2 mM EDTA at pH 7.2. Forty µL of ice-cold MACS buffer was used and 10 µL of biotin-antibody cocktail was added per 10^7 PBMCs, after which cells were

incubated for 5 minutes at 4°C. Subsequently, 30 µL of MACS buffer and 20 µL of anti-biotin magnetic microbeads were added per 10^7 PBMCs, and cells were incubated for another 10 minutes. The antibody cocktail contains biotin-conjugated antibodies directed against CD3 and CD4 (T cells), CD16 and CD56 (NK cells), CD14 (monocytes), CD15 (granulocytes), FcεRIa (basophils), CD34 (haematopoietic progenitor cells), CD61 (platelets) and CD235 (erythrocytes), which would then become bound to the anti-biotin magnetic beads. Cell types other than B lymphocytes would therefore be magnetically labelled. Upon application of the cell suspension to a separation column attached to a magnet (LS column; Miltenyl Biotec), CD19+ B cells would pass through the column as the elutant, whereas other cell types would become adhered to the magnetic column and hence depleted.

Enrichment for CD19+ CD5+ CLL cells. Isolated CD19+ cells were resuspended in ice-cold MACS buffer at 100 µL per 10^7 cells. One µL of human CD5-biotin antibody (clone UCHT2; Miltenyl Biotec) was added per 10^7 cells, and cells incubated at 4°C for 5 minutes. After washing the cells and resuspending them in 80 µL of fresh MACS buffer per 10^7 cells, 20 µL of anti-biotin microbeads per 10^7 cells (Miltenyl Biotec) was added, and cells were incubated at 4°C for another 10 minutes. Upon passing through an LS column (Miltenyl Biotech) attached to a magnet, the CD5+ CLL cells would adhere to the column whilst the remaining CD5 negative B lymphocytes would pass through. The bound CD19+ CD5+ CLL cells were then collected after removing the column from the magnet.

Confirmation of purity of the sorted population. The sorted cell fraction was confirmed to be >93% CD19+ CD5+ by flow cytometry (see section 2.4.4) prior to their use in experiments. In the majority of cases this was >95%. Representative flow cytometry plots in **Figure 2.1** illustrate the effectiveness of the cell sorting process.

Figure 2.1

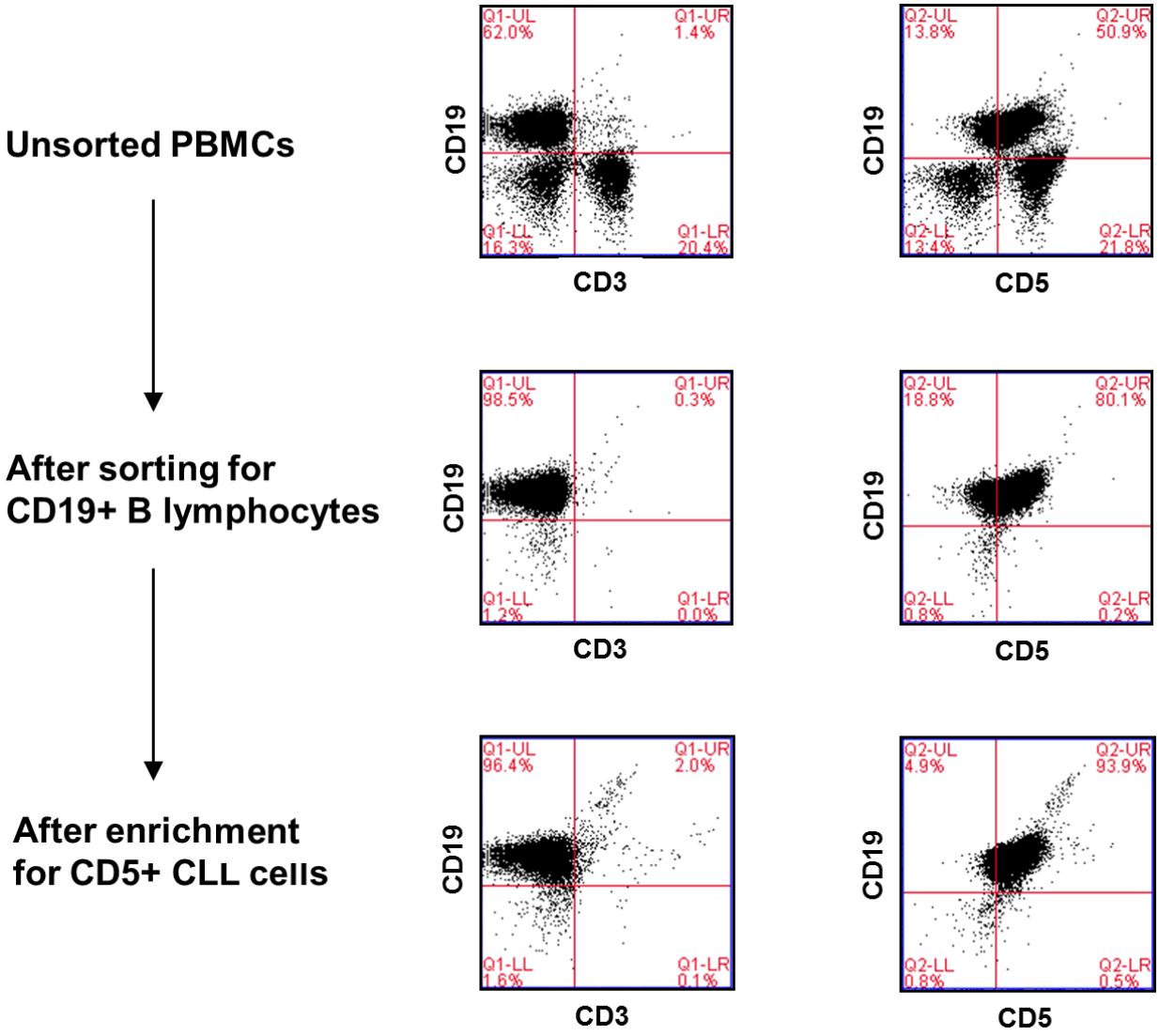

Methodology for the isolation of CD19+ CD5+ CLL cells from PBMCs. CLL cells were isolated from PBMCs using a two-step MACS sorting process. CD19+ B lymphocytes were first isolated from PBMCs using human B-CLL cell isolation kit (Miltenyl Biotec) which depletes cell types other than B lymphocytes. The sorted population was subsequently enriched for CD19+ CD5+ CLL cells using a human CD5-biotin antibody (Miltenyl Biotec). The sorted cell fraction was confirmed to be >93% CD19+ CD5+ prior to their use in experiments. The sorting of a representative PBMC sample from a patient with spontaneous CLL regression was shown.

2.1.5. DNA extraction

DNA was extracted from between 10^6 and 5 x 10^6 sorted CD19+ CD5+ CLL cells using the DNeasy blood and tissue kit (Qiagen) according to the manufacturer's instructions. Cells were resuspended in 200 µL of PBS. Twenty µL of proteinase K was then added, followed by 200 µL of lysis buffer (AL). After vortexing and incubation at 56°C for 10 minutes, 200 µL of 100% ethanol was added to the sample. Following further vortexing, the sample was applied onto the DNeasy Mini spin column and centrifuged at maximum speed (14,000 rpm) for 1 minute. The flow-through was discarded, 500 µL of wash buffer (AW1) was applied onto the spin column, and the column was centrifuged again for 1 minute at 14,000 rpm. A further wash step with 500 µL of AW2 was carried out after removal of the flow through from the previous wash, but on this occasion the column was centrifuged for 3 minutes at 14,000 rpm. Thereafter, the collection tube was replaced and the DNeasy membrane was dried by centrifuging the spin column for a further 3 minutes at 14,000 rpm. Finally, 50-100 µL of elution buffer (AE) was added to the spin column, and the elutant was collected in a DNase-free eppendorf tube by centrifuging the spin column for 1 minute at 14,000 rpm.

DNA samples were quantified and their purity confirmed using a NanoDrop spectrophotometer (Thermo Fisher Scientific). The A260/280 ratio was confirmed to be 1.7-1.9 to ensure minimal protein or phenol contamination, which would result in lower and higher readings respectively. For samples subjected to WES, the nucleic acid concentration was further verified by a Qubit 2.0 fluorometer (Thermo Fisher Scientific). DNA samples were stored at -20°C.

2.2. CLL cell lines

2.2.1. Cell lines

Two CLL cell lines were used in the ATR inhibitor study. Both were obtained from Prof. Anders Rosen, Linkoping University, Sweden. The details are as follows:

The CII cell line was derived from a 47 year old female with CLL who presented with lymphadenopathy, hepatosplenomegaly, a white cell count of 152 x 10^9/L with 88% lymphocytes, and increased lymphocytes in the bone marrow. This cell line was established by infecting mononuclear cells with the B95-8 strain of Epstein-Barr virus. The CII cell line shows expression of mature B cell markers (CD5+, CD19+, CD20+ and CD23+) with immunoglobulin production restricted to the IgM λ subtype, similar to the patient CLL clone. Moreover, the cell line is characterised by unmutated *IGHV*1-69/*IGHD*3-10/*IGHJ*-6 and *IGLV*1-4/IGLJ-3 gene rearrangements showing CDR3 sequence homology with stereotyped CLL subset 5. The CII cell line shows low CD38 but high ZAP-70 levels, and exhibits trisomy 12, which was also present in the in vivo CLL clone (Fialkow et al., 1978; Karande et al., 1980; Lanemo Myhrinder et al., 2013).

The Mec1 cell line was derived from a 58 year old male with CLL in prolymphocytoid transformation, clinically characterised by constitutional symptoms, lymphadenopathy and splenomegaly. The Mec1 cell line was established by spontaneous outgrowth from peripheral blood lymphocytes, taken prior to treatment at a time when the white cell count was 39 x 10^9/L. The Mec1 cell line displays mature B-cell markers (CD19+, CD20+ and CD23+) with mutated *IGHV*4-59/*IGHD*2-21/*IGHJ*-4 rearrangement identical to that of the patient's CLL clone. Mec1 cells lack CD5 and express low levels of CD38, with absent ZAP70 expression. Mec1 cells possess a deleterious *TP53* mutation, which results in a truncation at the N-terminus, producing a lower molecular weight protein (approx. 47 kDa

compared to wild-type p53 which is 53 kDa) that is non-functional and cannot be induced by DNA damaging agents such as fludarabine. Our lab has independently confirmed by *TP53* sequencing the presence of c.950insC insertion with absent wild-type allele in Mec1 cells (Almazi et al., 2012; Lanemo Myhrinder et al., 2013; Stacchini et al., 1999).

2.2.2. Generation of isogenic cell lines

Isogenic CII and Mec1 cell lines with different expression of ATM or p53 were previously generated in our laboratory.

Paired ATM-deficient and ATM-proficient CII cell lines. Isogenic CII cell lines were generated by shRNA transfections carried out using RNA oligonucleotide (Dharmacon) targeting either green fluorescent protein (GFP) as a negative control (CII-*GFP*sh), or ATM (CII-*ATM*sh) as described previously (Biton et al., 2006; Weston et al., 2010). In brief, stable knockdown of *ATM* was achieved using two shRNA sequences complementary to a 19 or 21 nucleotide sequence beginning at positions 912 and 8538 respectively of the *ATM* transcript. The two shRNA sequences were expressed in a retroviral vector. CII cells infected with the shRNA-expressing retroviral vector were selected using 1 μg/ml puromycin. The shRNA expressed in the vector-infected CII cells would be processed by the endoribonuclease Dicer, releasing siRNA sequences that cleave the *ATM* mRNA at the corresponding positions.

Paired p53-deficient and p53-proficient CII cell lines. To re-express wild-type *TP53* in this *TP53* mutant cell line, Mec1 cells were transfected by electroporation (Amaxa system; Lonza Biologics) with the vector pcDNA3.1 (kind gift from Dr. A. Turnell, University of Birmingham) containing either wild-type *TP53* (Mec1-p53-pcDNA3.1), or *GFP* as control (Mec1-GFP-pcDNA3.1). Forty-eight hours after transfection, the culture media was supplemented with Geneticin (Life Technologies) to select for the transfected cells.

2.3. CLL cell culture

2.3.1. Cell line and primary cell culture

Cell culture was performed under aseptic technique. CII-*GFP*sh and CII-*ATM*sh were cultured in RPMI-1640/10% FBS supplemented with 1 µg/ml puromycin to maintain selection of cells expressing the corresponding shRNA. The Mec1 cell line and CLL primary cells were cultured in RMPI-1640/10% FBS alone. Cells were incubated at 37°C with 5% CO_2 in an incubator. CII and Mec1 cells were passaged every 4 days.

2.3.2. Induction of CLL cell proliferation

To induce proliferation, primary CLL cells were co-cultured for 4 days in RPMI-1640/10% FBS with CD40 ligand (CD40L) expressing murine embryonic fibroblasts (MEFs), supplemented with IL-21 (eBiosciences) diluted to a final concentration of 25 ng/ml (Pascutti et al., 2013). The CD40L expressing MEFs, kindly supplied by Prof. John Gordon (University of Birmingham), were generated by transfection of the NIH3T3 MEF cell line with a vector expressing CD40L. Prior to their use, the CD40L expressing MEFs were expanded in Dulbecco's Modified Eagle's Medium (DMEM)/10% FBS culture for two weeks, after which they were irradiated with 50 Gy IR to render them non-proliferative. CLL cells and CD40L expressing MEFs were cultured in a 10:1 ratio.

Following the initial 4-day culture and subsequent drug treatment, CLL cells were harvested for analysis. The CLL cells were easily dislodged by gentle pipetting, while the MEFs remained adherent to the culture plate or flask. Pilot experiments have shown that there was negligible contamination of the harvested CLL cells with MEFs.

2.4. Flow cytometry

Flow cytometry was used within both the spontaneous CLL regression study and the ATR inhibitor study. Within the spontaneous CLL regression study, flow cytometry was used for peripheral blood immunophenotyping, for phosphoflow analysis of BCR signalling and for purity confirmation of cellular populations after MACS sorting. Within the ATR inhibitor study, flow cytometry was used for cell cycle analysis, for the measurement of drug-induced cytotoxicity (section 2.7.2) and for the measurement of tumour load *ex vivo* (section 2.10).

Flow cytometry enables the detection of both surface and intracellular proteins in individual cells. Cells are incubated with fluorochrome-conjugated antibodies that are directed against the surface and intracellular proteins of interest. In cases where intracellular proteins are investigated, cells are additionally fixed and their cell membrane permeabilised to allow antibodies to enter the cell and bind to intracellular proteins. These cells are then directed through a single file within the fluidics system, where they pass, one cell at a time, through several beams of laser, each with a different frequency. These lasers excite specific fluorophore bound to the cell surface or intracellular proteins. Each fluorophore is excited by a specific laser and emits fluorescence at a specific wavelength immediately following excitation. Each emission is then detected within a specific channel that incorporates a filter that permits passage only of emissions within a specific range of wavelengths.

2.4.1. Flow cytometer setup and controls

As detailed in the sections to follow, different flow cytometers were used for different investigations. The flow cytometer used include BD FACSCanto (for peripheral

blood immunophenotyping), BD LSRFortessa (for phosphoflow) and BD Accuri C6 (for all other investigations). The acquisition and analytical software used was BD FACSDiva, with the exception of acquisitions on the BD Accuri C6 which were analysed using the accompanying C6 software. All equipment and software were produced by Becton Dickinson Biosciences.

Unstained and compensation controls. All experiments incorporate an unstained control used for setting the voltages of each channel. Unstained controls were prepared in exactly the same way as the stained samples, with the exception that no antibody was added. Compensation enables the elimination of any spectral overlap, whereby the emissions of a fluorophore that is detected by one channel spills over to the adjacent channels. Compensation was carried out using anti-mouse immunoglobulin κ/negative control compensation particles set (BD Biosciences). A separate polystyrene round-bottom tube was prepared for each fluorophore, with each tube containing a mixture of anti-mouse immunoglobulin κ beads and negative control beads. The former binds to the κ light chain of the mouse antibody, while the latter does not have any antibody-binding capacity. An equivalent volume of a single antibody to that used in the samples was added to each tube. The tubes were then incubated at room temperature for 30 minutes in darkness. Thereafter the compensation beads in each tube were washed in PBS and resuspended in 200 µl of PBS for acquisition. This allows the establishment of two distinct populations, one with the antibody staining and one without. Using these single stained compensation controls, compensation was carried out either manually (for experiments on BD Accuri C6) or automatically through the FACSDiva software (for experiments on all other flow cytometers). This involves subtracting any spillover from the affected channels such that the median fluorescence intensity (MFI) of those channels return to that seen with the unstained control.

Biological controls and the setting of gates. To determine the settings of gates which demarcate the positive vs negative populations, biological controls were used. For many cell surface and intracellular targets, healthy cellular populations known to highly

express or not express a particular target protein were used as positive and negative controls respectively. For instance, B-progenitor cells were used as a positive control for ROR1, and T cells as a negative control. For some target proteins, such as Bcl-2, cell lines known to highly express the target were used as positive controls. Isotype controls, which are detects non-specific binding of antibodies, were used only where negative biological controls were not available.

Antibody titration. During the initial setup of the antibody panels, the manufacturer recommended antibody volume was used. However, excess antibody may bind at low affinity and/or create high levels of non-specific background staining. Therefore, antibody volumes used for staining were titrated down to achieve the greatest separation between the positive and negative populations.

2.4.2. Peripheral blood immunophenotyping

All immunophenotyping experiments carried out as part of the spontaneous CLL regression study was performed on fresh blood, with the exception of those experiments investigating changes across serial timepoints, in which case immunophenotyping was performed on archived PBMCs for all timepoints. To allow comparison of my immunophenotypic results from the spontaneous regression and indolent cases with the available data from the clinical trial cases, all immunophenotyping experiments were performed using the same experimental protocol, antibody panels, flow cytometer and analysis template as those used in the clinical trial cases.

Extracellular antibody staining. For immunophenotyping on fresh blood samples, a blood volume containing 2 x 10^7 white blood cells were added to 5 ml of ammonium chloride solution (8.6 g/L) in a round-bottom polystyrene tube, and incubated at 37°C for 10 minutes, in order to lyse the red blood cells within the blood sample. Following centrifugation

and removal of the supernatant, the cells were resuspended in 2.8 ml of FACSFlow (BD Biosciences) with 2% BSA. BSA acts as a blocking agent to reduce non-specific binding of antibodies to Fc receptors expressed on monocytes, dendritic cells and B lymphocytes, which could otherwise yield false positive results. Two hundred µl of the cell suspension (equivalent of 10^6 cells) was then applied to each well within a round-bottom 96-well plate, the number of wells applied being dependent on the number of antibody panels being used. For archived samples, 10^6 cells were applied to each well after cell thawing and revival (section 2.1.3). After centrifugation of the plate, removal of the supernatant and resuspension of the cells, cells were washed once with FACSFlow/BSA, and extracellular antibodies added to the appropriate wells. Cells were incubated with these antibodies for 30 minutes at 4°C, after which they were washed twice with FACSFlow/BSA, resuspended in 180 µl of FACSFlow, and transferred to a polystyrene tube for acquisition on a FACSCanto.

Intracellular antibody staining. For antibody panels where intracellular markers were included, 100 µl of Intrasure reagent A (BD Biosciences) was added immediately after the first wash step following extracellular antibody incubation, in order to fix the cells. After 5 minutes of incubation at room temperature with Intrasure A, the plate was centrifuged, the supernatant removed and 200 µl of FACSLyse reagent (BD Biosciences) was applied to the resuspended sample to remove any residual red blood cells. Following 10 minutes of incubation with FACSLyse at room temperature, and subsequent centrifugation and removal of the supernatant, 50 µl of Intrasure B reagent (BD Biosciences) was added to permeabilise the cells. Thereafter, intracellular antibodies were applied, and the plates were then incubated at 4°C for 15 minutes to allow for intracellular antibody binding. The cells were then washed twice with FACSFlow/BSA, and resuspended in FACSFlow for acquisition.

Antibody panels. For all antibody staining, master mixes were prepared to ensure staining consistency. Up to 8 different fluorophores (colours) per antibody panel is used. Example of an extracellular antibody panel, and an extracellular and intracellular antibody panel, is shown in **Figure 2.2.** A list of all antibodies used is provided in **Appendix 1.**

Figure 2.2

Example of an extracellular antibody panel

	Antigen	Source	Catalogue No.	Excitation laser	Filter	Volume (µl)/10 samples
BV421	CD23	BD Biosciences	562707	Violet (405 nm)	450 nm	10
BV510	CD43	BD Biosciences	563377	Violet (405 nm)	525 nm	10
FITC	CD81	BD Biosciences	551108	Blue (488 nm)	530 nm	50
PE	CD79b	Coulter	IM1612	Blue (488 nm)	575 nm	50
PerCP-Cy5.5	CD19	BD Biosciences	332780	Yellow-Green (561 nm)	695 nm	50
PE-Cy7	CD5	BD Biosciences	348810	Yellow-Green (561 nm)	780 nm	10
APC	ROR1	Miltenyi Biotec	130-098-320	Red (640 nm)	660 nm	50
APC-H7	CD20	BD Biosciences	641414	Red (640 nm)	780 nm	50
Buffer (FACSFlow/2% BSA)						120

Example of an antibody panel comprising extracellular and intracellular antibodies

	Antigen	Source	Catalogue No.	Excitation laser	Filter	Volume (µl)/10 samples	
						Extracellular Ab mix	Intracellular Ab mix
BV421	CD95/FasR	BD Biosciences	562616	Violet (405 nm)	450 nm	10	-
BV510	CD49d	BD Biosciences	563204	Violet (405 nm)	525 nm	10	-
FITC	**[Ki67]**	BD Biosciences	558616	Blue (488 nm)	530 nm	-	50
PE	**[ZAP70]**	BD Biosciences	344635	Blue (488 nm)	575 nm	-	200
PerCP-Cy5.5	CD19	BD Biosciences	332780	Yellow-Green (561 nm)	695 nm	50	-
PE-Cy7	CD5	BD Biosciences	348810	Yellow-Green (561 nm)	780 nm	10	-
APC	**[BCL2]**	BD Biosciences	563600	Red (640 nm)	660 nm	-	10
APC-H7	CD20	BD Biosciences	641414	Red (640 nm)	780 nm	50	-
Buffer (FACSFlow/2% BSA)						270	140

Examples of antibody panels used for peripheral blood immunophenotyping. The volume of each antibody and buffer required to produce master mixes for 10 samples are shown (400 µl). Forty µl of antibody master mix is dispensed to each sample. Events were acquired by a LSR Fortessa flow cytometer. In the tables, intracellular antibodies are displayed in boldface within brackets.

Data analysis **(Figure 2.3).** Following the setting of voltage and spectral compensation (section 2.4.1), different cellular populations were identified on the forward scatter (FSC) vs side scatter (SSC) plot by their relative position. The granulocyte population would have higher granularity and therefore higher SSC than mononuclear cells. On the other hand, apoptotic cells and cellular debris would have lower FSC and/or higher SSC than the mononuclear cell population. This allowed a gate (P1) to be applied on the FSC vs SSC plot to include the mononuclear cell population (shown in black), but exclude granulocytes, dead cells and debris (shown in green) **(Figure 2.3A)**. The positioning of this gate was confirmed by displaying the P1 gated events on a CD19 vs CD20 plot. The CD19+ population would represent the B lymphocytes, whereas the CD19− CD20− population would comprise other mononuclear cells. Any events that were CD20+ but CD19− would be considered possibly to be apoptotic or degenerate cells, and would prompt re-adjustment of the P1 gate to exclude those events. Such a gating strategy has been confirmed to exclude >98% of propidium iodide (PI) positive cells.

The P1 gated events were then displayed on a FSC-area (FSC-A) vs FSC-height (FSC-H) plot. A second gate (P2) was then applied to include singlets but exclude doublets, on the basis that doublets would have double the area as singlets while the height would remain the same **(Figure 2.3B)**.

For CLL immunophenotyping, events were displayed on a CD19 vs CD20 plot. CD20 provides the single best discriminator between the CLL cells and normal B cells (Rawstron et al., 2001). A third gate (P3) was applied to include all CD19+ CD20-low CLL cells, but exclude normal B cells that would be CD19+ CD20-high **(Figure 2.3C)**. For T cell immunophenotyping, events were displayed on a CD3 vs SSC plot, and the third gate was applied on the CD3+ T cell population, with further gating to differentiate between CD3+ CD4+ and CD3+ CD8+ T cells **(Figure 2.3E)**. The P1 + P2 + P3 gated singlet CLL or T cell population was then analysed for the expression of a variety of markers **(Figure 2.3D-E)**. A minimum of 200,000 events were acquired for each sample.

Figure 2.3

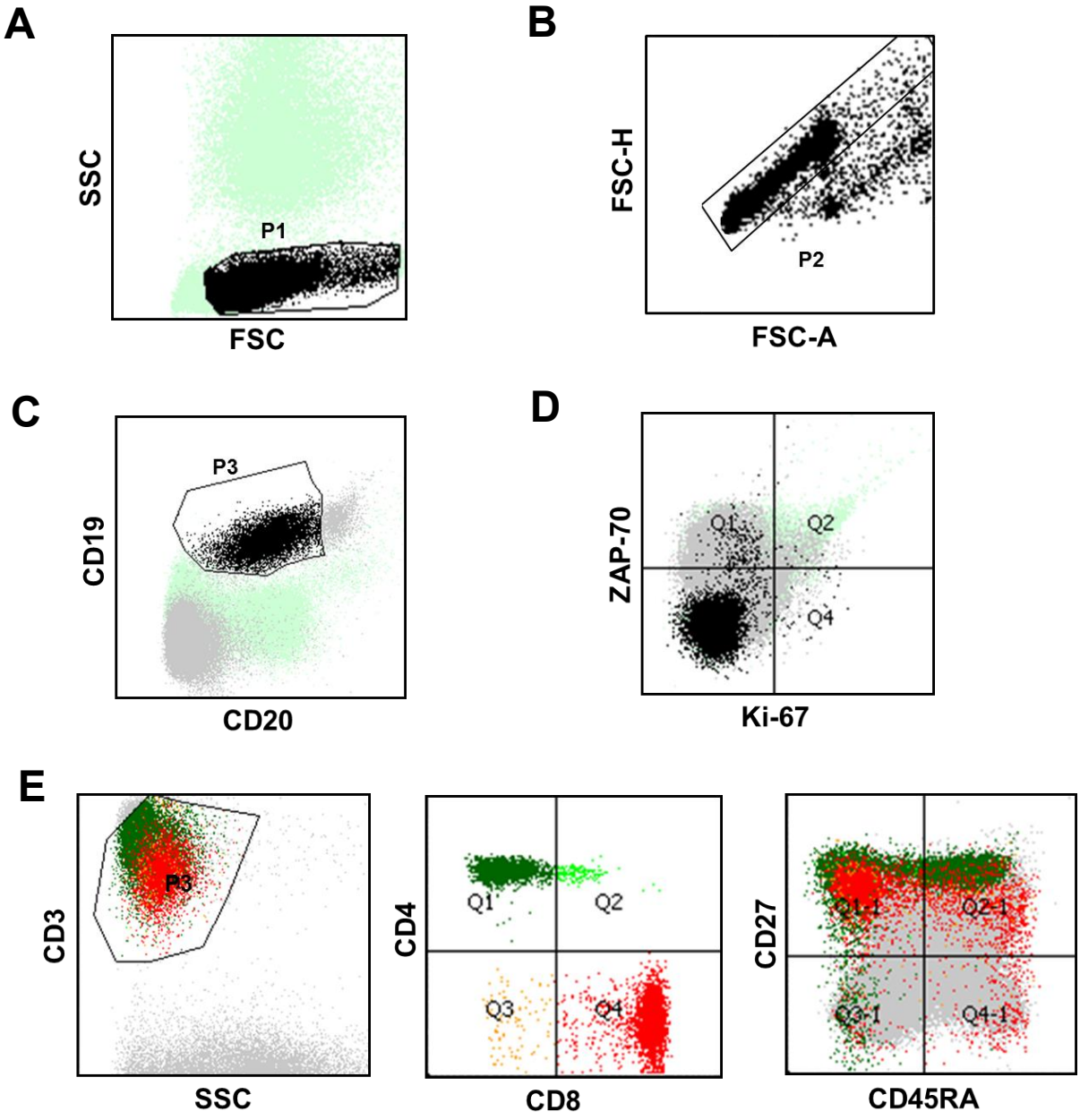

Gate settings in peripheral blood immunophenotyping experiments. (A) First, the viable mononuclear cell population is gated (P1) based on its position on the FSC vs SSC plot. **(B)** The P1 gated events are subjected to further gating to include singlets but exclude doublets (P2). **(C)** For immunophenotypic analysis of CLL cells, events are displayed on a CD19 vs CD20 plot, and a third gate (P3) applied to include CLL cells but exclude non-malignant B cells and CD19-negative mononuclear cells. The P1 + P2 + P3 gated events are displayed in black, while the P1 + P2 gated events that have fallen outside the P3 gate are displayed in grey. **(D)** The gated CLL singlet population (in black) is then analysed for the expression of various markers (e.g. ZAP-70 and Ki-67). **(E)** For immunophenotypic analysis of T cells, further gates (P3, and Q1-Q4) are applied to identify the singlet CD3+ CD4+ (P1 + P2 + P3 + Q1, in dark green) and the CD3+ CD8+ (P1 + P2 + P3 + Q4, in red) populations. These populations are then analysed for the expression of various markers (e.g. CD27 and CD45RA). All events outside the P1 + P2 + P3 gate are displayed in grey.

2.4.3. Phosphoflow analysis of BCR signalling

All phosphoflow analysis was performed on fresh blood samples. The experimental setup consists of four tubes per CLL sample, labelled as: (A) no IgM or IgD stimulation; (B) IgM stimulation only; (C) IgD stimulation only; and (D) IgM and IgD stimulation. A blood volume containing 10^6 white blood cells was applied to each tube, and PBS was added such that the total volume in each tube was 189 µl. Thereafter, a master mix containing the following extracellular antibodies (BD Biosciences) were made and dispensed to each tube:

CD20	APC-H7	5 µl per tube
CD19	PE-Cy7	1 µl per tube
CD5	PerCP-Cy5.5	5 µl per tube

The tubes were incubated in darkness at room temperature for 30 minutes, following which the cells in each tube were stimulated with 8 µl (to produce a final concentration of 20 µg/mL) of either anti-human IgM $F(ab')_2$ (Southern Biotech; tube B), anti-human IgD $F(ab')_2$ (Southern Biotech; tube C) or both (tube D), for 2 minutes in a 37°C water bath. Immediately after the 2 minute incubation, cells were fixed by adding 1 ml of pre-warmed Lyse/Fix buffer (BD Biosciences) and incubated in the water bath for a further 10 minutes. This incubation duration was adopted based on time course experiments showing that maximal effect of IgM/IgD stimulation was reached at 2 minutes.

After centrifugation to remove the fixative, cells were washed in 1ml PBS, and then permeabilised by adding 1 ml of Perm/Wash buffer (BD Biosciences), followed by 15 minutes' of incubation at room temperature. Cells were then washed again in Perm/Wash, after which a master mix containing the following intracellular phosphoantibodies (BD Biosciences) were made and dispensed to each tube:

Akt (pS473)	BV421	3 µl per tube
Syk (pY348)	PE	20 µl per tube
Erk 1/2 (pT202/pY204)	Alexa Fluor 488	20 µl per tube

Following incubation with these antibodies in darkness at room temperature, cells were washed with FACSFlow/BSA, and resuspended in 200 µl of FACSFlow for acquisition on an LSR Fortessa. A minimum of 200,000 events were recorded.

Data Analysis **(Figure 3.10A).** Cells were gated on the live, singlet, CD19+ CD20-low CLL population using the methodology outlined in section 2.4.2. Histograms corresponding to each phosphoprotein were then constructed. For each phosphoprotein, the positive vs negative gate was set such that 99% of unstimulated (tube A) cells would fall within the negative gate. The CD19− CD5+ T cell population was used as an internal negative control.

2.4.4. Purity confirmation of sorted cellular populations

This was carried out on the BD Accuri C6 flow cytometer using a combination of CD19 PE-Cy7, CD5 FITC and CD3 APC antibodies (all from eBiosciences). Antibody staining, acquisition and exclusion of dead cells, cellular debris and doublets were performed as described in section 2.4.2. The purity of the sorted CLL population was determined from the proportion of the remaining cells that were CD19+ CD5+. An illustrative example is provided in **Figure 2.1**.

2.4.5. Cell cycle analysis

Cell cycle analysis in response to drug treatment was performed as part of the ATR inhibitor study. Harvested cells were fixed and permeabilised in ice-cold 80% ethanol and stored overnight at −20°C. On the following day, the cells were washed in PBS, and then resuspended in 100 µl PBS. Thereafter a mastermix was prepared containing 2 µl of 1 mg/mL PI stock solution (Sigma) and 5 µl of 20 mg/mL PureLink RNase A (Invitrogen) per

sample. Seven µl of the mastermix was added to each sample, such that the final concentration of PI was 20 µg/mL and the final concentration of RNase A was 1 mg/mL. PI binds to cellular DNA, and therefore measurement of its level reflects the position of a cell within the cell cycle (i.e. G0/G1 phase: 2N; S phase: 2N-4N; G2/M phase: 4N). RNase A was added to prevent any binding of PI to double-stranded RNA. The samples were incubated in darkness at room temperature for 15 minutes, prior to acquisition on an Accuri C6 flow cytometer.

A minimum of 100,000 events were analysed. Following the exclusion of doublets and cellular debris, the events were displayed on a PI histogram for analysis. All cell cycle experiments were performed in triplicates.

2.5. DNA and genomic analysis

2.5.1. SNP array analysis

SNP array genotyping was provided by University College London (UCL) Genomics. Ten µl of DNA per sample at 50 ng/µl was submitted to UCL Genomics for genotyping on a HumanCoreExome BeadChip array (Illumina). The array contains oligonucleotide probes corresponding to >500,000 SNP-containing DNA sequences throughout the genome. The preparation of the array was carried out according to the Infinium High Throughput Screening (HTS) Assay protocol (Illumina).

Briefly, in a deep well plate 200 ng of DNA was whole genome amplified overnight (at 37°C for 20-24 hours), then fragmented (at 37ºC for 1 hour and 15 minutes in a hybridisation oven), precipitated and resuspended in hybridisation buffer. Using a liquid handling robot (Freedom Evo, Tecan Ltd), samples were hybridised onto the array containing oligonucleotide probes and incubated at 48°C for 16-24 hours. Unhybridised and non-specifically hybridised DNA was washed away. Using the captured DNA as a template, a single base, conjugated to a fluorophore, was then added to the end of the DNA-bound oligonucleotide probes on the array. Finally, the array was scanned using an iScan scanner with autoloader (Illumina). This involves using a laser to excite the fluorophore of the single-base extension on the oligonucleotide probes, and the image of light emitted from the fluorophores was captured and recorded by the scanner. This process allows the genotype to be determined for each of the markers contained within the array.

Raw data was sent by UCL Genomics for analysis using the GenomeStudio software Genotyping Module v.3.1 (Illumina) and OncoSNP v2.1. Log R ratio and B allele frequency values were generated across all 23 chromosome pairs. The log R ratio reflects the intensity of the signal observed at a particular SNP, compared to the expected intensity.

The log R ratio is normally zero, and any deviation above or below this reflects genomic duplication or deletion respectively at that particular position. The B allele frequency, on the other hand, reflects the ratio of the intensity of the two alleles (A and B) at the specific SNP. This is normally 0.5, and deviations from this value would be seen in duplications or deletions. However, such deviations in B allele frequency may also be seen in the presence of a normal log R ratio, in cases where there is copy-neutral loss of heterozygosity **(Figure 2.4)**.

2.5.2. *IGH* sequencing

Initial PCR. The rearranged *IGH* gene was amplified from genomic DNA extracted from MACS-sorted CLL cells (section 2.1.5) using the BIOMED-2 framework region 1 (FR1) multiplexed primers (Sigma) and a J_H consensus primer (Sigma) (van Krieken et al., 2007):

JH consensus	5' CTT ACC TGA GGA GAC GGT GAC C 3'
FR1 VH1	5' GGCCTCAGTGAAGGTCTCCTGCAAG 3'
FR1 VH2	5' GTCTGGTCCTACGCTGGTGAAACCC 3'
FR1 VH3	5' CTGGGGGGTCCCTGAGACTCTCCTG 3'
FR1 VH4	5' CTTCGGAGACCCTGTCCCTCACCTG 3'
FR1 VH5	5' CGGGGAGTCTCTGAAGATCTCCTGT 3'
FR1 VH6	5' TCGCAGACCCTCTCACTCACCTGTG 3'

A PCR mastermix was made containing: 1x PCR buffer, magnesium chloride (2 mM), deoxyribonucleotide (dNTP; 0.125 mM) and Taq polymerase (1 unit), all from Applied Biosystems, and 20 mM of each forward primer (FR1) and the reverse (J_H) primer. Twenty-four µl of the mastermix was dispensed to each PCR tube, following which 1 µl of DNA at 20-100 ng/µl was added. PCR was performed on a Veriti thermal cycler (Applied Biosystems) using the following settings: 95°C for 4 minutes, then 95°C for 30 seconds,

Figure 2.4

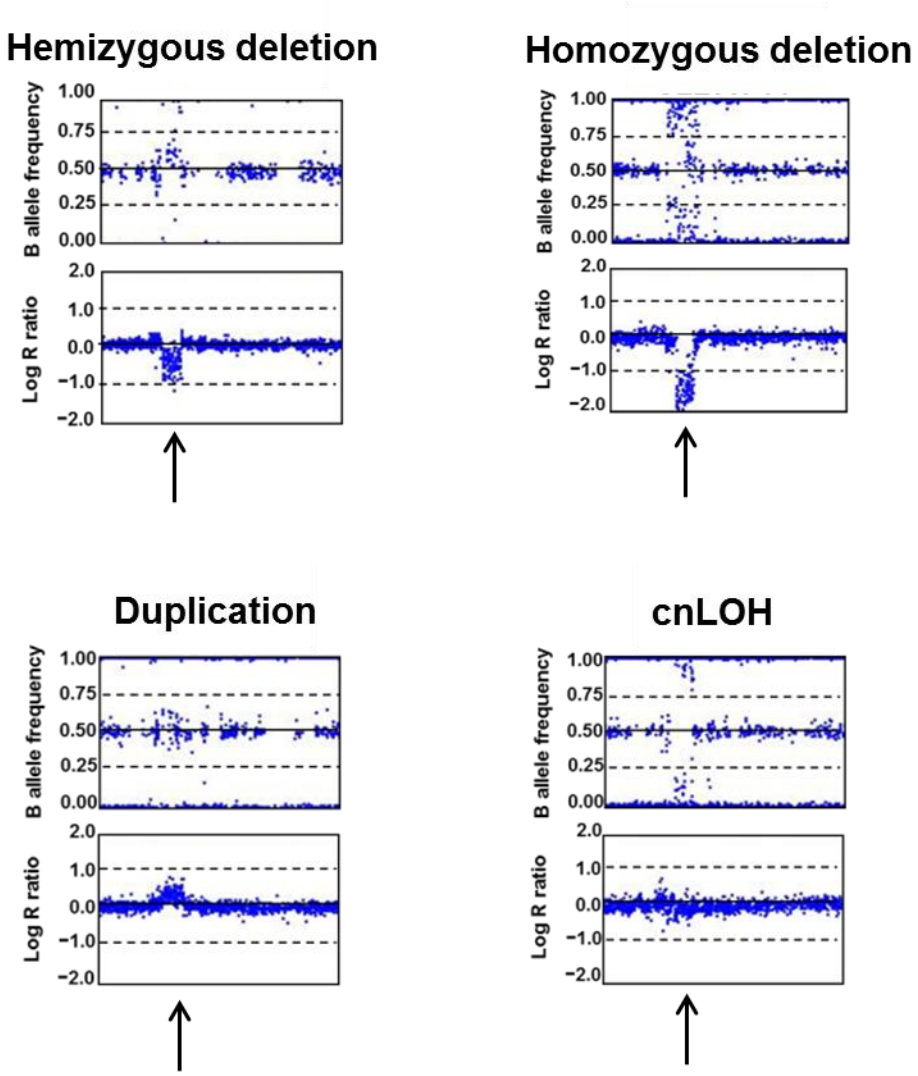

Copy number alterations detectable by SNP array analysis. Examples of copy alterations detectable by SNP array analysis are shown. These include hemizygous deletion (top left), homozygous deletion (top right), hemizygous duplication (bottom left) and copy-neutral loss of heterozygosity (cnLOH, bottom right). Intraclonal heterogeneity is evident in these examples with only a proportion of tumour cells harbouring deletion or duplication.

58°C for 30 seconds and 72°C for 45 seconds repeated 37 times, and finally 72°C for 7 minutes.

Gel electrophoresis and extraction. Three µl of the PCR product was mixed with 3 µl of a 1:5000 dilution of the SYBR Green nucleic acid gel stain (Invitrogen). The mixture was ran on 1% agarose gel (prepared by dissolving 1 g of agarose in 100 ml of Tris/Borate/EDTA (TBE) buffer) at 130V for 30 minutes, with a DNA ladder (Invitrogen). The PCR products were then visualised in an ultraviolet transilluminator, and the band with the appropriate product size was excised from the gel. DNA was extracted from the excised gel using a QIAquick gel extraction kit (Qiagen) according to the manufacturer's instructions. Briefly, buffer QG was added to the gel and the sample incubated at 50°C for 10 minutes to dissolve the gel. Isopropanol was then added to the sample and the mixture transferred to a QIAquick spin column. The flow through was discarded after centrifugation of the spin column and further QG buffer was applied. Thereafter the spin column was washed with buffer PE, and the DNA was eluted in 50 µl of buffer EB.

Sequencing. Gel extracted PCR products were then subjected to a sequencing PCR reaction using a BigDye Terminator v3.1 cycle sequencing kit (Applied Biosystems). The BigDye reagent consists of a mixture of dNTPs, fluorescently labelled dideoxynucleotides (ddNTPs) and Taq polymerase. In this PCR reaction, sequence extension by the addition of dNTPs proceeds as usual until the DNA polymerase inserts a fluorescently labelled ddNTP, which stops the chain elongation process. This generates DNA sequences with one of four coloured ddNTPs. A BigDye mastermix was produced containing the BigDye reagent, 1x PCR buffer and the J_H primer (at 0.06 µM). One µl of the gel extraction product was added to 19 µl of the mastermix, and BigDye PCR was performed on a Veriti thermal cycler: 96°C for 2 minutes, followed by 96°C for 10 seconds, 50°C for 5 seconds and 60°C for 4 minutes repeated 29 times.

Following the PCR reaction, the fluorescently labelled DNA product was precipitated with 50 µl of 100% ethanol and 2 µl of 3M sodium acetate at room temperature for 30 minutes, and then centrifuged at 2000 rpm for 20 minutes. This removes any unwanted products, such as residual primers, dNTPs and ddNTPs, form the sequencing reaction. Finally, the DNA product was washed twice in 70% ethanol, and allowed to air dry for 30 minutes, before being Sanger sequenced on an ABI 3500 capillary sequencer (Applied Biosystems). Prior to loading onto the sequencer, 10 µl of HiDi-Formamide (Applied Biosystems) was added to the samples, which were then denatured by heating to 95°C for 5 minutes. Capillary electrophoresis allows separation of the different-sized DNA fragments within the sample. Base calling was made on the basis of the specific fluorescence emissions detected from the ddNTP ends of each DNA fragment, upon laser excitation.

For the spontaneous CLL regression cases, all *IGH* sequencing results generated by myself were independently validated by Dr Paul Evans (HMDS, Leeds) using V_H leader peptide primers combined with a consensus J_H primer (Rosenquist et al., 2017). The *IGHV* sequences were aligned and analysed using the international immunogenetics information (IGMT) online database and analytical platform. These sequences were also checked for *IGHV* stereotypy using the online ARResT/AssignSubsets tool (Bystry et al., 2015).

2.5.3. Whole exome sequencing

Qubit-quantified DNA from sorted CD19+ CD5+ CLL cells or the granulocyte-containing fraction isolated during Lymphoprep (as germline controls) was used to produce paired-end libraries for WES. Library preparation was carried out using the Nextera Rapid Capture Exome Kit (Illumina) according to the instructions detailed in the Nextera Rapid Capture guide (Illumina). DNA from each sample was first diluted in 10 mM Tris-Cl buffer (pH 8.5) to produce a final volume of 10 µl at 5 ng/µl. The diluted DNA sample was then subjected to the following steps in sequential order **(Figure 2.5)**:

Figure 2.5

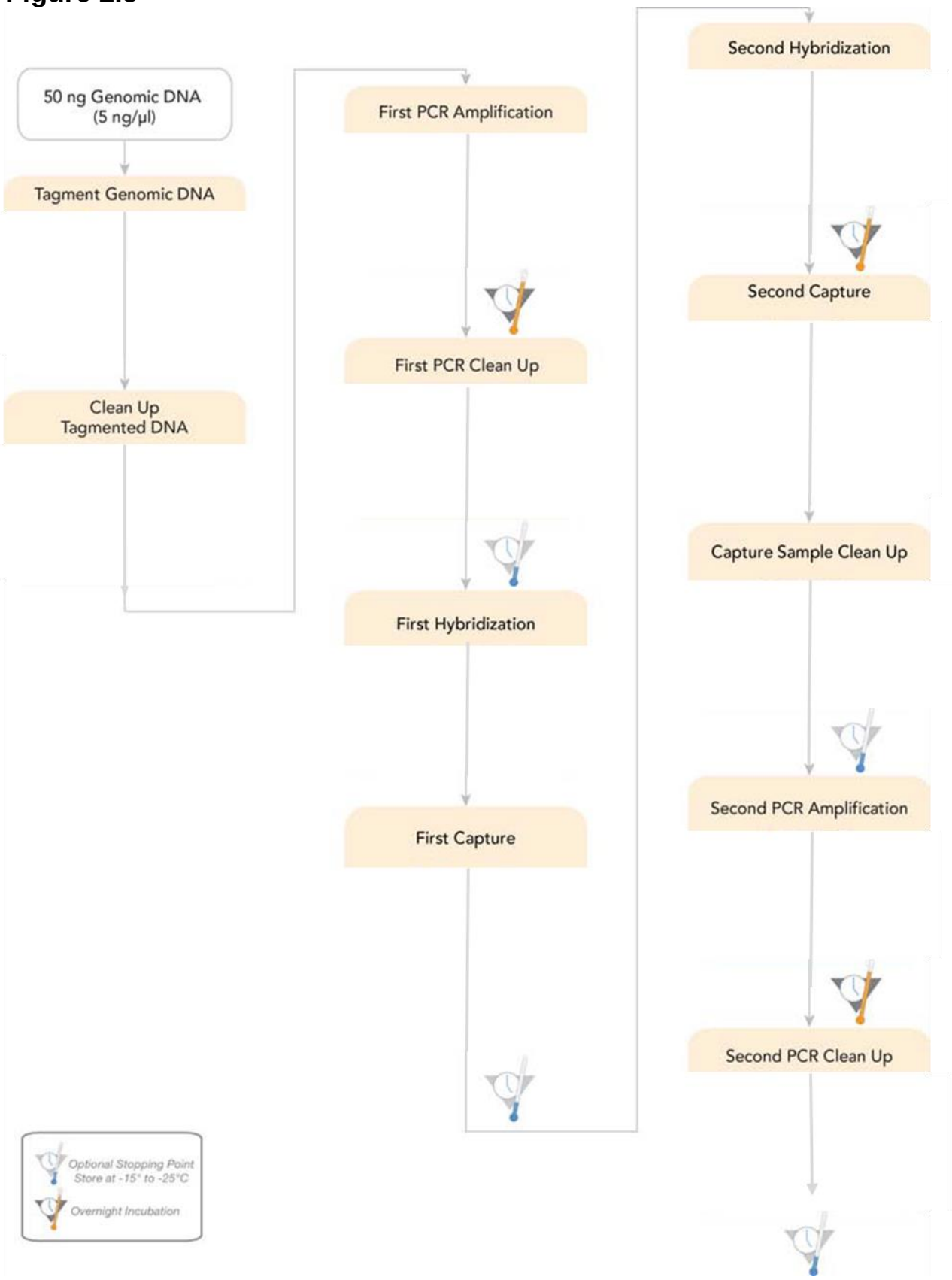

Library preparation workflow for whole exome sequencing. Reproduced with minor modification from the Nextera Rapid Capture Guide (Illumina, February 2013).

Tagmentation. Tagmentation is a process through which the genomic DNA is fragmented and adapter sequences added to the ends of the DNA fragment, thereby allowing primer binding during subsequent PCR amplification. Twenty five µl and 15 µl respectively of tagment DNA buffer and tagment DNA enzyme was added to the DNA sample in a deep-well plate. The plate was then heated for 10 minutes at 58°C, following which 15 µl of stop tagment buffer was added and the sample incubated for another 4 minutes. Thereafter, the tagmented DNA was purified from the tagment enzyme in a clean-up process. This involves adding sample purification beads which bind to the tagmented DNA, and washing each well of the plate with 80% ethanol with the plate placed on a magnetic stand. The tagmented DNA was then resuspended in 22.5 µl of resuspension buffer, and the sample purification beads were removed.

First PCR Amplification. In this step, the tagmented DNA is PCR amplified. During the PCR amplification process, an index is added to the DNA to identify the sample, and common adaptors are added to facilitate subsequent cluster generation and sequencing. Five µl each of the corresponding index 1 and index 2 primers, and 20 µl of the Nextera library amplification mix were added to the purified tagmented DNA. PCR was performed on a Veriti thermal cycler according to the following programme: 72°C for 3 minutes and 98°C for 30 seconds, then 98°C for 10 seconds, 60°C for 30 seconds and 72°C for 30 seconds repeated 10 times, and finally 72°C for 5 minutes. Thereafter, the PCR amplified DNA sample was purified in a clean-up process using sample purification beads as described above. The PCR-amplified sample, now known as a DNA library, was then quantified using Qubit. Finally, 500 ng of DNA each from 8 DNA libraries with different indices were combined into a volume totalling 40 µL.

Hybridisation and capture. Probes that target specific coding DNA regions bind to the DNA library in a process known as hybridisation. The probe-hybridised DNA is then selectively captured, allowing enrichment of the DNA library for coding exomes. Ten µl of coding exome oligos and 50 µl of enrichment hybridisation buffer were added to the pooled

DNA libraries. The pooled libraries were then hybridised to the oligos in a Veriti thermal cycler using the following programme: 95°C for 10 minutes, followed by 18 cycles of 1 minute incubations, starting at 94°C, and decreasing 2°C each cycle. Next, 250 µl of streptavidin magnetic beads were added to the probe-hybridised libraries. Following 25 minutes of incubation which allowed capture of the probe-hybridised libraries by the streptavidin magnetic beads, the supernatant was removed with the sample placed on a magnetic stand. Two hundred µl of enrichment wash solution was subsequently added to the bead-captured libraries and incubated at 50°C for 30 minutes, after which the sample was returned to the magnetic stand and the wash solution was removed. This process was repeated for a total of two washes. Finally, the exome-enriched libraries were separated from the streptavidin beads by the addition of enrichment elution buffer to the sample, and by the subsequent removal of the supernatant containing the exome-enriched libraries while the sample was placed on a magnetic stand.

This hybridisation and capture process was repeated a second time using the eluted DNA library from the first enrichment. This allowed enhanced exome enrichment, thus ensuring that the libraries contained specifically the coding DNA regions. Prior to the second PCR amplification, the sample containing exome-enriched libraries was purified in a clean-up process using sample purification beads as described above.

Second PCR amplification. This final PCR step amplifies the exome-enriched libraries. Five µl of the PCR primer cocktail and 20 µl of the Nextera library amplification mix were added to the sample containing exome-enriched libraries. PCR was performed on a Veriti thermal cycler according to the following programme: 98°C for 30 seconds, then 98°C for 10 seconds, 60°C for 30 seconds and 72°C for 30 seconds repeated 10 times, and finally 72°C for 5 minutes. Thereafter, the sample was purified in a clean-up process using sample purification beads described above, and quantified using Qubit. In addition, the sample was assessed for quality using TapeStation 2200 (Agilent Technologies). A distribution of DNA fragments ranging from 200 to 1000 base pairs was considered acceptable (**Figure 2.6A**).

Figure 2.6

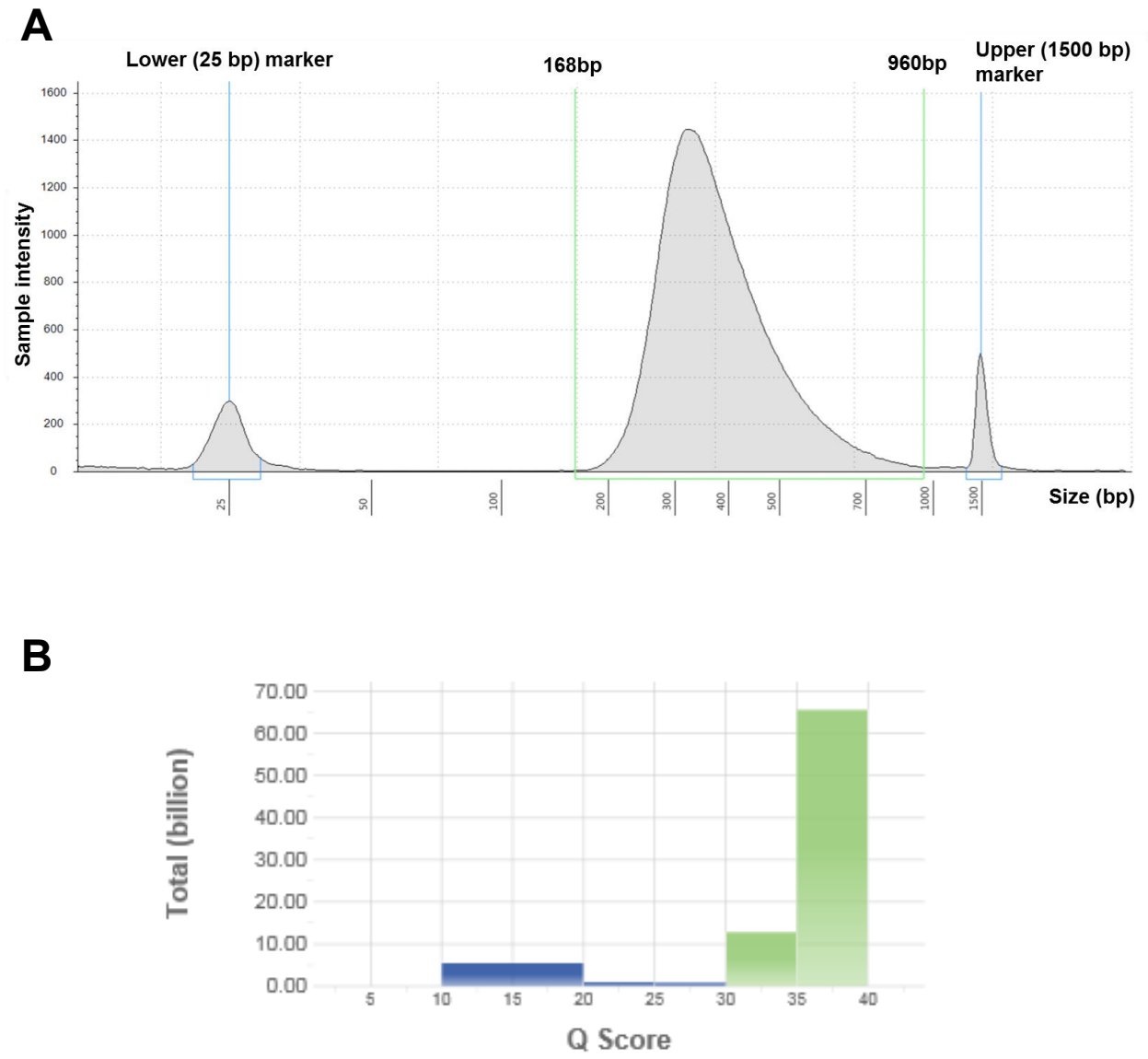

Quality checks following library preparation and sequencing. **(A)** TapeStation trace showing the majority of DNA fragments in the sequencing library falling within the 200 to 1000 base pairs (bp) range. **(B)** The Phred quality score (Q score) after the sequencing run showing a Q score of >30 for the majority of bases.

Exome sequencing. The prepared WES library pool from 8 DNA libraries was submitted to the University of Birmingham genomics facility for sequencing using the NextSeq 500/550 High Output Kit v2 (Illumina). The sequencing process involved loading the pooled library onto the reagent cartridge which then flows through the lanes of the flow cell. The flow cell is filled with a lawn of oligonucleotides, which binds to the adaptor region of the DNA fragments in the library. Using the DNA fragment as a template, the DNA polymerase then adds complementary bases to the end of the oligonucleotide, thus creating a sequence that is complementary to the DNA fragment. The double-stranded DNA produced is then denatured with the original DNA fragment being washed away, leaving behind the newly created complementary strand. The strand is then amplified through bridge amplification, in which the strand bends over before being duplicated through the activity of the DNA polymerase. This process is repeated simultaneously throughout the flow cell, generating clusters of strands, and resulting in the amplification of all DNA fragments within the library pool. These amplified strands in turn serve as a template for a process known as sequencing by synthesis. In this process, fluorescently-tagged bases complementary to the template are added to the elongating DNA chain. After the addition of each nucleotide, the strands are excited by a light source, resulting in emissions from the base-specific fluorophores which are then detected by the sequencer. A base is assigned according to the specific emissions from the fluorophore. Each time a strand is sequenced is known as a read. This sequencing process occurs simultaneously in all clusters throughout the flow cell, and is repeated numerous times, resulting in all DNA fragments being sequenced. Altogether 8 DNA samples were sequenced within a single flow cell, allowing an average of 50 million reads per sample.

Following each sequencing run, a Phred quality score (Q score) was generated by the sequencer which reflects the probability of a base calling error (**Figure 2.6B**). A score of 30 or above, which indicates a base calling accuracy of 99.9%, for the majority of reads would be considered acceptable. The sequencing output (FASTQ) files were downloaded

from my BaseSpace (Illumina) account, and uploaded to a shared folder within the University of Birmingham Linux-based high performance computing cluster known as BlueBEAR for bioinformatics analysis.

2.5.4. Bioinformatics analysis of whole exome sequencing data

Bioinformatics analysis of WES data was carried out by Dr Anshita Goel, Dr Archana Sharma-Oates and Prof. Jean-Baptiste Cazier. The major steps are briefly summarised here and illustrated in **Figure 2.7A**.

Raw FASTQ files were first processed using FastQC which makes diagnostic plots for indicators such as base quality distribution, GC content, sequence length distribution and adapter content. Trimmomatic was then used to remove adaptors and trim low quality bases from sequence end. Reads were aligned and mapped to the human reference genome (GRCh37) using Burrows-Wheeler Aligner (BWA). Picard tools was used to coordinate sort the aligned reads, mark PCR duplicates and create the BAM file (a text file containing the sequence alignment data) that would be used as input to the Genome Analysis Tool Kit (GATK). Local realignment and base quality score recalibration was performed to refine the alignments around known variations (indels and SNPs) using GATK. Subsequently, somatic mutations were identified independently through two separate programmes, MuTect and Platypus, by comparing paired tumour (i.e. CLL) and germline (i.e. granulocyte) samples. The somatic mutations identified were annotated using Variant Effect Predictor (VEP), SIFT and Polyphen, and only variants that were predicted to be of high or moderate impact by VEP and functionally deleterious by SIFT and Polyphen were retained. Finally, MutSigCV was used to identify genes with statistically significant mutation occurrence in the CLL whole exome sequencing dataset. A p value threshold of <0.05 was used to identify significantly mutated genes.

Figure 2.7

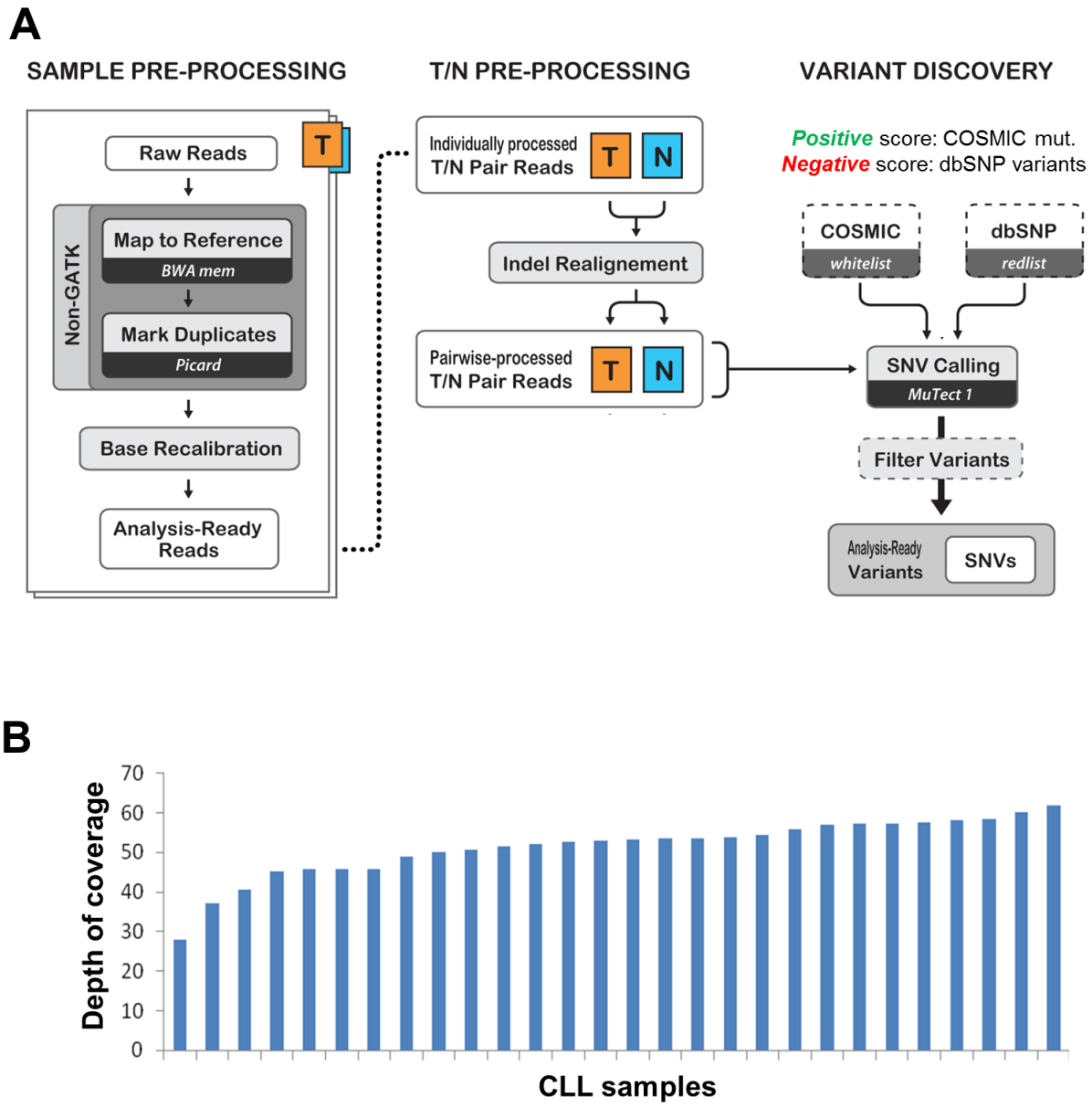

Bioinformatics analysis of whole exome sequencing data. **(A)** Schematic diagram showing the major steps involved in the processing of raw exome sequencing data. MuTect utilises a scoring system that takes into account of whether a variant is present in the COSMIC database of known somatic mutations or the dbSNP database of known polymorphisms. The former confers a positive score whereas the latter a negative score. Thus, polymorphisms that are unlikely to be genuine mutations are filtered out. Reproduced with modification from *Best Practices for Somatic SNPs in Whole Genomes and Exomes*, GATK website, Broad Institute, https://software.broadinstitute.org/gatk/best-practices. **(B)** Diagram showing the mean depth of coverage of the CLL samples to be approximately 50x.

2.6. Analysis of telomeres and cellular senescence

2.6.1. Telomere length analysis

Allele-specific single telomere length analysis (STELA) was carried out at the University of Cardiff by Prof. Duncan Baird and his team, as previously described (Lin et al., 2010). This is a single molecule PCR technique that analyses the length of specific telomere repeat regions in individual single cells. The technique employs an adaptor that attaches to the telomeric ends, as well as PCR primers that bind to the adaptor and to a known DNA sequence in the sub-telomeric region of chromosome arms Xp and Yp. In brief, multiple PCR steps were carried out on 10 ng of DNA in the presence of Taq (ABGene) and Pwo polymerase (Roche), the Telorette2 linker (adaptor), the sub-telomeric primer XpYpE2 and the Teltail primer which binds to the Telorette2 linker. The PCR products were resolved by agarose gel electrophoresis, and detected by Southern blot hybridisations using α-^{33}P–labelled TTAGGG repeat probes (GE Healthcare), sub-telomeric probes and probes recognising the molecular weight markers (Bio-rad). The Southern blot hybridisations were visualised by a phosphoimager (GE Healthcare), with each single band on the blot representing a single telomeric molecule. Hence, the molecular weight of a band reflects the telomere length of Xp/Yp in a cell.

2.6.2. Analysis of telomerase activity

Analysis of telomerase activity was carried out using the TeloTAGGG telomerase PCR enzyme-linked immunosorbent assay (ELISA) kit (Roche), which incorporates a telomeric repeat amplification protocol (TRAP) followed by detection of the PCR amplified telomerase-mediated elongation products using ELISA. The assay was performed according to the manufacturer's instructions, as outlined below:

DNA elongation and PCR amplification. The addition of telomeric repeats (TTAGGG) to telomeric ends is dependent on the activity of telomerase. Therefore, the amount of TTAGGG added to a telomerase substrate would reflect the level of telomerase activity. A total of 10^6 MACS-sorted CD19+ CD5+ CLL cells were used for each sample. These cells were pelleted and washed in PBS. The pelleted cells were then lysed in 200 µl of lysis reagent, and incubated on ice for 30 minutes. The lysate was centrifuged at 14,000 rpm following which the supernatant was collected and used for the TRAP reaction. The TRAP reaction mixture contains the biotin labelled telomerase substrate P1-TS (5'-Biotin-AATCCGTCGAGCAGAGTT-3'), the reverse P2 primer (5'-CCCTTACCCTTACCCTTAC CCTAA-3'), nucleotides and Taq polymerase. Three µl of the cell lysate was added to 25 µl of the TRAP reaction mixture in a PCR tube, and sterile water added to a final volume of 50 µl. The sample was first incubated at 25°C for 30 minutes in a Veriti thermal cycler to allow the addition of telomeric repeats to the 3' end of P1-TS by the telomerase present in the sample. Thereafter, the sample was heated to 94°C for 5 minutes to inactivate the telomerase. Finally, PCR amplification was performed, with 30 cycles of 94°C for 30 seconds, 50°C for 30 seconds and 72°C for 90 seconds, followed by 72°C for 10 minutes. Cell lysates that were heat-treated for 10 minutes at 85°C, which inactivates the telomerase, were used as negative controls. The positive control cell extract supplied with the kit, and the Mec1 cell line, were used as positive controls.

Hybridisation and ELISA. Five µl of the PCR product per sample was denatured by incubating with 20 µl of denaturation reagent at room temperature for 10 minutes. Hybridisation buffer (225 µl) was then added and 100 µl of the mixture was transferred to a streptavidin-coated microplate well, which was incubated at 37°C in a shaker (300 rpm) for 2 hours. This allows the biotin-labelled elongation products to adhere to streptavidin, and the digoxigenin-labelled telomeric repeat detection probe, contained within the hybridisation buffer, to bind to the TTAGGG repeats. Subsequently, the hybridisation buffer was removed and the wells on the microplate were washed three times with washing buffer. The

immobilised PCR product was then detected by the addition of 100 µl of a peroxidase-conjugated antibody against digoxigenin. Following 30 minutes' incubation and further washing steps, the elongation products were visualised by the addition of tetramethylbenzidine which was converted to a coloured product by peroxidase. A stop reagent was added after 10 minutes, and the absorbance of the samples were detected at 450 nm using an iMark microplate absorbance reader (Bio-rad). The mean absorbance of the blank wells were subtracted form all other wells, and the mean absorbance of the negative controls were subtracted form those of the samples. Absorbance values of <0.25 and >1.5 were considered acceptable for the negative and positive controls respectively.

2.6.3. β-galactosidase assay

β-galactosidase expression and activity at pH 6 is a characteristic unique to senescent cells (Dimri et al., 1995). β-galactosidase hydrolyses β-D-galactosides (e.g. X-gal) that may yield products emitting a specific colour (e.g. a blue precipitate), and can therefore be detected. A senescence β-galactosidase staining kit (Cell Signaling Technology) was used for this purpose. MACS-sorted CD19+ CD5+ CLL cells were plated onto a 96-well plate at 10^5 cells per well. The cells were then fixed in fixative solution for 15 minutes at room temperature. During this time, the β-galactosidase staining solution was prepared by combining X-gal stock solution and other staining solutions as per the supplier's instructions, and adjusted to a pH of 6. The plate was washed two times with PBS, following which 200 µl of the prepared galactosidase staining solution was added to each well. The plate was incubated at 37°C in a dry incubator overnight, in the absence of CO_2 which might alter the pH of the staining solution. Thereafter, with the staining solution still in place, the cells were examined under an inverted microscope (Nikon) for the development of a blue colour.

2.7. Cytotoxicity assays

For the assessment of drug-induced cytotoxicity carried out as part of the ATR inhibitor study, two different methodologies were employed: the CellTiter-Glo luminescent cell viability assay (Promega), and a flow cytometric method using PI. The former is a high-throughput, albeit indirect, method of assessing the number of viable cells in multiple samples, and was used in all experiments involving cell lines. However, due to the presence of CD40L-expressing MEFs within the primary CLL co-culture system, the CellTiter-Glo assay could not be used in experiments involving primary CLL cells. Therefore, for these experiments, the flow cytometric method was employed.

2.7.1. CellTiter-Glo luminescent cell viability assay

The CellTiter-Glo luminescent cell viability assay utilises a thermostable luciferase, which catalyses a reaction involving the mono-oxygenation of luciferin, producing a luminescent signal in this process. This reaction is dependent on adenosine triphosphate (ATP), and the intensity of the luminescent signal is directly proportional to the amount of ATP present. Since the absolute quantity of ATP within a sample is directly proportional to the number of viable, metabolically active cells, it follows that the luminescent signal intensity must also be proportional to the number of viable cells in the sample.

Cell density. Cells were plated on a flat-bottomed, opaque-walled 96-well microplate, with each well capable of holding a maximum volume of 200 µl. The plating density of the CII and Mec1 cell line was tested in a pilot experiment using a variety of plating densities, and the optimal plating density for both CII and Mec1 cells was found to be 10^4 cells per well. When analysed after 4 days of incubation, such a plating density produced

the maximum luminescent signal, whereas increasing the plating density beyond this did not improve the signal. A plating density of 10^4 cells per well was therefore adopted for all subsequent experiments. Cells were resuspended in RPMI-1640/10% FBS at 10^5 cells/mL, and 100 µl of cells were dispensed into each well using a multichannel pipette. The exception to this was the outer wells forming the perimeter of the microplate, which were filled instead with 200 µl of culture medium. The purpose of this was to reduce evaporation from the sample wells during culture which could otherwise affect result interpretation.

Drug dilutions. For experiments involving a single drug, a doubling dilution of 9 drug doses was used to construct the dose response curve. A stock solution containing twice the highest drug concentration was prepared by dissolving the appropriate amount of drug in RPMI-1640/10% FBS. A two-fold serial dilution in RPMI-1640/10% FBS was then carried out starting with the stock solution. Therefore, for each dose, a solution containing twice the desired drug concentration was made. One hundred µl of the 2x drug solution was dispensed and mixed with the 100 µl of cells in each well, such that the final drug concentration was 1x. Triplicate wells were used for each drug dose, and triplicate wells containing untreated cells were included as negative control.

For experiments involving a combination of two drugs, a solution containing four-fold the desired drug concentration was made for each dose of the two drugs. Fifty µl of the 4x solution of each drug was added to 100 µl of cells in each well, such that the final concentration of each drug was 1x. Triplicate wells were used for each dose combination. In addition, single-agent treated wells and untreated negative controls were included. An example microplate setup for experiments involving a single drug and drug combinations are displayed in **Figure 2.8A** and **Figure 2.8B** respectively.

Plate reading and analysis. The microplate was incubated at 37°C with 5% CO_2 for 4 days, after which the plate was equilibrated at room temperature for 30 minutes.

Figure 2.8

A

	1	2	3	4	5	6	7	8	9	10	11	12
A	Blank	Blank	Blank	Blank	Blank	Blank	Blank	Blank	Blank	Blank	Blank	Blank
B	Blank	0 μM	0.125 μM	0.25 μM	0.5 μM	1 μM	2 μM	4 μM	8 μM	16 μM	32 μM	Blank
C	Blank									AZD6738		Blank
D	Blank	CII-*ATM*sh cell line										Blank
E	Blank	0 μM	0.125 μM	0.25 μM	0.5 μM	1 μM	2 μM	4 μM	8 μM	16 μM	32 μM	Blank
F	Blank									AZD6738		Blank
G	Blank	CII-*GFP*sh cell line										Blank
H	Blank	Blank	Blank	Blank	Blank	Blank	Blank	Blank	Blank	Blank	Blank	Blank

B

	1	2	3	4	5	6	7	8	9	10	11	12
A	Blank	Blank	Blank	Blank	Blank	Blank	Blank	Blank	Blank	Blank	Blank	Blank
B	Blank	0 μM	1 μM	2.5 μM	5 μM	10 μM	0 μM	1 μM	2.5 μM	5 μM	10 μM	Blank
C	Blank		Fludarabine					Fludarabine +				Blank
D	Blank							AZD6738 (1 μM)				Blank
E	Blank	0 μM	0.25 μM	0.5 μM	1 μM	2 μM	0 μM	0.25 μM	0.5 μM	1 μM	2 μM	Blank
F	Blank			4HC					4HC +			Blank
G	Blank							AZD6738 (1 μM)				Blank
H	Blank	Blank	Blank	Blank	Blank	Blank	Blank	Blank	Blank	Blank	Blank	Blank

Example microplate setups for CellTiter-Glo luminescent cell viability assay. (A) An example microplate setup involving a single drug. Isogenic CLL cell lines (CII-*ATM*sh and CII-*GFP*sh) were incubated in doubling dilutions of AZD6738. **(B)** An example microplate setup involving drug combinations. A single cell line was incubated with various doses of fludarabine or 4HC, with and without AZD6738 (1 μM). Triplicate wells were included for each drug dose or dose combination. Blank wells contained culture medium only.

Twenty µl of the CellTiter-Glo reagent was dispensed to each well using a multichannel pipette. The microplate was placed on an orbital shaker for 2 minutes to lyse the cells, after which it was incubated for 10 minutes at room temperature to stabilise the luminescent signal. Finally, the microplate was read in a luminescent plate reader (Bio-Tek). The mean luminescence of the medium-only wells were subtracted form all other wells, and the relative survival fraction at each drug dose was calculated through dividing the mean luminescence corresponding to the drug dose by the mean luminescence of the untreated controls.

2.7.2. Flow cytometric assessment of cell viability

Cytotoxicity assessments in primary CLL cells involved several experimental procedures carried out in succession. These were: (1) carboxyflourescein succinindyl ester (CFSE) labelling of CLL cells; (2) induction of CLL cell proliferation; (3) addition of drug or drug combination; (4) cell harvesting and labelling; and (5) flow cytometric analysis.

CFSE labelling. CLL cells were labelled with 5 µM CFSE (Cell Technologies). CFSE is a fluorescent dye that covalently binds to intracellular molecules. CFSE fluorescent intensity would be expected to halve with each cell division, and can therefore be used to confirm proliferation. To perform CFSE labelling, cells were first washed with serum-free PBS and up to 10^8 cells were resuspended in 1 ml serum-free PBS. Five µl of 1 mM CFSE was added to produce a final concentration of 5 µM, after which the cell suspension was incubated for 5 minutes at room temperature with gentle swerving. Following this, the labelling was stopped by adding 10 ml of RMPI-1640/10% FBS. Cells were then washed with RMPI-1640/10% FBS to remove unlabelled CFSE.

Induction of CLL cell proliferation. CFSE-labelled primary CLL cells were induced to proliferate in transparent flat-bottomed 96-well microplates using the CD40L/IL-21 co-culture system described in section 2.3.2. In pilot experiments, the optimal plating density

was found to be 10^5 CLL cells and 10^4 MEFs per well **(Figure 2.9A)**. Increasing the plating density or the ratio of MEFs to CLL cells did not improve CLL cell viability or the number of viable CLL cells. An 8-day co-culture period was used, and shortening this to 6 days in pilot experiments did not improve CLL cell viability. Hence, all subsequent experiments adopted a plating density of 10^5 CLL cells and 10^4 MEFs, and a co-culture period of 8 days. This includes 4 days to allow CLL cells to proliferate before the addition of drugs, and 4 days after drug treatment. Similar to the setup for CellTiter-Glo experiments, the outer wells forming the perimeter of the microplate were not plated with cells, but rather were filled with 200 µl of culture medium.

Addition of drug or drug combination. Following 4 days of CLL cell culture within the CD40L/IL-21 co-culture system, the microplates were examined under an inverted microscope to confirm CLL proliferation. Proliferating CLL cells appeared as cells of varying sizes congregating around the adherent fibroblasts. One hundred µl of culture medium was removed from each well without disrupting the CLL cells. This was replaced by 100 µl of drug or drug combination, prepared in the same way as for the CellTiter-Glo experiments described in section 2.8.1 **(Figure 2.9B)**. Similar to the CellTiter-Glo experiments, triplicate wells were used for each drug dose or dose combination, and untreated controls were included. The CellTiter-Glo experimental layouts shown in **Figure 2.8** are also reflective of the microplate layout used for drug studies involving primary CLL cells. Following drug treatment, the cells were incubated at 37°C with 5% CO_2 for 4 further days.

Cell harvesting and labelling. CLL cells were harvested after a total of 8 days of culture. CLL cells were dislodged by gentle pipetting as described in section 2.3.2, and transferred to a new 96-well round-bottom microplate using a multichannel pipette. These cells were washed in PBS with 2% BSA, after which they were incubated in CD19 APC antibody (eBiosciences) for 30 minutes at 4°C. After a further wash in PBS/BSA, 10 µl of 10 µg/mL PI solution (Sigma) was dispensed to each well, and the microplate was immediately loaded onto the plate handler for automated acquisition using an Accuri C6 flow cytometer.

Figure 2.9

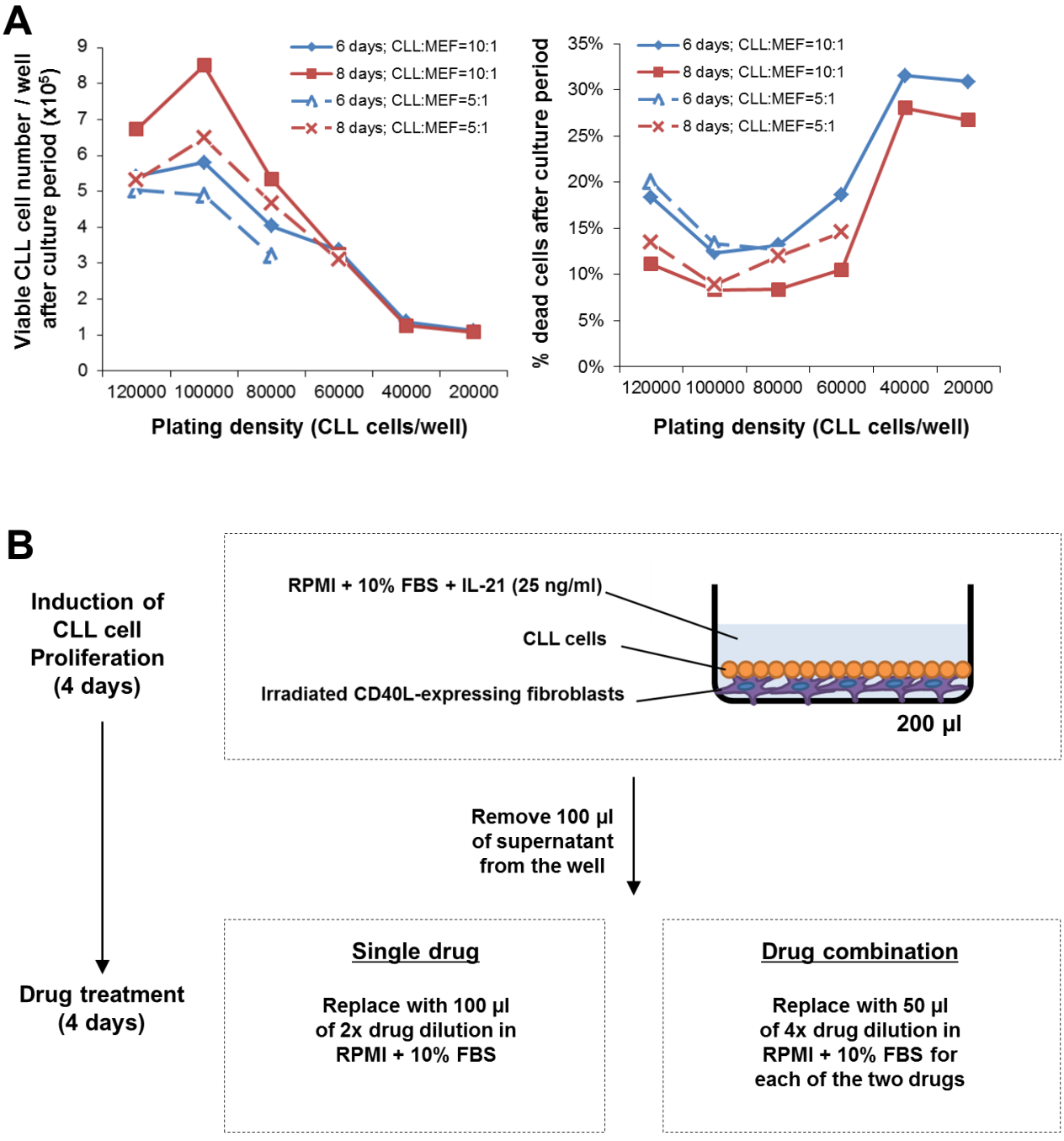

Drug cytotoxicity assays on primary CLL cells. (A) Results of optimisation experiments in 96-well microtitre plates showing the total viable CLL cell number per well (left panel) and the proportion of dead CLL cells (right panel) at the end of the culture period, with different initial plating densities, incubation durations (8 days vs 6 days) and ratios of CD40L-expressing MEFs to CLL cells (10:1 vs 5:1). A plating density was 10^5 CLL cells and 10^4 MEFs per well, and a total culture period of 8 days was found to be optimal. **(B)** Schematic diagram showing the key steps involved in the experimental setup for the assessment of drug cytotoxicity in primary CLL cells.

***Flow cytometric analysis* (Figure 2.10).** The flow cytometer was set up as described in section 2.4.1. A mixture of CFSE-labelled and unlabelled CLL cells was used as the compensation control for CFSE, whereas a mixture of fludarabine treated and untreated PI-labelled CLL cells was used as the compensation control for PI. Prior to sample acquisition, the flow cytometer was pre-programmed to acquire 20,000 gated events for each sample. Following the exclusion of doublets and debris (which had lower FSC and SSC compared to live cells), but not dead cells (which had lower FSC but similar or higher SSC compared to live cells) **(Figure 2.10A-B)**, the acquired events were displayed in a CFSE histogram. The rightmost peak represents non-cycling cells. Each cell division was accompanied by reduction in CFSE fluorescence intensity indicated by a shift of the peaks to its left. Cellular proliferation could therefore be confirmed using by the CFSE histogram which demonstrates successive reduction in CFSE fluorescence intensity **(Figure 2.10C)**. The CD19+ population that had undergone at least one round of cell division was gated in a CFSE vs CD19 plot **(Figure 2.10D)**, and the gated events were analysed on a PI histogram **(Figure 2.10E)**. The viability of each sample is calculated by: Viability = 1 – (% of PI positive events). The relative surviving fraction at each drug dose was calculated through dividing the mean viability corresponding to the drug dose by the mean viability of the untreated controls.

2.7.3. Calculation of drug combination indices

Drug doses which would produce 50% cell killing (EC_{50}) and drug combination indices (CI) were calculated using Calcusyn (Biosoft), which employs a mathematical modelling algorithm known as the median effect method (Chou and Talalay, 1984). Synergism was observed when the combined use of two drugs produced an effect exceeding the use of the two drugs separately (i.e. 1 + 1 > 2). Antagonism, on the other hand, was reported when the combined use of two drugs was less effective than either of

Figure 2.10

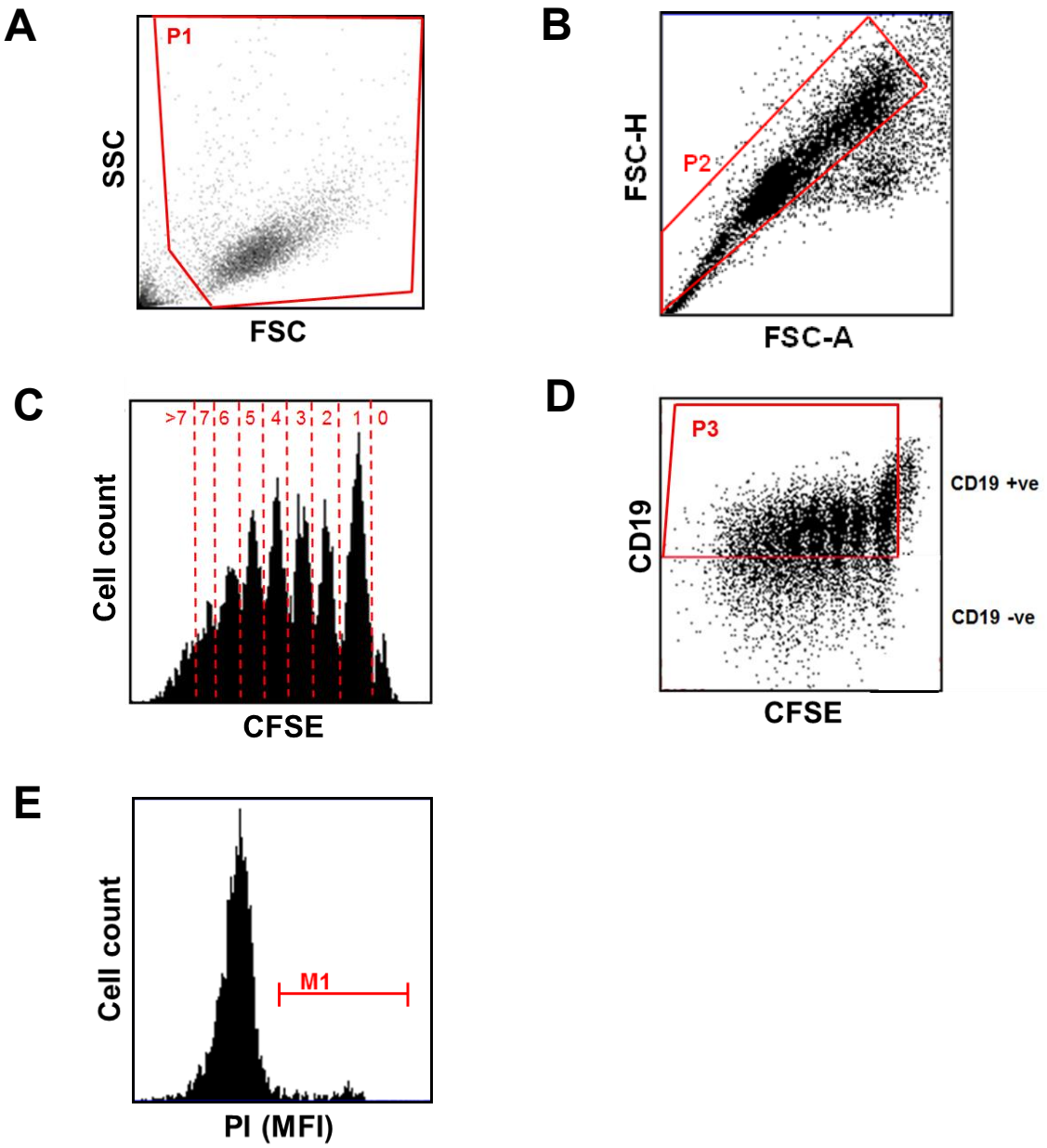

Gate settings in flow cytometric assessments of cell viability. **(A)** First, events on the FSC vs SSC plot are gated (P1) to exclude cellular debris. **(B)** The P1 gated events are subjected to further gating to include singlets but exclude doublets (P2). **(C)** Cellular proliferation can be confirmed on a CFSE histogram. Only P1 + P2 gated events are displayed. The rightmost peak represents non-cycling cells. Each cell division is accompanied by reduction in CFSE fluorescence intensity indicated by a shift of the peaks to its left. Each peak represents cells that have undergone a particular number of cell divisions, indicated on the top of the histogram (in red). **(D)** The P1 + P2 gated events are displayed in a CFSE vs CD19 plot, which is used to identify CLL cells (CD19+) that have undergone at least one round of cell division (P3). **(E)** The viability of the gated P3 population is analysed on a PI histogram. The PI positive events (dead cells) fall within the M1 gate and viability is calculated accordingly, i.e. viability = 1 – (M1 gated events/P3 gated events).

the two agents (i.e. 1+1 < 1) (Bijnsdorp et al., 2011). A list of CI values and their indications is provided below:

CI	<0.1	+++++	Very strong synergism
CI	0.1-0.3	++++	Strong synergism
CI	0.3-0.7	+++	Synergism
CI	0.7-0.85	++	Moderate synergism
CI	0.9-1.1	+	Slight synergism
CI	0.9-1.1	±	Additive
CI	1.1-1.2	−	Slight antagonism
CI	1.2-1.45	−−	Moderate antagonism
CI	1.45-3.3	−−−	Antagonism
CI	3.3-10	−−−−	Strong antagonism
CI	>10	−−−−−	Very strong antagonism

2.7.4. Drugs and inhibitors

Drug and inhibitors used in the cytotoxicity assays and other experiments within the ATR inhibitor study are summarised here. AZD6738, hydroxyurea (Sigma), chlorambucil (Sigma), fludarabine (Teva), bendamustine (Sigma) and ibrutinib (Seleckchem) were dissolved in DMSO and used at the specified concentration. *In vitro* studies involving cyclophosphamide were conducted using 4-hydroperoxycyclophosphamide (Niomech). Pharmacological inhibition of ATM, DNA protein kinase (DNA-PK) and caspases was carried out respectively using the ATM inhibitor KU-55933 (Calbiochem), the DNA-PK inhibitor NU7441 (Seleckchem) and Z-VAD-FMK (Enzo).

2.8. Western blotting

2.8.1. Sample preparation and protein quantification

Harvested cells were lysed and protein extracted in urea/Tris buffer (UTB), prepared by dissolving urea, Tris and 2-mercaptoethanol in distilled water to a concentration of 9 M urea, 75 mM Tris and 150 mM 2-mercaptoethanol, and then adjusting the pH to 7.5. Cells were washed with PBS and pelleted at 4°C in a universal tube, after which 50 µl of ice-cold UTB buffer was added and mixed with the cells. Cells were then sonicated twice in UTB buffer for 15 seconds each, in order to ensure complete cell lysis and to reduce sample viscosity by shearing the DNA. Sonicated samples were transferred to an eppendorf, and centrifuged at 14,000 rpm for 20 minutes at 4°C. The supernatant containing the extracted proteins was then transferred to a new eppendorf, and the pellet remaining in the previous eppendorf was discarded.

Protein determination was then carried out in a colorimetric assay using the Bradford dye binding method (Bradford, 1976). This method utilises a Coomassie Brilliant Blue dye, which changes from red to blue upon binding to protein. A set of 6 concentrations of BSA (0, 100, 200, 300, 400 and 500 µg/ml) was prepared by diluting a 1 mg/ml BSA stock solution with distilled water. This was used as the protein standard. Ten µl of each BSA standard and 10 µl of a 1:10 dilution (in distilled water) of each sample was added in triplicates to a transparent, flat-bottomed 96-well microplate, after which 200 µl of a 1:5 dilution (in distilled water) of the Bradford reagent (Biorad) was dispensed to each well. The microplate was allowed to equilibrate for 5 minutes before absorbance was measured at 595 nm by an iMark microplate reader (Bio-rad). A linear standard curve was constructed by plotting the absorbance readings against known concentrations of the BSA standard. The standard curve was then used to convert absorbance readings of the samples to protein

concentrations. The actual protein concentration of each sample was calculated by multiplying the value obtained from the standard curve by 10.

2.8.2. Gel electrophoresis and transfer

A polyacrylamide gel was used to resolve the proteins in each sample. Gels can be made with different acrylamide percentages. A 10% gel was used if the proteins of interest were <50 kDa; otherwise, a 6% gel was used. The gels were made according to the following recipe:

	6% gel	10% gel
Distilled water	27.4 ml	19.4 ml
1M Tris	4 ml	4 ml
30% acrylamide	8 ml	13.4 ml
10% sodium dodecyl sulphate (SDS)	400 µl	400 µl
Tetramethylethylenediamine (TEMED)	80 µl	80 µl
10% ammonium persulphate (APS)	200 µl	200 µl

TEMED and APS were used to catalyse the polymerisation of acrylamide to form the gel. SDS was used to denature the proteins such that the mobility during gel electrophoresis would depend primarily on its molecular size.

The gel was cast and allowed to set for 2 hours. Thereafter, 20 µg of each protein sample, prepared in loading buffer (made with bromophenol blue, 2-mercaptoethanol, SDS and glycerol in Tris buffer, pH 6.8), was denatured by heating to 99°C for 5 minutes, and loaded into individual wells. A multicolour broad range protein ladder (Thermo Fischer Scientific) was also loaded. The gel was run at 25 mA for 5 hours in gel running buffer (prepared by adding 50 ml of 1M Tris and 5 ml of 10% SDS to 445 ml of distilled water).

The resolved proteins were then transferred onto a nitrocellulose membrane (Thermo Fischer Scientific). First, the transfer buffer was made by dissolving 1.4 L of methanol, 203 g of glycine and 40.6 g of Tris in 7 L of distilled water. Next, the transfer cassette was assembled by placing the gel and the nitrocellulose membrane in between two sponges and filter papers soaked in transfer buffer, with the membrane facing the cathode and the gel facing the anode. The assembled cassette was then placed in a tank filled with transfer buffer, and the transfer was run for 18 hours at 200 mA.

2.8.3. Antibody staining and visualisation

Following protein transfer, the nitrocellulose membrane was rinsed in water and stained with Ponceau S solution (Sigma) to visualise and confirm equal loading of proteins. Using the protein ladder and Ponceau staining as a guide, the membrane was then separated into several strips, each containing a single protein of interest. The membrane strips were washed in TBST (50 mM Tris, 150 mM NaCl and 0.1% Tween 20, at pH 7.5) to remove the Ponceau stain, and blocked in 5% non-fat dry milk (20 g of milk powder dissolved in 400 ml of TBST) for 2 hours to reduce subsequent non-specific antibody binding. After a further wash in TBST, the membrane strips were incubated overnight at 4°C with their respective primary antibody made up in TBST with 5% BSA. A list of antibodies used is provided in **Appendix 2**. Antibodies were generally used at dilutions recommended by the supplier, with optimisation required only for a minority of antibodies.

Following three further wash in TBST, the membrane strips were incubated for 1 hour at room temperature with an anti-mouse, anti-goat or anti-rabbit antibody (Dako) conjugated to horseradish peroxidase (HRP), depending on the animal species from which the primary antibody was raised. Thereafter, the membrane strips were washed for three times in TBST before the addition of the enhanced chemiluminescence (ECL) reagent (Thermo Fischer Scientific). The ECL reagent is a substrate for HRP, and emits signals that

can be detected on an X-ray film. The membrane strips were incubated in ECL reagent for 1 minute, following which excess ECL reagent was removed. The strips were wrapped in cling film and placed in a cassette with the protein side facing up. X-ray films (Thermo Fischer Scientific) were placed on top of the membrane in a dark room for exposures of varying durations. These films were then developed in a dark room.

2.9. Immunofluorescence microscopy

2.9.1. Analysis of DNA damage foci

Slide preparation. Harvested cells were pelleted in a universal tube, washed once with PBS and resuspended in PBS at a concentration of 10^6 cells/mL. Multispot glass slides (4 spots/slide; Hendley-Essex) were prepared the previous day by immersing in 70% ethanol with 1% hydrochloric acid for 1 hour, rinsing with distilled water and drying overnight in a 37°C incubator. A blob of poly-L-lysine (Sigma) was added to each spot on the slide, and left for 20 minutes at room temperature. The poly-L-lysine was then removed and each spot was washed with a blob of distilled water. The slide was left to dry at room temperature for 30 minutes, after which 100 µl of cells (containing 10^5 cells) was applied to each spot.

Extraction, fixing and blocking. The cells were left to adhere onto the glass slide for 30 minutes, and fixed in ice cold 4% paraformaldehyde for 5 minutes in a coplin jar. Thereafter, extraction buffer (containing 10 mM piperazine-N,N′-bis(2-ethanesulfonic acid), 300 mM sucrose, 20 mM sodium chloride, 3 mM magnesium chloride and 0.5% Triton X-100) was applied to each spot, in order to permeabilise the cell membrane to allow subsequent antibody entry and binding. Slides were then washed three times in PBS at room temperature, after which blocking was carried out by immersing the slides in PBS with 10% FBS for 1 hour. This prevents subsequent non-specific antibody binding.

Antibody labelling and microscopy. Following blocking, the slides were washed three times in PBS, and labelled with primary antibody. The primary antibodies used include those against γH2AX (Millipore), 53BP1 (Santa Cruz), lamin B (Santa Cruz) and phosphohistone H3 serine 10 (pH3; Cell Signaling). All antibodies were used at the supplier's recommended dilution, and dilutions were made in PBS with 1% FBS. One hundred µl of the primary antibody dilution was added to each spot. The slides were then

incubated at 4°C in a moist chamber overnight. After three further washes in PBS, 100 µl of the secondary antibody dilution, made in PBS with 1% FBS, was applied to each spot. A fluorophore-conjugated anti-mouse or anti-rabbit antibody (Dako) was used as the secondary antibody, depending on the animal species from which the primary antibody was raised. The slides were incubated with the secondary antibody for 1 hour at room temperature in darkness. Thereafter, three further washing steps were performed, and the slides were mounted in Vectashield mounting medium with 4',6-diamidino-2-phenylindole (DAPI; Vector Laboratories) which stains the cellular DNA content. The slides were examined under an immunofluorescence microscope (Nikon) using a x60 lens and analysed using the Volocity software (Perkin Elmer).

2.9.2. DNA fibre analysis

DNA fibre analysis performed as part of the ATR inhibitor study was carried out by Dr Eva Petermann (University of Birmingham).

First, cells were pulse-labelled sequentially with thymidine analogues 5-chloro-2'-deoxyuridine (CidU; Sigma) and 5-iodo-2'-deoxyuridine (IdU; Sigma) as previously described (Jackson and Pombo, 1998; Petermann et al., 2010). This involved incubating the cells with 25 µM of CidU for 20 minutes, and then 250 µM of IdU for the next 20 minutes, such that CidU and IdU was incorporated into newly synthesised DNA during the first and second 20 minutes respectively. Cells were then lysed and DNA molecules were stretched and fixed onto a microscope slide. Thereafter, the slide was stained with antibodies directed against CiDU and IdU respectively.

DNA replication tracts were examined using an immunofluorescence microscope. Replication rates in kb/min were obtained by measuring DNA fibre length in microscopy images. Fibre length in µm was converted into kb using the factor 2.59 kb/µm as determined by spreading and staining viral genomes of a defined length (Jackson and Pombo, 1998).

2.10. Animal experimentation

All animal experimentation conducted as part of the ATR inhibitor study was carried out by Dr Nicholas Davies (University of Birmingham) under a UK Home Office animal license (PPL 70/8151).

Generation of primary CLL xenografts. Primary CLL xenografts were generated by injecting 2-5 x 10^7 CLL cells intravenously into irradiated (1.25 Gy X-ray) NOD/Shi-scid/IL-2Rγ (NOG) mice, alongside 10^5 autologous T lymphocytes. Autologous T lymphocytes were stimulated for 3-7 days prior to inoculation into mice with CD3/CD28 Dynal beads (Life Technologies) in the presence of human IL-2 (30 units/ml; Peprotec, London, UK) in accordance with a published protocol (Patten et al., 2011). Engraftment was ascertained by the presence of ≥1% human CD45+ CD19+ cells in peripheral blood, assessed using flow cytometry.

Drug treatment. Animals were treated with AZD6738 (12.5 mg/kg orally 5 days per week for 2 weeks) and/or chlorambucil (16mg/kg on day 1 and 5mg/kg on day 3, intraperitoneally), or vehicle, and sacrificed 3 weeks following the initiation of treatment.

Assessment of tumour load and cytogenetics. Tumour load was assessed by flow cytometric quantification of murine CD45−, human CD45+ CD19+ cells in infiltrated murine spleens. FISH was carried out on these murine CD45−, human CD45+ CD19+ cells using 11q FISH probes (Abbott Molecular).

2.11. Statistical analysis

All statistical analysis was carried out using the GraphPad Prism software, with the exception of survival analysis which was performed using SPSS Statistics (IBM Corporation). The range of values which has a 95% probability of containing the true value was determined by the 95% confidence interval (CI), and p values of <0.05 were considered statistically significant. The specific statistical tests used are described below:

Student's t-test. This test was applied to compare a single variable between two groups. Paired t-tests were used to compare the same patients or samples between two timepoints, whereas unpaired t-tests were used for comparisons between two distinct groups of patients or samples.

Analysis of variance (ANOVA). This test was employed for comparison of a single variable across more than two groups. The one-way ANOVA and the two-way ANOVA were used for comparisons across three or more distinct groups of patients or samples, defined by a single factor and by two different factors, respectively. In all ANOVA tests, a Bonferroni post-hoc analysis was additionally performed to generate a significance value for all possible pairwise comparisons, where the results of each group was compared to the results of each of the remaining groups.

***Kaplan-Meier analysis*.** This methodology was used to estimate the PFS and OS of specific groups of patients. Such estimation of PFS and OS was based on the last known clinical status (i.e. remission vs progression for PFS; alive vs dead for OS) and time to event for each individual within a group, calculated from the date of end of treatment to clinical progression or death respectively. Events were censored at the time of the last clinic appointment for patients who remained untreated or were lost to follow up. These statistics were used to construct survival curves, in which the proportion of patients who remained

progression-free or alive was plotted against time. In these curves, each downward step or deflection represents one or more progression or death events, whereas a tick reflects a censored event.

Log-rank test. The univariate log-rank test was employed to compare the survival outcomes of two distinct groups of patients. For each comparison, the statistical significance and hazard ratio were reported. The hazard ratio (HR) refers to the ratio of the rate of progression (for PFS) or death (OS) in one group of patients compared to the other group. For instance, an HR of 2 would indicate that the rate of death in one group was twice that of the other group.

***Cox proportional hazards model*.** This multivariate Cox regression analysis was used to assess the relative impact of and the relationship between several different co-variates which, as a single variable, had demonstrable impact on clinical outcome. Similar to the log-rank test, the statistical significance and HR were reported. A significant result from this test indicates that the variable under consideration has clinical impact independent of all the other co-variables analysed.

CHAPTER 3

FEATURES AND MECHANISMS UNDERPINNING SPONTANEOUS DISEASE REGRESSION IN CLL

Understanding the features and probable mechanism of spontaneous disease regression could inform the therapeutic management of CLL. Multiple lines of evidence now suggest that the clinical course of individual patients is shaped both by the biological properties of their CLL clone and by the dynamics of its interaction with the microenvironment. Disease progression in CLL is often accompanied by increased CLL cell trafficking to proliferation centres, BCR positive signalling, and proliferation (Herishanu et al., 2011; Messmer et al., 2005; Stevenson et al., 2011). Moreover, the emergence of driver mutations and genomic complexity may result in the outgrowth of CLL cells with greater proliferative and survival advantage (Landau et al., 2013; Landau et al., 2015; Puente et al., 2015). These changes, facilitated by impaired tumor immunity and a microenvironment conducive to CLL proliferation and apoptotic evasion (Burger, 2011; Forconi and Moss, 2015; Herishanu et al., 2011; Nunes et al., 2012; Ramsay et al., 2008; Riches et al., 2013), may shift the balance of CLL turnover in favour of clonal expansion (Messmer et al., 2005). I therefore postulated that, conversely, spontaneous CLL regression may occur under some or all of the following conditions: low CLL BCR signalling and proliferative capacity, high susceptibility of CLL cells to apoptosis, low tumour mutational burden and improved immunity.

To evaluate this hypothesis, and to identify features underpinning spontaneous CLL regression, I conducted an integrative analysis using phenotypic, functional and genomic approaches on peripheral blood samples from 19 subjects who have undergone spontaneous CLL regression. The analysis revealed unique features that were seen consistently across these subjects, providing novel insights into spontaneous disease regression in CLL.

3.1. Results

I reviewed the clinical records of all patients with untreated CLL from 4 UK haematology centres who either attended a CLL clinic or participated in the community monitoring program between 2010 and 2016. Subjects with *complete* spontaneous disease regression were identified on the basis of a sustained reduction in lymphocyte count (ALC) to below 4 x 10^9/L, with complete resolution of CLL-related symptoms, anaemia (<100 g/L), thrombocytopenia (<100 x 10^9/L) or clinically detectable lymphadenopathy or hepatosplenomegaly that may be present at diagnosis. Subjects with *partial* spontaneous disease regression were identified based on evidence of sustained reduction of lymphocytosis by ≥ 50% from the peak level with regressing nodal disease. Individuals with an alternative explanation for the disease regression were excluded. These comprise patients with concurrent infections or second malignancies and those receiving treatment with cytotoxic or immunosuppressive drugs, including long-term or high-dose corticosteroids, immediately preceding or coinciding with the onset of CLL regression. Subjects diagnosed with a second malignancy following the onset of spontaneous CLL regression were not excluded, but were considered within a separate category if the subsequent malignancy was diagnosed within 5 years of the onset of CLL regression. These patients were categorised separately from other spontaneous regressors because pro-inflammatory responses could potentially be developed against the second malignancy, and these responses could have potential anti-tumour effects that might have impacted on the initial CLL.

For comparison purposes, untreated CLL cases with indolent disease were recruited locally, while progressive cases were sourced from UK multicentre clinical trials, as detailed in **Table 3.1**. Indolent CLL was defined as Binet stage A disease with a lymphocyte doubling time of ≥ 2 years monitored over ≥ 5 years. For progressive cases, a sample

Table 3.1. Demographic and clinical features of patient cohorts in this study.

(A) Patient cohorts used in section 3.2.3 (phenotypic analysis)

		Spontaneous regression	Indolent	Progressive
Cohort size	N	17	54	40
Age	Median	77.4	71.3	61.5
	Range	44-86	45-89	42-83
Binet stage		A	A	B/C
Previous treatment	% treated	0	0	50
***IGHV* mutational status**	% U-CLL	0	8	70
Source		Local hospitals	Local hospitals	UK IciCLLe trial

(B) Patient cohorts used in section 3.2.5 (BCR signalling analysis)

		Spontaneous regression	Indolent mutated	Indolent unmutated
Cohort size	N	14	35	4
Age	Median	78.6	71.3	70.5
	Range	67-86	45-89	66-80
Binet stage		A	A	A
Previous treatment	% treated	0	0	0
***IGHV* mutational status**	% U-CLL	0	0	100
Source		Local hospitals	Local hospitals	Local hospitals

(C) Patient cohorts used in section 3.2.7 (T cell analysis)

		Healthy controls	Spontaneous regression	Indolent
Cohort size	N	6	16	31
Age	Median	62.0	76.6	71.3
	Range	47-70	44-86	60-89
Binet stage		-	A	A
Previous treatment	% treated	-	0	0
CMV serostatus	% anti-CMV IgG positive	50.0	68.8	67.7
Source		Local donors	Local hospitals	Local hospitals

obtained immediately before treatment was used. Details of patient recruitment and the clinical trial cohorts used in this study were provided in section 2.1.1 and 2.1.2.

3.1.1. Spontaneous disease regression occurs at a frequency of 1.4% in CLL

Twenty individuals who fulfilled the criteria for spontaneous disease regression were identified from a review of 1425 patients with CLL. The prevalence of spontaneous CLL regression in this cohort was 1.4%, which approximates the frequency reported in earlier studies (Del Giudice et al., 2009; Thomas et al., 2002). The clinical details of these 20 individuals are described in **Figure 3.1** and **Table 3.2**. These 20 individuals include 11 subjects who underwent complete spontaneous regression (Category A; CLL01 to CLL11); 6 who experienced partial spontaneous regression (Category B; CLL12 to CLL17); 2 whose onset of CLL regression preceded the diagnosis of a second malignancy by ≤ 5 years, and thus may potentially be related to the concurrent malignancy (Category C, CLL 18 and CLL19); and 1 who experienced spontaneous regression over a 14-year period, but whose ALC has recently increased (Category D, CLL20). In the absence of a reactive cause, the latter may represent CLL relapse following spontaneous regression.

Subjects were followed for a median of 15.2 years (range 3.6-30 years). Among the complete spontaneous regressors, CLL regression occurred over a median of 8.6 years (range 5.3-26.2 years). At the time of the study, lymphocytosis and CLL-related clinical features have been absent for a median of 2.7 years for the complete spontaneous regressors (range 0.9-11.8 years). Lymphopenia is a rare, idiosyncratic effect of certain drugs (e.g. levetiracetam); however, no temporal relationship was apparent between the initiation of these drugs and spontaneous CLL regression. Therefore, CLL regression in individuals other than CLL18 and CLL19 could not be explained by their medical or drug history (**Table 3.2**).

Figure 3.1

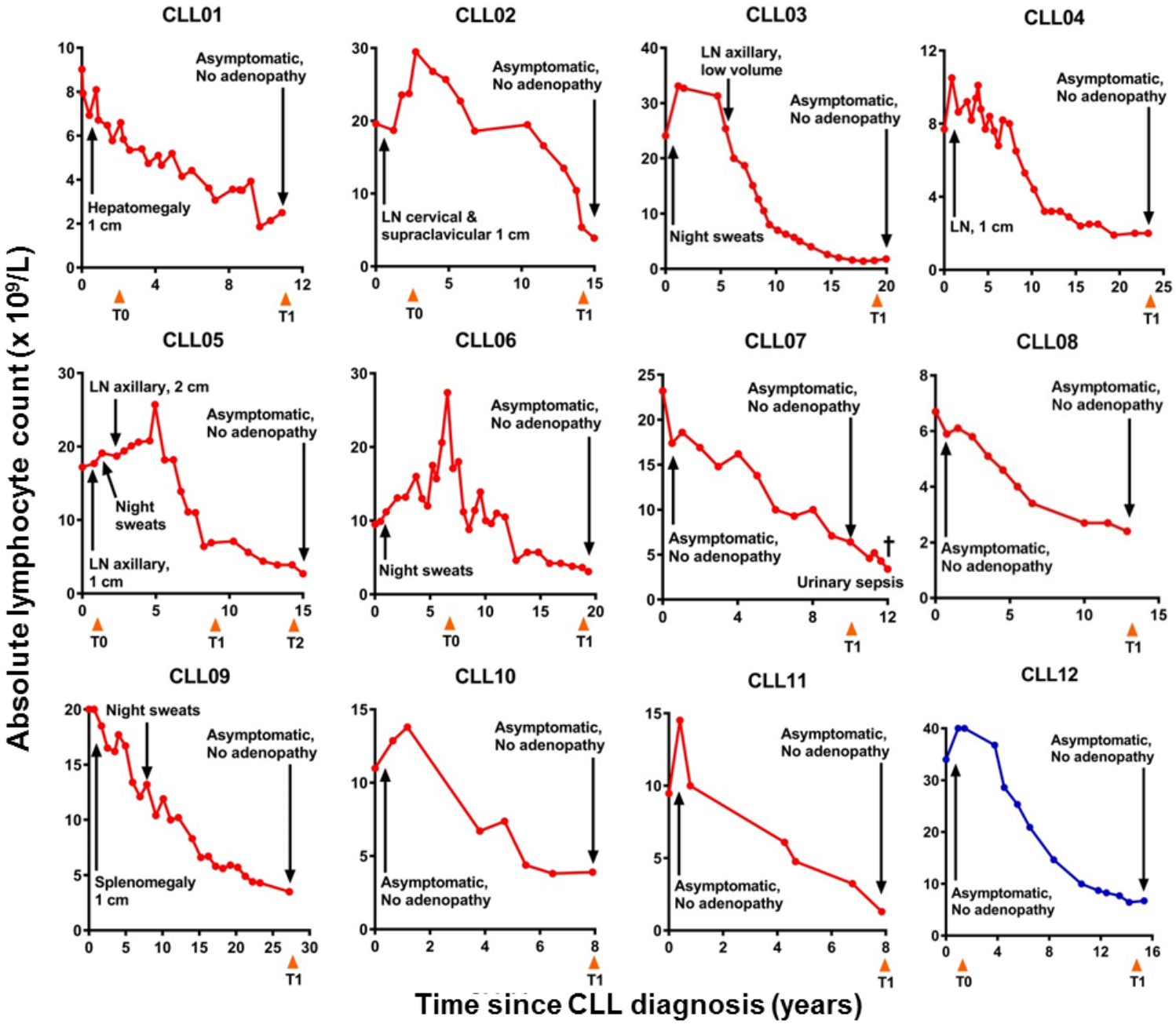
CLL01
Asymptomatic, No adenopathy
Hepatomegaly 1 cm
T0
T1
CLL02
Asymptomatic, No adenopathy
LN cervical & supraclavicular 1 cm
T0
T1
CLL03
LN axillary, low volume
Asymptomatic, No adenopathy
Night sweats
T1
CLL04
Asymptomatic, No adenopathy
LN, 1 cm
T1
CLL05
LN axillary, 2 cm
Asymptomatic, No adenopathy
Night sweats
LN axillary, 1 cm
T0
T1
T2
CLL06
Asymptomatic, No adenopathy
Night sweats
T0
T1
CLL07
Asymptomatic, No adenopathy
Asymptomatic, No adenopathy
Urinary sepsis
†
T1
CLL08
Asymptomatic, No adenopathy
Asymptomatic, No adenopathy
T1
CLL09
Night sweats
Asymptomatic, No adenopathy
Splenomegaly 1 cm
T1
CLL10
Asymptomatic, No adenopathy
Asymptomatic, No adenopathy
T1
CLL11
Asymptomatic, No adenopathy
Asymptomatic, No adenopathy
T1
CLL12
Asymptomatic, No adenopathy
Asymptomatic, No adenopathy
T0
T1
Absolute lymphocyte count (x 10⁹/L)
Time since CLL diagnosis (years)

Figure 3.1 (cont'd)

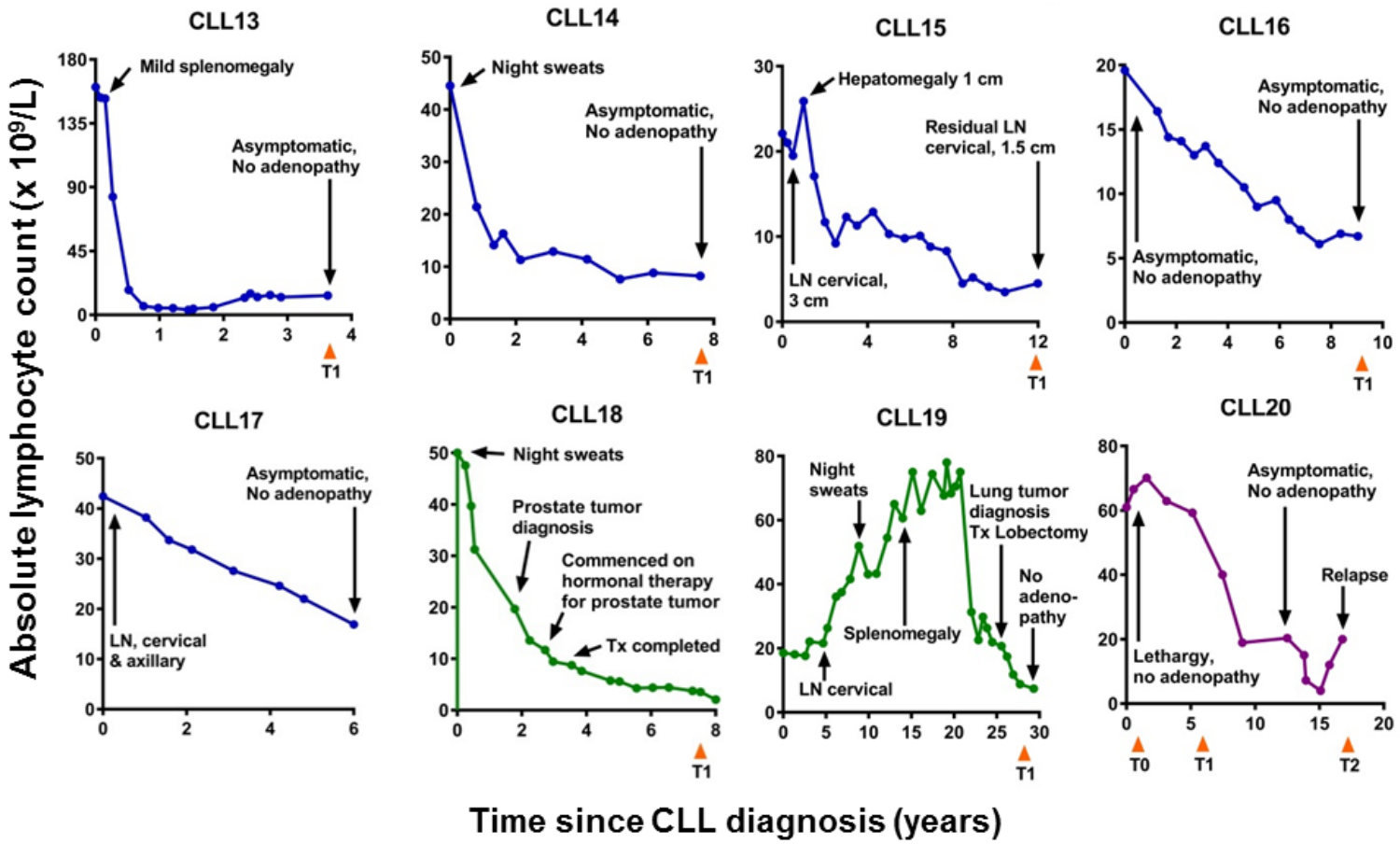

Clinical features of 20 spontaneous CLL regression cases. Spontaneous CLL regression cases were categorised into 4 groups: complete spontaneous regression (Category A; represented by red-coloured curves), partial spontaneous regression (Category B; blue-coloured curves), spontaneous regression potentially associated with a second malignancy (Category C; green-coloured curves) and relapsed spontaneous regression (Category D; purple-coloured curves). The absolute lymphocyte count for each patient is plotted against the time elapsed from the date of diagnosis. Clinical features are annotated, and the time of peripheral blood sampling is displayed at the bottom each chart. T0 represents the diagnostic timepoint, whereas T1 and T2 represent the regression timepoints, except in CLL20 where T2 represents the relapse timepoint. LN, lymphadenopathy (the measurement that follows denote the size of the largest palpable node); Tx, treatment.

Table 3.2. Clinical features of subjects with spontaneous CLL regression.

	Diagnosis		Sex	ALC (x10^9/L)		Medical history and co-morbidities	Second malignancy		Drug history
	Year	Age		Peak	Current		Site	Diagnosis	
Complete spontaneous regression (Category A)									
CLL01	2005	58	M	9.0	3.2	Osteoarthritis, hypertension, Hypercholesterolaemia	Prostate	2014	Atorvastatin, amlodipine (discontinued)
CLL02	2001	52	M	29.5	3.3	Hypertension, diabetes mellitus	-	-	Metformin, ramipril, bendroflumethiazide, doxazosin, verapamil
CLL03	1996	66	M	32.7	1.5	Ischaemic heart disease, peripheral vascular disease, diabetes mellitus, bronchiectasis (since 2010), hypertension	-	-	Alfuzosin, aspirin, bendroflumethiazide, doxazosin, felodipine, lisinopril, simvastatin
CLL04	1994	58	M	10.5	1.7	Hypertension, benign prostatic hypertrophy, previous neurofibroma, osteoarthritis	-	-	Finasteride, amlodipine, ibersartan
CLL05	2000	56	M	25.7	2.6	Previous rectal polyp (non-malignant), diabetes mellitus	-	-	Metformin
CLL06	1997	61	M	27.4	3.5	Diabetes mellitus, hypertension	-	-	Metformin, furosemide
CLL07	2002	83	M	23.2	3.6	Hypothyroidism, diabetes mellitus, hypertension, benign prostatic hypertrophy	Skin (SCC)	2010	Aspirin, linagliptin, tamsulosin, levothyroxine
CLL08	2002	72	F	6.7	2.4	Atrial fibrillation, diverticulosis, hypertension, hyperthyroidism, cholecystitis (in 2014)	-	-	Bisoprolol
CLL09	1990	46	M	20.2	3.1	Hypertension, Hypercholesterolaemia	-	-	Ramipril, simvastatin
CLL10	2008	70	M	13.8	3.2	Hypertension, abdominal aortic aneurysm, previous TIA, Hypercholesterolaemia	-	-	Simvastatin, aspirin, lansoprazole, indapamide
CLL11	2007	75	M	14.5	1.2	Atrial fibrillation, gout	Skin (SCC)	2013	Warfarin, bisoprolol, lansoprazole, febuxostat, donepezil
Partial spontaneous regression (Category B)									
CLL12	2000	66	M	40.6	5.6	Previous iron deficiency anaemia	Skin (BCC)	2010	Omeprazole, temazepam, aspirin
CLL13	2013	73	M	161.0	11.3	Abdominal aortic aneurysm, COPD	-	-	Tiotropium and salbutamol inhalers
CLL14	2002	73	F	44.5	8.5	Ischaemic heart disease, osteoarthritis, hypertension, Hypercholesterolaemia	-	-	Aspirin, ramipril, furosemide, ropinirole, levetiracetam
CLL15	2004	61	M	25.9	5.5	Diabetes mellitus, hypertension, Hypercholesterolaemia			Simvastatin, doxazosin
CLL16	2007	36	F	19.6	7.0	Eczema, mild depression	-	-	Nil
CLL17	2009	81	M	42.4	16.9	Lewy body dementia, previous ischaemic heart disease, depression	-	-	Bumetanide, citalopram, donepezil
Spontaneous regression associated with second malignancy (Category C)									
CLL18	2008	60	M	50.2	3.0	Diabetes mellitus, hypertension	Prostate	2010	Aspirin, enalapril, metformin, pioglitazone, simvastatin, tamsulosin
CLL19	1987	55	M	78.0	7.7	Diverticulosis, COPD, gout	Lung	2010	Carbocisteine, tamsulosin, tiotropium/fluticasone/ salmeterol inhalers
Relapsed spontaneous regression (Category D)									
CLL20	1993	38	M	52.4	20.0	Hypercholesterolaemia, asthma, previous hip replacement	-	-	Simvastatin, salbutamol/formoterol inhalers

ALC, absolute lymphocyte count; TIA, transient ischaemic attack; COPD, chronic obstructive pulmonary disease; SCC, squamous cell carcinoma; BCC, basal cell carcinoma.

3.1.2. Spontaneously regressed CLL tumours utilise mutated *IGVH3* and *IGVH4* genes

All subjects except one (CLL07) were alive at the time of analysis. CLL07 died from complications of sepsis, arising from an ascending urinary tract infection associated with an indwelling urinary catheter. The cause of death was therefore not directly related to CLL. Peripheral blood samples were available at the time of CLL regression from 19 individuals (T1/T2 timepoint), and at the time of diagnosis in 6 individuals (T0 timepoint). The blood sampling timepoints for each subject is displayed in **Figure 3.1** beneath their respective lymphocyte count charts.

In all cases, a residual monoclonal B lymphocyte population with CLL phenotype (CD19, CD5, CD23 and CD43 positive, CD20, CD79b and CD81 weak, CD10 negative and Igκ/λ-restricted) could be identified by multiparameter flow cytometry in the regression blood sample (T1 timepoint). These cases were therefore genuine cases of CLL. Furthermore, the residual CLL population could be distinguished from the normal B cell population and quantified based on several cell surface markers. Both normal B cells and CLL cells are CD19 positive; however, whereas normal B cells have high expression levels of CD20, CD79b and CD81 and low expression levels of CD43, CLL cells typically have high expression levels of CD43 and low expression levels of CD20, CD79b and CD81, as shown in **Figure 3.2A** (Rawstron et al., 2016). On this basis, it could be determined that residual CLL cells accounted for a median of 92.5% of B cells (range 71.6-99.8%) at the time of regression (**Table 3.3**). Furthermore, by taking into account of the lymphocyte count and determining the proportion of lymphocytes that were B cells (CD19+), T cells (CD3+) or NK cells (CD3− CD4− CD16+), as shown in **Figure 3.2B**, the B cell, T cell, NK cell and residual CLL cell count could be estimated for each case (**Table 3.3**). At the time of regression, the median residual CLL count was 1.8 x 10^9/L (range 0.4-6.5 x 10^9/L), and these residual

Figure 3.2

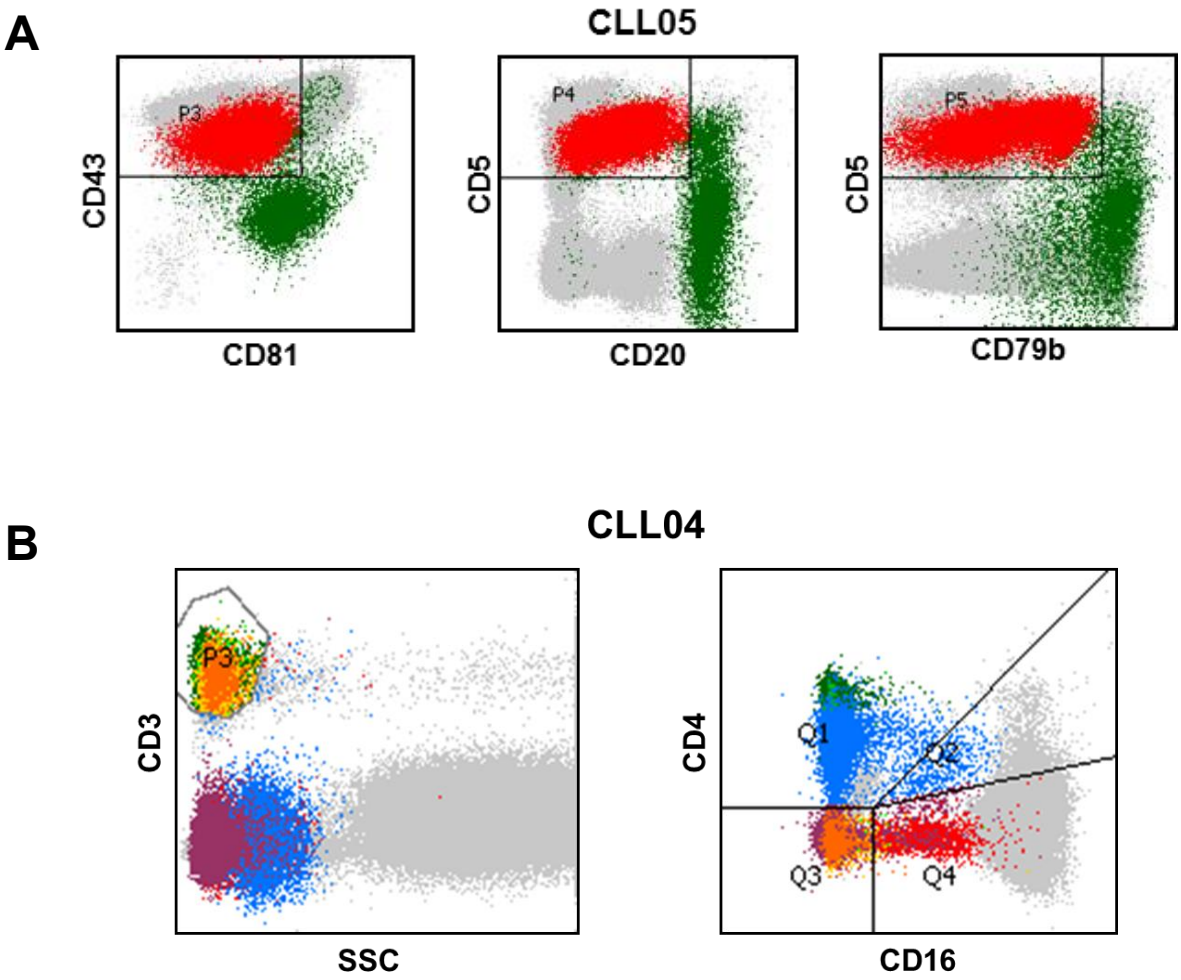

Gating strategies to differentiate various lymphocyte populations in CLL patients. In both (A) and (B), singlet mononuclear cells are first selected using the gating strategy shown in Figure 2.3A-B. **(A)** A CD19 gate is then applied to select for CD19+ B lymphocytes (not shown). The CLL population (shown in red) is distinguished from the non-malignant B lymphocyte population (shown in green) by their immunophenotype. CLL cells have high CD5 and CD43 expression and low CD20, CD79b and CD81 expression. Non-malignant B lymphocytes and progenitors have high CD20, CD79b and/or CD81 expression. **(B)** Different mononuclear cell populations are distinguished based on their CD3, CD4 and CD16 expression. B lymphocytes (in purple) are CD3−CD4−CD16−, CD4 T lymphocytes (in green) are CD3+CD4+CD16−, CD8 T lymphocytes (in orange) are CD3+CD4−CD16−, NK cells (in red) are CD3−CD4−CD16+, and monocytes (in blue) are CD3−CD4+ with variable CD16 expression.

Table 3.3. Lymphocyte count and characteristics of the *IGH* gene in subjects with spontaneous CLL regression.

	B-cell count x10^9/L	CLL count x10^9/L	% CLL cells of B-cells	% CLL cells of lymph ocytes	*IGH* gene usage			*IGHV* % homology to germline	T-cell count x10^9/L	CD4+ T-cell count x10^9/L	CD8+ T-cell count x10^9/L	NK-cell count x10^9/L
					V_H	D_H	J_H					
CLL01	1.0	0.9	92.0	28.8	3-30	4-17	4	95.5	1.9	1.2	0.7	0.3
CLL02	2.1	2.1	99.0	63.6	3-53	2-21	4	93.7	1.0	0.6	0.4	0.2
CLL03	0.4	0.4	91.6	23.8	1-69	5-12	3	91.7	0.8	0.4	0.4	0.3
CLL04	0.5	0.5	91.5	28.0	3-48	5-18	1	95.5	1.0	0.7	0.3	0.2
CLL05	1.4	1.0	71.6	38.5	2-5	2-15	4	96.3	1.1	0.5	0.4	0.1
CLL06	1.7	1.7	98.8	48.0	4-34	6-13	4	87.9	1.7	0.6	1.0	0.1
CLL07	2.2	2.2	98.0	59.9	3-23	6-19	3	93.1	1.2	0.7	0.5	0.2
CLL08	-	-	86.1	-	3-15	1-1	3	89.1	-	-	-	-
CLL09	2.0	1.8	92.2	58.0	4-39	2-8	5	91.8	0.7	0.5	0.2	0.4
CLL10	1.3	1.2	92.5	37.6	3-13	3-16	6	92.6	1.8	1.0	0.7	0.1
CLL11	0.7	0.7	98.3	57.3	4-4	3-22	4	94.8	0.4	0.3	0.2	0.1
CLL12	1.6	1.2	75.0	21.4	3-30	3-10	4	91.7	3.9	1.0	2.7	0.1
CLL13	5.3	5.3	99.8	46.8	3-74	2-21	5	88.9	4.4	3.6	0.6	1.6
CLL14	6.6	6.5	98.2	76.2	4-39 3-23	1-26 6-6	4 2	95.9 89.9	1.6	0.8	0.6	0.3
CLL15	3.4	3.4	99.2	61.3	3-30	1-1	3	97.6	1.8	0.9	0.9	0.3
CLL16	6.1	5.9	96.4	84.0	3-23	4-17	5	92.7	0.6	0.3	0.3	0.3
CLL18	1.9	1.8	92.4	58.5	3-23	6-19	5	93.1	0.9	0.4	0.4	0.3
CLL19	6.7	6.2	92.0	80.0	4-34	5-18	6	95.1	0.7	0.4	0.3	0.3
CLL20	-	-	-	-	4-34	6-19	3	94.7	-	-	-	-

B-cell, CD4+ T cell, CD8+ T cell and NK cell count were derived from the ALC taking into consideration the proportion of lymphocytes that were CD19+, CD3+CD4+, CD3+CD8+ and CD16+CD3−CD4− respectively. The CLL count was derived from the B-cell count taking into account of the proportion of CLL cells in the B lymphocyte population, determined using the methodology illustrated in Figure 3.2. *IGH* sequencing was performed on DNA from sorted CLL cells. Gene usage and % homology to the germline *IGHV* sequence was determined using the international immunogenetics information (IGMT) platform.

CLL cells accounted for a median of 57.3% of circulating lymphocytes (range 21.4-84%).

Analysis of the CLL *IGH* gene locus by Sanger sequencing revealed that every spontaneous regression case possessed mutated *IGHV*, consistent with findings from the Italian spontaneous CLL regression study (Del Giudice et al., 2009). There was usage of *IGVH3* genes in 12 cases. In addition to the use of *IGVH3* genes, *IGVH4* gene usage was also observed in 6 cases in the present cohort, and a single case each of *IGVH1* and *IGVH2* usage was seen (**Table 3.3**). None exhibited stereotyped BCR usage. Importantly, in all 6 individuals with sequential samples, the *IGH* sequence of the diagnostic (T0) and regression (T1/T2) samples were indistinguishable, indicating that the CLL cells at the diagnostic and regression timepoints belonged to the same CLL clone.

3.1.3. Spontaneously regressed CLL tumours exhibit specific phenotypic features

To identify biological features within the CLL clone among spontaneous regressors, a comprehensive immunophenotypic analysis was performed comparing regressors (n=17) at the regression (T1) timepoint against non-regressing indolent (n=54) and progressive CLL cases (n=40). Gated CLL cells (**Figure 2.3**) were analysed for molecules of relevance to CLL pathogenesis, including the proliferation marker Ki-67, key CLL prognostic biomarkers (CD38, ZAP-70) (Crespo et al., 2003; Del Poeta et al., 2001; Ibrahim et al., 2001), adhesion molecules (CD49d, CD62L/L-selectin) (Brachtl et al., 2014; Bulian et al., 2014), chemokine receptors (CXCR4, CXCR5, CCR6, CCR7) (Burkle et al., 2007; Krzysiek et al., 2000; Mohle et al., 1999; Till et al., 2002; Vlad et al., 2009), antiapoptotic proteins (Bcl-2, Mcl-1), CD95/Fas receptor (FasR) and ROR1 (Cui et al., 2016; Yu et al., 2016).

CLL cells from regression cases had uniformly low Ki-67 expression. Indeed, Ki-67 was positive in <1% of CLL cells in all spontaneous regression cases, with Ki-67 <0.5% in the majority, indicating absent or negligible CLL proliferation (**Figure 3.3A**). Spontaneously regressed CLL tumours were generally CD38 and ZAP-70 negative, but these markers did not distinguish regressors from non-regressing indolent cases, with the majority of regression and indolent cases being negative for both CD38 and ZAP-70 (<30% positivity), whereas a substantial proportion of the progressive cases were CD38 and/or ZAP-70 positive using a 30% cut-off (**Figure 3.3B**).

Adhesion molecules, particularly CD49d, are important for the homing of CLL cells from the peripheral blood to the lymph nodes where CLL proliferation takes place. CD49d expression was significantly lower among spontaneous CLL regression cases compared to both indolent and progressive cases, with less than 2% of CLL cells being CD49d positive in the majority of the spontaneous CLL regression cases (**Figure 3.4A**). On the other hand, there was no significant difference in CD62L expression across the comparator groups (**Figure 3.4B**).

The interaction between chemokine and chemokine receptors also plays a crucial role in CLL cell trafficking between the proliferative compartment and the peripheral blood. As discussed in section 1.2.3.1, the interaction between the chemokine CXCL12 and the chemokine receptor CXCR4 on CLL cells is of particular biological significance. Newly proliferated CLL cells downregulate cell surface CXCR4 expression to allow their exit from lymph nodes into the peripheral circulation (Vlad et al., 2009). Over time, these CLL cells recover their CXCR4 expression (Calissano et al., 2011). Hence, CLL cells with low CXCR4 expression are those that have recently proliferated and emerged from the lymph nodes (Coelho et al., 2013). CXCR4 expression was found to be significantly higher in the spontaneous regression cases compared to the indolent and progressive cases (**Figure 3.4C**). Indeed, >95% of CLL cells were CXCR4 positive in the majority of the spontaneous CLL regression cases, indicating that very few have recently proliferated. On the other hand,

Figure 3.3

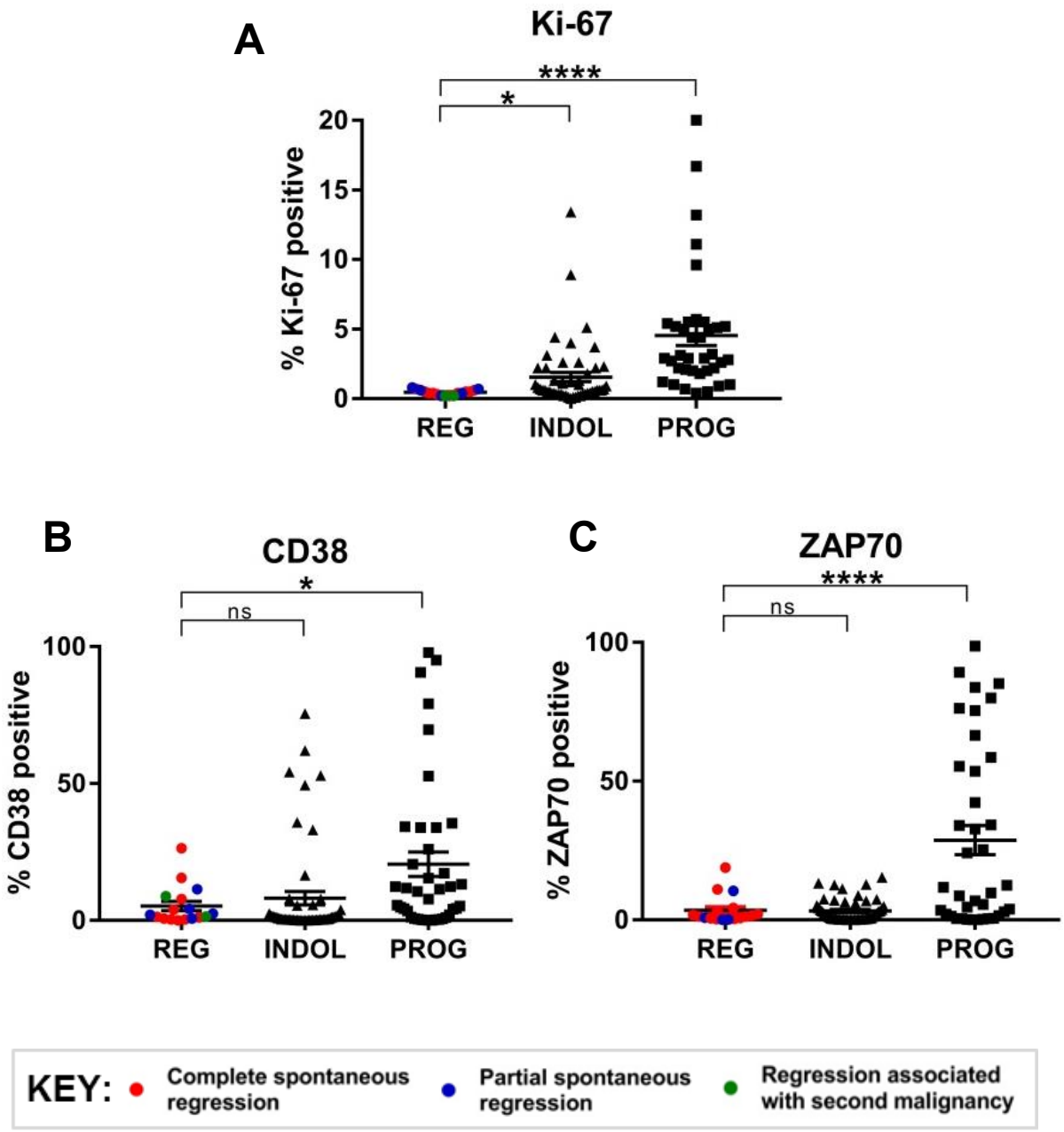

Spontaneously regressed CLL tumours have low Ki-67, CD38 and ZAP-70 expression. CLL cells were gated on the basis of their expression of CD19 and CD20 (CD19+ CD20-low), as shown in Figure 2.3. The gated CLL population was analysed for the expression of the respective markers shown in each panel. For all comparisons, the regression (T1) samples from 17 spontaneous regression cases were compared against 54 indolent and 40 progressive CLL cases. Complete spontaneous regression cases, partial spontaneous regression cases and regression cases associated with second malignancy were represented by red, blue and green dots respectively as shown by the key. Statistical significance was determined using one-way ANOVA with Bonferroni post-hoc analysis. Statistical significance is indicated by *p<0.05, **p<0.01, ***p<0.001 and ****p<0.0001; n.s. denotes comparisons that are not statistically significant.

Figure 3.4

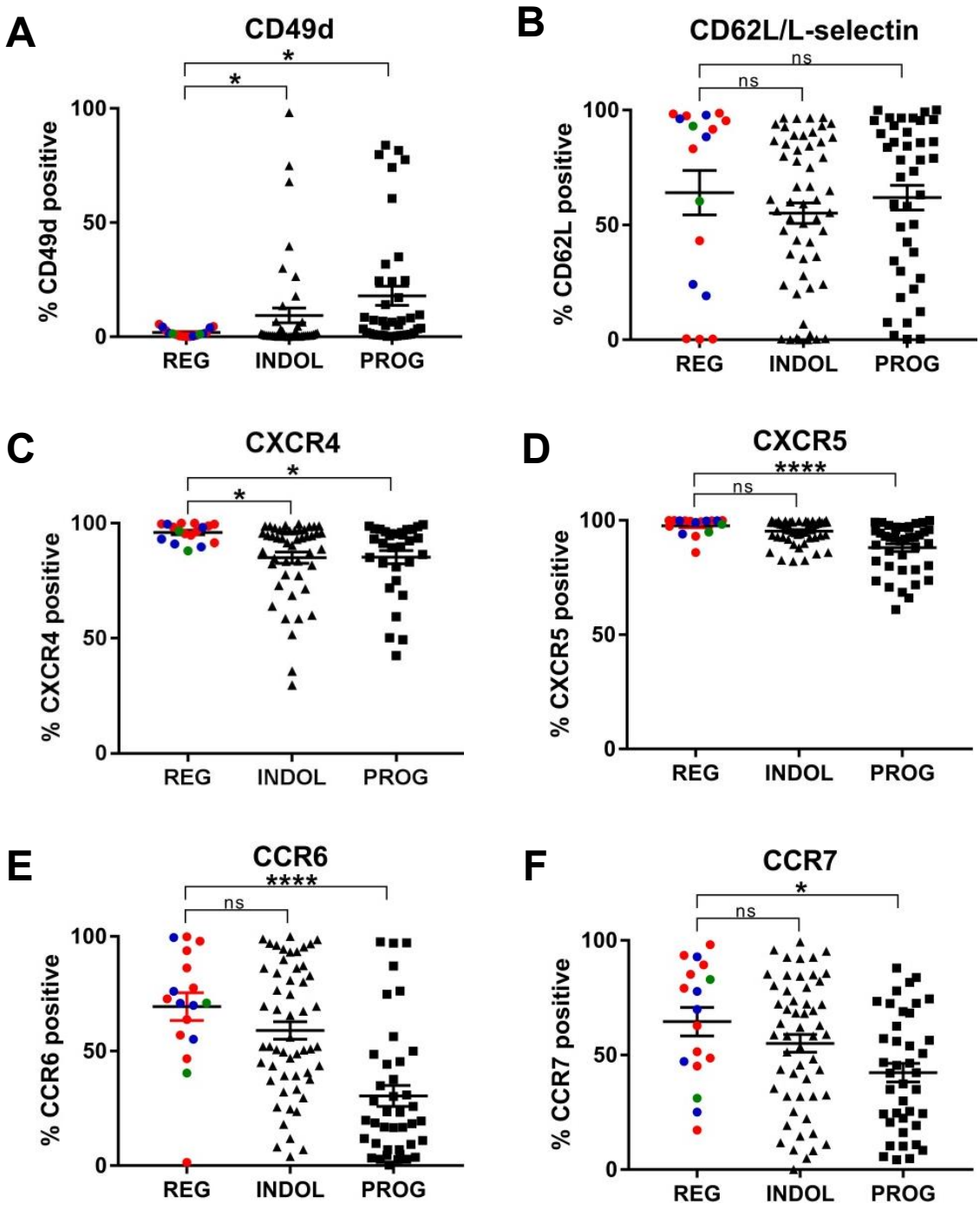

Spontaneously regressed CLL tumours have low CD49d and high CXCR4 expression. The gated CLL population was analysed for the expression of the respective markers shown in each panel. For all comparisons, 17 spontaneous regression cases were compared against 54 indolent and 40 progressive CLL cases. Complete spontaneous regression cases, partial spontaneous regression cases and regression cases associated with second malignancy were represented by red, blue and green dots respectively as shown by the key in Figure 3.3. Statistical significance was determined using one-way ANOVA with Bonferroni post-hoc analysis. Statistical significance is indicated by *p<0.05, **p<0.01, ***p<0.001 and ****p<0.0001; n.s. denotes comparisons that are not statistically significant.

there was no significant difference in CXCR5, CCR6 or CCR7 expression between the spontaneous regression and indolent groups (**Figure 3.4D-F**). However, progressive cases had comparatively lower expression of all four chemokine receptors. Lower CXCR4, CXCR5 and CCR6 levels may reflect a higher proportion of recently proliferated CLL cells that have undergone BCR signalling among the progressive cases (Calissano et al., 2011; Krzysiek et al., 2000; Saint-Georges et al., 2016; Vlad et al., 2009).

With regards to anti-apoptotic proteins, there was no difference in Bcl-2 or Mcl-1 expression levels between regression and indolent CLL, but Mcl-1 levels were higher in progressive CLL cases (**Figure 3.5A-B**). It is of particular importance to highlight the observation that CLL cells from spontaneous regressing patients retained high levels of Bcl-2 expression. On the other hand, spontaneously regressed CLL tumours had significantly higher CD95/FasR expression compared to both indolent and progressive CLL cases (**Figure 3.5C**), implicating a potential role of the extrinsic apoptotic pathway in spontaneous CLL regression.

Finally, ROR1 has generated considerable interest recently because of its high expression in many CLL cells. Functionally, ROR1 is a tyrosine kinase receptor that binds Wnt5a, and enhances chemokine-mediated CLL cell migration and CD40L-induced proliferation through the activation of RhoA and Rac1 respectively which forms part of the non-canonical Wnt signalling pathway (Yu et al., 2016). A recent study has demonstrated that high expression level of ROR1 is associated with accelerated disease progression in CLL (Cui et al., 2016). Although not significant, I found that there was a trend towards lower ROR1 expression in spontaneously regressed CLL tumours compared to indolent CLL cases (**Figure 3.5D**). No significant difference was observed with respect to the expression of each of the phenotypic markers studied among the different categories of spontaneous regression (i.e. Category A-D as detailed in section 3.2.1 and **Table 3.2**).

To determine whether the phenotypic features among spontaneous regressors

Figure 3.5

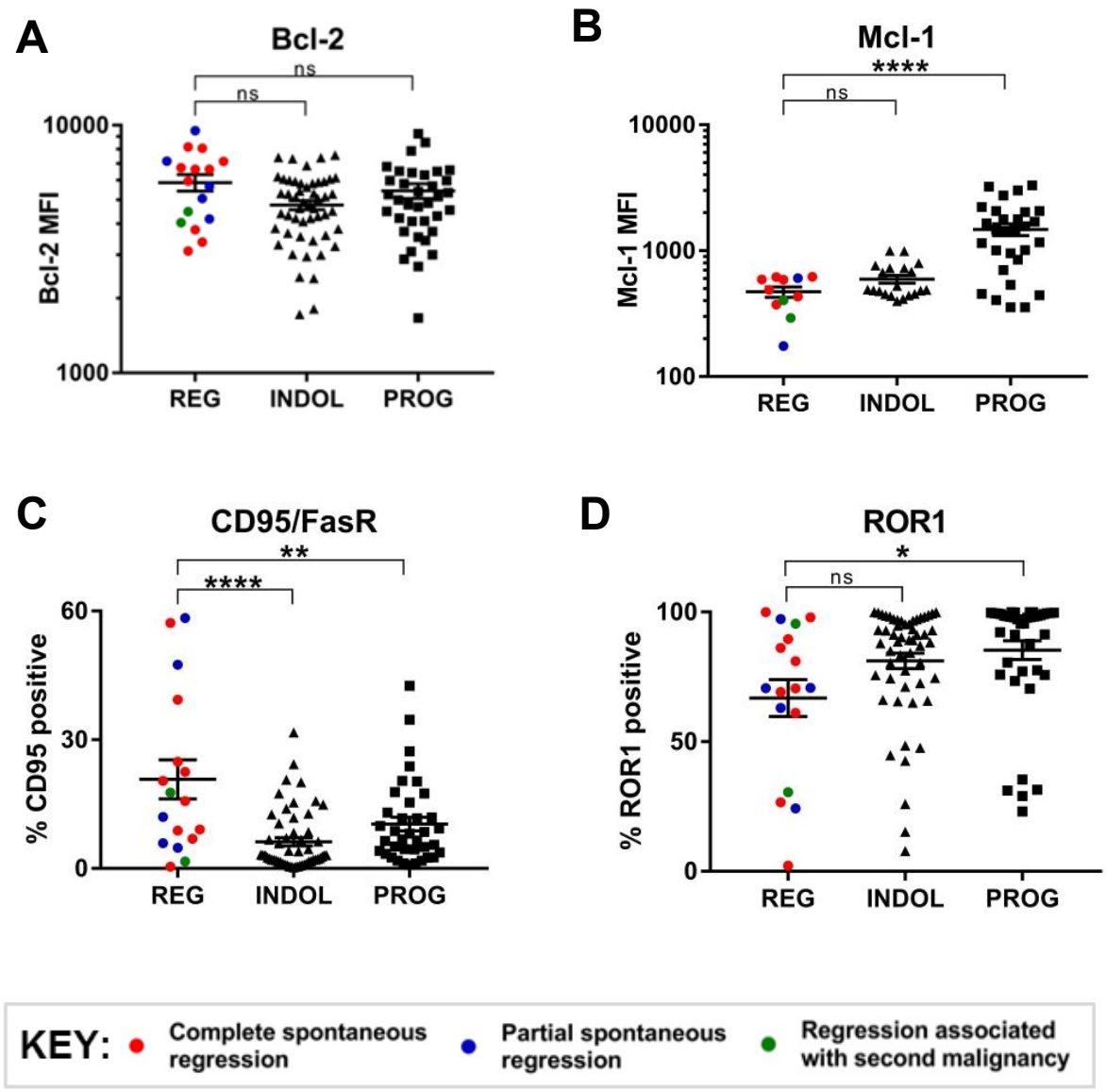

Spontaneously regressed CLL tumours retain high Bcl-2 expression, and have increased FasR and reduced ROR1 expression. The gated CLL population was analysed for the expression of the respective markers shown in each panel. For all comparisons except Mcl-1, 17 spontaneous regression cases were compared against 54 indolent and 40 progressive CLL cases. For Mcl-1, 11 spontaneous regression cases were compared against 20 indolent and 29 progressive cases. Complete spontaneous regression cases, partial spontaneous regression cases and regression cases associated with second malignancy were represented by red, blue and green dots respectively as shown by the key. Statistical significance was determined using one-way ANOVA with Bonferroni post-hoc analysis. Statistical significance is indicated by *p<0.05, **p<0.01, ***p<0.001 and ****p<0.0001; n.s. denotes comparisons that are not statistically significant.

were pre-existing or were acquired during the course of regression, I compared samples from the diagnostic (T0) and regression (T1) timepoints in up to 5 spontaneous CLL regression cases (**Figure 3.6**). A reduction in Ki-67 positivity was observed across all 5 cases. In addition, there was a trend towards an increase in CXCR4 expression and a reduction in CD38 expression. These changes were consistent with reduced CLL proliferation over time. They were accompanied by a trend towards a reduction in cell surface CD49d expression, and an increase in CD95/FasR expression. Collectively, these results on sequential samples suggest that these unique phenotypic features in spontaneous regressors were acquired during course of disease regression.

3.1.4. Reduction in CLL proliferation during spontaneous regression is not due to cellular senescence

Since the major finding emerging from the phenotypic analysis has been that of decreased CLL proliferation in spontaneous disease regression, I next investigated its potential cause and underlying mechanism.

To examine the proliferation history of CLL cells from individuals with spontaneous disease regression, single-cell telomere length analysis was performed on DNA from sorted CLL cells, through collaboration with Prof. Duncan Baird (Cardiff University) and his team as detailed in section 2.6.1. Indolent CLL cases displayed variable telomere lengths. This observation is likely to reflect the clinical heterogeneity of this group of indolent CLL patients, with variable lymphocyte doubling times ranging from 3 years to not reached. Importantly, the mean telomere length of the spontaneous regressing cases was not longer than that of the indolent cases. Indeed, the mean telomere length among spontaneous regressors was generally <5 kb, indicating that the regressed CLL clone was likely to have proliferated at some point during its natural history **(Figure 3.7)**. In most spontaneous regression cases, a

Figure 3.6

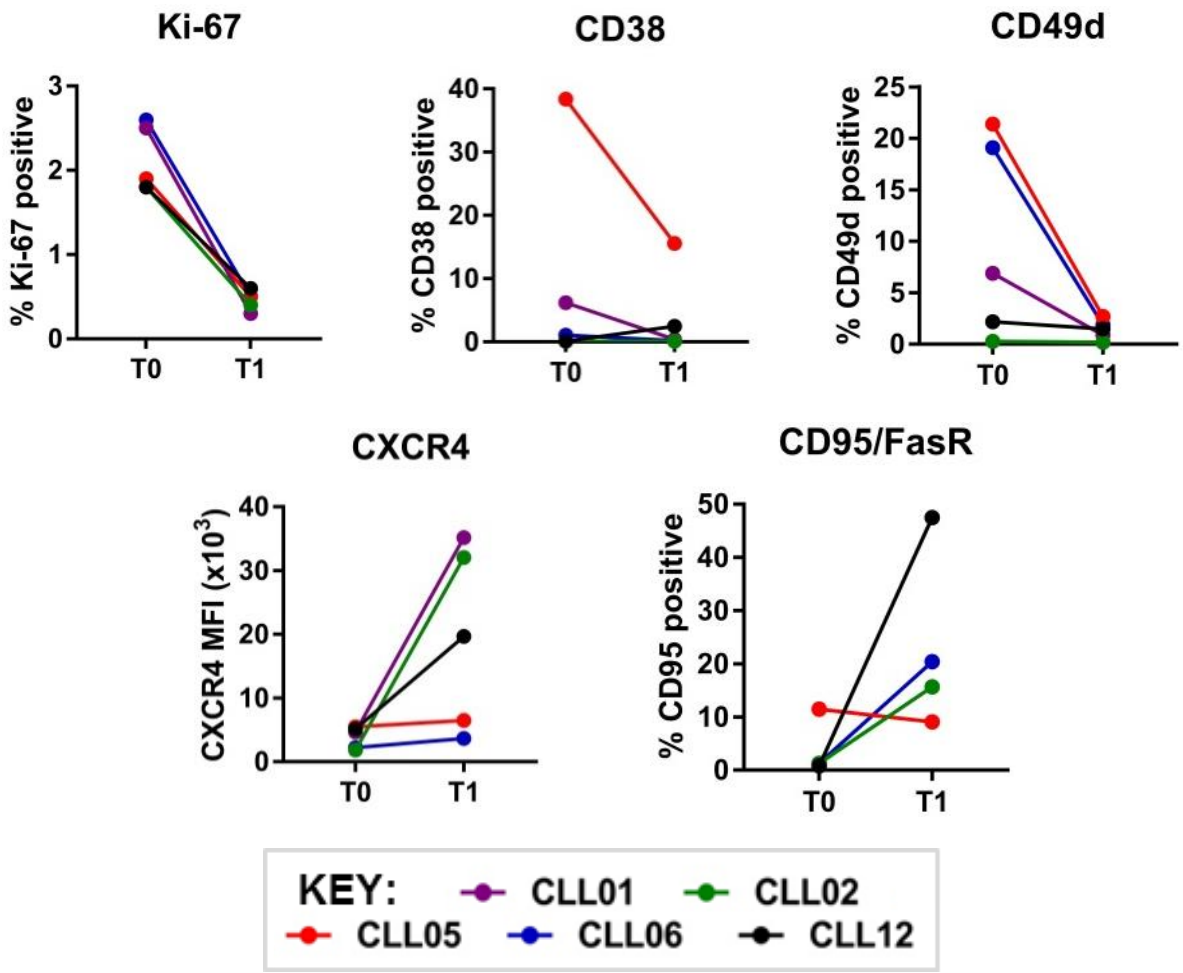

CLL proliferation and cell surface CD49d expression are reduced and CD95/FasR expression is increased during spontaneous regression. Expression of Ki-67, CD38, CD49d, CXCR4 and CD95/FasR were compared between two sequential timepoints in individual spontaneous regression cases. T0 represents the diagnostic timepoint, whereas T1 represents the regression timepoint. Each coloured line represents a specific case, as indicated by the key.

Figure 3.7

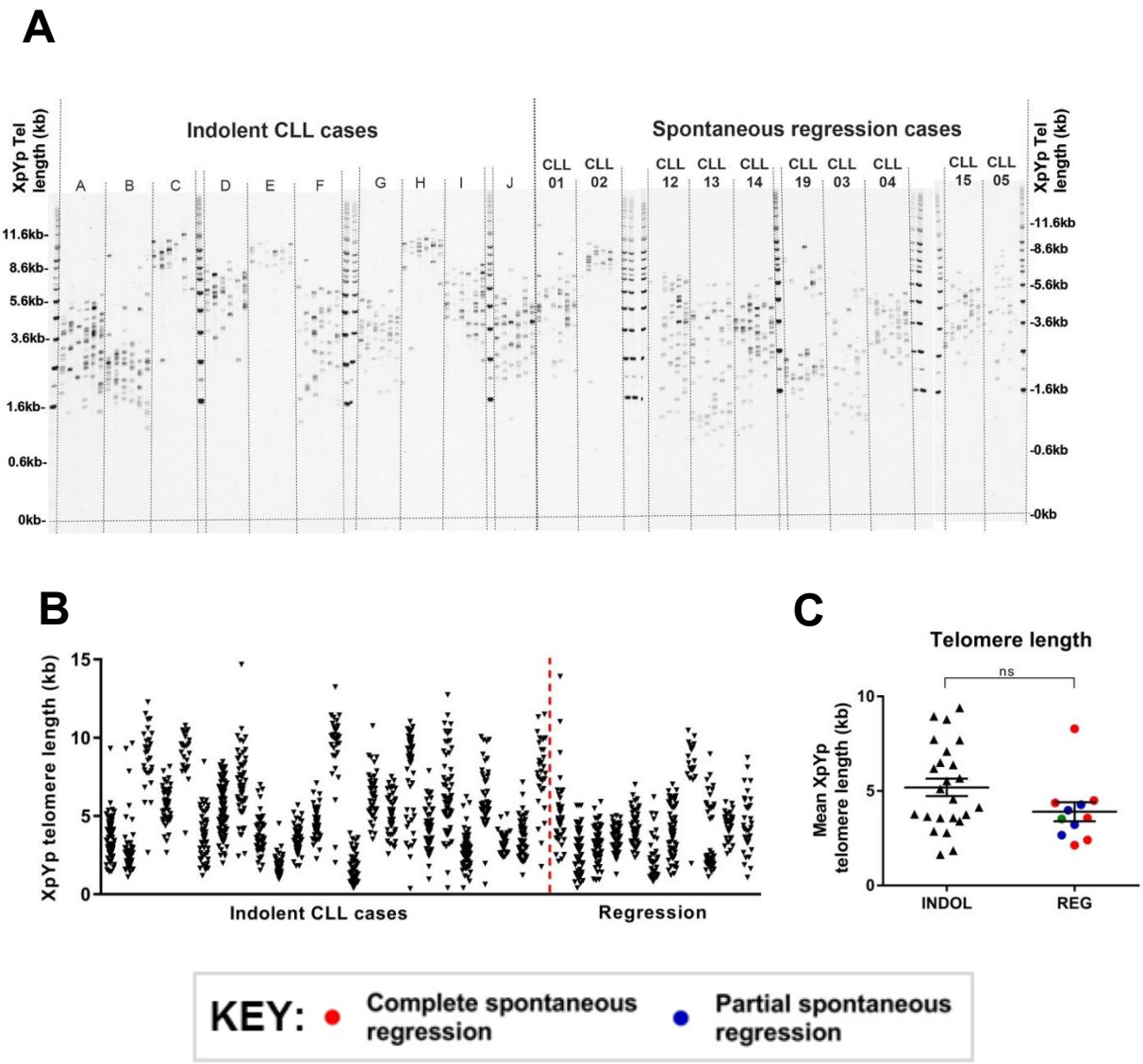

Telomere lengths of spontaneously regressed and non-regressing indolent CLL tumours are comparable. (A) STELA was performed to assess the telomere length of chromosomes Xp and Yp of the CLL cells in each case. The Southern blot shows the telomere length distribution of typical indolent and spontaneous regression cases. **(B)** The telomere length distribution of the CLL Xp and Yp chromosomes in all of the analysed indolent and spontaneous regression cases is summarised. **(C)** The mean CLL XpYp telomere length was compared between the spontaneous regression and indolent cases. Complete spontaneous regression cases and partial spontaneous regression cases were represented by red and blue dots respectively as shown by the key. Statistical significance was determined using Student's T test; n.s. denotes comparisons that are not statistically significant.

range of telomere lengths was seen within individual samples, suggesting intraclonal heterogeneity. When the telomere length of the diagnostic (T0) and regression (T1/T2) samples in individual regression cases were compared, the telomere length distributions were found to be largely similar across timepoints, suggesting the presence of the same CLL clone (**Figure 3.8**). Thus, this finding corroborates the *IGH* sequencing results detailed in section 3.1.2 showing identical *IGH* sequence across timepoints within individual spontaneous CLL regression cases.

Given the rather short CLL telomere length in some of the spontaneous regression cases, I questioned whether the reduction in proliferation seen during spontaneous regression was due to the CLL cells becoming senescent. To address this, I first measured the telomerase activity of the CLL cells from each regression (T1) sample using methodology outlined in section 2.7.2, and compared that with samples from indolent CLL cases. Interestingly, and contrary to expectation, high CLL telomerase activity was observed among the spontaneous regressors compared to patients with indolent disease (**Figure 3.9A**). I next proceeded to stain the CLL cells from patients who have undergone spontaneous disease regression with beta-galactosidase, a marker of cellular senescence. The CLL cells from these patients were negative for beta-galactosidase staining (**Figure 3.9B**). Collectively, these results exclude cellular senescence as a cause of decreased CLL proliferation during spontaneous regression.

3.1.5. Spontaneously regressed CLL tumours are unresponsive to IgM and IgD BCR stimulation

BCR positive signalling is the major driver of CLL proliferation (Herishanu et al., 2011; Stevenson et al., 2011). Having excluded cellular senescence as a cause of decreased CLL proliferation in spontaneous regression, I asked whether this could be due

Figure 3.8

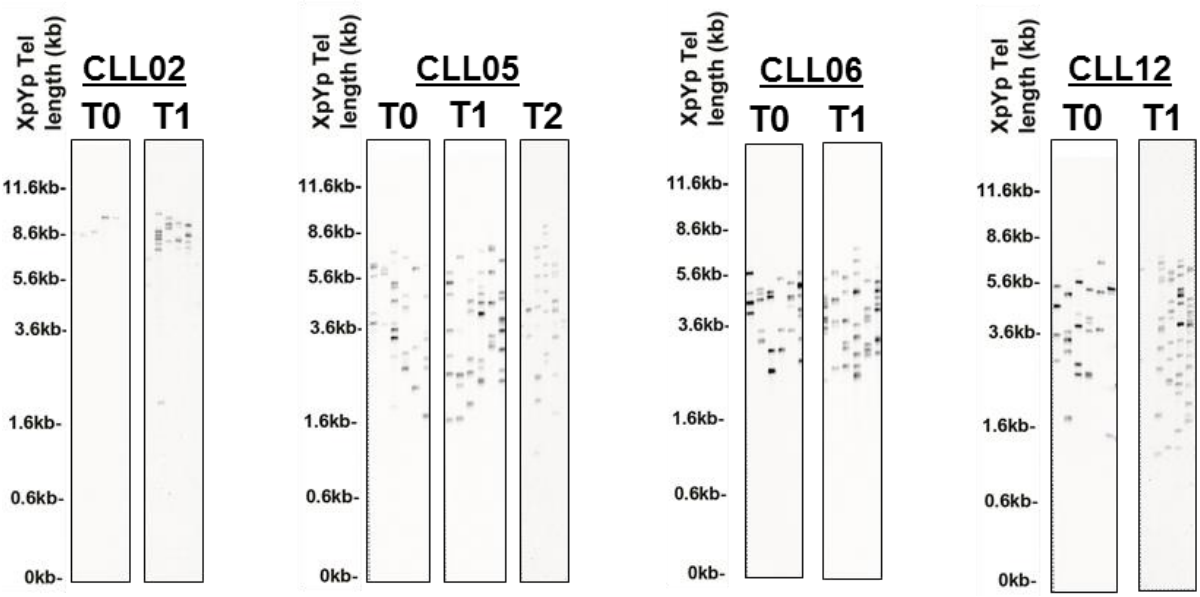

Telomere length distributions are similar across sequential timepoints in spontaneous CLL regression cases. STELA was performed to assess the telomere length of chromosomes Xp and Yp of CLL cells from sequential samples in 4 spontaneous regression case. T0 represents the diagnostic timepoint, whereas T1/T2 represents the regression timepoint(s). The Southern blot shows the telomere length distribution of each sample.

Figure 3.9

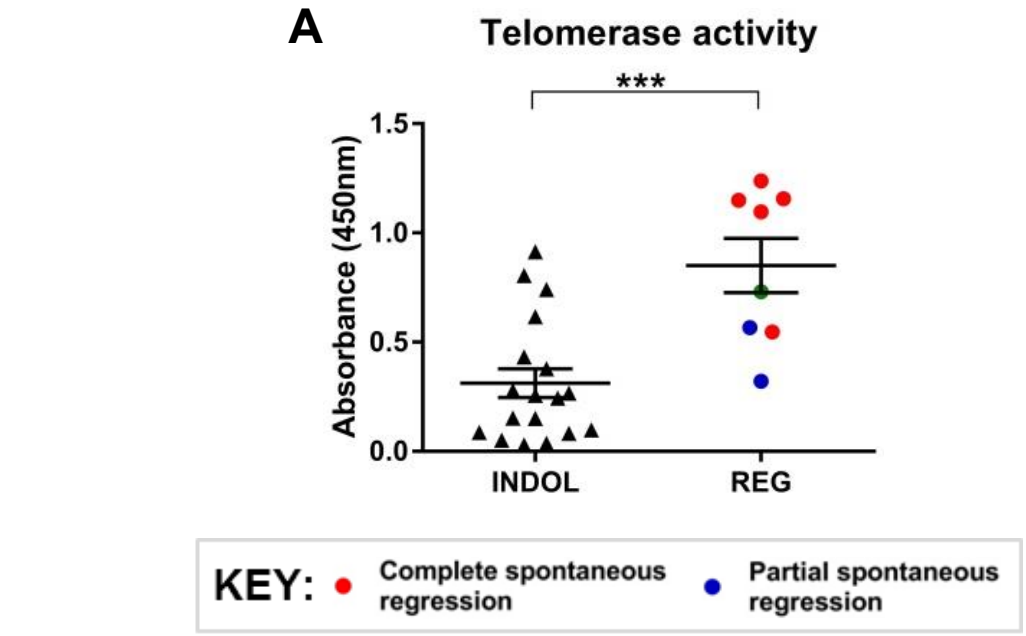

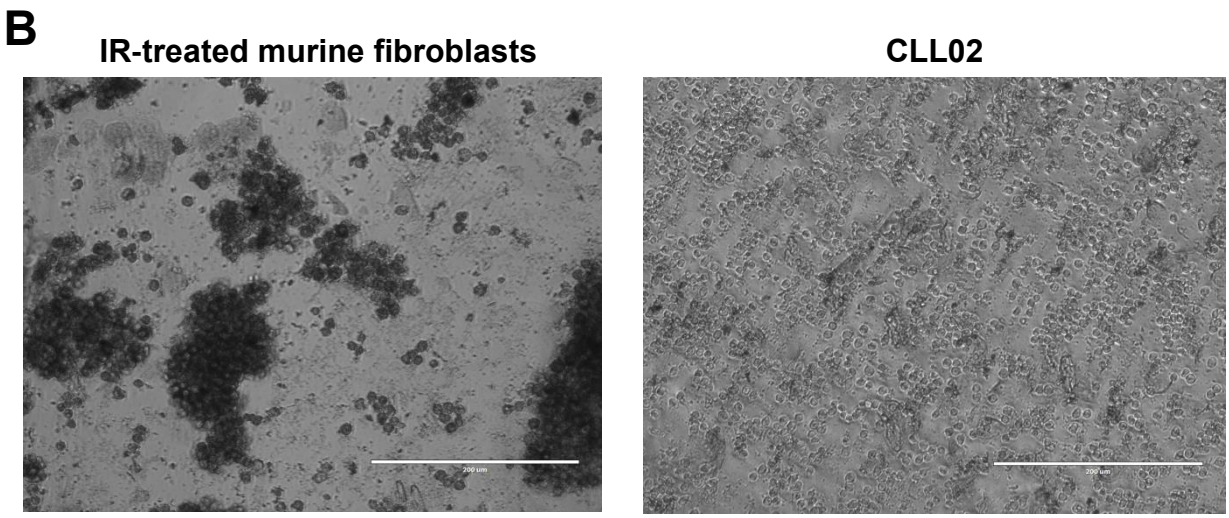

Reduction in CLL proliferation during spontaneous regression is not due to cellular senescence. (A) Telomerase activity of sorted CLL cells was assessed using the Telo*TAGGG* telomerase PCR enzyme-linked immunosorbent assay kit. The absorbance at 450 nm, which is proportional to the telomerase activity, was compared between the spontaneous regression and indolent cases. Complete spontaneous regression cases and partial spontaneous regression cases were represented by red and blue dots respectively as shown by the key. Statistical significance was determined using Student's T test. Statistical significance is indicated by ***p<0.001. **(B)** Sorted CLL cells were assessed for β-galactosidase staining. The staining pattern of a typical spontaneous regression case (CLL02) was shown in comparison with the positive control (murine embryonic fibroblasts induced to senesce by exposure to a sublethal dose of ionising radiation).

to the attenuation of CLL BCR signalling responses in patients with spontaneous CLL regression.

I therefore assessed BCR signalling response by phosphoflow analysis on gated CLL cells, comparing spontaneous regression cases at the regression (T1) timepoint against *IGHV* mutated and unmutated indolent cases (**Figure 3.10**). The combined effect of IgM and IgD stimulation was first examined, which reflects BCR stimulation *in vivo*. Indolent M-CLLs displayed variable BCR signalling response to combined stimulation with anti-IgM and anti-IgD $F(ab)_2$ antibodies, with many cases showing substantial response as evidenced by high levels of Syk, Erk and Akt phosphorylation. On the contrary, the response to combined IgM and IgD BCR stimulation was uniformly low among spontaneous regressors, as evidenced by <10% of CLL cells in these cases displaying p-Syk, p-Erk and p-Akt positivity following BCR stimulation. No significant difference in BCR signalling response was apparent between individuals with complete spontaneous regression and those with partial spontaneous regression.

In order to dissect the relative contribution of IgM and IgD response to the overall BCR signalling response in each comparator group, I next stimulated the CLL cells in each sample separately with anti-IgM or anti-IgD $F(ab)_2$ antibodies. As expected, there was a marked difference in IgM response between indolent M-CLL and UM-CLL, with much greater IgM response in UM-CLL. This was consistent with data presented in several previously published studies (Guarini et al., 2008; Lanham et al., 2003; Mockridge et al., 2007). In addition, there was a smaller but significant difference in IgM response between the regression group and the indolent M-CLL group, such that whereas all the regression cases were unresponsive to IgM BCR stimulation, many indolent M-CLL cases retained a low level of response. Moreover, the IgD response was both significantly and substantially lower in the regression group compared to the indolent M-CLL group (**Figure 3.11**). This was reflected in the differential expression of CLL cell surface immunoglobulins across the three

Figure 3.10

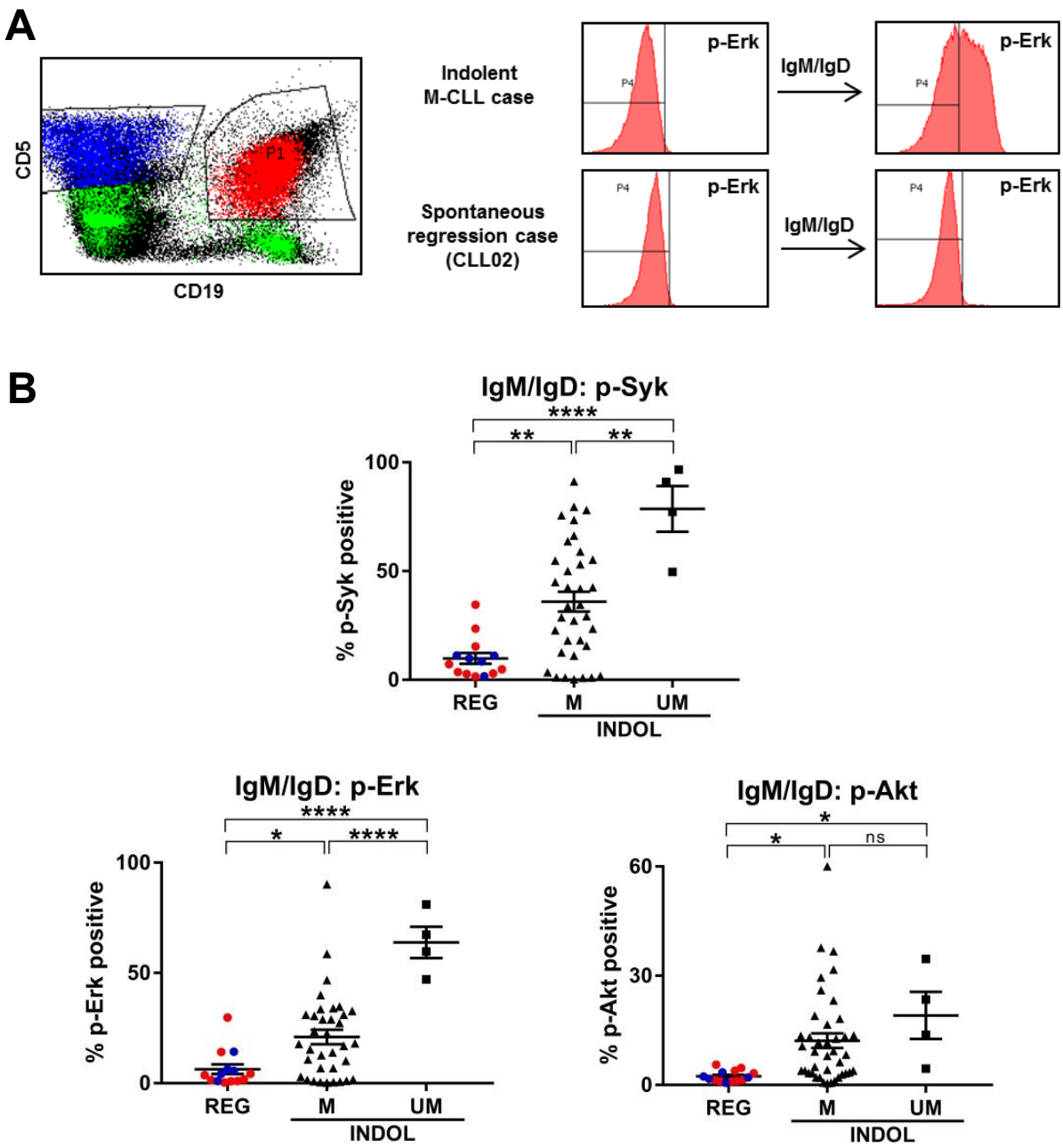

Spontaneously regressed CLL tumours are unresponsive to combined IgM and IgD BCR stimulation. (A) BCR signalling responses to IgM and IgD stimulation can be assessed by phosphoflow. Cells were stimulated with anti-human IgM and IgD $F(ab')_2$ antibodies prior to acquisition on a flow cytometer. Left panel: The CD19− CD5+ T-cell population (shown in blue) was used as the internal negative control, and the CD19+ CD5+ CLL population (shown in red) was gated and analysed for the phosphorylation of Syk, Erk and Akt. The positive vs negative gate for p-Syk, p-Erk and p-Akt was set such that 99% of unstimulated cells would fall within the negative gate. Right panel: Example histograms showing results of a typical indolent M-CLL case and a spontaneous regression case. While many M-CLL cases were responsive to IgM/IgD stimulation (>10% p-Syk, p-Erk and p-Akt positivity), spontaneous regression cases were not. **(B)** Phosphoprotein levels of spontaneous regression cases (n=14) in response to combined IgM and IgD stimulation were compared against indolent M-CLL (n=35) and UM-CLL (n=4) cases. Complete spontaneous regression cases and partial spontaneous regression cases were represented by red and blue dots respectively as shown by the key in Figure 3.9A. Statistical significance was determined using one-way ANOVA with Bonferroni post-hoc analysis. Statistical significance is indicated by *p<0.05, **p<0.01 and ****p<0.0001; n.s. denotes comparisons that are not statistically significant.

Figure 3.11

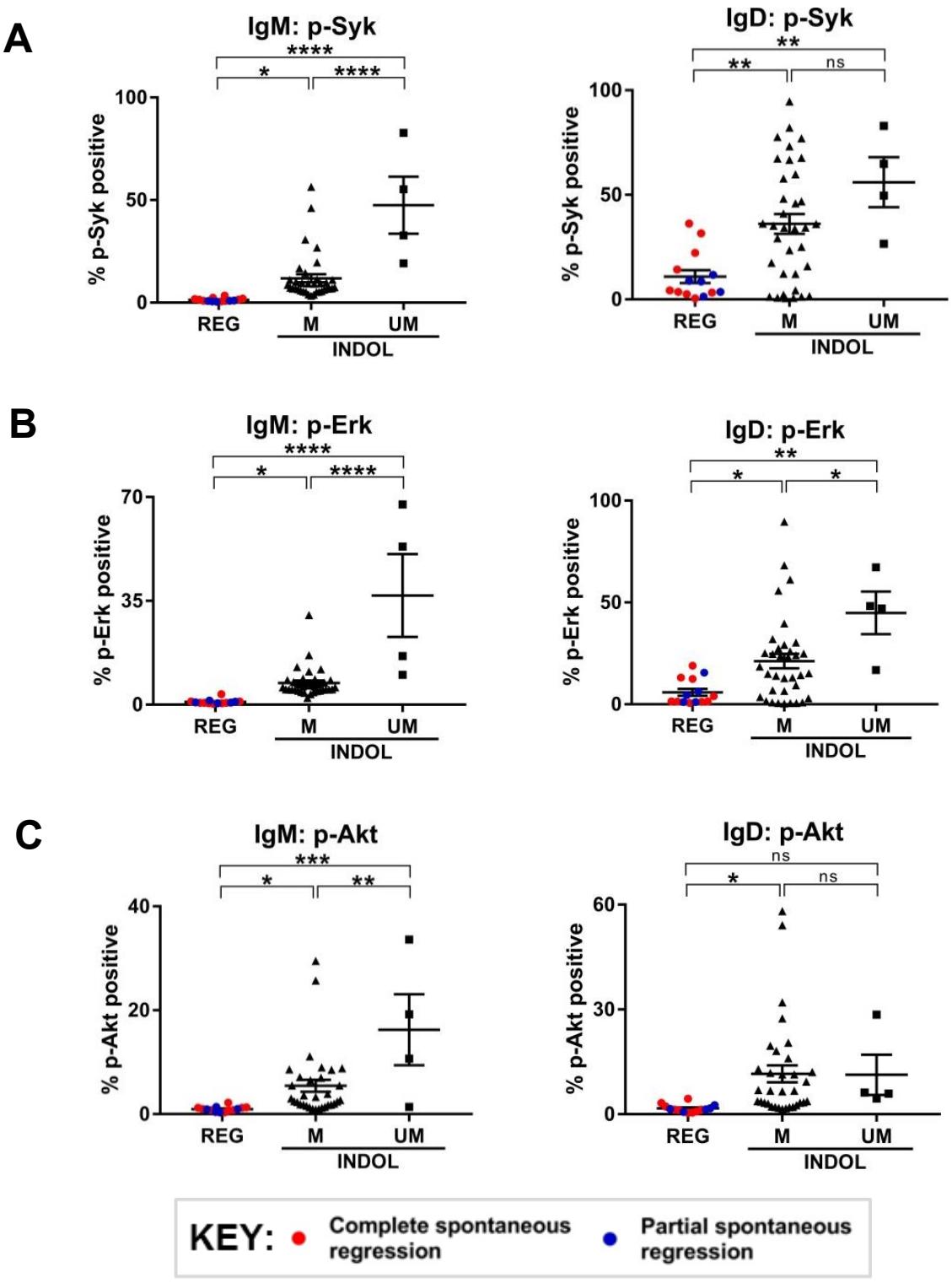

Spontaneously regressed CLL tumours are unresponsive to separate IgM BCR stimulation and IgD BCR stimulation. Phosphoprotein levels of spontaneous regression cases (n=14) in response to separate stimulation with anti-human IgM or IgD $F(ab')_2$ antibody stimulation were compared against indolent M-CLL (n=35) and UM-CLL (n=4) cases. Complete spontaneous regression cases and partial spontaneous regression cases were represented by red and blue dots respectively as shown by the key. Statistical significance was determined using one-way ANOVA with Bonferroni post-hoc analysis. Statistical significance is indicated by *p<0.05, **p<0.01, ***p<0.001 and ****p<0.0001; n.s. denotes comparisons that are not statistically significant.

comparator groups, i.e. spontaneous regression, indolent M-CLL and indolent UM-CLL. Spontaneous regression cases had low CLL surface IgM (sIgM) and modest surface IgD (sIgD) expression. However, whereas indolent M-CLLs also had low sIgM expression compared to UM-CLL cases, many of these cases retained high sIgD expression that was comparable to their UM-CLL counterpart and significantly higher than that of spontaneous CLL regressors (**Figure 3.12**). Because low sIgM and sIgD expression in CLL can sometimes be due to class-switch recombination, I examined the expression of IgG in all cases. All samples had negligible IgG expression with the exception of a single spontaneous regression case and an indolent M-CLL case.

The unresponsiveness to BCR stimulation seen in CLL cells from spontaneously regressing CLL cases, coupled with low cell surface immunoglobulin expression, are hallmark features of B cell anergy (Packham et al., 2014). I therefore proceeded to evaluate, by flow cytometry, the spontaneous CLL regression cases for constitutive Erk phosphorylation and the expression of the B cell inhibitory receptor LAIR1 that could corroborate these features (Muzio et al., 2008; Packham et al., 2014; Perbellini et al., 2014). High levels of constitutive Erk phosphorylation, but not constitutive Akt phosphorylation, was apparent in CLL cells from the spontaneous regression cases, particularly when compared to the indolent M-CLL and UM-CLL cases (**Figure 3.13A-B**). In addition, CLL cells from spontaneous regressors displayed higher levels of expression of LAIR1, a B cell inhibitory receptor, on their cell surface compared to both indolent M-CLL and UM-CLL cases (**Figure 3.13C**). Taken together, these results indicate CLL anergy as a mechanism accounting for the reduction in CLL proliferation during spontaneous regression.

Figure 3.12

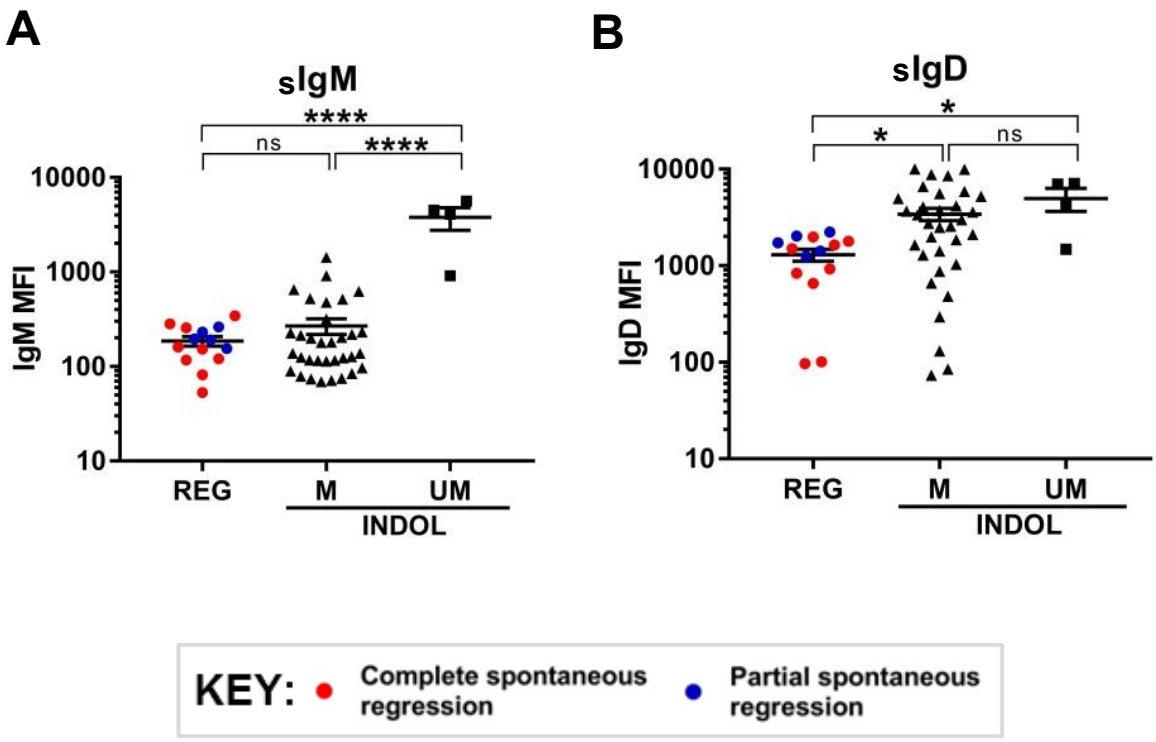

Spontaneously regressed CLL tumours have low cell surface IgM and IgD expression. CLL cells were gated on the basis of their expression of CD19 and CD20 (CD19+ CD20-low), as shown in Figure 2.3. The gated CLL population was analysed for the expression of cell surface IgM (sIgM; **A**) and IgD (sIgD; **B**). Spontaneous regression cases (n=14) were compared against indolent M-CLL (n=35) and UM-CLL (n=4) cases. Complete spontaneous regression cases and partial spontaneous regression cases were represented by red and blue dots respectively as shown by the key. Statistical significance was determined using one-way ANOVA with Bonferroni post-hoc analysis. Statistical significance is indicated by *p<0.05 and ****p<0.0001; n.s. denotes comparisons that are not statistically significant.

Figure 3.13

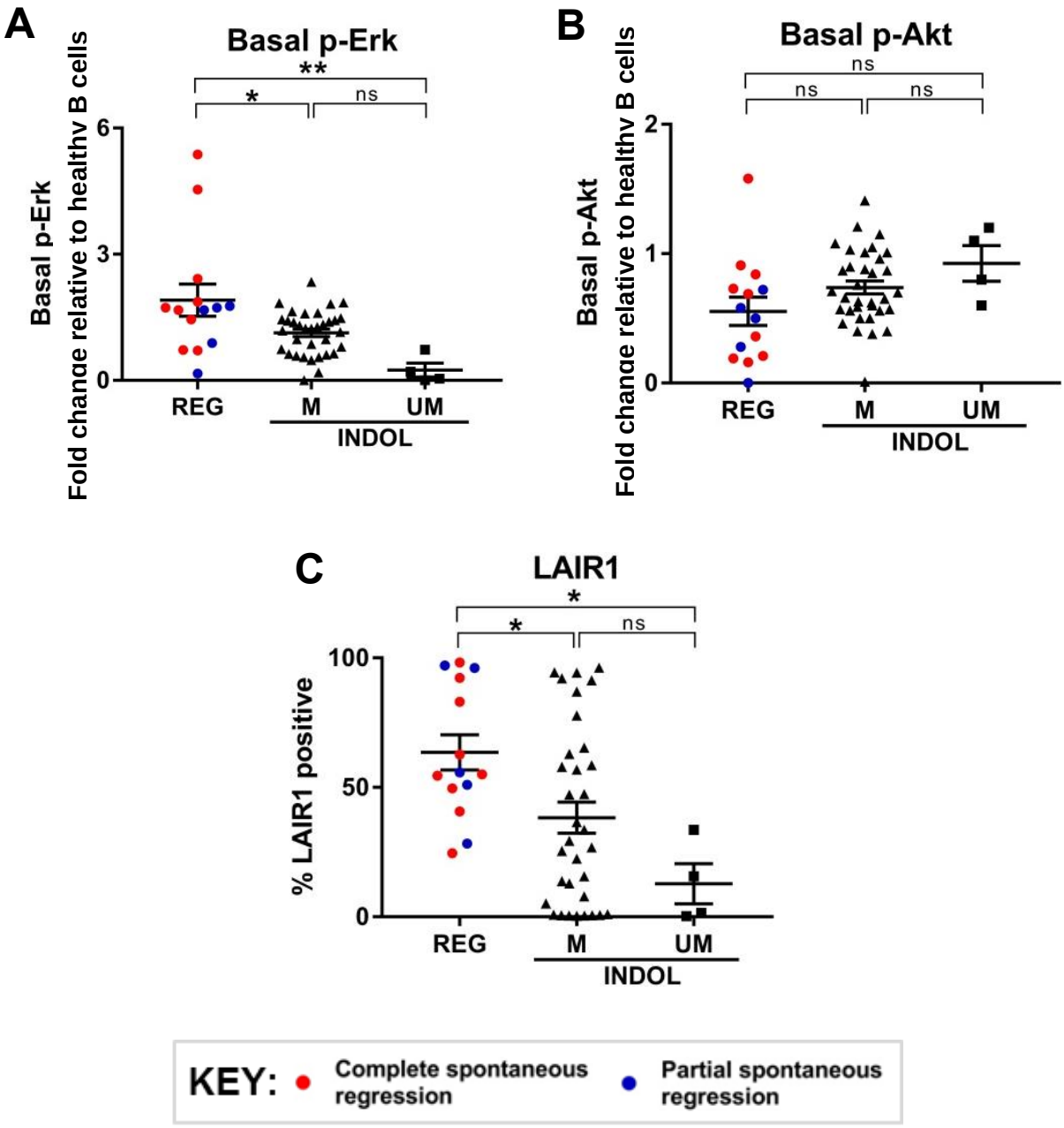

Spontaneously regressed CLL tumours have high levels of constitutive Erk phosphorylation and LAIR1 expression. The gated CLL population was analysed for basal Erk and Akt phosphorylation (A-B) and cell surface LAIR1 expression (B). Spontaneous regression cases (n=14) were compared against indolent M-CLL (n=35) and UM-CLL (n=4) cases. Basal Erk and Akt phosphorylation in CLL cells was normalised to B cells from 3 age-matched healthy donors, and was expressed as fold change compared to these controls. Complete spontaneous regression cases and partial spontaneous regression cases were represented by red and blue dots respectively as shown by the key. Statistical significance was determined using one-way ANOVA with Bonferroni post-hoc analysis. Statistical significance is indicated by *p<0.05 and ****p<0.0001; n.s. denotes comparisons that are not statistically significant.

3.1.6. The genomic landscape of spontaneously regressed CLL tumours

The genomic landscape of CLL in general is well characterised, with several major WES or WGS studies published over recent years. However, these studies focused on indolent CLL cases (Kasar et al., 2015; Puente et al., 2015) or progressive cases (Landau et al., 2015; Puente et al., 2015). On the other hand, the genomic landscape of spontaneously regressing CLL is unknown.

To elucidate the genomic landscape of this group of CLL patients, I undertook SNP array analysis and WES on 19 spontaneous regression cases, using a CLL sample from the regression (T1) timepoint and a germline sample (either the granulocyte or the T cell fraction, as outlined in section 2.5) for each case. SNP array analysis revealed a median of 1 somatic copy number aberrations (CNAs; range 0-3) per case that were not present in the germline DNA. These are listed in **Table 3.4** for each spontaneous CLL regression case. A summary of the recurrent and/or functionally important CNAs is provided in **Figure 3.14**, alongside the recurrent single nucleotide variations (SNVs) for each case.

The most frequent CNA was 13q14.2-3 deletion, seen in 12 of 19 cases (63%), with all deletions encompassing the minimally deleted region involving the *DLEU2*/miR-15a/16-1 cluster. Most 13q14 deletions also encompassed both *DLEU7* and *RNASEH2B* genes that are adjacent to *DLEU2*. In addition, 2 cases (10%; CLL14 and CLL16) carried a larger 13q14 deletion that included the retinoblastoma (*RB1*) gene (**Table 3.4**). Two of these 13q14 deletions were homozygous (CLL05 and CLL06), whereas others were hemizygous. Consistent with acquisition of del(13q14) being an early genomic event, in the majority (10 of 12) of cases del(13q14) was clonal, and was present in all CLL cells. The frequency of del(13q14) in this spontaneous regression cohort was comparable to a typical non-regressing CLL cohort. There was no recurrent CNAs in the spontaneous regression cohort

Table 3.4. Copy number variations (CNV) in 19 spontaneously regressed CLL tumours

	CNV
CLL01	8q24.13 del (x1; *TRIB1*; *NSMCE2*); 13q14.2- q14.3 del (x1; miR15a/16-1, *DLEU7; RNASEH2B)*
CLL02	**10q26.3 gain** (x3); 13q14.2- q14.3 del (x1; miR15a/16-1, *DLEU7; RNASEH2B*)
CLL03	13q14.2- q14.3 del (x1; miR15a/16-1, *DLEU7*)
CLL04	2q13 del (x1); **3p24.2-p24.3 gain** (x3; *NKIRAS1*)
CLL05	13q14.2- q14.3 del (x0; miR15a/16-1, *DLEU7*)
CLL06	**3q23 gain** (x3); 13q14.2-q14.3 del (x0; miR15a/16-1, *DLEU7; RNASEH2B*)
CLL07	3q11.1-q11.2 gain (x3) ; **4q28.3 gain** (x3); **11p13-p14.1 gain** (x3; *WT1*)
CLL08	No detectable CNV
CLL09	**7q11.23 del** (x1)
CLL10	7q31.33-q32.1 gain (x3; *POT1*); 13q14.2- q14.3 del (x1; miR15a/16-1, *DLEU7; RNASEH2B*)
CLL11	13q14.2-q14.3 del (x1; miR15a/16-1, *DLEU7*)
CLL12	2p16.1 del (x1)
CLL13	8p del (x1; *TNFRSF10A*); 13q14.2-q14.3 del (x1; miR15a/16-1, *DLEU7*); 17p del (x1; *TP53*)
CLL14	**10q21.2 gain** (x3); 13q14.2-q14.3, q21-q22 del (x1; miR15a/16-1, *DLEU7*, *RNASEH2B*; *RB1*); 20q11.21-11.22, q13.31-q13.32 gain (x3)
CLL15	**12q21.2-q31 gain** (x3; *PAWR*); 13q14.2-q14.3 del (x1; miR15a/16-1, *DLEU7; RNASEH2B*); **16q11.2-q12.1 gain** (x3)
CLL16	13q14.2-q14.3 del (x1; miR15a/16-1, *RNASEH2B*; *RB1*)
CLL18	6p22.3 gain (x3)
CLL19	**7p12.1 gain** (x3)
CLL20	13q14.2-q14.3 del (x1; miR15a/16-1, *DLEU7; RNASEH2B*)

Shown in brackets following each CNV are the copy number within the cytoband, followed by any genes within the cytoband that could potentially be functionally significant. Highlighted in bold are CNVs that have not been previously reported in major CLL genomic studies.

other than del(13q14), although additional CNAs were found in isolated cases. One spontaneous regression case (CLL13) harboured clonal del(17p) and del(8p), which are well-described genomic aberrations in CLL, in addition to del(13q14). Other CNAs of potential functional significance include deletion of 8q24 (clonal), as well as duplications of 3p24, 7q31, 11p13-14 and 12q21-31 (all clonal) as shown in **Table 3.4**.

In addition to CNAs, a number of SNVs which include missense, nonsense, stop loss and splice donor site mutations were detected by WES across the spontaneous CLL regression cohort. Included in **Figure 3.14** are all SNVs that were identified by MuTect and/or Platypus, found to be significantly mutated by MuSigCV, and predicted to have a functional impact by VEP, SIFT and Polyphen. All were validated independently by Sanger sequencing or allele-specific PCR. The mutational burden as revealed by WES was generally low in spontaneously regressed CLLs, with a median of 2 SNVs per case (range 0-5) and no significant indels identified in any case. Recurrent SNVs were seen in only 3 genes: *TP53* (occurring in 3 cases), *PCMTD1* (in 3 cases) and *NAV3* (in 2 cases). Mutations within known putative CLL drivers were found in 5 spontaneous regression cases (26%). In addition to *TP53* mutations, *MYD88* and *HIST1H1B* mutations were each observed in one case. All *TP53* and *MYD88* mutations were previously described and reported in the Catalogue of Somatic Mutations in Cancer (COSMIC), whereas the *HIST1H1B* mutation identified was novel. Of note, CLL13 harboured a biallelic *TP53* defect, consisting of a 17p deletion and a c.484A>T *TP53* mutation. With the exception of the *TP53* mutation in CLL13 which was clonal with variant allelic frequency (VAF) of 100%, all driver mutations were subclonal with VAF of 12-44%. These results collectively demonstrate that spontaneous CLL regression can occur in the presence of mutations in putative CLL drivers.

Among SNVs that were identified in genes not known to be CLL drivers, all have previously been reported in cancer, but only 19 of 30 (63%) have previously been reported in CLL. The majority were subclonal and occur in isolated spontaneous regression cases.

Figure 3.14

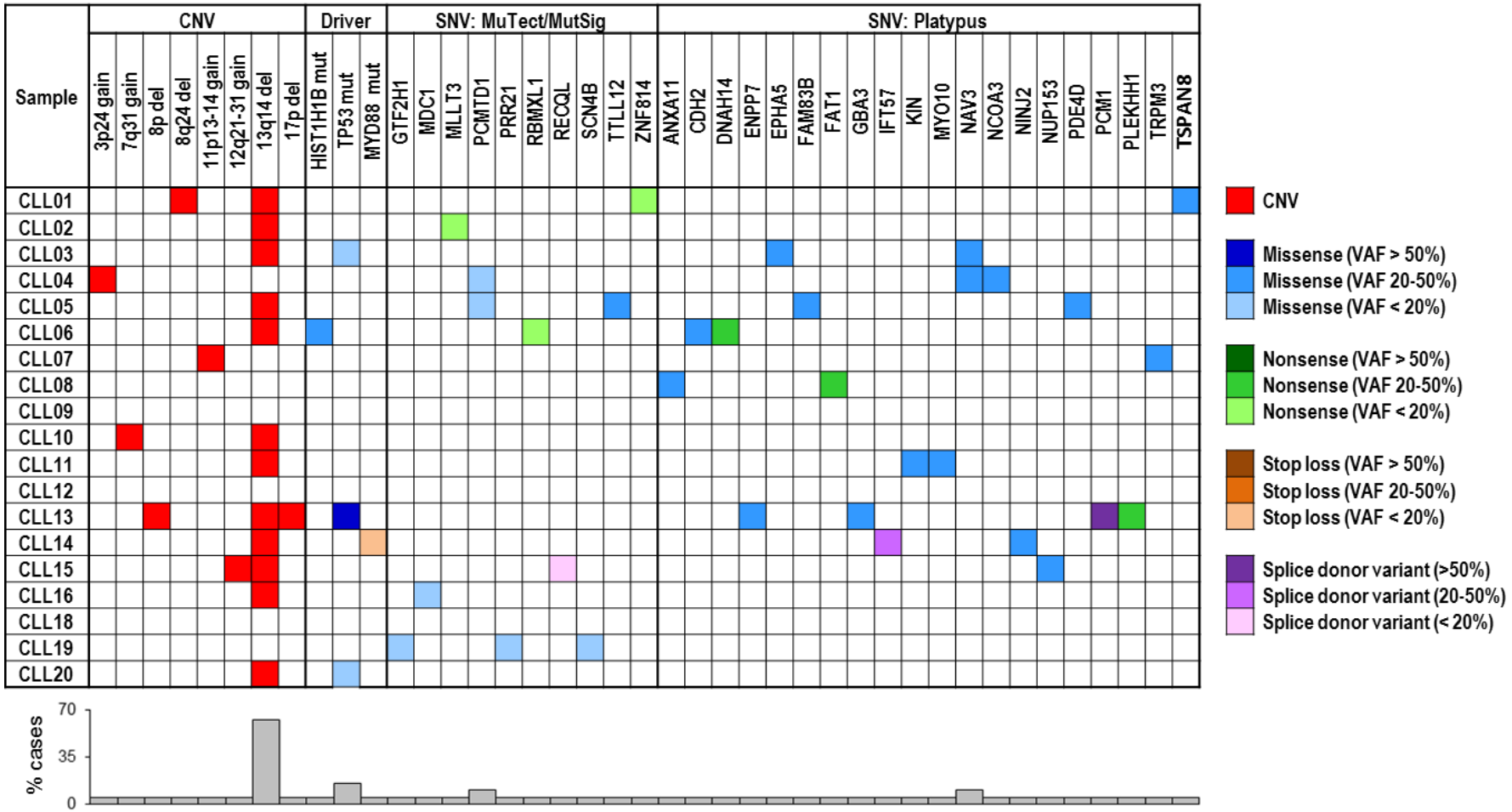

The genomic landscape of 19 spontaneously regressed CLL tumours. The CNV data of each spontaneous regression case was combined with their respective SNV data obtained from WES. Different types of genomic events are represented by different colours, with the colour code displayed next to the table. The frequency of each genomic event is represented in the bar chart beneath the table. CNV, copy number variation; SNV, single nucleotide variation; VAF, variant allelic fraction.

3.1.7. Spontaneous CLL regression leads to partial recovery of normal immune phenotype

CLL is associated with immune dysfunction. In T cells this is manifested in the accumulation of terminally differentiated memory T cells, leading to expanded T cell numbers, as well as T cell exhaustion (Forconi and Moss, 2015; Nunes et al., 2012; Ramsay et al., 2008; Riches et al., 2013). Likewise, NK cells numbers are expanded in CLL, and NK cell function is defective (Huergo-Zapico et al., 2014). To determine whether the defective immune phenotype is reversed in spontaneous CLL regression, I analysed T cell and NK cell number, as well as the T cell phenotype, in patients with spontaneous CLL regression and compared this to non-regressing indolent CLL patients.

Spontaneous CLL regression was associated with a reduction in CD4+ and CD8+ T cell number, both when compared to non-regressing indolent cases **(Figure 3.15A, left panel)**, and when compared across sequential timepoints in individual regression cases **(Figure 3.15B)**. CD4+ and CD8+ T cells can be further differentiated into four subsets on the basis of their CD27 and CD45RA expression. These are namely naïve (CD27+ CD45RA+), central memory (CM; CD27+ CD45RA−), effector memory (EM; CD27− CD45RA−) and effector memory RA (EMRA; CD27− CD45RA+) T cell subsets. Patients who have undergone spontaneous CLL regression had lower CD4 and CD8 T cell number compared to patients with non-regressing indolent CLL across all T cell subsets **(Figure 3.15A, left panel)**, and no difference was observed in T cell subset distribution between spontaneous regression and indolent CLL groups (**Figure 3.15A, right panel**).

As explained in section 1.2.1.4, the inversion of CD4:CD8 ratio (CD4:CD8 < 1) is an abnormality seen in some CLL patients. Inversion of CD4:CD8 ratio was found to persist in several subjects who have undergone spontaneous CLL regression (**Figure 3.15C**). On the other hand, spontaneous regression was associated with a significant reduction in the expression of the T cell exhaustion marker PD-1 in CD8+ but not CD4+ T cells (**Figure**

Figure 3.15

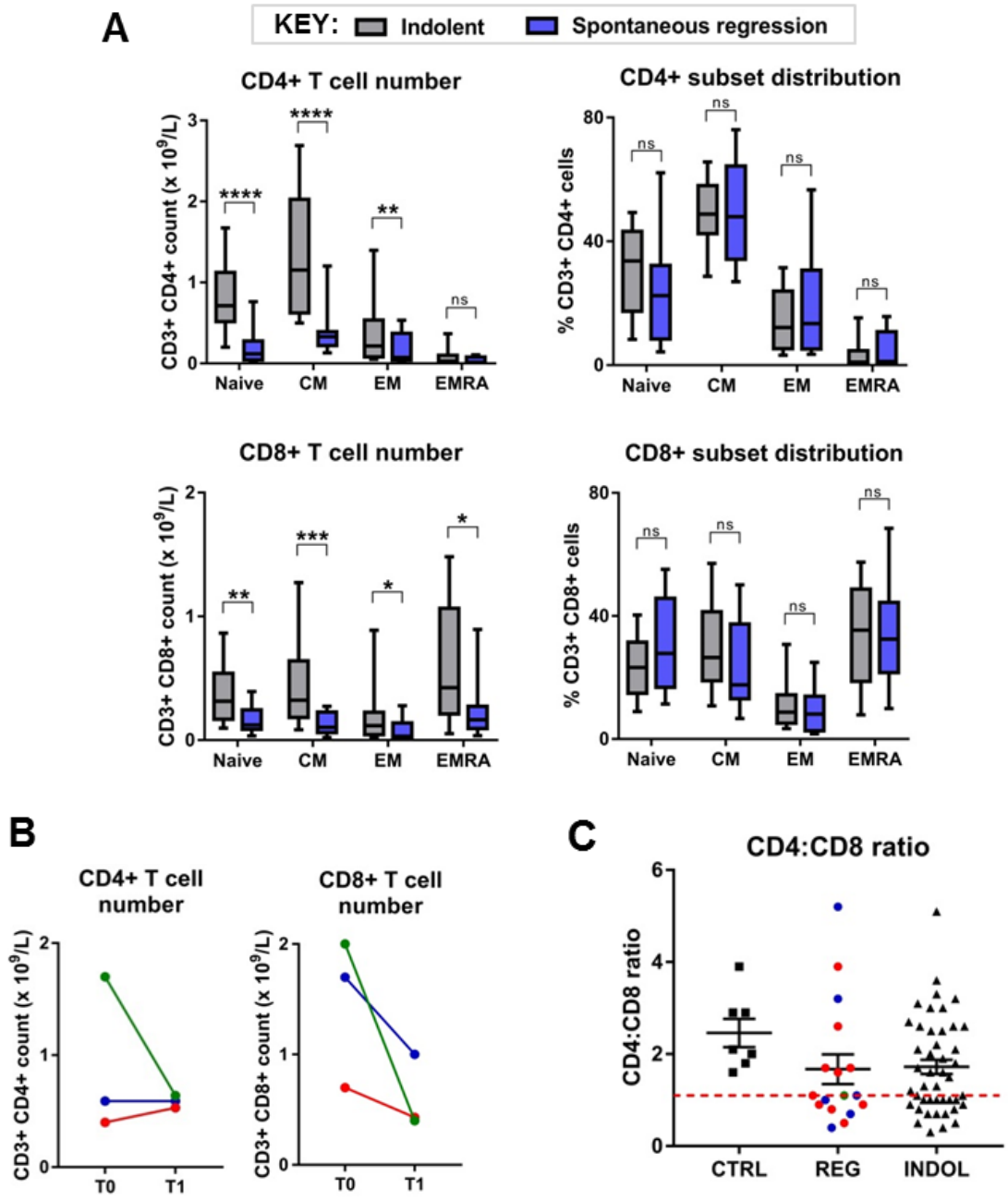

Spontaneous CLL regression is accompanied by a reduction in T cell number. (A) Subsets of CD4+ and CD8+ T cells were defined by the markers CD27 and CD45RA, with naïve cells being CD27+ CD45RA+, central memory (CM) cells being CD27+CD45RA−, effector memory (EM) cells being CD27−CD45RA−, and effector memory RA (EMRA) cells being CD27−CD45RA+. The number of T cells within each subset was determined from the CD4 or CD8 count by taking into consideration of the subset distribution within the CD4+ or CD8+ T cell population respectively. Spontaneous regression cases were compared to indolent cases, and statistical significance was determined using Student's T test. Statistical significance is indicated by *p<0.05, **p<0.01, ***p<0.001 and ****p<0.0001; n.s. denotes comparisons that are not statistically significant. **(B)** The CD4+ and CD8+ T cell number was compared between the diagnostic (T0) and the regression (T1) timepoint in 3 individuals with spontaneous CLL regression. **(C)** The CD4:CD8 ratio in spontaneous regression cases (REG; n=16) were compared against indolent cases (INDOL; n=31) and age-matched healthy controls (CTRL; n=6). Complete spontaneous regression cases, partial spontaneous regression cases and regression cases associated with second malignancy were represented by red, blue and green dots respectively as shown by the key in Figure 3.5.

Figure 3.16

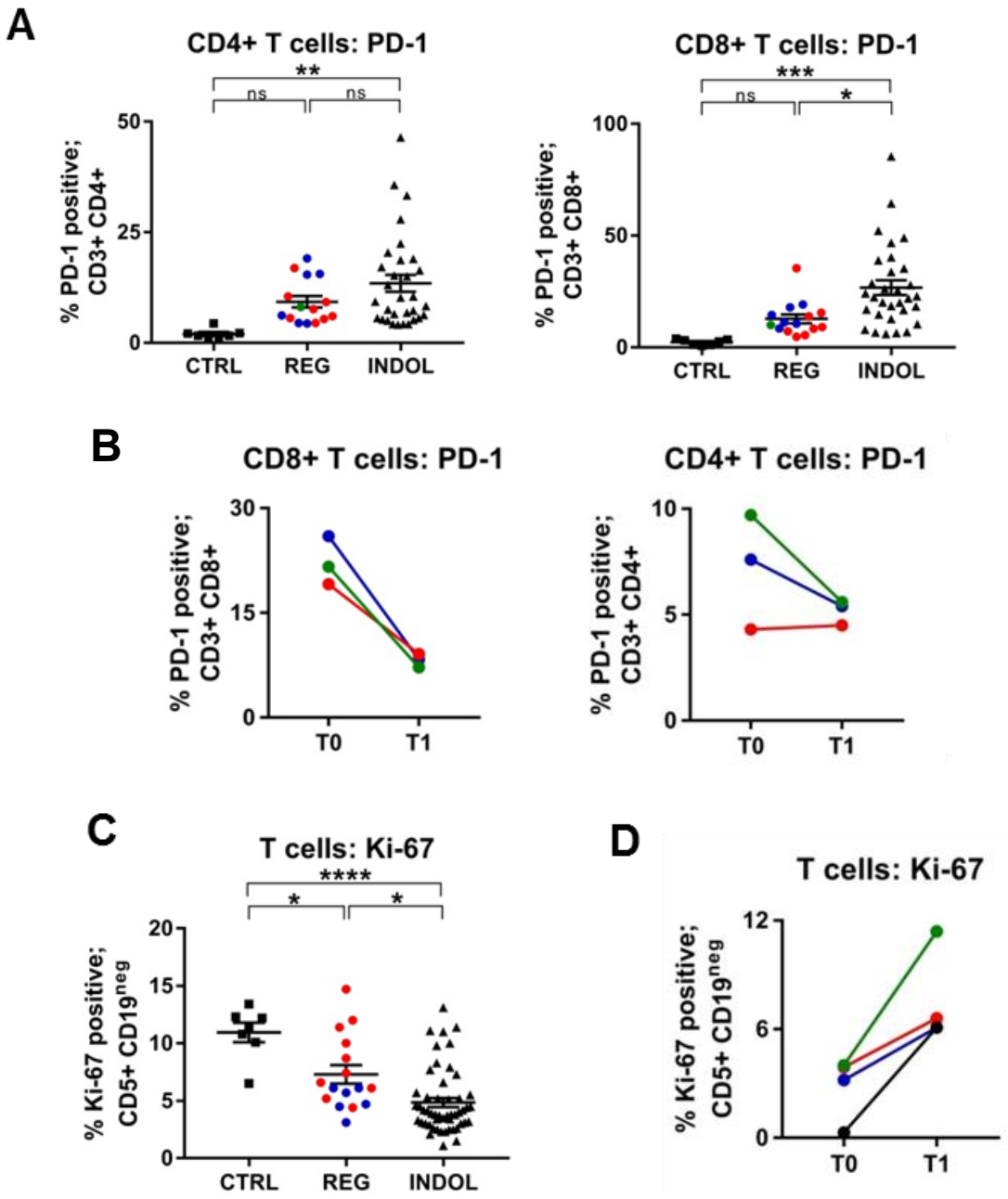

Spontaneous CLL regression is accompanied by decreased PD-1 expression and increased T cell proliferation. **(A)** PD-1 expression in CD4+ and CD8+ T cells in spontaneous regression cases (REG; n=16) were compared against indolent cases (INDOL; n=31) and age-matched healthy controls (CTRL; n=6). **(B)** PD-1 expression in CD4+ and CD8+ T cells was compared between the diagnostic (T0) and the regression (T1) timepoint in 3 individuals with spontaneous CLL regression. **(C)** Ki-67 expression in T cells in spontaneous regression cases (CTRL; n=16) were compared against indolent cases (INDOL; n=31) and age-matched healthy controls (CTRL; n=6). **(D)** Ki-67 expression in T cells was compared between the diagnostic (T0) and the regression (T1) timepoint in 3 individual subjects with spontaneous CLL regression. In (A) and (C), complete spontaneous regression cases, partial spontaneous regression cases and regression cases associated with second malignancy were represented by red, blue and green dots respectively as shown by the key in Figure 3.5. Statistical significance is indicated by *p<0.05, **p<0.01, ***p<0.001 and ****p<0.0001; n.s. denotes comparisons that are not statistically significant.

3.16A-B), and a recovery of T cell proliferation (**Figure 3.16C-D**). This was demonstrated by comparing spontaneous regression cases against indolent CLL cases, and by comparing results across sequential timepoints in patients who have undergone spontaneous CLL regression. The recovery of T cell proliferation was particularly marked among patients who have undergone complete spontaneous CLL regression (Figure 3.16C). However, the reduction of PD-1 expression on CD8+ T cells and the recovery of T cell proliferation was only partial, and a significant difference in these parameters between spontaneously regressed CLL cases and age-matched healthy controls remained (**Figure 3.16A,C**).

A reduction in NK cell number was also evident in spontaneous CLL regression from a comparison of spontaneous CLL regression cases with non-regressing indolent cases **(Figure 3.17A)** and from an analysis of individual spontaneous regression cases across sequential timepoints **(Figure 3.17B)**. Collectively, these data on T cells and NK cells suggest that there may be a partial recovery of immune dysfunction in spontaneous CLL regression. However, a degree of immune defect remains apparent in the majority of individuals in the present cohort who have undergone spontaneous CLL regression.

Figure 3.17

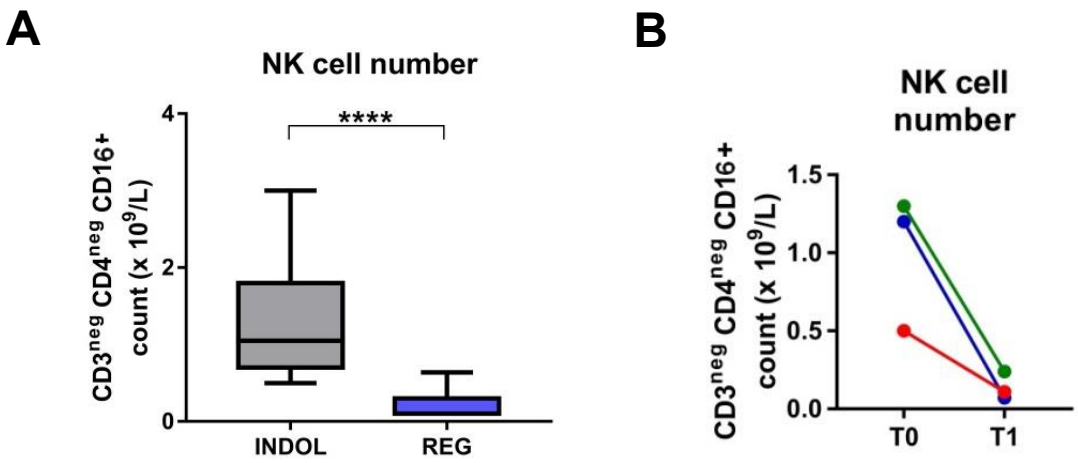

Spontaneous CLL regression is accompanied by a reduction in NK cell number. NK cells were identified from the gated mononuclear cell population on the basis of expression of cell surface markers (CD16+CD3−CD4−), as shown in Figure 3.2B. The NK cell count was derived from the ALC taking into consideration the proportion of lymphocytes that were NK cells (CD16+CD3−CD4−). **(A)** NK cell numbers in spontaneous regression cases (REG; n=16) were compared against indolent cases (INDOL; n=31). Statistical significance was determined using Student's T test. Statistical significance is indicated by ****p<0.0001. **(B)** The NK cell number was compared between the diagnostic (T0) and the regression (T1) timepoint in 3 individuals with spontaneous CLL regression.

3.2. Discussion

3.2.1. Competing models of CLL clonality in spontaneous disease regression

In this study, I collated clinical data and performed biological study on a substantial spontaneous CLL regression cohort, including analysis of sequential samples taken before and after regression. However, the interpretation of all experimental results requires an understanding of the changes, if any, in CLL clonality before and after the onset of regression. Is the CLL clone at the time of diagnosis the same as the CLL clone at the time of regression in an individual patient? This question is important because, owing to limitation in sample availability at earlier timepoints, many of the experimentation and analyses in this study were carried out on samples taken at the regression timepoint.

As illustrated in **Figure 3.**18, there are two possible scenarios that could occur during spontaneous CLL regression. The first scenario (Model 1) involves a single CLL clone, which has initially proliferated and subsequently regressed but not completely disappeared. The second scenario (Model 2) involves two CLL clones, one of which (Clone 1) has initially proliferated but subsequently regressed and disappeared, leaving behind a second CLL clone (Clone 2) that has always been dormant and never proliferated. If the second model (Model B) was correct, then one would expect two CLL clones to be present at the time of diagnosis, but only one would remain at the time of regression.

However, Model B was not consistent with the experimental data presented in the previous section. Using spontaneous CLL regression cases with sequential samples, I confirmed that CLL cells at the diagnostic and regression timepoints belonged to the same CLL clone based on identical *IGH* sequence and similar telomere length patterns

Figure 3.18

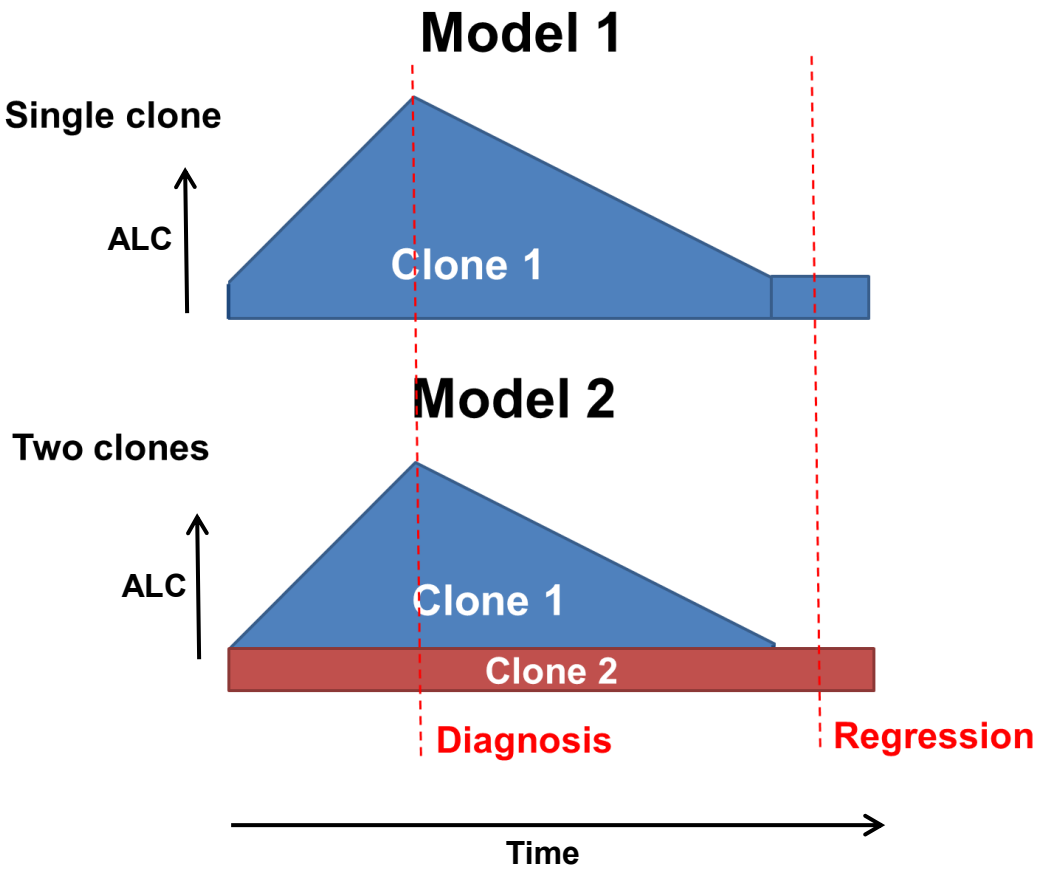

Two possible models of CLL clonality in spontaneous CLL regression. In the above schematic diagram, the absolute lymphocyte count (ALC) is displayed against time. Two possible scenarios (Model 1 and Model 2) are shown. Both scenarios involve an initial proliferative phase followed by a spontaneous regression phase, with residual disease remaining following spontaneous regression. However, Model 1 involves a single CLL clone that that has initially proliferated, then regressed but not completely disappeared, whereas Model 2 involves two clones, one of which (Clone 1) has proliferated but subsequently regressed and disappeared, leaving behind a second clone (Clone 2) that has always been dormant. Experimental data from this study (*IGH* sequence and telomere length distribution pattern) support Model 1 rather than Model 2.

(**Figure 3.8**), consistent with Model 1. This was the case in all the paired diagnostic and regression samples analysed as part of this study. These results therefore indicate that the residual CLL cells in the regression blood samples (T1/T2 timepoints) were likely to be derived from the CLL clone that has regressed.

3.2.2. Phenotypic features of spontaneously regressed CLL tumours

In the ensuing investigations, I compared the phenotype of spontaneously regressed CLL tumours against non-regressing indolent CLLs or untreated progressive CLLs, focusing on molecules of particular relevance to CLL pathogenesis. This permits the identification of specific phenotypic features among individuals who have undergone spontaneous CLL regression. These phenotypic features include low or absent CLL proliferation and a lack of recently proliferated CLL cells. as evidenced by low or negligible Ki-67 and high CXCR4 expression respectively in the CLL cells from spontaneous regression cases (**Figure 3.3A** and **Figure 3.4C**) (Calissano et al., 2009; Calissano et al., 2011; Coelho et al., 2013). My analysis also identified low cell surface CD49d expression as a consistent feature of spontaneously regressed CLL tumours (**Figure 3.4A**), as well as comparatively higher CD95/FasR expression (**Figure 3.5C**) and a trend towards lower CLL cell surface ROR1 expression **(Figure 3.5D)** in these tumours. Finally, spontaneous regression CLL cases were exclusively *IGHV* mutated, and exhibited low expression of cell surface IgM and IgD and high expression of LAIR1, but none displayed stereotyped BCR usage (**Table 3.3**; **Figure 3.12**; **Figure 3.13C**).

3.2.3. Potential mechanisms underpinning spontaneous disease regression in CLL

Analysis of the phenotype in spontaneous regression CLL cases revealed evidence of phenotypic changes across sequential timepoints, particularly a reduction in Ki-67 and CD38 expression, and an increase in CXCR4 expression (**Figure 3.6**). Moreover, the telomere length of the CLL clone in many of the spontaneous regression cases was rather short. Telomere erosion typically occurs at an average rate of 111 base pairs (bp)/year in M-CLLs (Damle et al., 2004). While many of spontaneous regression cases in the present cohort have telomere lengths that would fall within the short (1.9-2.9 kb) or intermediate (2.9-3.6 kb) categories based on the UK CLL4 trial data (Strefford et al., 2015) **(Figure 3.7)**, the telomere length distribution data of these cases remains largely similar between the time of diagnosis and regression, with minimal telomere length erosion at <50 bp/year between these two timepoints in all cases examined **(Figure 3.8)**. Although the latter may reflect telomerase activity in regressing CLL tumours, the above observations collectively support the presence of an initial proliferation phase and the subsequent reduction in CLL proliferation during spontaneous regression.

Initially, I hypothesised that the reduction in CLL proliferation might be due to CLL cellular senescence; however, the high telomerase activity and negative beta-galactosidase staining in these cells were incompatible with such a hypothesis (**Figure 3.9**). The higher telomerase activity in the spontaneous regression cases compared to the indolent cases is interesting but difficult to explain. One hypothesis could be that the regressing CLL clone could be composed of cells with different telomerase activity, and the subclonal population with lower telomerase activity might have preferentially regressed over the population with higher telomerase activity. If this was the case, one might expect changes in the telomere length distribution pattern over time to reflect the subclonal selection of cells with shorter telomeres, which are associated with higher telomerase activity (Damle et al., 2004).

However, there was minimal change in the telomere length patterns over time across the spontaneous regression subjects **(Figure 3.8)**. In any case, the difference in telomerase activity between the spontaneous regression and indolent groups should be interpreted with caution. This is because this data was derived from CLL cells that are quiescent. CLL cells upregulate telomerase activity when they are induced to proliferate, such as when stimulated by BCR agonists (Damle et al., 2012). Unpublished data from our group also shows that telomerase activity in CLL cells is upregulated when co-cultured with CD40L/IL-21. It is therefore of interest to compare the extent to which spontaneous regression and indolent CLL tumours upregulate telomerase activity when induced to cycle.

Strikingly, spontaneously regressing CLL tumours displayed a consistent unresponsiveness to BCR stimulation and low surface immunoglobulin expression (**Figure 3.10**, **Figure 3.12**) that are characteristic of CLL anergy (Packham et al., 2014). These CLL cells also exhibited high levels of basal Erk phosphorylation, which is another B cell anergic feature (**Figure 3.13**) (Muzio et al., 2008). Collectively, these findings suggest clonal anergy as a mechanism underpinning reduced CLL proliferation in spontaneous regression. LAIR1 is a BCR inhibitory receptor that binds extracellular matrix collagen and the complement protein C1q (Perbellini et al., 2014), and its high expression levels may potentially contribute to clonal anergy in spontaneously regressing CLL tumours. Further experiments to demonstrate features of anergy in these tumours could include measuring constitutive SHIP1 phosphorylation levels and assessing proliferative responses to CD40L and IL-4 or IL-21. It would also be important to compare BCR signalling responses across diagnostic and regression timepoints in the spontaneous CLL regression cases where samples are available. This is currently being carried out in collaboration with Dr Francesco Forconi (Southampton), and preliminary data in two cases suggest that there was indeed a reduction in BCR signalling response over time as measured by calcium flux.

Consistent with previous studies, I found that the majority of indolent M-CLL cases retained high CLL IgD expression and IgD response (**Figure 3.11**) (D'Avola et al., 2016; Mockridge et al., 2007). Interestingly, and in contrast to the indolent cases, CLL cells from spontaneous regressing individuals expressed low sIgM and sIgD (**Figure 3.12**), and displayed unresponsiveness to both IgM and IgD triggering (**Figure 3.11**). At present, the functional significance of IgD BCR signalling in CLL is unclear. Two previous studies from the same group demonstrated that IgD BCR stimulation can promote the survival of CLL cells. In one study, the exposure of CLL cells to anti-IgD but not anti-IgM antibodies prolonged the survival of these cells when cultured *in vitro* for up to 10 days (Zupo et al., 2000). In the second study, analysis of the CLL IgD BCR responses in a group of Binet stage A CLL patients showed that IgD BCR triggering by anti-IgD antibodies can lead to inhibition of spontaneous apoptosis in some cases (33 of 106 cases; 31.1%), but not in others (Morabito et al., 2010). A recent study however suggested that, in contrast to IgM BCR signalling that results in prolonged downstream activation (e.g. Erk phosphorylation), the more transient downstream responses elicited through IgD signalling do not support CLL survival *in vitro* (Ten Hacken et al., 2016). On the other hand, my phosphoflow data herein indicate the possibility that IgD signalling may contribute to *in vivo* disease persistence in highly indolent M-CLLs, whereas absence of IgD and IgM signalling together may lead to spontaneous disease regression (**Figure 3.11**).

In addition to anergy leading to decreased CLL proliferation, there may be other potential mechanisms that could contribute to spontaneous CLL regression. Firstly, the low CD49d +/- low ROR1 expression on CLL cells from spontaneous regression cases (**Figure 3.4A**, **Figure 3.5D**) could potentially contribute to reduced CLL proliferation through reduced CLL cell migration to proliferation centres. This potential mechanism could be studied further *in vitro* by assessing transwell migration responses of CLL cells to chemokines such as CXCL12. Secondly, increased apoptosis might also play a role in spontaneous CLL regression through increased levels of CD95/FasR expression on regressing CLL tumours

(Figure 3.5C). However, CLL cells are known to be resistant to Fas-mediated apoptosis (Greaney et al., 2006; Panayiotidis et al., 1995), in part through overexpression of TOSO. Upon activation of FasR by Fas ligand, FADD is recruited to the FasR which leads to cleavage and activation of procaspase 8. TOSO binds to FADD and inhibits procaspase 8 activation (Proto-Siqueira et al., 2008). On the other hand, CD40L-activated CLL cells are highly susceptible to Fas-mediated apoptosis by cells expressing Fas ligand such as T cells and NK cells. This is mediated through upregulation of FADD and downregulation of FLIP, the latter of which is another inhibitor of the Fas signalling pathway that binds to FADD and inhibits procaspase 8 activation (Chu et al., 2002). Additionally, CD40L-activated CLL cells also upregulate TRAIL receptor, which acts together with FasR in mediating apoptosis through the extrinsic apoptotic pathway (Dicker et al., 2005). It is therefore of relevance to examine the expression of molecules such as FADD, FLIP, TOSO and TRAIL receptor (DR4/DR5) in spontaneously regressing CLL tumours, and to determine their sensitivity to FasR agonists compared to non-regressing CLL tumours. It is possible that spontaneously regressing CLL tumours may have an intrinsic sensitivity to Fas-mediated apoptosis. Additionally, clonal anergy and a lack of IgM and IgD BCR signalling may potentially contribute to increased CD95/Fas expression and/or sensitivity to Fas-mediated apoptosis during the course of spontaneous CLL regression. Indeed, Fas-mediated cell death plays an important role in the elimination of anergic non-malignant B cells (Rathmell et al., 1995). In CLL, the transcription factor NFAT has been shown to be a crucial mediator of clonal anergy (Marklin et al., 2017), and one important action of NFAT is the induction of Fas ligand upregulation (Rengarajan et al., 2000). It remains to be ascertained whether anergy-associated NFAT activation also leads to FasR upregulation, or whether alternative mechanisms are involved.

A limitation of phenotypic analysis by flow cytometry is the restricted number of markers that can be assessed. To comprehensively elucidate the features and potential mechanisms underpinning spontaneous CLL regression, an unbiased approach is

preferable. I have therefore carried out RNA sequencing (RNA-seq) and initiated transcriptomic analysis on spontaneously regressing CLL tumours (n=15) comparing them to indolent (n=17) and untreated progressive (n=12) M-CLLs, as well as normal B cells from healthy donors (n=3). Preliminary data from this analysis shows that the transcriptomic profile from spontaneous regression cases were distinct from those of healthy controls and the majority of indolent and progressive case. In particular, consistent with reduced proliferation in spontaneously regressing tumours, RNA-seq data showed downregulation of cell cycle genes, as well as pathways involved in cell proliferation, RNA processing and cellular metabolism in these tumours compared to indolent and progressive M-CLLs. Corroborating my flow cytometry data, *ITGA4* (CD49d) and *FAS* (FasR) expression was also downregulated in spontaneously regressed CLL tumours. In addition, gene set enrichment analysis showed downregulation of *MYC* and Myc target genes in spontaneous regression cases compared to their non-regressing indolent M-CLL counterpart, and analysis is currently underway to determine if a signature of B cell anergy is present in the RNA-seq data of spontaneous regressing CLLs. Finally, genes involved in DNA repair and telomere maintenance were upregulated in spontaneous regressing CLL cases. The upregulation of these processes could reduce the level of genomic instability and may potentially play a role in spontaneous regression.

Finally, analysis of the immune compartment revealed that spontaneous CLL regression is associated with a partial reversal of T-cell defects that are ubiquitous in patients with CLL **(Figure 3.15, Figure 3.16)**. It is therefore plausible that enhanced T-cell immunosurveillance could contribute to the later stages of CLL regression and the maintenance of regressed state following spontaneous regression, but is unlikely be a major mediator of early regression when substantial T-cell dysfunction exists. Furthermore, it is possible that spontaneous regressing CLL tumours are more immunogenic than their non-regressing counterparts, and are therefore more capable of inducing an adaptive immune response. The determinants of CLL immunogenicity is unclear and is an area that warrants

further investigation. It is possible that the genomic and epigenomic landscape could influence expression of immunogenic antigens on individual CLL tumours. In addition, the levels of HLA expression on tumour cells, and the presence or otherwise of immunosuppressive mechanisms such as tumour PD-L1 expression and regulatory T cell recruitment, are also likely to influence tumour immunogenicity (Blankenstein et al., 2012).

3.2.4. Genomic features of spontaneously regressed CLL tumours

The 13q14 deletion seen among spontaneously regressing CLL tumours is mostly clonal and is likely to be the main genomic event driving the initial proliferative phase before the onset of spontaneous disease regression. This is likely to be mediated primarily through loss of the *DLEU2*/miR-15a/16-1 cluster. However, there are other genes in 13q14 that were co-deleted with *DLEU2*/miR-15a/16-1, including *DLEU1*, *DLEU5*, *DLEU7*, *KCNRG* and *RNASEH2B*. The function of *DLEU1*, *DLEU5, RNASEH2B* and *KCNRG* is unknown in CLL (Lia et al., 2012), but *DLEU7* has been shown in a single study to have inhibitory effect on the transcription activatory activity of NF-kB and NFAT (Palamarchuk et al., 2010). In addition, in two of the cases del(13q14) involved loss of the *RB1* gene which encodes for the retinoblastoma protein that negatively regulates cell cycle entry (Lia et al., 2012). *RB1* deletion could therefore co-operate with miR-15a/16-1 deletion in promoting CLL proliferation during the initial proliferative phase.

There are a number of other clonal CNVs that may have arisen early during disease development in this cohort. Of particular interest are duplications of 3p24 (*NKIRAS1*), 12q21-31 (*PAWR*), 7q31-32 (*POT1*) and 11p13-14 (*WT1),* where the duplications encompass respective genes of functional significance (shown in brackets). *NKIRAS1* encodes for a Ras-like protein that is known to inhibit NF-kB signalling by preventing the degradation of the NF-kB inhibitory molecule IkB-β (Fenwick et al., 2000). *PAWR* encodes

for Par-4, which has been shown to also have an inhibitory effect on NF-kB signalling and additionally causes tumour regression in prostate cancer by enhancing the cell membrane trafficking of FasR and Fas ligand, and activating Fas-mediated apoptosis (Chakraborty et al., 2001). *POT1* encodes for a protein that forms part of the shelterin complex, which is important in maintaining telomere length and genome integrity (Maciejowski and de Lange, 2017), and indeed *POT1* loss-of-function mutations are known to cause telomere dysfunction in CLL (Ramsay et al., 2013). Finally, *WT1* encodes for a transcription factor that has both oncogenic and tumour suppressor activities (Yang et al., 2007). It is unclear whether these gene duplications have any effect in mediating subsequent spontaneous tumour regression. It is important to highlight the fact that these duplications were found only in isolated spontaneous regression cases. Moreover, it remains to be determined whether these gene duplications translate into increased gene expression, and if so whether this leads to any functional consequences.

Exome sequencing revealed the presence of mutations in known putative CLL drivers in several spontaneous regression cases. These include mutations in *TP53*, *MYD88* and *HIST1H1B*. The functional role of *TP53* has been described in detail in sections 1.2.4.2 and 1.4.1. *MYD88* encodes for an intracellular adaptor protein involved in the TLR signalling pathway. The *MYD88* mutation in CLL14 occurs at L265 of *MYD88*, which leads to increased downstream activation of TLR signalling through enhanced binding of MYD88 to IRAK1, resulting in increased activation of targets such as NF-kB (Fabbri and Dalla-Favera, 2016). *HIST1H1B*, on the other hand, encodes for a histone that is involved in chromatin remodelling by packaging and organising DNA into nucleosomes (Landau et al., 2015). The presence of these mutations, together with del(13q14) found in the majority of spontaneously regressed tumours, suggest that the forces underpinning disease regression must have been sufficient to overcome the growth advantage conferred by these genomic aberrations. This is particular the case with CLL13, which harboured multiple clonal genomic

aberrations including del(8p) involving the TRAIL receptor gene and biallelic *TP53* defects, in addition to del(13q14).

Of the two recurrent SNVs that were not known CLL driver mutations, one involved *PCMTD1*, which encodes for a component of a methyltransferase, and the other *NAV3*, which may have some T cell regulatory function (Karenko et al., 2005). There were also a substantial number of significantly mutated genes occurring in isolated spontaneous regression cases. Examples of genes with potential functional significance include *MDC1* (involved in DNA damage response), *PCM1* (involved in centrosome assembly and function), as well as *FAT1* and *CDH2* (which encodes for cadherins that may be involved in cell migration and adhesion). Most of these mutations were subclonal and it is likely that the majority would be passenger mutations. It would be of interest to investigate whether there is any clonal selection or evolution during the course of spontaneous CLL regression, and work is currently under way to compare CNVs and SNVs in spontaneous regression cases where paired diagnosis and regression samples are available.

3.2.5. Limitations of the current study and a mechanistic model of spontaneous CLL regression

A limitation of this study is the lack of CT imaging and bone marrow samples; hence, it was not possible to determine the full extent of residual nodal and marrow disease, if any, after spontaneous regression. Notwithstanding this limitation, there is strong evidence in our subjects for spontaneous regression, at least of peripheral CLL. Moreover, CLL cells from complete and partial spontaneous regressors displayed similar phenotypic features, suggesting that partial regressors were merely at an earlier stage of regression, and with time, complete regression of CLL clinical features could become apparent.

A further limitation is the unavailability of samples from the initial proliferative phase, prior to CLL diagnosis and the onset of spontaneous regression. It is therefore not possible to establish the biological features of these cases during the early stages of their natural history. Nevertheless, a possible model for spontaneous CLL regression can be inferred from the literature and from the available data within this study (**Figure 3.19**). Initially, antigenic BCR stimulation in the presence of co-stimulatory signals may account for CLL proliferation. With increasing proliferation, the demand for co-stimulation may also increase (Bagnara et al., 2011; Os et al., 2013). Concomitantly, T cells may become more dysfunctional as CLL progresses (Palma et al., 2017), with reduced ability to provide the required co-stimulation (Packham et al., 2014). Continued chronic antigenic BCR stimulation, in the absence of adequate co-stimulation, results in CLL anergy (Cambier et al., 2007; Gauld et al., 2005). In non-regressing indolent CLLs, the consequences of anergy could potentially be counteracted by high ROR1 and Bcl-2 levels, CD49d expression and IgD BCR signalling, resulting in disease persistence. In the rare scenarios where CLL anergy occurs in the absence of both IgM and IgD BCR signalling, reduced CD49d and ROR1 expression, high FasR levels and/or enhanced tumour immunosurveillance, spontaneous CLL regression ensues.

It is important to emphasise that the above remains largely a hypothetical model. To provide further evidence to support this model, experimental work will need to be conducted to demonstrate impaired *in vitro* signalling and proliferative response to BCR stimulation that can be reversed with CD40L/IL-4 co-stimulation, and that impaired *in vivo* engraftment in immunodeficient mice of CLL cells from spontaneous regressors can be reversed by suppression of inhibitory BCR signalling, re-expression of CD49d and ROR1, and/or inhibition of Fas-mediated signalling.

Figure 3.19

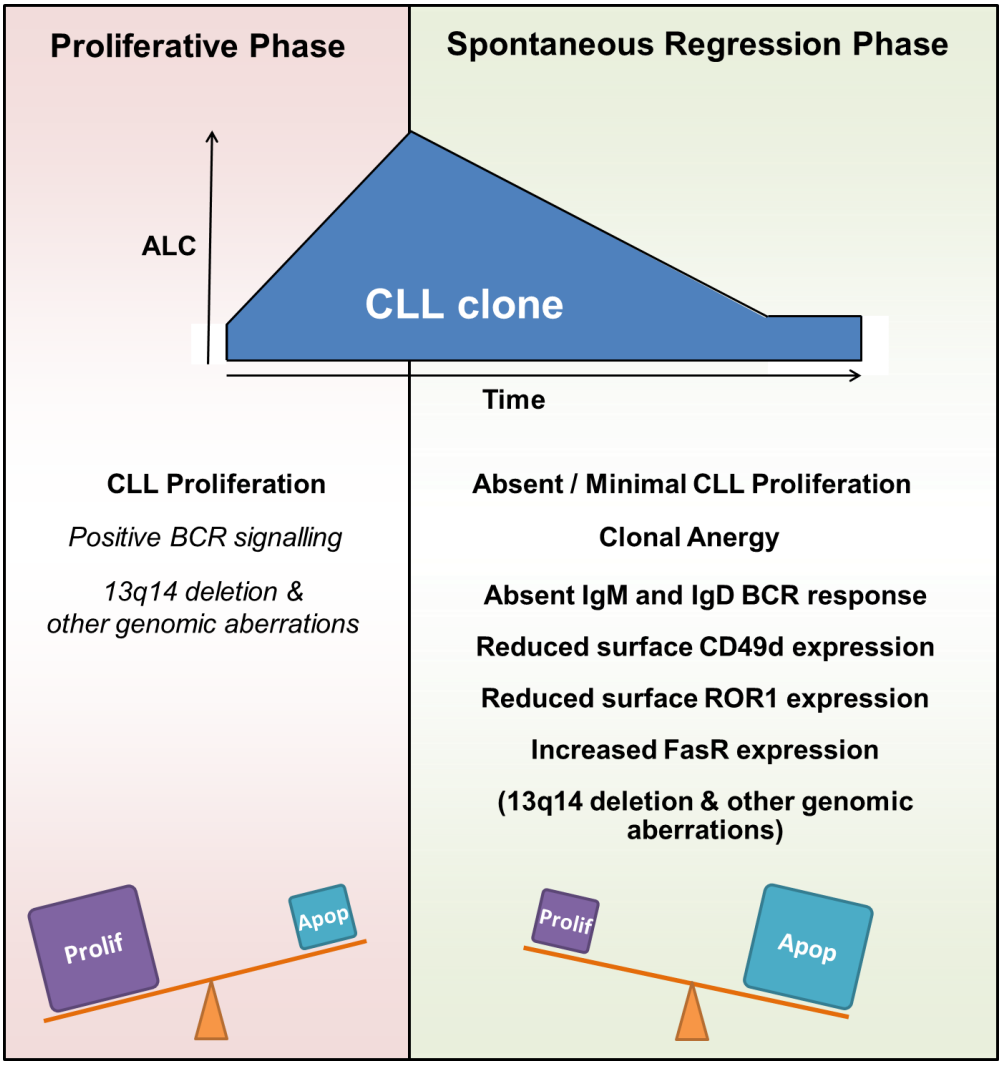

A possible mechanistic model of spontaneous CLL regression. The features pertaining to the spontaneous regression phase (shown in bold) are supported by experiential evidence from this study. Due to the unavailability of samples, the features pertaining to the initial proliferative phase (shown in italics) are speculative. Disease regression may occur when the balance of cell turnover is shifted in favour of cell death rather than cell proliferation. ALC, absolute lymphocyte count; Prolif, CLL proliferation; Apop, CLL cell death.

3.2.6. Clinical implications of this study

My experimental findings from this study support the continued use of BCR signalling inhibitors for the treatment of CLL. The finding of decreased CD49d and ROR1 and increased FasR expression on CLL cells in patients with spontaneous disease regression suggests approaches to downregulate CD49d and ROR1 expression and upregulate FasR expression may also potentially be useful for the treatment of CLL in combination with BCR signalling inhibition. At present, gene therapy for the treatment of cancer is still in its infancy, and delivery systems that are selective for tumour cells are limited to platforms such as those that utilises oncolytic adenoviruses (Choi et al., 2012) and lipid nanoparticles conjugated to monoclonal antibodies, which allows delivery of antisense oligonucleotides targeting a specific mRNA (Petrilli et al., 2014). Alternatively, combined use of ROR1 mAb and BCR signalling inhibitor may show promise (Yu et al., 2016).

Finally, it is important to highlight the substantial level of minimal residual disease in all of the spontaneous regression cases in this study, and its potential clinical significance. Firstly, since T cell dysfunction arises from their interaction with CLL cells, it is plausible that residual disease may contribute to persistent T cell defects seen among CLL patients even after spontaneous disease regression (**Figure 3.15 and Figure 3.16**) (Gorgun et al., 2005; Ramsay et al., 2008). Indeed, the *partial* normalisation of T cell numbers and phenotype seen in spontaneous CLL regressors is reminiscent of that observed in patients treated with BCR signalling inhibitors such as ibrutinib (Niemann et al., 2016). It is possible that *complete* immune recovery in CLL might require disease eradication (i.e. MRD negativity); this hypothesis will necessitate investigation in future studies. Moreover, as my experimental data indicates, residual CLL cells remaining after spontaneous regression are quiescent and anergic rather than senescent. Quiescence and anergy are reversible (Mockridge et al., 2007; Nossal, 1996), as exemplified by CLL20 in this cohort, where the patient experienced disease relapse following complete spontaneous regression. Therefore, there remains the

case for disease eradication rather than merely disease control, especially for CLL with poor-risk features such as *TP53* defects. This will be the focus of the next two chapters of this thesis.

CHAPTER 4

PRE-CLINICAL EFFICACY AND MECHANISM OF ATR INHIBITION IN CLL

This chapter has been published as:

Kwok M, et al. (2016). ATR inhibition induces synthetic lethality and overcomes chemoresistance in TP53 or ATM defective chronic lymphocytic leukemia cells. Blood. *127*, 582-595.

ATR regulates replication initiation, preventing aberrant or excessive replication origin initiation that depletes the cellular pool of nucleotides and replication proteins. Inhibition of ATR therefore induces replication stress, manifested by the accumulation of slowed and stalled replication forks with unprotected ssDNA that inevitably collapses into DSBs. Specifically, the breakage of ssDNA results in the formation of partially replicated DNA fragments with DNA double-stranded ends. ATR also mediates the response to replication stress, delaying cell cycle progression, as well as stabilising and repairing DNA replication forks (Couch et al., 2013; Toledo et al., 2013; Zeman and Cimprich, 2014). If ATR is inhibited, maintenance of genome integrity becomes dependent upon functional ATM and p53, with ATM being essential for HRR to repair DSBs and hence restore the original structure of the replication fork, and both ATM and p53 for arresting cell cycle progression to permit repair. ATR therefore represents an attractive synthetically lethal target for p53 or ATM deficiency. Evidence for this synthetically lethal interaction has previously been provided by the deletion of ATR in p53-deficient mice (Ruzankina et al., 2009) and by inhibition of ATR in tumour cell lines which resulted in selective killing of cells harbouring p53 or ATM defects (Nghiem et al., 2001; Reaper et al., 2011; Sangster-Guity et al., 2011). These studies have been outlined in section 1.4.

On the other hand, no study to date has addressed the impact of ATR inhibition on primary tumour samples of CLL or other haematological malignancies in which DDR defects are present. In this study, I utilised AZD6738 (AstraZeneca), a novel, highly specific and orally bioavailable ATR kinase inhibitor to examine the effect of ATR inhibition in CLL cell lines, primary CLL cells and primary CLL xenotransplantation models. The study demonstrated synthetic lethality and selective cytotoxicity of the ATR inhibitor AZD6738 in CLL cells with *TP53* or *ATM* defects, as well as the sensitisation of these cells to chemotherapeutic agents and ibrutinib by ATR inhibition.

4.1. Results

To investigate the therapeutic efficacy and mechanism of action of AZD6738 in CLL cells, I employed two pairs of isogenic cell lines: CII-*GFP*sh (ATM wild-type) and CII-*ATM*sh (ATM deficient), as well as Mec1-p53-pcDNA3.1 (p53 mutant) and Mec1-GFP-pcDNA3.1 (p53 wild-type). These two cell line pairs were previously established in our laboratory as outlined in section 2.2.2.

In addition to cell lines, primary CLL PBMC samples from a panel of previously characterised CLL cases (n=36) were utilised. These 36 CLL cases include patients of a variety of age, disease stage, treatment status, as well as *IGHV* mutational status, as shown in **Table 4.1**. The panel comprises 18 CLL cases with wild-type *ATM* and *TP53,* 10 cases with an *ATM* defect and 8 cases a *TP53* defect. All *ATM* defective or *TP53* defective cases harboured del(11q) and del(17p) respectively in ≥80% of CLL cells, as assessed by FISH. Moreover, the majority of *ATM* defective or *TP53* defective cases also harboured *ATM* or *TP53* mutations of varying allelic frequencies.

In all cases, the functional status of ATM and p53 had been previously ascertained by Western blotting. Two strategies were used to determine ATM/p53 function. This first strategy assessed p53 and p21 expression in response to IR. The absence of p53 and p21 induction is a feature common to both ATM and p53 functional loss; however, p53 mutation may be accompanied by a high p53 basal level (**Figure 4.1A**). The second strategy assessed the phosphorylation of ATM targets, including ATM, SMC1 and p53, in response to IR. ATM functional loss results in defective phosphorylation response to all three ATM targets, whereas p53 functional loss results in defective phosphorylation of only p53 (**Figure 4.1B**). Each of the 18 *ATM* defective or *TP53* defective cases was associated with an ATM

Figure 4.1

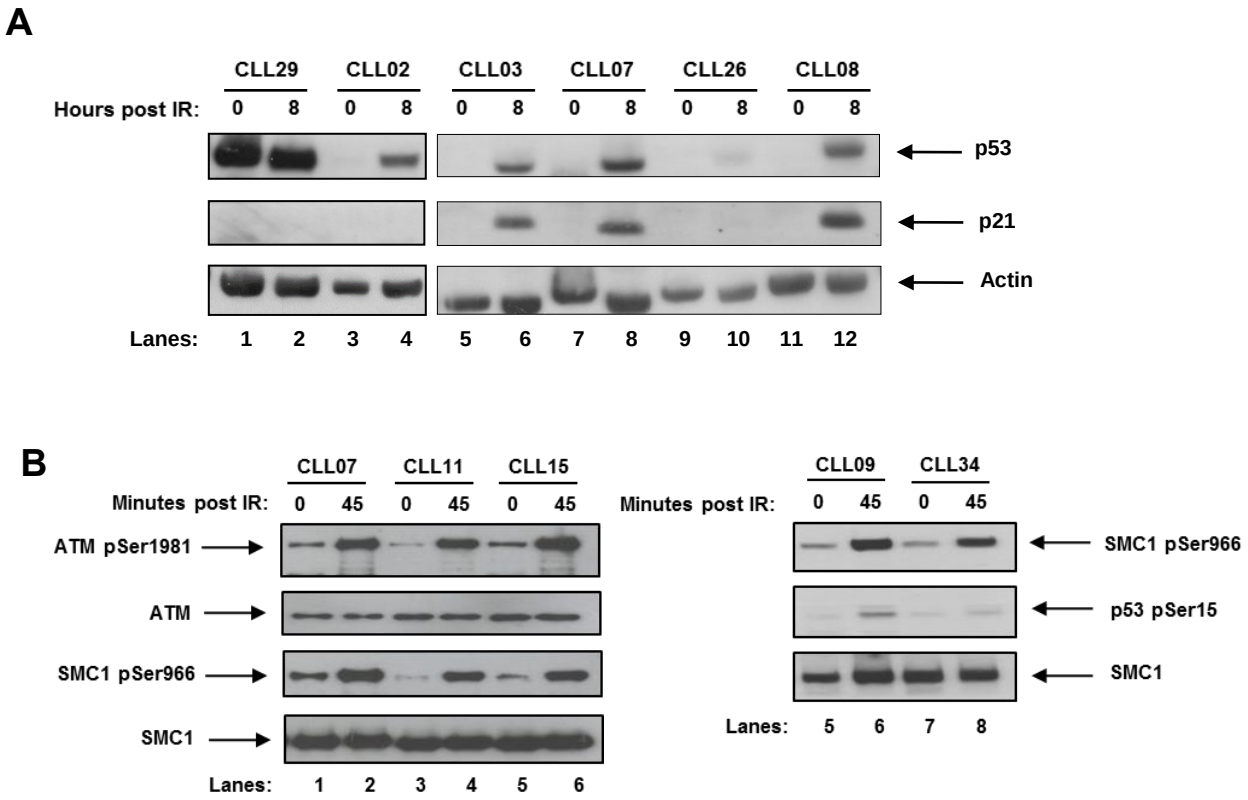

Determination of DNA damage response (DDR) in primary CLL samples. Two strategies were used to assess DDR in primary CLL samples and the impact of the identified mutations in the *ATM* or *TP53* gene. **(A)** Cellular lysates were obtained from CLL cells before and 8 hours following in vitro treatment with 5 Gy IR. Subsequent assessment of the levels of p53 and its target p21 allowed identification of defective p53 function in CLL29 and defective ATM function in CLL26. Both samples are characterised by the absence of IR-induced p53 and p21 levels, but in the p53 mutant CLL29 this is coupled with a high p53 basal level. **(B)** Analysis of IR-induced ATM targets (phosphorylated ATM/p53 and SMC1) 45 minutes after 5 Gy IR allows detection of normal ATM function in CLL07, CLL11, CLL15 and CLL09 and defective p53 function in CLL34 where p53 cannot be phosphorylated, despite normal SMC1 phosphorylation that is suggestive of functional ATM.

or p53 functional defect. Due to limited sample availability, not every case was used for each experiment. The samples used for each experiment are listed in **Table 4.1**.

Using these CLL cell lines and primary CLL samples, a pre-clinical study of AZD6738 was carried out to address: (1) the inhibitory activity of AZD6738 on the ATR pathway; (2) the single-agent efficacy of AZD6738; (3) the mechanism underpinning the cytotoxic effect of ATR inhibition; and (4) the effect of combining AZD6738 with chemotherapy and ibrutinib.

4.1.1. ATR signalling is active in proliferating CLL cells and is inhibited by AZD6738

The ATR pathway has previously been shown to be suppressed in quiescent lymphocytes in both healthy individuals and patients with CLL. This was evidenced by the absence of detectable ATR protein expression in non-proliferating CLL cells or healthy PBMCs, and by a lack of p53 induction and phosphorylation upon exposure of quiescent lymphocytes to ultraviolet radiation, a known activator of ATR (Jones et al., 2004). Consistent with this, I found, using Western blotting, that ATR protein expression was low in quiescent CLL PBMCs obtained from peripheral blood sampling of patients with CLL. However, ATR expression was induced when cells were stimulated to proliferate by co-culturing for 4 days with CD40L/IL-21, a method described in section 2.3.2. This was consistently observed across all 12 CLL cases tested, irrespective of the presence, or otherwise, of p53 or ATM defects (**Figure 4.2A**; showing the results of 8 of these 12 cases).

Next, I used phosphorylation of the checkpoint kinases Chk1 (at Ser345) and Chk2 (at Thr68), which are downstream targets of ATR and ATM respectively, as surrogate markers for ATR and ATM pathway activation. Primary CLL cells were cultured for 4 days with CD40L/IL-21 to induce proliferation, or for 1 day in RPMI-1640 without CD40/IL-21.

Table 4.1. Clinical and biological characteristics of primary CLL samples

ID	Age	Sex	Binet stage	Number of prior therapies	Flud refractory	*IGHV* mut status	Cytogenetics	*ATM* mutation	*TP53* mutation	% cells with *ATM*/*TP53* mutation	DNA damage response*	Other known mutations	AZD6738 EC_{50}	Sample used in
CLL01	66	M	A	0	No	nk	Normal	No	No	-	nk	No	66.8	Figure 4.2, 4.8
CLL02	73	M	C	2	Yes	U	Normal	No	No	-	Normal	NOTCH1	38.9	Figure 4.2, 4.8, 4.9
CLL03	74	F	B	1	Yes	M	Normal	No	No	-	Normal	No	-	Figure 4.2
CLL04	58	F	A	0	No	M	Normal	No	No	-	Normal	No	9.3	Figure 4.2, 4.8
CLL05	70	M	A	0	No	nk	Normal	No	No	-	nk	No	19.6	Figure 4.8
CLL06	67	M	A	2	No	U	Normal	No	No	-	Normal	No	21.2	Figure 4.2, 4.8, 4.9
CLL07	72	F	C	1	No	M	del13q, trisomy12	No	No	-	Normal	No	25.6	Figure 4.2, 4.8, 4.9
CLL08	80	M	C	1	No	nk	del13q	No	No	-	Normal	No	67.4	Figure 4.8
CLL09	57	F	A	0	No	M	Normal	No	No	-	Normal	No	40.2	Figure 4.8
CLL10	66	F	A	0	No	M	del13q	No	No	-	Normal	No	26.8	Figure 4.8
CLL11	70	M	B	2	No	M	Normal	No	No	-	Normal	No	45.0	Figure 4.8
CLL12	61	M	A	2	No	nk	Normal	No	No	-	nk	No	29.4	Figure 4.8
CLL13	51	F	A	0	No	M	Normal	No	No	-	Normal	No	33.2	Figure 4.8
CLL14	65	M	A	0	No	U	del13q	No	No	-	Normal	No	76.0	Figure 4.8
CLL15	69	F	C	1	No	M	Normal	No	No	-	Normal	No	44.1	Figure 4.8
CLL16	35	F	A	1	No	nk	trisomy12	No	No	-	nk	No	22.9	Figure 4.8
CLL17	77	F	A	4	No	M	Normal	No	No	-	nk	No	52.2	Figure 4.8
CLL18	55	F	A	1	No	M	Normal	No	No	-	Normal	No	32.9	Figure 4.8
CLL19	70	M	A	1	No	U	del11q, trisomy12	c.5224G>C, p.A1724P	No	nk	Defective	No	7.1	Figure 4.8
CLL20	70	M	A	1	No	nk	del11q	c.2282delCT, p.761fs	No	nk	Defective	No	9.2	Figure 4.8
CLL21	79	M	A	0	No	U	del11q	c.2466+2T>G, splicing site	No	nk	Defective	No	18.5	Figure 4.2, 4.8
CLL22	88	M	A	0	No	M	del11q	c.222T>A, p.C74X	No	41.7	Defective	No	5.8	Figure 4.2, 4.8, 4.21
CLL23	61	F	A	1	No	M	del13q	c.1229T>C, p.V410A	No	48.0	Defective	No	5.1	Figure 4.2, 4.8, 4.21, 4.9

Table 4.1. (cont'd)

ID	Age	Sex	Binet stage	Number of prior therapies	Flud refractory	*IGHV* mut status	Cytogenetics	*ATM* mutation	*TP53* mutation	% cells with *ATM*/*TP53* mutation	DNA damage response*	Other known mutations	AZD6738 EC_{50}	Sample used in
CLL24	61	M	A	1	No	M	Normal	c.6067G>A, p.G2023R	No	56.4	Defective	No	6.3	Figure 4.8, 4.21
CLL25	78	F	C	2	No	nk	del11q, del6q, trisomy12	c.4220T>C, p.I1407T	No	nk	Defective	BIRC3, NOTCH1	-	Figure 4.10, 4.25
CLL26	74	M	B	1	No	U	del11q	c.9038T>A, p.L3013Q	No	65.0	Defective	No	-	Figure 4.10
CLL27	65	F	A	3	No	U	del11q, trisomy12	c.4220T>C, p.I1407T	No	76.0	Defective	BIRC3	-	Figure 4.9
CLL28	80	M	A	0	No	M	del11q, trisomy12	c.6966C>G, p.S2322R	No	46.6	Defective	No	-	Figure 4.9
CLL29	56	M	C	2	Yes	U	del17p, trisomy12	No	c.752T>G, p.I251S	27.2	Defective	BIRC3	16.0	Figure 4.8, 4.10, 4.21, 4.9
CLL30	55	F	C	4	Yes	U	del17p	c.968T>A, p.I323K	No	30.1	Defective	No	15.7	Figure 4.8†
CLL31	78	F	C	2	Yes	M	del17p, del13q, trisomy12	No	c.711G>A, p.M237I	98.2	Defective	No	2.8	Figure 4.8, 4.10, 4.21
CLL32	65	M	A	1	Yes	M	del17p, del13q	No	c.377A>G, p.Y126C	75.3	Defective	No	2.9	Figure 4.2, 4.8, 4.21
CLL33	77	M	A	1	No	M	del17p	No	No	50.8	nk	SF3B1	-	Figure 4.2
CLL34	74	F	C	2	No	U	Normal	No	c.849_850insC, p.T284fs	54.7	Defective	No	5.6	Figure 4.8, 4.9
CLL35	86	F	B	2	No	nk	Normal	No	c.626_627del, p.209_209del	90.3	Defective	No	15.7	Figure 4.8, 4.9
CLL36	60	M	B	3	No	M	del17p, del13q	No	c.743G>A, p.R248Q	53.5	Defective	SF3B1	7.0	Figure 4.8, 4.9

ID, sample identifier; Flud refractory, fludarabine refractory; *IGHV* mut status, *IGHV* mutational status; U, unmutated; M, mutated; nk, not known

* DNA damage response (ATM and p53 function) was assessed using methodology specified in Figure 4.1.

† This sample was originally used in the experiment presented in Figure 4.8 but subsequently was excluded from analysis, as it contained both *ATM* and *TP53* defects.

Thereafter, hydroxyurea (HU), a known inducer of replication stress, was added. Cells were then harvested for analysis following 1, 5 and 24 hours of HU exposure. Upon treatment with HU, ATR-dependent Chk1 phosphorylation was observed in proliferating (**Figure 4.2B**; lanes 2-3, 10) but not quiescent CLL cells (lanes 6 & 8). Indeed, in proliferating CLL cells, Chk1 phosphorylation was observed as early as 1 hour (lane 2) after exposure to HU, with maximal Chk1 phosphorylation being seen at 5 hours (lane 3). The background Chk2 phosphorylation in quiescent cells (lanes 5-6) likely reflected the accumulation of cellular stress in cryopreserved primary CLL samples when resuspended and cultured in RPMI medium for 1 day, without access to survival signals afforded by the CD40L/IL-21 co-culture system. Such background Chk2 phosphorylation was absent when the experiment was repeated using CLL PBMCs isolated from fresh peripheral blood samples without prior culture (lanes 7-8).

It has been reported that prolonged incubation with replication inhibitors, including ATR inhibitors, can lead to S phase checkpoint adaptation, a process in which Chk1 phosphorylation is lost despite persistent replication stress. The underlying mechanism is likely to be attributable to ubiquitin-mediated degradation of the Chk1 adaptor protein Claspin, which is required for recruiting Chk1 and mediating Chk1 phosphorylation (Syljuasen, 2007; Yoo et al., 2004). Because 24-hour HU treatments (lane 4) appeared to be associated with S phase checkpoint adaptation, in which Chk1 phosphorylation was lost despite persistent replication stress, 24-hour HU treatments do not provide optimal conditions for the assessment of ATR activity. Therefore, 5-hour HU treatments were adopted for all subsequent experiments. The specificity of Chk1 as a marker for ATR activation was evident by minimal Chk1 phosphorylation following IR. Specifically, exposure to IR generates DNA DSBs and activates the ATM pathway rather than ATR, hence leading to ATM and Chk2 phosphorylation at Ser1981 and Thr68 respectively, rather than Chk1 phosphorylation (**Figure 4.3**, lanes 8-11).

Figure 4.2

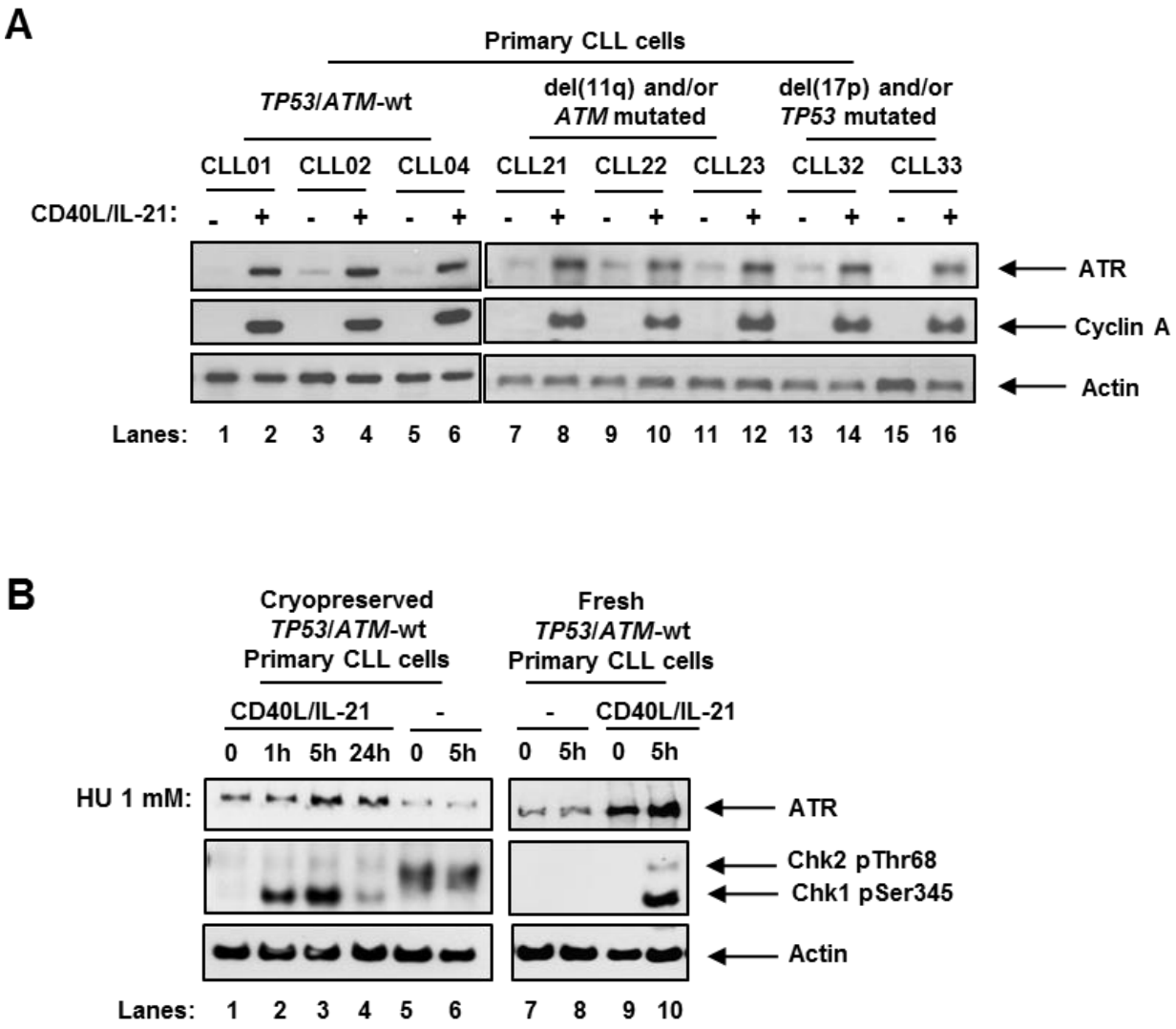

ATR signalling is activated in response to replication stress in proliferating primary CLL cells. (A) Stimulation of primary CLL cell proliferation by co-culture with CD40L-expressing murine embryonic fibroblasts in the presence of IL-21 (CD40L/IL-21) for 4 days resulted in induction of ATR expression in primary CLL cells irrespective of ATM or TP53 status. Cyclin A expression is a marker of proliferating cells. Actin is the loading control. **(B)** Cryopreserved or fresh primary CLL cells cultured with or without CD40L/IL-21 (lanes 1-4 and 9-10, and lanes 5-8 respectively) were treated with HU. Cryopreserved samples not co-cultured with CD40L/IL-21 were resuspended and pre-incubated in culture media for 24 hours prior to treatment (lanes 5-6), whereas fresh cells were treated immediately upon isolation from peripheral blood without pre-incubation (lanes 7-8). Exposure to HU (1 mM) which induces replication stress led to Chk1 phosphorylation in primary CLL cells co-cultured with CD40L/IL-21 (lanes 2-3, 10).

To investigate the effect of AZD6738 on ATR and ATM pathways, *TP53*/*ATM* wild-type primary CLL cells induced to proliferate within the CD40/IL-21 co-culture system (**Figure 4.3**), as well as the CII-*GFP*sh and CII-*ATM*sh isogenic cell lines (**Figure 4.4**), were employed. The ATM functional status of these cell lines were confirmed by their response to IR. In the CII-*GFP*sh cell line, exposure to 6 Gy of IR led to activation of the ATM pathway, as evidenced by the phosphorylation of ATM and Chk2 (**Figure 4.4**, lane 5). This was not seen in the CII-*ATM*sh cell line, indicating that the ATM response was defective in this cell line (**Figure 4.4**, lane 11).

Proliferating primary CLL cells and cell lines were treated with 1 μM of AZD6738 and/or 10 μM of the ATM inhibitor KU-55933 for 2 hours prior to HU or IR exposure. These drug doses and treatment durations were chosen with reference to both published studies (Reaper et al., 2011) and unpublished data (AZD6738 Investigator's Brochure, AstraZeneca, 2013) of these inhibitors on tumour cell lines, and on the basis of the results of my pilot experiments. Pilot experiments showed that treatment at these doses and for these durations produced the desired inhibition of the ATR or ATM pathway, without incurring any substantial impact on CLL cell viability. Moreover, the maximal inhibitory effect on these pathways was reached at 2 hours, with no observable difference in inhibitory effect when the treatment duration was extended from 2 hours to 24 hours.

AZD6738 treatment led to the suppression of ATR signalling as indicated by a reduction in HU-induced Chk1 phosphorylation, independent of ATM functional status (**Figure 4.3**, lane 4 vs 6, 5 vs 7; **Figure 4.4**, lanes 3 vs 4, 9 vs 10). Complete abolition of HU-induced Chk1 phosphorylation was evident at AZD6738 doses ≥3 μM (**Figure 4.5A**). The specificity of AZD6738 for ATR inhibition was demonstrated by its lack of effect on IR-induced ATM/Chk2 phosphorylation (**Figure 4.3**, lane 8 vs 10; **Figure 4.4**, lane 5 vs 6). Instead, ATM/Chk2 phosphorylation was suppressed by the ATM inhibitor (**Figure 4.3**, lane 8 vs 10; **Figure 4.4**, lane 5 vs 6). Importantly, in ATM-proficient primary CLL cells and cell line, AZD6738 treatment resulted in ATM activation as evidenced by ATM phosphorylation

Figure 4.3

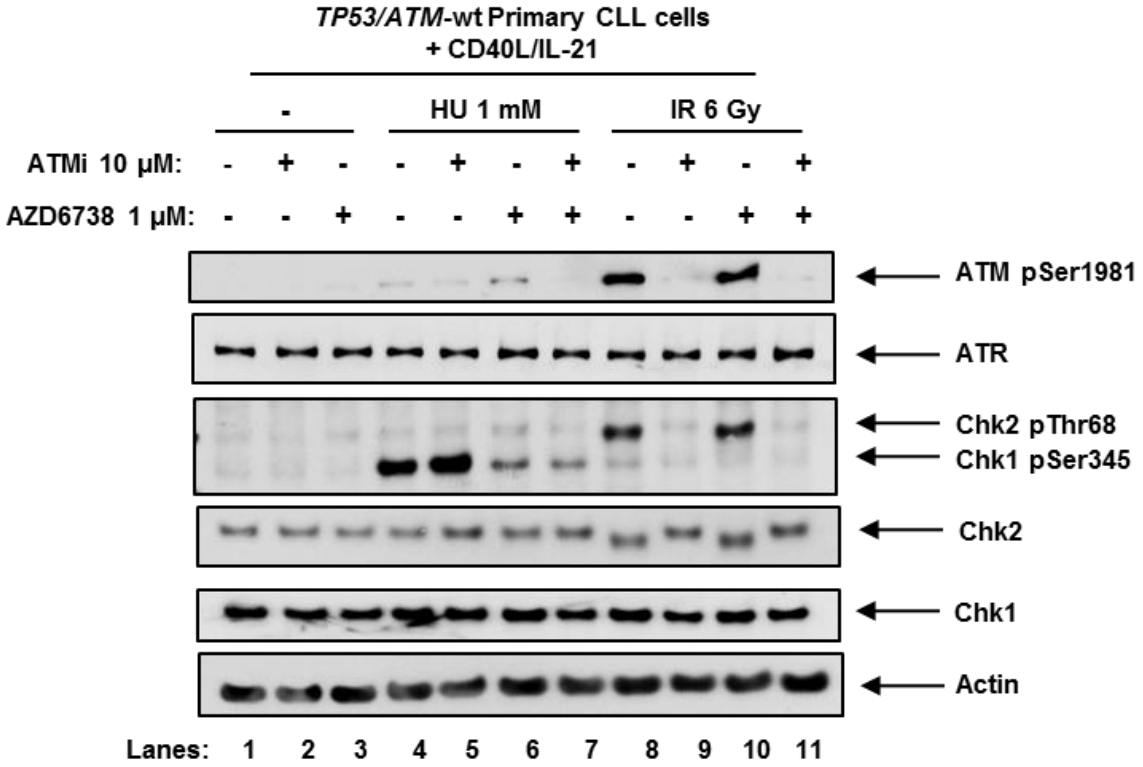

ATR signalling in primary CLL cells is inhibited by AZD6738. ATM/p53-wild type (wt) primary CLL cells co-cultured with CD40L/IL-21 were treated with AZD6738 (1 μM) and/or the ATM inhibitor KU-55933 (ATMi; 10 μM) for 2 hours, or left untreated, prior to exposure to HU (1 mM) or IR (6 Gy) for a further 5 hours. AZD6738 treatment inhibited ATR signalling as indicated by a reduction in HU-induced Chk1 phosphorylation (lane 4 vs 6). In ATM-proficient CLL cells this also led to ATM activation as evidenced by ATM phosphorylation and Chk2 phosphorylation (lane 4 vs 6). Representative blots from experiments on 3 CLL samples are shown.

Figure 4.4

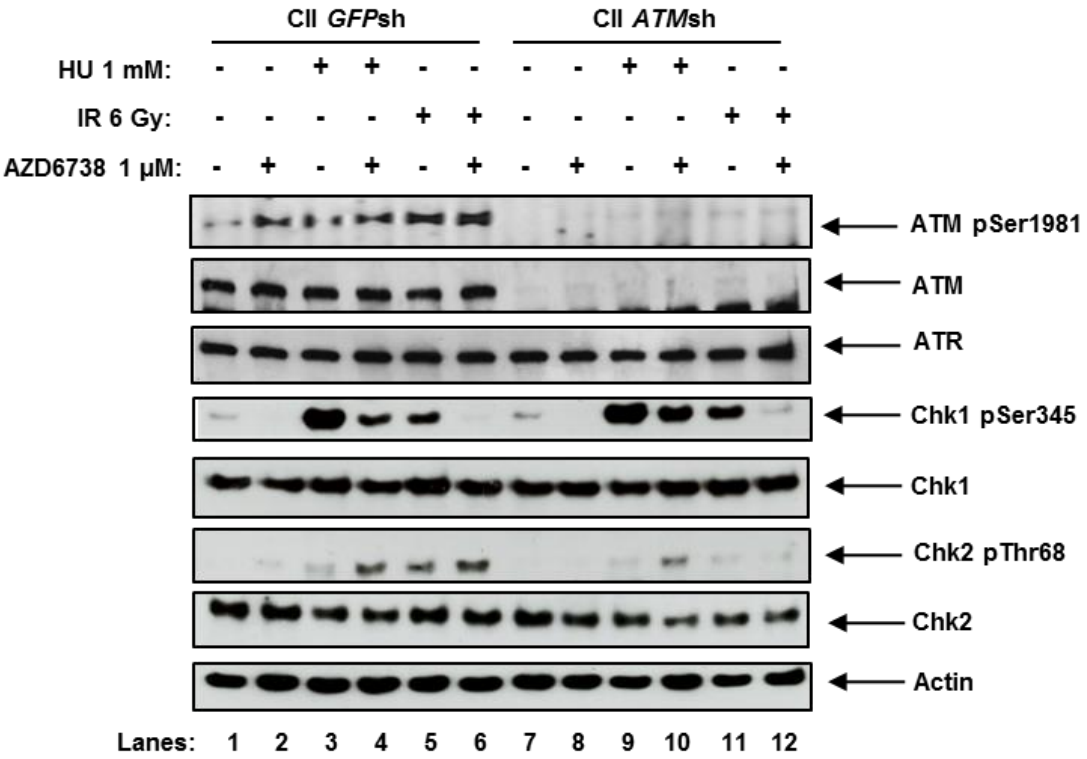

ATR signalling in CLL cell lines is inhibited by AZD6738. CII cells, both CII-GFPsh and CII-ATMsh, were treated with AZD6738 (1 μM) and/or the ATM inhibitor KU-55933 (ATMi; 10 μM) for 2 hours, or left untreated, prior to exposure to HU (1 mM) or IR (6 Gy) for a further 5 hours. AZD6738 treatment inhibited ATR signalling as indicated by a reduction in HU-induced Chk1 phosphorylation (lanes 3 vs 4, and 9 vs 10). In ATM-proficient CLL cells this also led to ATM activation as evidenced by ATM phosphorylation and Chk2 phosphorylation (lane 3 vs 4).

and HU-induced Chk2 phosphorylation (**Figure 4.3**, lane 4 vs 6; **Figure 4.4**, lane 1 vs 2 and 3 vs 4). This indicated activation of the ATM pathway in the absence of functional ATR.

DNA-dependent protein kinase (DNA-PK) is a protein that functions alongside ATM to mediate the repair of DSBs. Whereas ATM repairs DSBs through HRR and NHEJ, DNA-PK is capable of repairing DSBs solely through NHEJ. Recently, DNA-PK was reported to possess some redundant activity with ATR. In one study, DNA-PK was shown to play a role in regulating Claspin expression, maintaining Chk1 stability and promoting Chk1 phosphorylation in cervical and colorectal cancer cell lines in response to replications stress. This was evidenced from the knockdown of DNA-PK in these cells, which led to decreased Claspin expression, Chk1 protein levels, as well as Chk1 phosphorylation in response to HU (Lin et al., 2014). In view of this, I assessed the impact of DNA-PK inhibition in primary CLL cells co-cultured with CD40L/IL-21, using the DNA-PK inhibitor NU7441. Cells were pre-treated with NU7441 and/or AZD6738, or neither, for 1 hour. Thereafter, cells were exposed to HU or IR, and incubated for a further 5 hours prior to protein extraction and analysis using Western blotting. The results are displayed in **Figure 4.5B**. Treatment with 10 μM NU7441 resulted in a reduction of IR-induc ed DNA-PK phosphorylation by >60% (lane 5 vs 6). However, treatment with 10 μM NU7441, either alone (lane 1 vs 2) or in combination with low dose AZD6738 (lane 3 vs 4), did not produce any observable impact on HU-induced Chk1 phosphorylation in primary CLL cells. The lack of impact on HU-induced Chk1 phosphorylation upon treatment with the DNA-PK inhibitor suggests a possibility that such a functional redundancy between ATR and DNA-PK may not be present in CLL cells.

4.1.2. ATR inhibition is selectively cytotoxic to *TP53* or *ATM* defective CLL cells *in vitro* and *in vivo*

To assess the therapeutic potential of ATR inhibition for DDR-defective CLL, I investigated the cytotoxic effects of AZD6738 on CLL cells. The cytotoxic effect of AZD6738

Figure 4.5

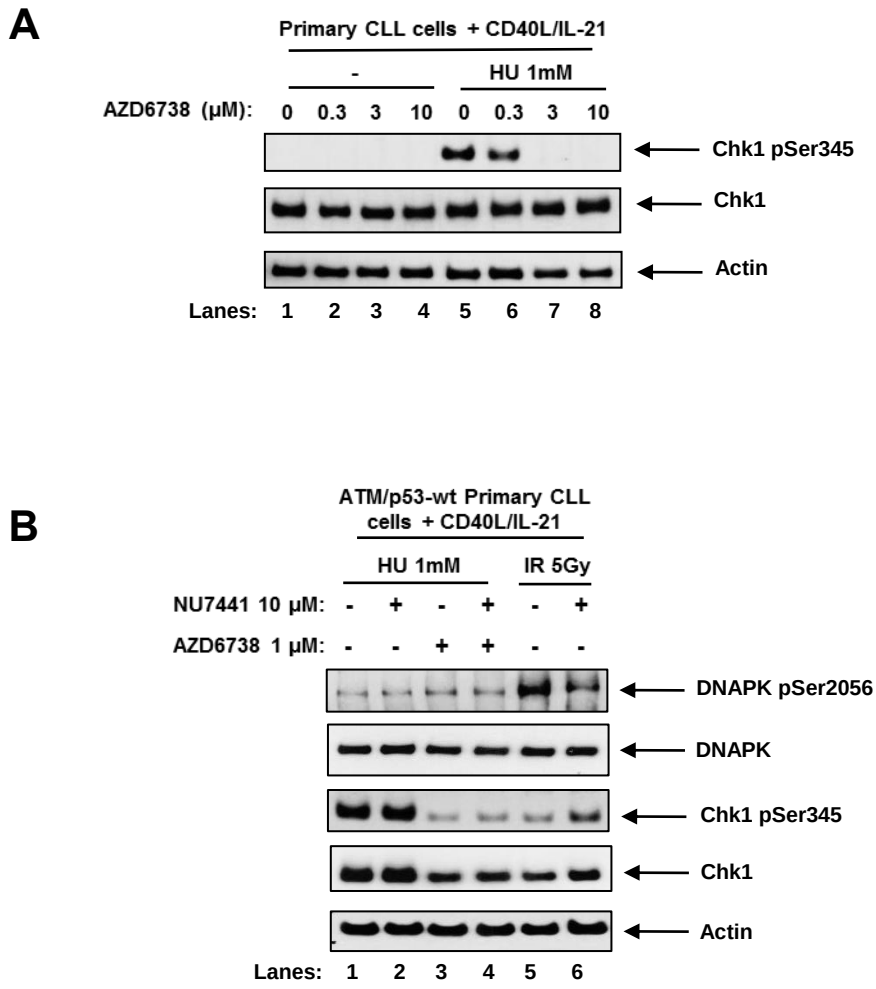

Complete abolition of Chk1 activity can be achieved with higher doses of AZD6738 and is not dependent on DNA-PK activity. (A) Primary CLL cells were treated with escalating doses of AZD6738 for 1 hour prior to exposure to HU. Complete elimination of HU-induced Chk1 phosphorylation was observed at 3 μM AZD6738 or above (lanes 7-8). **(B)** Cells were pre-treated with the DNA-PK inhibitor NU7441 and/or AZD6738, or neither, for 1 hour, exposed to HU or IR, and incubated for a further 5 hours before analysis. Treatment with 10 μM NU7441 resulted in >60% reduction of IR-induced DNA-PK phosphorylation (lane 5 vs 6). However, treatment with NU7441, either alone (lane 1 vs 2) or in combination with 1 μM AZD6738 (lane 3 vs 4) did not produce a detectable impact on HU-induced Chk1 phosphorylation in primary CLL cells.

was first assessed in CLL cell lines. The ATM-deficient CII-*ATM*sh cell line and the p53-mutant Mec1 cell line displayed significantly greater AZD6738 sensitivity (EC_{50} 1.6 μM and 1.1 μM respectively) following 96 hours of drug treatment compared to the ATM/p53-proficient CII-*GFP*sh cell line (EC_{50} 8.4 μM; **Figure 4.6**), as assessed by CellTiter-Glo luminescent cell viability assay. The differential sensitivity of the CII-*ATM*sh and Mec1 cell lines relative to the CII-*GFP*sh cell line to AZD6738 was apparent across a range of AZD6738 doses.

Although Mec1 CLL cells lack p53 function, they are not isogenic with the p53-proficient Cll cell lines. Therefore, observations regarding the effects of AZD6738 based solely on comparisons between these cell lines may not be conclusive. Therefore, I performed additional experimentation on separate paired cell lines that are either proficient or deficient in p53. To achieve this, I utilised Mec1 cells that were transfected by electroporation with the vector pcDNA3.1 containing either wild-type *TP53*, or *GFP* as control, as outlined in section 2.2.2. The expression of the wild-type *TP53* was confirmed on Western blot by the presence of a 53 kDa wild-type p53 protein, located above the smaller 47 kDa truncated mutant p53 protein, as shown in **Figure 4.7A**. The expression of wild-type p53 significantly reduced the sensitivity of Mec1 cells to AZD6738 (EC_{50} 3.2 μM vs 1.0 μM; **Figure 4.7B**), as assessed by CellTiter-Glo luminescent cell viability assay.

Having demonstrated, using cell lines, the selectivity of ATR inhibition for ATM or p53 defective CLL cells, I then proceeded to confirm this in a panel of 29 primary CLL samples. As outlined in section 2.8.2, CFSE-labelled CLL PBMCs from each patient were co-cultured with CD40L/IL-21 for 4 days to induce proliferation, following which cells were treated for 4 days with AZD6738. Viability was measured by PI exclusion of the proliferating CLL population identified by CD19 positivity and a reduction in CFSE fluorescence intensity

Figure 4.6

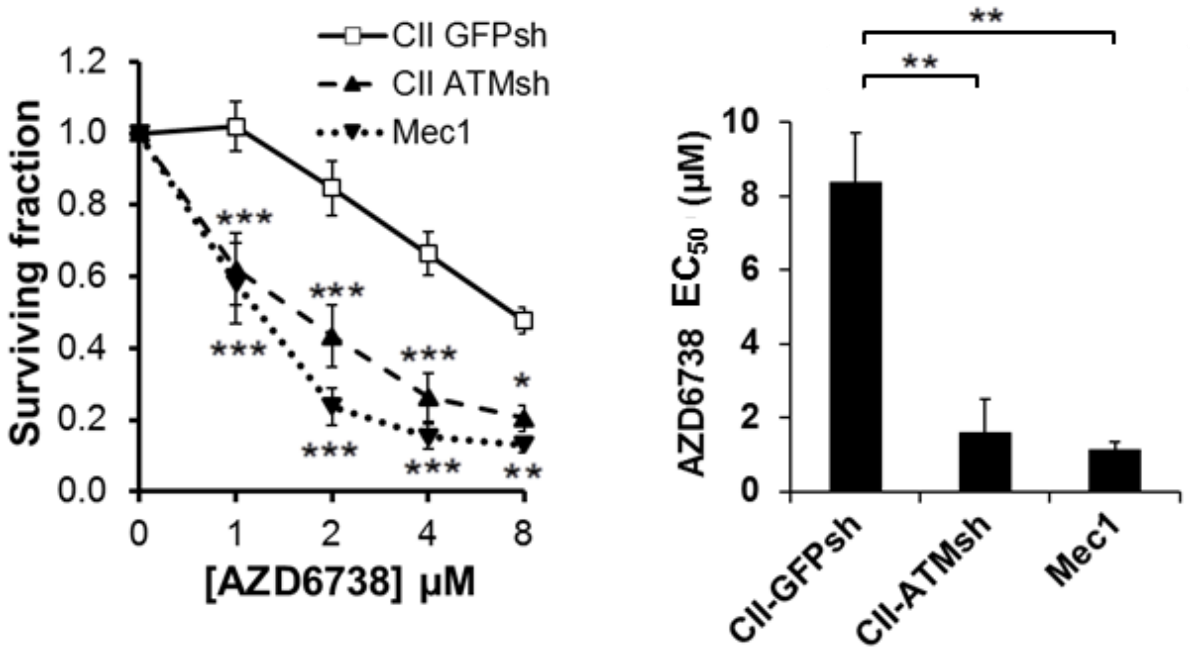

ATR inhibition is selectively cytotoxic to both *ATM*-deficient and *TP53*-deficient CLL cell lines. CII-GFPsh, CII-ATMsh (ATM-deficient) and Mec1 (p53-defective) cells were treated with AZD6738 for 4 days and viability measured using the CellTiter-Glo assay. Surviving fraction is expressed relative to untreated controls. AZD6738 induced significantly greater dose-dependent cytotoxicity with significantly lower AZD6738 EC_{50} in CII-ATMsh and Mec1 cells compared to CII-GFPsh cells. All data is displayed as mean ± SEM. Statistical significance was determined using two-way ANOVA with Bonferroni post-hoc analysis (left panel) or one-way ANOVA (right panel). Statistical significance is indicated by *p<0.05, **p<0.01 and ***p<0.001.

Figure 4.7

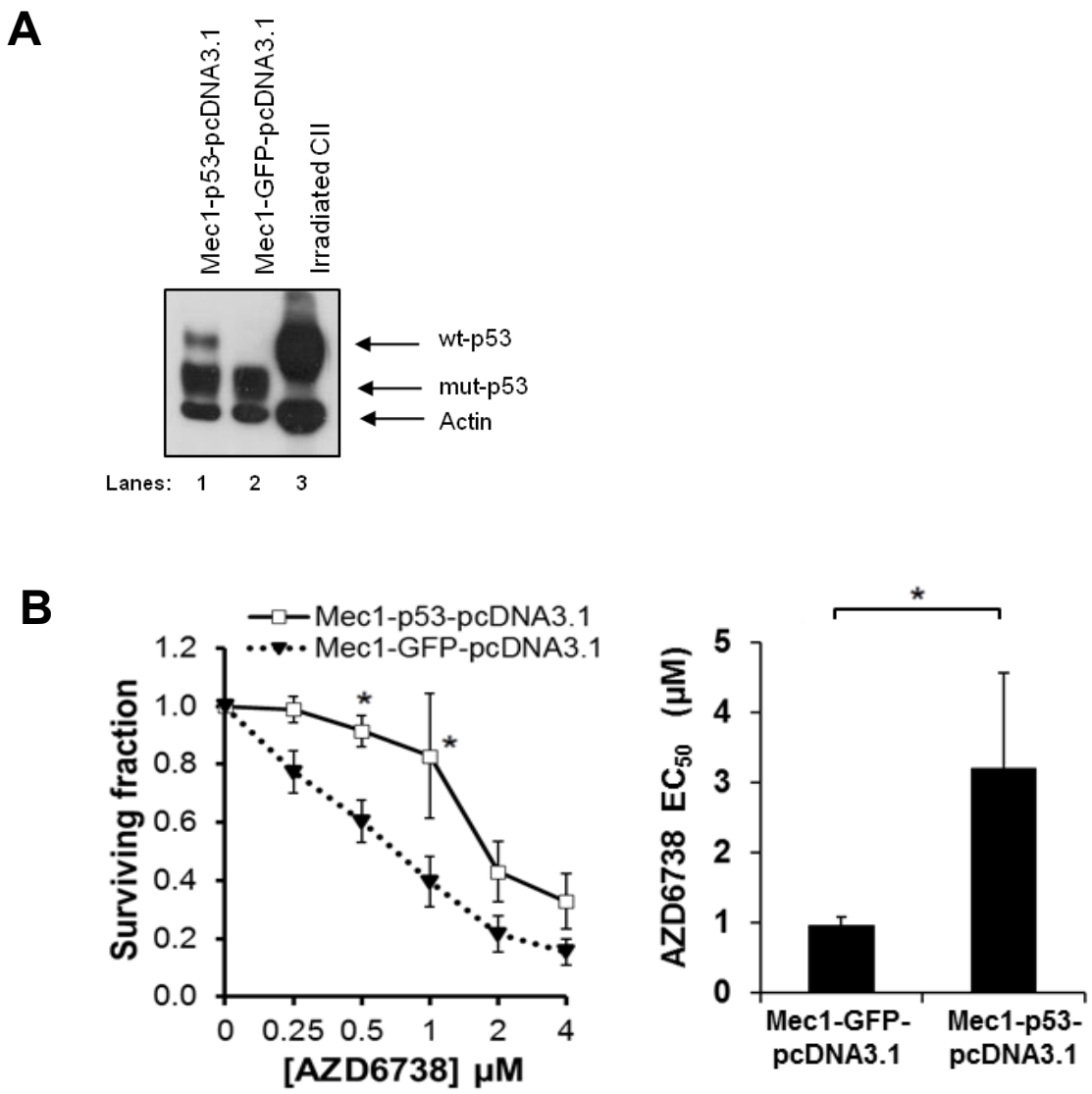

Reintroduction of wild-type *TP53* in Mec1 cells decreased their sensitivity to ATR inhibition. (A) Western blotting shows expression of wild type p53 (wt-p53) in p53-pcDNA3.1 transfected Mec1 cells. Irradiated CII cells were loaded as control for wt-p53 and the position of the mutant p53 (mut-p53) expressed by Mec1 cells is indicated. Actin was used for loading control. **(B)** Mec1 cells transfected with either wild-type *TP53* (Mec1-p53-pcDNA3.1) or GFP (Mec1-GFP-pcDNA3.1, as control) were treated with AZD6738 for 4 days and viability measured using the CellTiter-Glo assay. Surviving fraction is expressed relative to untreated controls. AZD6738-induced cytotoxicity was reduced with significantly higher AZD6738 EC50 in Mec1-p53-pcDNA3.1 cells compared to Mec1-GFP-pcDNA3.1 cells. All data is displayed as mean ± SEM. Statistical significance was determined using two-way ANOVA with Bonferroni post-hoc analysis (left panel) or Student's t-test (right panel). Statistical significance is indicated by *p<0.05, **p<0.01 and ***p<0.001.

(**Figure 2.11**). Selective cytotoxicity towards CLLs with DDR defects was evidenced by a significantly lower EC_{50} in *ATM*-defective (8.7 μM; 95% CI 3.4-13.9 μM; n=6) and *TP53*-defective CLL samples (8.2 μM; 95% CI 3.5-12.9 μM; n=6) compared to either *ATM*/*TP53*-wild-type CLLs (38.3 μM; 95% CI 28.8-47.8 μM; n=17) or healthy donor PBMCs (87.6 μM; 95% CI 50.0-125.3 μM; n=4). As with CLL cell lines, the differential sensitivity of *ATM*-defective or *TP53*-defective CLL samples to AZD6738, relative to the *ATM*/*TP53*-wild-type CLL samples and healthy donor PBMCs, was seen across a range of AZD6738 doses. These results are displayed in **Figure 4.8A-B**, and individual results are included in **Table 4.1**.

No significant difference in AZD6738 sensitivity was found when these samples were analysed according to clinical stage, prior treatment or *IGHV* mutational status (**Figure 4.8C**). As discussed earlier, all of the *ATM*/*TP53*-defective cases harboured del(11q) or del(17p) in the majority of CLL cells. No significant correlation was found between the mutant allelic frequency of the remaining *ATM* or *TP53* allele, and sensitivity to AZD6738 (**Table 4.1**). The lack of such correlation may be due to the small sample size of CLL cases with *ATM* or *TP53* defect. Finally, as expected from a loss of the G1/S checkpoint, there was a trend towards a higher level of proliferation among CLL samples carrying *ATM* or *TP53* defects, as estimated from the proportion of cells that have cycled ≥1 and ≥4 times during the 8-day culture period. However, the differences were not statistically significant, indicating that *ATM* or *TP53* defective CLL cells possess intrinsic sensitivity to ATR inhibition, rather than increased sensitivity simply because of a higher proliferation rate.

To investigate the effect of ATR inhibition in quiescent CLL cells, I treated 10 primary CLL samples (3 *TP53/ATM*-wild type, 3 *ATM*-defective and 4 *TP53*-defective samples) with escalating doses of AZD6738 without CD40L/IL-21 co-culture, and measured cytotoxicity at 24 hours and 96 hours using PI labelling and flow cytometric analysis. As expected, AZD6738 had little, if any, cytotoxic effect on cells cultured without CD40L/IL-21, regardless of *TP53* or *ATM* status (**Figure 4.9**). This is consistent with my earlier finding that

Figure 4.8

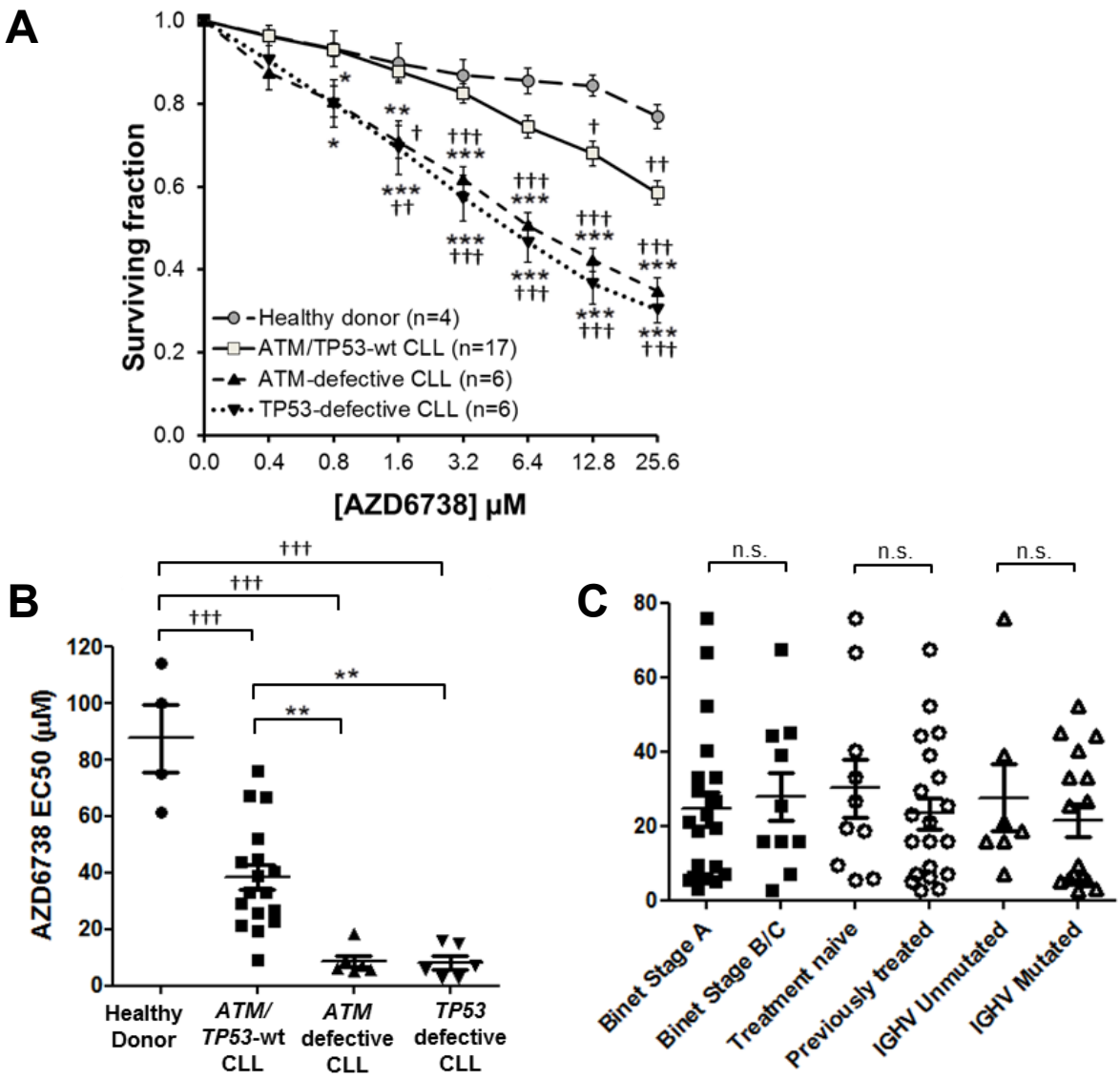

ATR inhibition is selectively cytotoxic to both *ATM*-defective and *TP53*-defective CLL primary cells. (A) CFSE-labelled primary CLL cells with or without ATM/TP53 defects and healthy donor PBMCs co-cultured with CD40L/IL-21 were treated with AZD6738 for 4 days. Viability was measured by propidium iodide exclusion of the proliferating cell population that was identified by reduction in CFSE fluorescence intensity. Surviving fraction is expressed relative to untreated controls. AZD6738 induced significantly greater dose-dependent cytotoxicity in *ATM/TP53*-defective CLL cells than either *ATM/TP53*-wild type CLL cells or healthy donor PBMCs. **(B)** The EC50 of AZD6738 was significantly lower for *ATM/TP53*-defective primary CLL samples than both *ATM/TP53*-wild type samples and healthy donor PBMCs. A list of CLL samples assessed and their respective EC50 are provided in Table 4.1. **(C)** There was no significant difference in the EC50 of AZD6738 between subgroups of CLL samples stratified according to Binet stage, prior treatment and *IGHV* mutational status. All data is displayed as mean ± SEM. Statistical significance was determined using two-way ANOVA with Bonferroni post-hoc analysis (A), one-way ANOVA (B) or Student's t-test (C). Statistical significance vs *ATM/TP53*-wild type samples (*) or healthy donor PBMCs (†) (C,D), or vehicle (F-H) is indicated by *,†p<0.05, **,††p<0.01 and ***,†††p<0.001. Non-significant results are denoted by n.s.

Figure 4.9

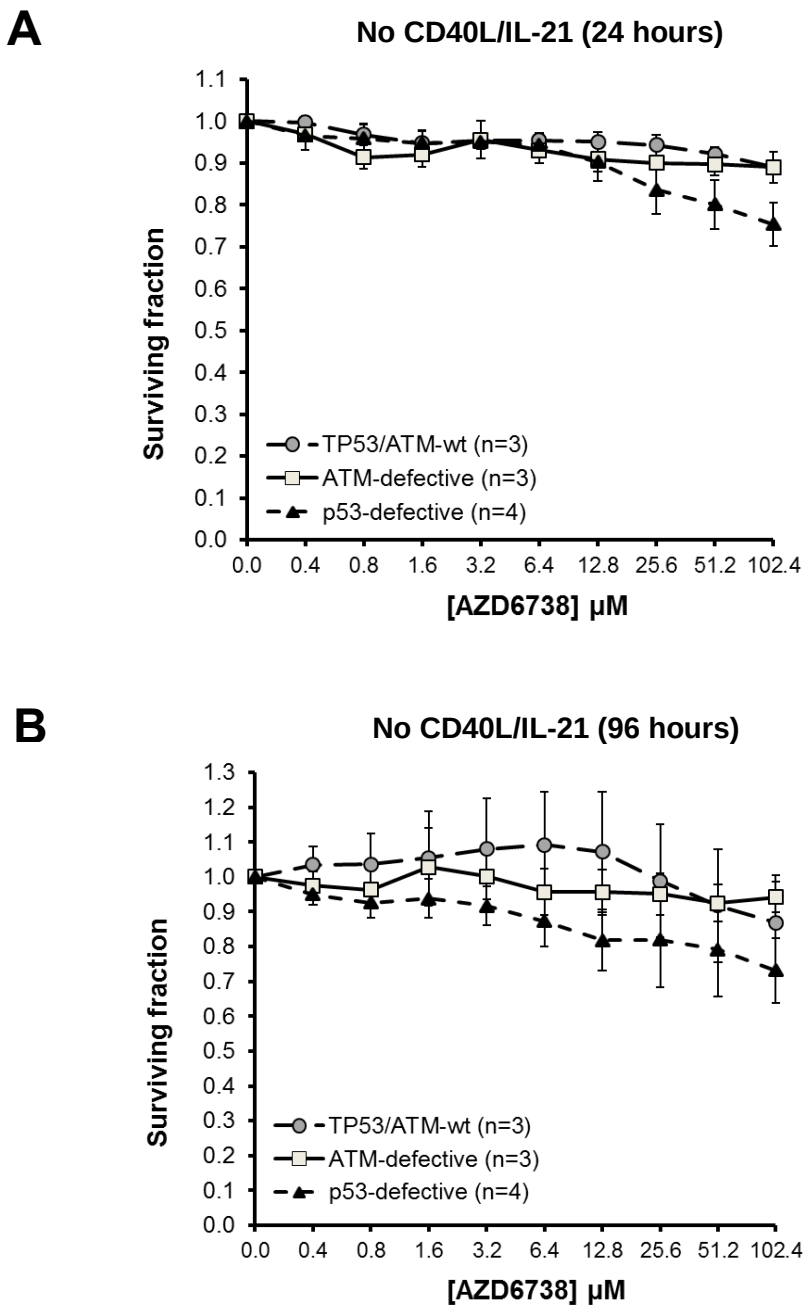

The cytotoxic effect of AZD6738 monotherapy is dependent on CLL cell proliferation. Primary CLL samples [n=10, including 3 *TP53*/*ATM*-wild type (CLL02, CLL06 and CLL07), 3 *ATM*-defective (CLL23, CLL27 and CLL28), and 4 *TP53*-defective samples (CLL29, CLL34, CLL35 and CLL36)] were treated with escalating doses of AZD6738 without co-culture with CD40L/IL-21. Cytotoxicity was assessed using flow cytometric measurement of PI uptake. Surviving fraction was expressed as a percentage of untreated controls. In the absence of cycling induced by CD40L/IL-21, AZD6738 had little impact on the viability of CLL cells, regardless of *TP53* or *ATM* status.

the ATR pathway in CLL cells is active only upon induction of cell cycling (**Figure 4.2**). Therefore, AZD6738, when used as a single agent, specifically targets the proliferating CLL population.

To assess the effectiveness of ATR inhibition in vivo, primary CLL xenografts were employed. In a set of experiments carried out by Dr Nicholas Davies, four representative primary CLL samples carrying either del(17p) and a *TP53* mutation (p.I251S or p.M237I) or del(11q) and an *ATM* mutation (p.I1407T or p.L3013Q) were engrafted into NOD/Shi-scid/IL-2Rγ^{null} mice. Following treatment with AZD6738 (n=10) or vehicle (n=11) for two weeks, tumour load was significantly reduced in AZD6738-treated animals compared to vehicle-treated controls (**Figure 4.10A**). When analysed separately according to genotype, both *TP53* and *ATM* defective AZD6738-treated xenografts showed significant reduction in tumour load (**Figure 4.10B**). Furthermore, in the CLL26 xenograft where tumour cell recovery allowed monitoring of del(11q) cells, a significant reduction in the percentage of cells with del(11q) (37% vs 100%) was observed in AZD6738-treated animals compared to vehicle-treated controls (**Figure 4.10C**). Taken together, the *in vitro* and *in vivo* data demonstrates efficacy and specificity of AZD6738 for *TP53* or *ATM* defective CLL.

4.1.3. ATR inhibition induces DNA damage and mitotic catastrophe in *TP53* or *ATM* defective CLL cells

As discussed in section 1.4.2.1, suppression of aberrant or excessive replication origin initiation is an important mechanism whereby ATR protects DNA replication forks from collapse and breakage (Couch et al., 2013; Toledo et al., 2013; Zeman and Cimprich, 2014). I therefore hypothesised that ATR inhibition in CLL cells would result in increased replication origin initiation. To verify this, I first determined the impact of ATR inhibition on DNA replication in CII-*ATM*sh and Mec1 cells. I collaborated with Dr Eva Petermann, who performed, on these cells, DNA fibre analysis that visualises origins of replication and

Figure 4.10

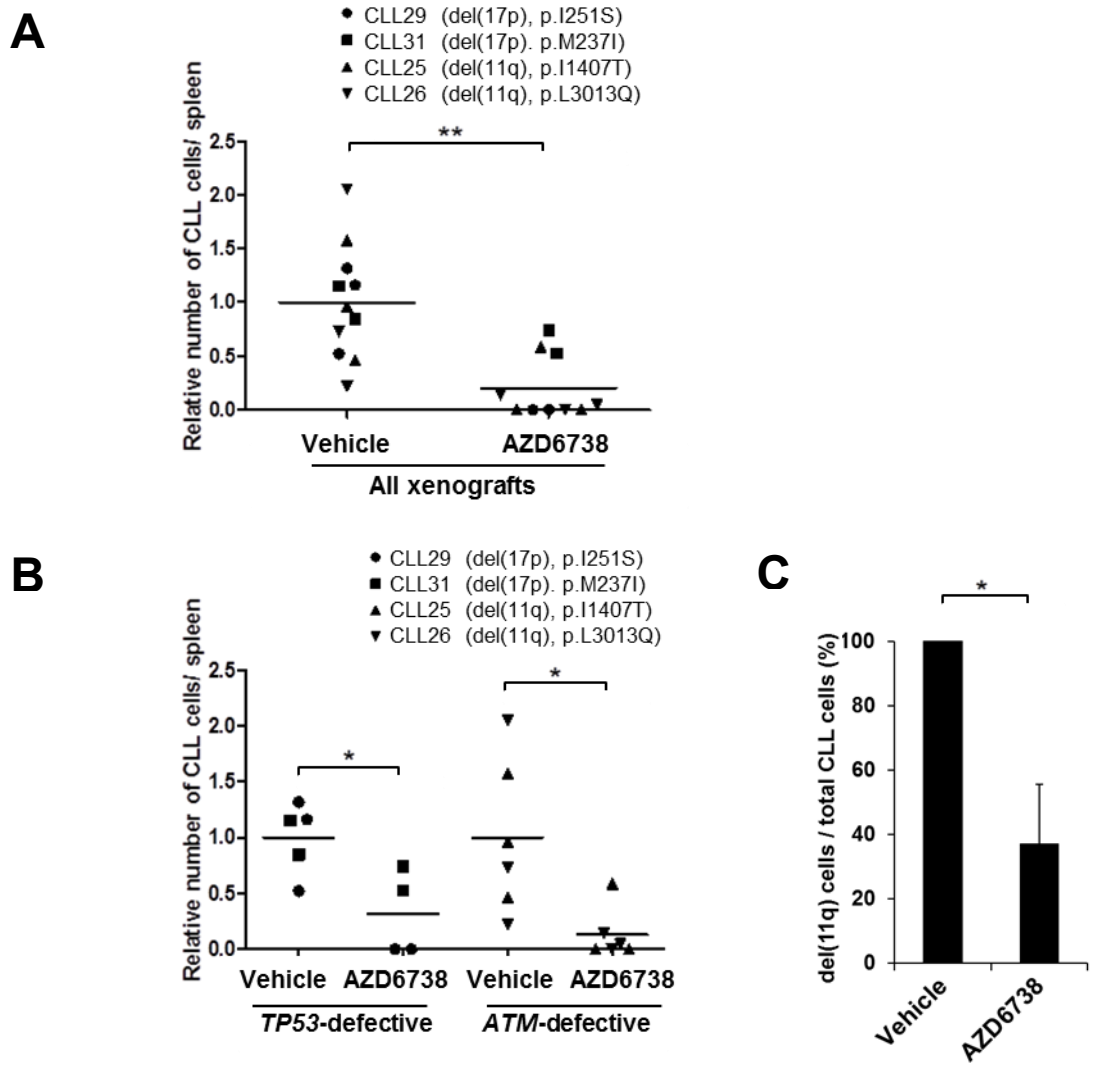

ATR inhibition is selectively cytotoxic to both *ATM*-defective and *TP53*-defective CLL cells *in vivo*. (A) Primary CLL samples (CLL29, CLL31, CLL25, CLL26) with biallelic *TP53* or *ATM* defects were engrafted into NOD/Shi-scid/IL-2Rγ^{null} mice and treated with vehicle (n=11) or AZD6738 (n=10). Treatments were carried out according to the schedule outlined in section 2.10. Collectively, AZD6738 treatment significantly reduced tumour load compared to vehicle treatment in *TP53/ATM*-defective xenografts. **(B)** When analysed separately, both *TP53* and *ATM* defective xenografts showed significant reduction in tumour load following AZD6738 treatment compared to vehicle-treated controls. **(C)** FISH probes for 11q were applied on human CD45+ CD19+ cells collected from the spleens of CLL26 xenografts (harbouring del(11q) and L3013Q ATM mutation) treated with AZD6738 (n=3) or vehicle (n=3). Two hundred cells were analysed per mouse. The proportion of CLL cells with del(11q) was significantly reduced following AZD6738 treatment compared to vehicle-treated controls. All data is displayed as mean ± SEM. Statistical significance was determined using two-way ANOVA with Bonferroni post-hoc analysis (B) or Student's t-test (A,C). Statistical significance is indicated by *p<0.05, **p<0.01 and ***p<0.001.

replication fork progression (**Figure 4.11**). One hour after treatment with AZD6738, increased replication origin initiation was observed as indicated by decreased inter-origin distance (**Figure 4.11A-B**). Decreased DNA fibre length and hence decreased replication fork progression rates was also observed (**Figure 4.11A, C**), consistent with fork slowing or stalling and therefore increased replication stress upon ATR inhibition (Couch et al., 2013; Petermann et al., 2010; Toledo et al., 2013).

Next, I assessed the impact of ATR inhibition on cell cycle progression. I performed cell cycle analyses on CII-*GFP*sh, CII-*ATM*sh and Mec1 cells following 24-hour and 48-hour treatment with either AZD6738 (1 μM or 3 μM) or RPMI-1640 medium. A representative cell cycle profile is displayed in **Figure 4.12**, and data from three independent experiments are presented in **Figure 4.13**. In response to AZD6738, CII-*GFP*sh cells accumulated in G0/G1 consistent with G1/S cell cycle arrest. Specifically, there was a significant increase in the proportion of G0/G1 cells by a magnitude of 10-13% following treatment with AZD6738, seen both at the 24-hour and the 48-hour timepoint (**Figure 4.12; Figure 4.13A**). In contrast, neither G1/S nor G2/M arrest was evident in CII-*ATM*sh and Mec1 cells despite replication stress. Indeed, AZD6738 treatment in the Mec1 cell line resulted in a reduction in the proportion of G0/G1 cells with a corresponding increase in the proportion of cells in S phase, indicating that the G0/G1 checkpoint was bypassed in these cells. This was accompanied by an accumulation of dead cells, represented by an increase of cells in the sub-G phase, particularly with 3 μM of AZD6738 and at the 48-hour timepoint (**Figure 4.12; Figure 4.13B-C**). Together, these results indicate that CLL cells depend on ATM and p53 for cell cycle regulation in the absence of ATR function.

ATR inhibition results in the collapse of stalled replication forks into DNA fragments with double-stranded ends (Couch et al., 2013; Toledo et al., 2013), for which effective resolution requires ATM-mediated HRR and ATM/p53-dependent cell cycle checkpoint activation (Bieging et al., 2014; Shiloh and Ziv, 2013). This was reflected by ATM/Chk2 phosphorylation upon ATR inhibition **(Figure 4.3; Figure 4.4)**. Therefore, I reasoned that

Figure 4.11

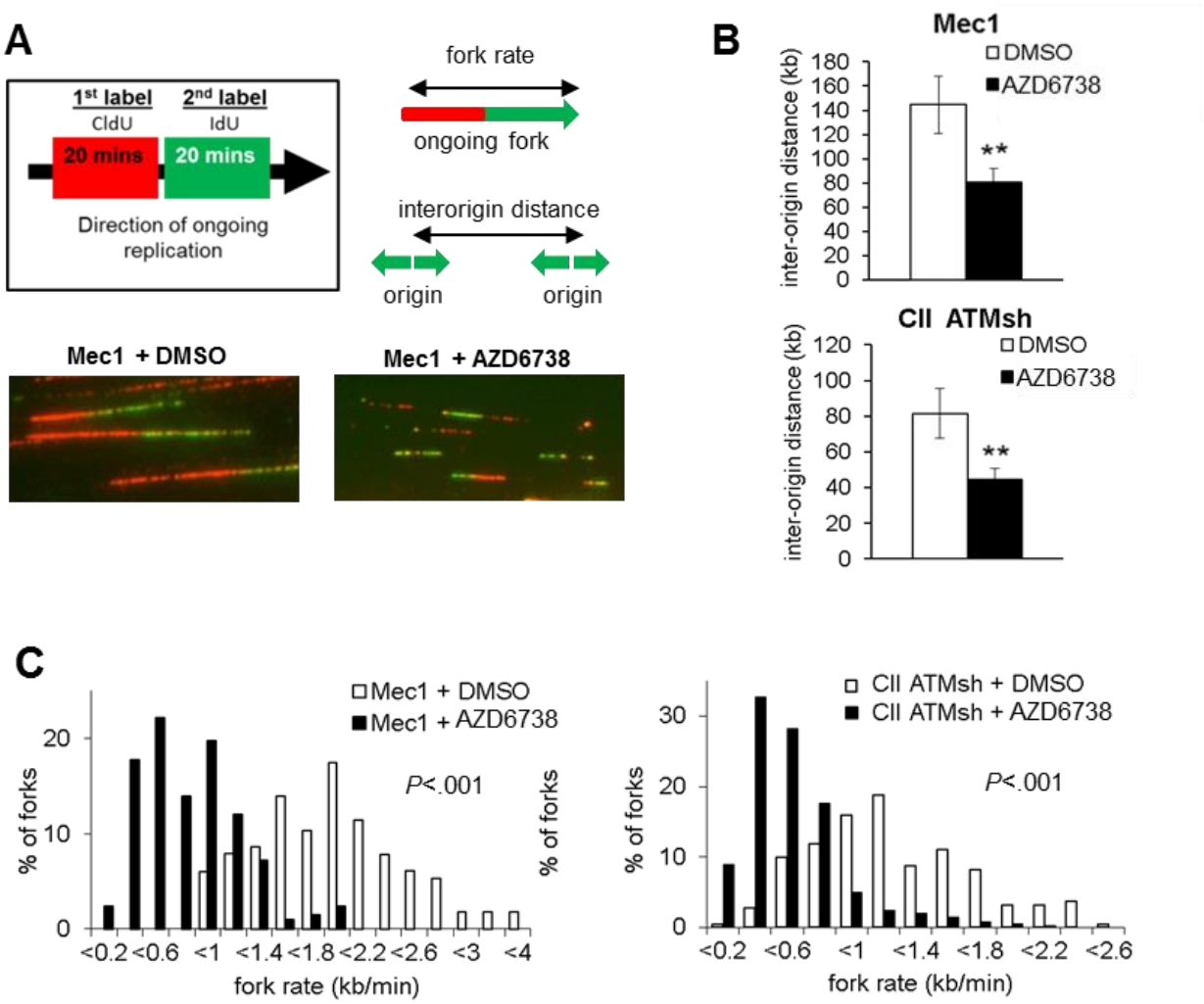

ATR inhibition leads to increased replication stress in CLL cells. (A) AZD6738 (1 μM) treatment for 1 hour led to increased replication stress in Mec1 (p53-defective) and CII-*ATM*sh (ATM-deficient) cells as demonstrated by DNA fibre analysis. Replicating DNA in cycling cells was sequentially labelled with CldU and IdU for 20 min each, after which DNA fibres were analysed by immunofluorescence microscopy. Representative images are displayed. **(B-C)** AZD6738 (1 μM) treatment for 1 hour significantly reduced (B) inter-origin distance and (C) fork progression rate in Mec1 and CII-*ATM*sh cells. Statistical significance was determined using Student's t-test (B) or Mann Whitney U test (C). In (B), statistical significance vs DMSO-treated controls is indicated by **p<0.01.

Figure 4.12

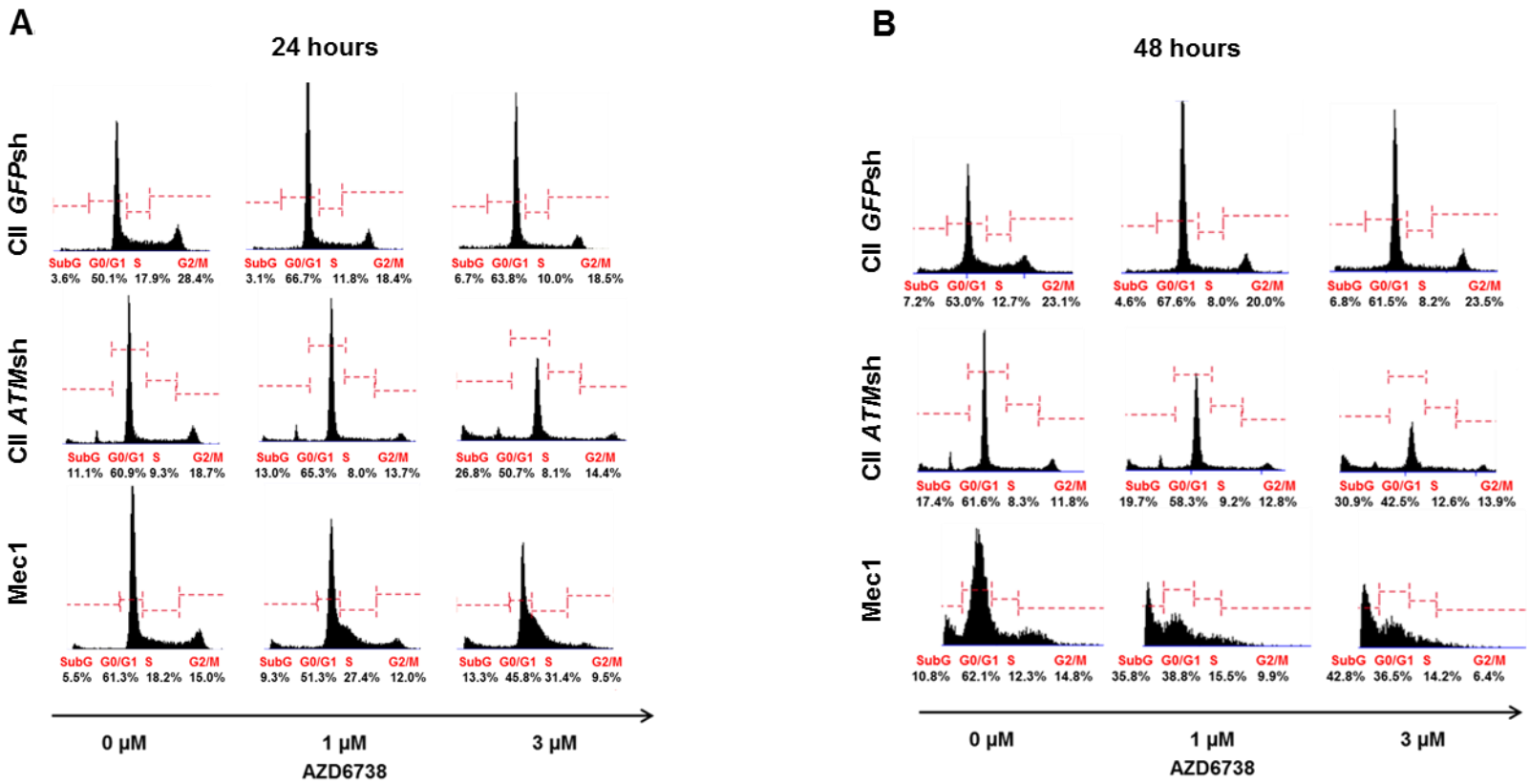

The effect of ATR inhibition on the cell cycle profiles of CLL cells with defective ATM or p53. CII-*GFP*sh, CII-*ATM*sh and Mec1 cells were analysed 24 (A) or 48 (B) hours after treatment with either AZD6738 (1 μM or 3 μM) or RPMI media. AZD6738 treatment induced G1/S cell cycle arrest in CII-*GFP*sh cells but not in CII-*ATM*sh or Mec1 cells. Representative cell cycle profiles from 3 independent experiments are displayed. The percentages shown represent the proportion of cells within each phase of the cell cycle.

Figure 4.13

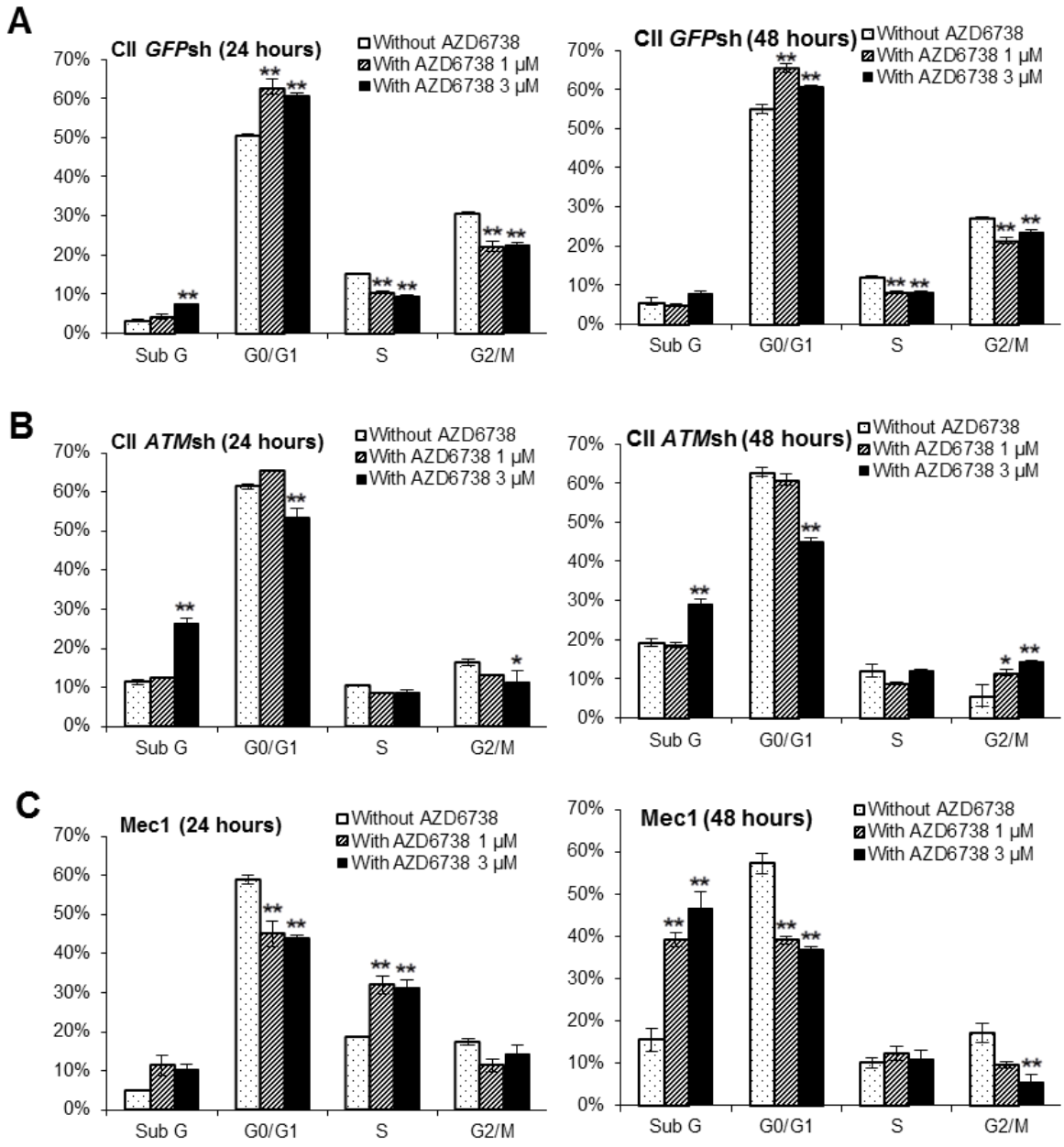

ATR inhibition leads to ATM/p53 dependent G1/S cell cycle arrest in CLL cells. Cell cycle analysis on (A) CII-*GFP*sh, (B) CII-*ATM*sh and (C) Mec1 cells were carried out following 24 or 48 hour treatment with either AZD6738 (1 μM or 3 μM) or RPMI media. AZD6738 treatment induced G1/S cell cycle arrest in CII-*GFP*sh cells but not CII-*ATM*sh or Mec1 cells. Data is displayed as mean ± SEM of triplicate experiments. Statistical significance was determined using two-way ANOVA with Bonferroni post-hoc analysis. Statistical significance vs untreated controls is indicated by *p<0.05 and **p<0.01.

ATR inhibition should produce more fragmented DNA in ATM/p53-defective CLL cells. To assess the amount of DNA damage accrued through ATR inhibition, I utilised CII cells pre-treated for 2 hours with 10 μM of ATM inhibitor, CII cells without ATM inhibitor pre-treatment, and Mec1 cells. I treated these cells with 1 μM of AZD6738 for 24 or 48 hours, after which the cells were harvested, labelled with anti-γH2AX and anti-53BP1 antibodies and the appropriate secondary antibodies, and analysed by immunofluorescence microscopy. As discussed in section 1.4.1, ATM can phosphorylate histone H2AX to produce γH2AX. However, H2AX can also be phosphorylated by numerous other DDR proteins, such as ATR and DNA-PK, leading to their accumulation at sites of DNA DSBs, even in the absence of ATM (Rothkamm et al., 2015). Likewise, 53BP1 accumulates at sites of DSBs. The aggregation of these proteins at damaged sites can be visualised as DNA damage foci. These foci serve as biomarkers of DNA damage, or more specifically of DSBs. Consistent with the above hypothesis that ATM/p53-defective CLL cells should preferentially accumulate DNA fragments arising from collapsed replication forks, I observed accumulation of these markers of DSBs, namely γH2AX and 53BP1 foci, in Mec1 and ATMi pre-treated CII cells but not in CII cells without ATMi pre-treatment, 24 and 48 hours respectively following exposure to 1 μM of AZD6738 (**Figure 4.14A-C; Figure 4.15A-C**).

To assess the amount of DNA damage specifically in CLL cells that are undergoing mitosis, I co-labelled these cells with anti-γH2AX antibody and an antibody against phosphohistone H3 ser-10 (pH3). The phosphorylation of histone H3 at Ser10 (as well as Ser28 and Thr11) is associated with chromosome condensation that occurs during mitosis. Hence, pH3 serves as a specific marker for mitosis. Co-labelling for γH2AX and pH3 revealed dual positivity for these markers following 24-hour incubation with 1 μM AZD6738 in Mec1 and ATMi pre-treated CII cells. Indeed, among Mec1 and ATMi pre-treated CII cells, a substantial proportion of cells undergoing mitosis was γH2AX positive (**Figure 4.14A-B, D)**. Therefore, consistent with the loss of both G1/S and G2/M checkpoints in the absence of functional ATM/p53 and ATR, Mec1 and ATMi pre-treated CII cells, when treated with AZD6738, progressed into mitosis despite carrying unrepaired DNA damage.

Figure 4.14

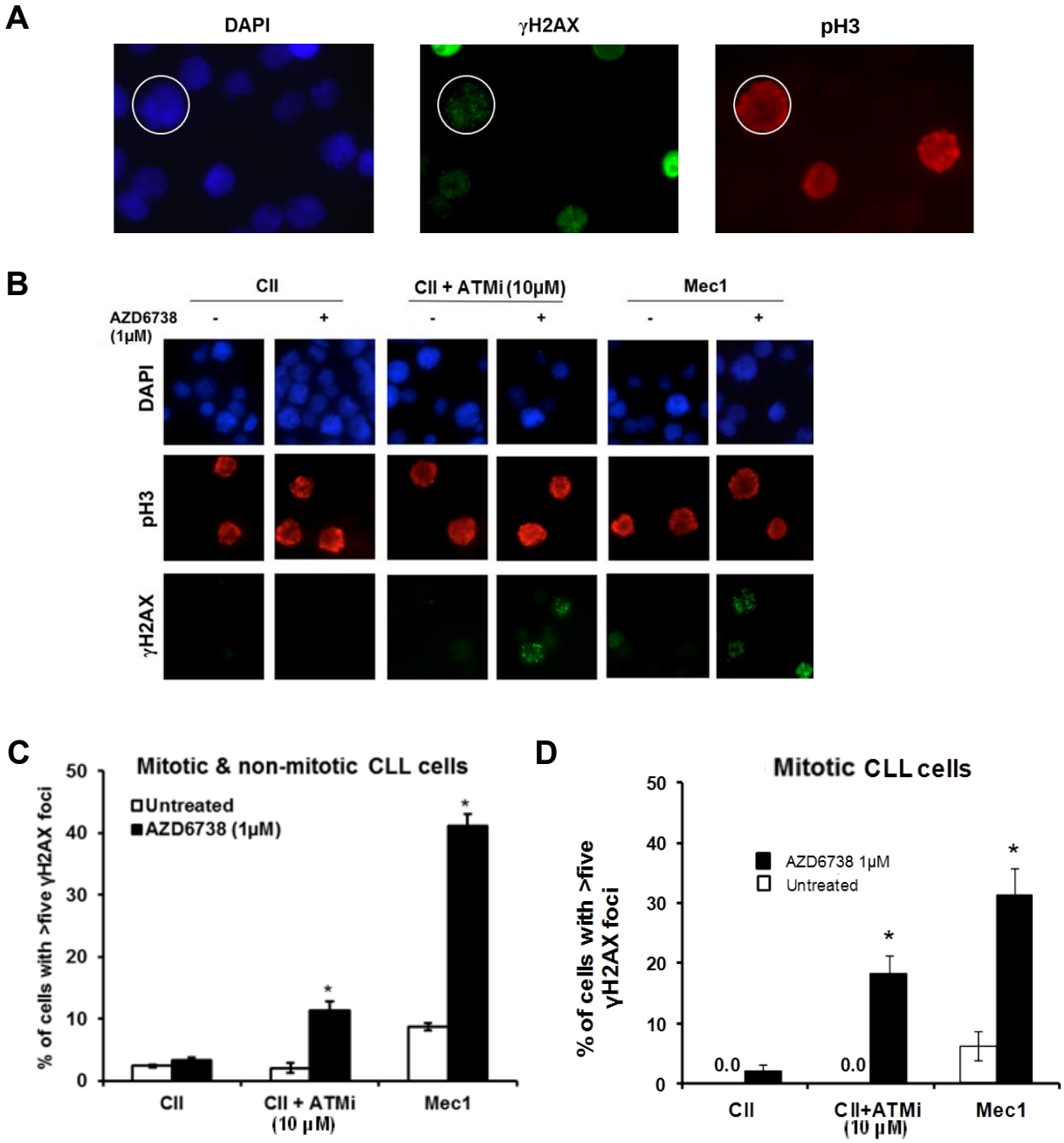

ATR inhibition results in accumulation of γH2AX foci in CLL cells with ATM or p53 deficiency. (A) Co-labelling of CLL cells with γH2AX and pH3 allows identification of both mitotic (pH3-positive) and non-mitotic (pH3-negative) cells that have accumulated DNA damage (γH2AX). Images were captured using a 60x lens. **(B)** Cells treated with AZD6738 (1 μM) for 24 hours were co-labelled with anti-γH2AX and anti-pH3 antibodies, and analysed by immunofluorescence microscopy. A cell was considered γH2AX positive if more than five γH2AX foci were present. At least 200 cells were analysed in each sample. AZD6738 induced γH2AX foci in Mec1 and ATMi pre-treated CII cells, but not in CII cells without ATMi pre-treatment. **(C-D)** The effect of AZD6738 (1 μM) treatment on the proportion of mitotic and non-mitotic γH2AX-positive CLL cells. Data is displayed as mean ± SEM of triplicate results from a representative experiment. Statistical significance compared to untreated controls, assessed by Student's t-test, is indicated by *p<0.05.

ATR inhibition results in replication stress, which leads to replication fork slowing and stalling and hence increasing the amount of incompletely replicated regions within the genome (Zeman and Cimprich, 2014). As outlined in section 1.4.2.3, ATR-mediated G2/M arrest would normally occur in the presence of replication stress, allowing resolution of stalled forks and completion of DNA replication prior to entry into mitosis. In the absence of functional ATR, some cells could enter mitosis despite incomplete genomic duplication. During the metaphase stage of mitosis, chromosomes align at the equatorial region of the cell. The sister chromatids of each duplicated chromosome are held together by protein complexes called cohesins, which are cleaved before the chromatids separate during anaphase, and by DNA catenanes. DNA catenanes are two DNA strands located within each of the two sister chromatids that become intertwined and entangled with each other. DNA catenanes can arise during normal DNA replication but these are normally resolved, by a hitherto unknown mechanism, prior to chromatid separation. In contrast, DNA catenanes that arises from partially replicated DNA, as a result of replication stress during the previous S phase, remain unresolved (Mankouri et al., 2013). As the sister chromatids try to separate during anaphase, these catenated regions of DNA result in ultra-fine DNA bridges, which are chromatin that remain connected to both chromatids (Liu et al., 2014). As the sister chromatids continue to separate, these ultra-fine DNA bridges often break and are transmitted to daughter cells at the following G1. These lesions are sequestered within nuclear compartments called 53BP1 nuclear bodies which serve to protect DNA from endonuclease degradation during G1, and facilitate their repair during the subsequent S phase (Harrigan et al., 2011; Lukas et al., 2011).

53BP1 foci appear as discrete dots or points on immunofluorescence microscopy. On the contrary, 53BP1 nuclear bodies are characterised by robust, block-like staining (Harrigan et al., 2011; Lukas et al., 2011). As shown in **Figure 4.15A**, 53BP1 foci reflect unrepaired DSBs, whereas 53BP1 bodies represent under-replicated DNA. As expected, I observed an accumulation of 53BP1 bodies in ATM/p53-proficient CII cells following 48

Figure 4.15

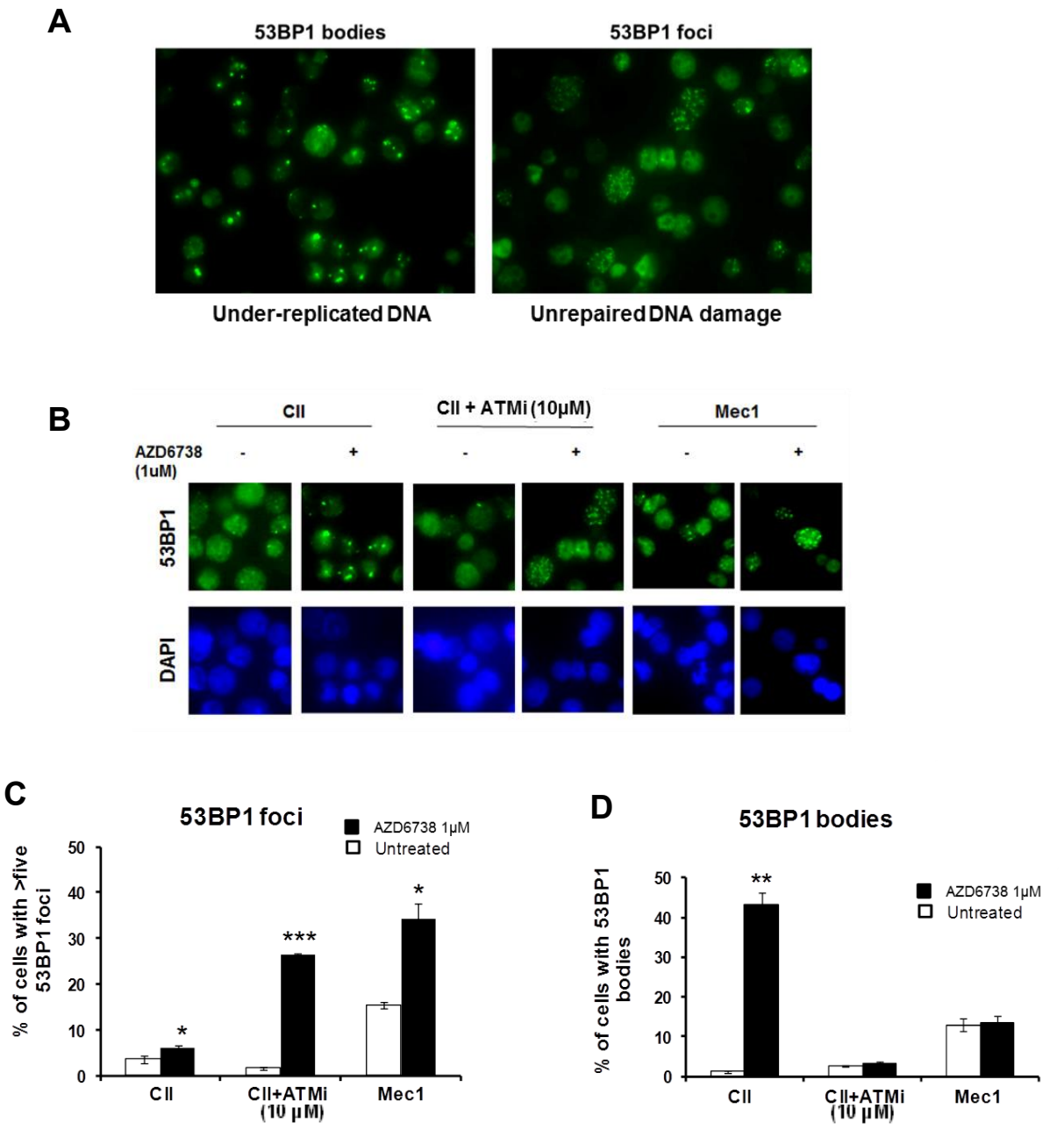

ATR inhibition results in accumulation of 53BP1 foci in CLL cells with ATM or p53 deficiency. (A) The pattern of 53BP1 labelling distinguishes 53BP1 bodies from 53BP1 foci. 53BP1 bodies are characterised by robust block-like staining, and indicate under-replicated DNA. 53BP1 foci are characterised by discrete punctate staining, and indicate DNA damage. A cell was considered 53BP1 foci positive if more than five 53BP1 foci were present. **(B-D)** Cells treated with AZD6738 (1 μM) for 48 hours were labelled with anti-53BP1 antibodies, and at least 200 cells were then analysed in each sample using a 60x lens. AZD6738 treatment led to an accumulation of 53BP1 foci in Mec1 and ATMi pre-treated CII cells, and an accumulation of 53BP1 bodies in CII cells without ATMi pre-treatment. Data is displayed as mean ± SEM of triplicate results from a representative experiment. Statistical significance compared to untreated controls, assessed by Student's t-test, is indicated by *p<0.05, **p<0.01 and ***p<0.001.

hours of AZD6738 treatment (**Figure 4.15A-B, D**). In contrast, this was not seen in ATM/p53-defective CLL cells, suggesting that formation of 53BP1 bodies was dependent on the ATM pathway as previously demonstrated using rapidly dividing fibroblast cell lines (Harrigan et al., 2011). Failure to initiate this protective mechanism could precipitate further DNA damage in ATM/p53-defective CLL cells.

Based on the results so far, I postulated that the abolition of both G1/S and G2/M cell cycle checkpoints due to the combined loss of functional ATM/p53 and ATR would permit entry into mitosis despite the accumulation of unrepaired DNA DSBs and partially replicated DNA fragments, resulting in mitotic catastrophe. Mitotic catastrophe is a form of cell death occurring during mitosis, as DNA damaged cells engage in an aberrant attempt at chromosomal segregation. Mitotic catastrophe is characterised by premature chromatin condensation, and the formation of micronuclei, which are distinct, oval-shaped DNA mass positioned next to the nucleus within the cytoplasm, and arise from failure of DNA or DNA fragments to incorporate into the daughter nuclei during mitosis. The exact mechanism of cell death occurring during mitotic catastrophe is, however, unclear (Vitale et al., 2011).

Experimentally, cells undergoing mitotic catastrophe can be distinguished from those undergoing apoptosis by immunofluorescence labelling of pH3 and lamin B (Weston et al., 2010). Lamin B is a nuclear membrane protein. Cells undergoing normal mitosis stain positive for pH3 but lose lamin B staining, because of dissolution of the nuclear membrane during mitosis. In contrast, cells undergoing mitotic catastrophe do not stain for pH3 but retain lamin B staining due to failed nuclear membrane disassembly. In addition, cells undergoing mitotic catastrophe can be identified and distinguished from quiescent cells by multiple micronuclei that are visible with DAPI staining. On the other hand, the expression of both pH3 and lamin B is lost when cells undergo apoptosis, because the nuclear membrane is targeted by caspases for proteolytic degradation. Apoptotic cells can also be recognised by their characteristic appearance upon DAPI staining, consistent with apoptosis-associated nuclear fragmentation (**Figure 4.16A**). Therefore, in order to confirm the cytotoxic

Figure 4.16

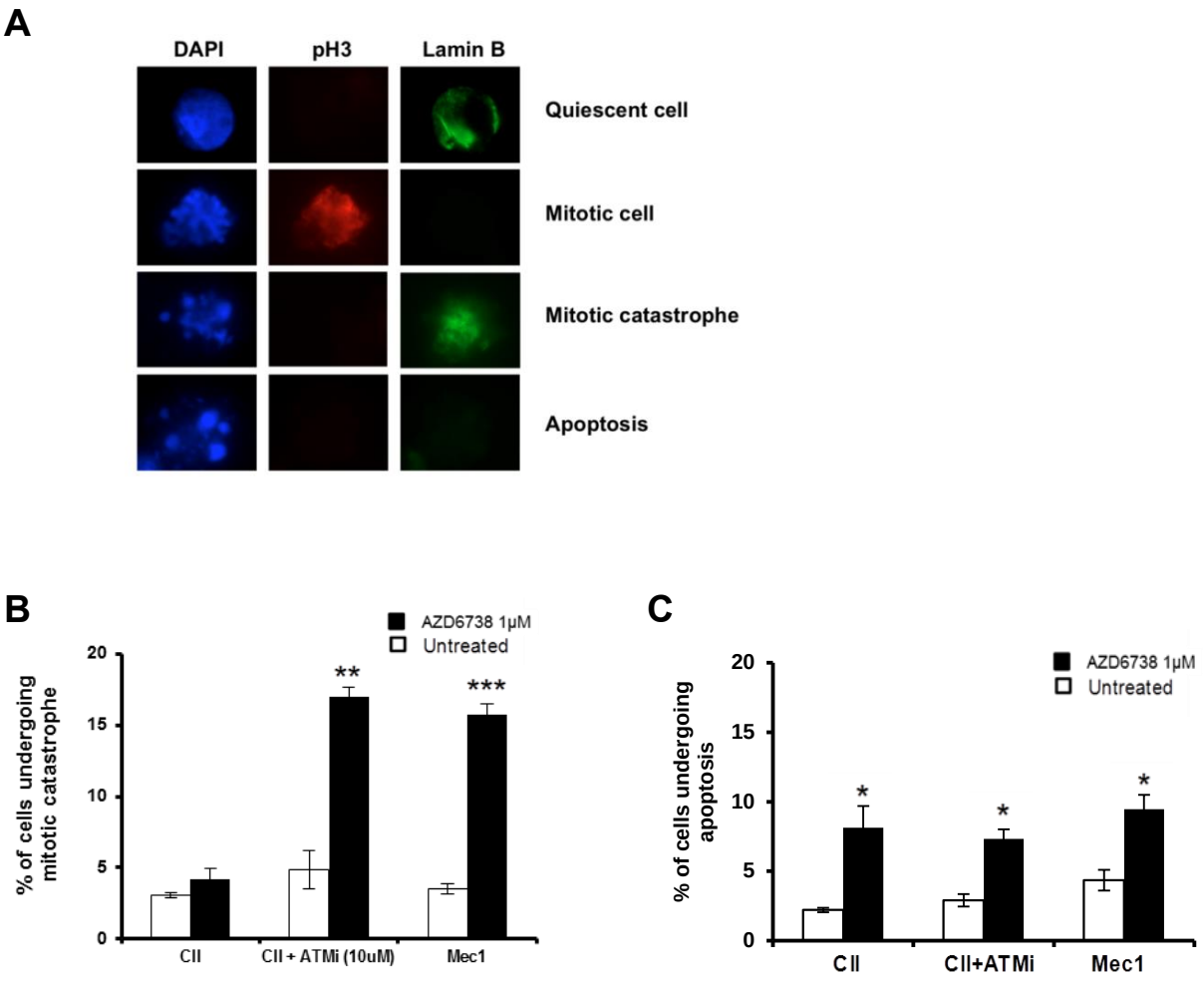

ATR inhibition results in mitotic catastrophe in CLL cells with ATM or p53 deficiency. **(A)** Co-labelling with anti-lamin B and anti-pH3 antibodies allows apoptotic CLL cells to be distinguished from cells undergoing mitotic catastrophe. At least 200 cells were analysed in each sample. **(B)** AZD6738 exposure for 72 hours resulted in significantly elevated levels of mitotic catastrophe in Mec1 and ATMi pre-treated CII cells. Data is displayed as mean ± SEM of triplicate results from a representative experiment. Statistical significance was determined using Student's t-test. Statistical significance compared to untreated controls, assessed by Student's t-test, is indicated by *p<0.05, **p<0.01 and ***p<0.001.

mechanism underpinning ATR inhibition, I probed CLL cells for pH3 and lamin B. I found significant levels of mitotic catastrophe 72 hours following 1 μM AZD6738 in Mec1 and ATMi pre-treated CII cells, but not in CII cells without ATMi pre-treatment (**Figure 4.16B**).

It has been reported in a previous study that mitotic catastrophe could be accompanied by an accumulation of tetraploid cells (4N, corresponding to the G2/M population) that have failed to complete mitosis (Huang et al., 2005). However, I did not observe this in CLL cells treated with AZD6738. A potential explanation relates to the effect of ATR inhibition on DNA replication. As alluded to previously, cells subjected to ATR inhibition enter mitosis having undergone incomplete DNA replication. They are therefore expected to have DNA content between 2N and 4N, rather than 4N. Therefore, mitotic arrest would be manifested by the accumulation of cells with DNA content between 2N and 4N (corresponding to S phase) rather than 4N, as observed from the changes in the Mec1 cell cycle profile in response to AZD6738 (**Figure 4.12**; **Figure 4.13C**).

In ATM/p53-proficient CII cells, I detected low level apoptotic activity after AZD6738 treatment by both immunofluorescence microscopy (**Figure 4.16C**) and Western blotting, where I used PARP and caspase 7 cleavage as markers of apoptosis. AZD6738 induced a modest reduction in full-length caspase 7, as well as an increase in cleaved PARP (**Figure 4.17A**). The modest change in the levels of these markers is indicative of a low level of apoptotic activity being induced by AZD6738. In these ATM/p53-proficient CLL cells, the apoptotic activity is likely to be a result of p53 activation in response to replication stress. Mec1 cells also exhibited low levels of apoptotic markers PARP and caspase cleavage (**Figure 4.17B**), but such levels were unlikely to account for their differential sensitivity to ATR inhibition compared to DDR-proficient cells. Indeed, in response to AZD6738, similar levels of apoptotic induction was seen across Mec1 cells and CII cells with and without ATM inhibitor pre-treatment (**Figure 4.16C**). Moreover, the negligible impact of pan-caspase inhibitor Z-VAD-FMK on the viability of AZD6738-treated Mec1 cells supports this notion (**Figure 4.17C**).

Figure 4.17

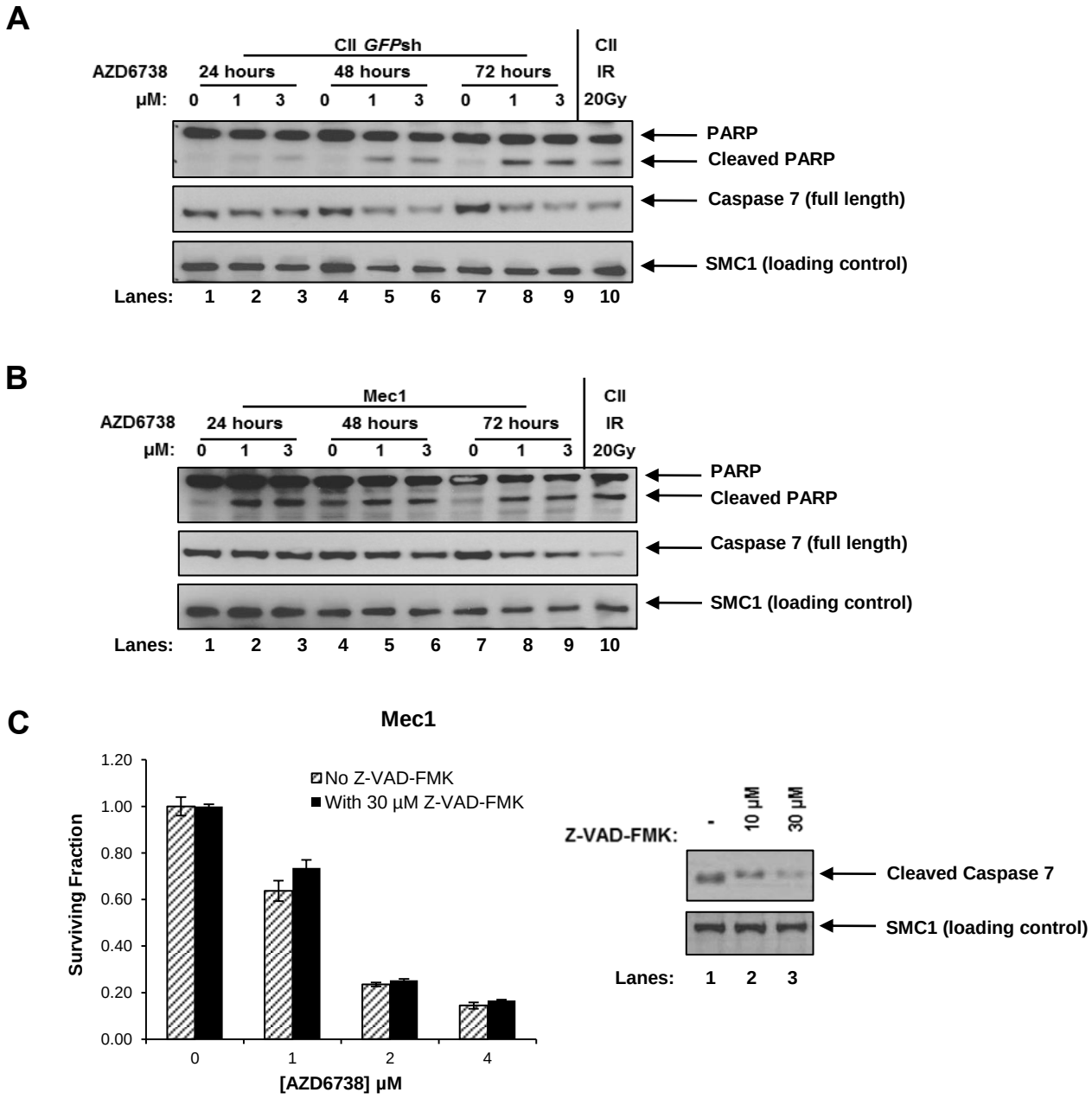

ATR inhibition induces a low-level of apoptotic activity in both DDR-proficient and DDR-deficient CLL cells. (A) CII-*GFP*sh (DDR-proficient) and **(B)** Mec1 (DDR-deficient) cells treated with AZD6738 (0, 1 or 3 μM) for 24-72 hours or 20 Gy IR as a positive control were analysed by Western blotting. AZD6738 induced a small reduction in full-length PARP and full-length caspase 7, as well as an increase in cleaved PARP. Taken together the minimal changes in the levels of these markers are indicative of a low level of apoptotic activity being induced. SMC1 was the loading control. **(C)** Mec1 cells were treated with AZD6738 in the presence or absence of the pan-caspase inhibitor Z-VAD-FMK (30 μM). Following 96 hours of incubation cells were analysed using the CellTiter-Glo assay. Z-VAD-FMK displayed minimal effect on the cytotoxic activity of AZD6738. Error bars represent SEM.

4.1.4. ATR inhibition sensitises *TP53* or *ATM* defective CLL cells to chemotherapy and ibrutinib

I reasoned that the synthetically lethal effects of ATR inhibition on *ATM* or *TP53* defective CLL cells could sensitise these chemoresistant cells to chemotherapeutic agents through potentiation of DNA damage. I therefore assessed the impact of combining AZD6738 with chemotherapy in CLL cell lines and primary CLL PBMCs. The chemotherapeutic agents chosen to combine with AZD6738 reflect the range of agents currently used in clinical practice: the alkylating agents chlorambucil, cyclophosphamide and bendamustine, and the purine analogue fludarabine. Cyclophosphamide is a pro-drug that requires metabolic activation *in vivo* by liver cytochrome P450. Therefore, its active form, 4-hydroperoxycyclophosphamide (4HC), was used in all *in vitro* experiments.

Since the goal of drug combination is to reduce the drug dose required to achieve the desired therapeutic effect, a low dose of AZD6738, at 1 μM, was used for the *in vitro* drug combination studies. At 1 μM, AZD6738 produced a cytotoxic effect that approximates the EC_{25} (the dose that produces 25% cell killing): slightly above the EC_{25} in *ATM*/*TP53*-defective CLL cell lines, and slightly below the EC_{25} in *ATM*/*TP53*-defective primary CLL cells (**Figure 4.6**; **Figure 4.8**). On the other hand, the choice of drug doses for chemotherapeutic agents was made with reference to their physiologically achievable dose range, calculated based on the maximal plasma concentrations (Cmax) obtained from patients treated with conventional doses of the drug in published *in vivo* pharmacokinetics studies. These are 5.7 μM, 5.4 μM, 0.6 μM / 11 μM (depending on the dose and route of administration) and 25 μM respectively for chlorambucil (Silvennoinen et al., 2000), fludarabine (Foran et al., 1999), 4HC (Anderson et al., 1996; Struck et al., 1987) and bendamustine (Ogura et al., 2011). Because these Cmax values were derived from a single drug dose and do not take into account the effect of repeat or continuous dosing, I have included several chemotherapy doses that are slightly higher than the Cmax (<4x Cmax).

While resistance to chlorambucil, fludarabine, 4HC or bendamustine monotherapy was evident in the *ATM* defective CII-*ATM*sh cells and the *TP53* defective Mec1 cells even at the highest chemotherapy dose, I discovered significant sensitisation to a range of doses of these agents upon addition of 1 μM AZD6738. This is evidenced by marked dose-dependent response of these cells to all four chemotherapeutic agents upon the addition of 1 μM AZD6738, as assessed by CellTiter-Glo luminescent cell viability assay after 4 days of treatment (**Figure 4.18**). Additive effect was seen in several dose combinations involving lower doses of fludarabine and bendamustine. However, highly synergistic interaction was evident with dose combinations involving higher chemotherapy doses that produce 50% cell killing or above, across all four drug combinations (**Figure 4.19**; **Table 4.2**). Of note, CII-*GFP*sh cells were sensitive to chemotherapy. However, addition of AZD6738 to chemotherapeutic agents led to further sensitisation (**Figure 4.20A**). AZD6738 was synergistic with chlorambucil, 4HC and bendamustine but mostly additive with fludarabine in CII-*GFP*sh CLL cells (**Figure 4.20B; Table 4.3**).

I then proceeded to evaluate these findings in DDR-defective primary CLL cells co-cultured with CD40L/IL-21. AZD6738 (at 1 μM) enhanced sensitivity to (**Figure 4.21**) and synergised with (**Figure 4.22**; **Table 4.4**) chlorambucil, fludarabine and 4HC in primary CLL samples with defective *ATM* or *TP53* (n=6) across a range of chemotherapy doses, as assessed by flow cytometric analysis of cell viability on the proliferating CLL cell population. However, due to pro-survival properties of the co-culture system the sensitisation effect in primary CLL cells (**Figure 4.21**) was less profound than in CLL cell lines (**Figure 4.18**). In order to assess the interaction of AZD6738 with chemotherapeutic agents across a broader range of cytotoxic effect, I additionally carried out combination experiments with 3 μM AZD6738 on these CLL samples. The interaction was highly synergistic for these drug combinations (**Table 4.4**).

Interestingly, in these primary CLL samples I also found additive to synergistic interaction between AZD6738 and cytotoxic doses of ibrutinib (Herman et al., 2011), as

Figure 4.18

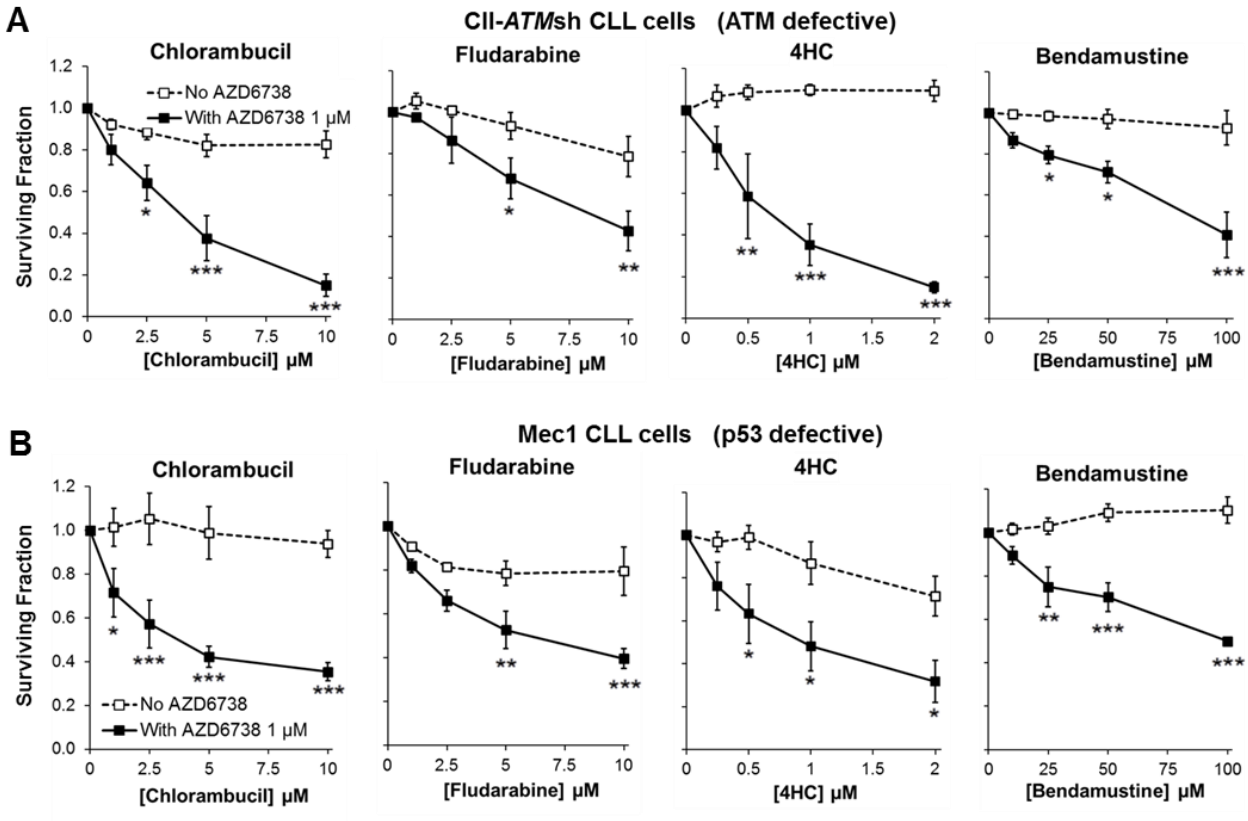

ATR inhibition sensitises CII-*ATM*sh and Mec1 CLL cells to cytotoxic chemotherapy. **(A)** CII-sh*ATM* and **(B)** Mec1 cells were treated with chlorambucil, fludarabine, 4-hydroperoxycyclophosphamide (4HC) or bendamustine with or without co-administration of AZD6738 (1 μM). Viability was assessed 96 hours later by the CellTiter-Glo assay. Surviving fraction is expressed relative to untreated controls for chemotherapy treatment alone (no AZD6738) and relative to 1 μM AZD6738 monotherapy for the co-treated samples. Addition of AZD6738 significantly enhanced sensitivity of CII-sh*ATM* and Mec1 cells to cytotoxic chemotherapeutic agents. Data is displayed as mean ± SEM of triplicate experiments. Statistical significance was determined using two-way ANOVA with Bonferroni post-hoc analysis. Statistical significance vs no AZD6738 is indicated by *p<0.05, **p<0.01 and ***p<0.001.

Figure 4.19

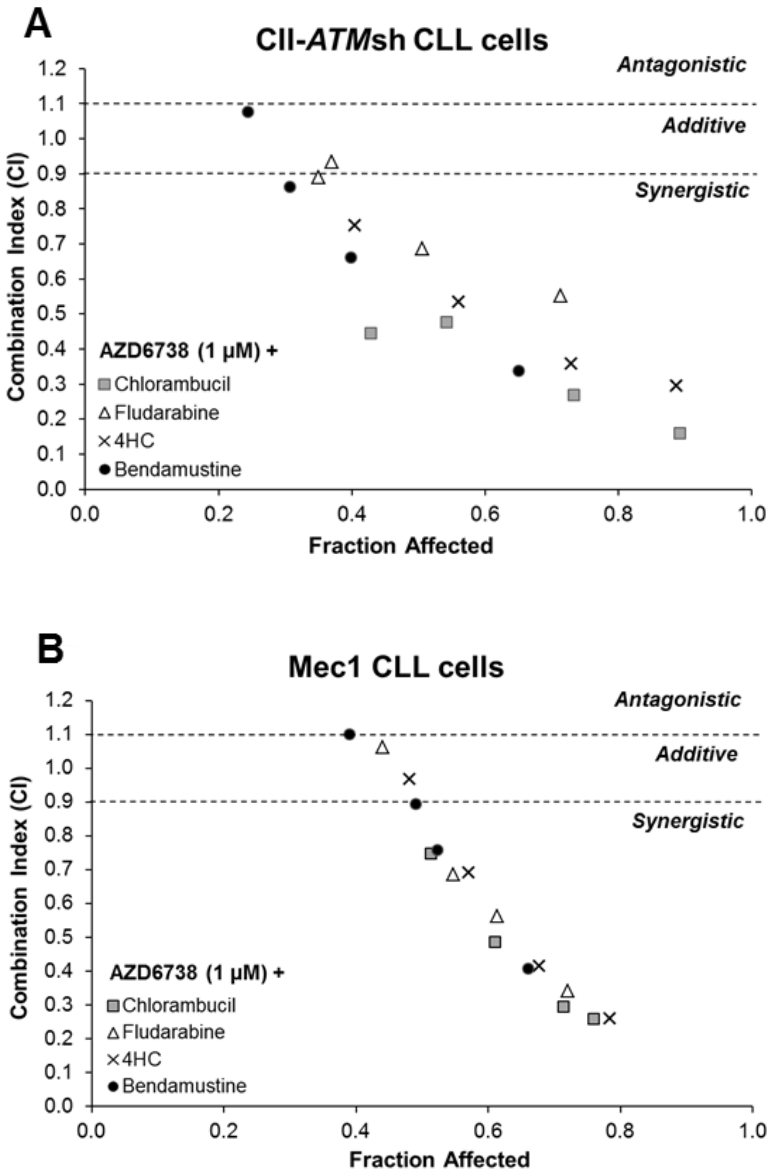

ATR inhibition synergises with cytotoxic chemotherapy in CII-*ATM*sh and Mec1 CLL cells. AZD6738 is synergistic with chlorambucil, fludarabine, 4HC and bendamustine in **(A)** CII-sh*ATM* and **(B)** Mec1 cells across a range of effective drug doses. Combination indices (CI) were calculated using the median-effect method. Each point represents the mean CI value obtained from 3 independent experiments plotted against the corresponding affected fraction that is expressed relative to untreated controls. CI < 0.9 represents synergism, CI 0.9-1.1 represents additive effect, and CI > 1.1 represents antagonism. The actual values are presented in Table 4.2.

Table 4.2. Combination indices of AZD6738 (1 μM) with cytotoxic chemotherapy in CII-*ATM*sh and Mec1 cells

		CII-*ATM*sh			Mec1		
Drug combined with AZD6738	**Dose, μM**	**Fraction Affected**	**Combination Index (mean ± SEM)**	**Synergism**	**Fraction Affected**	**Combination Index (mean ± SEM)**	**Synergism**
Chlorambucil	1	0.43	0.45 ± 0.16	+++	0.51	0.75 ± 0.16	++
	2.5	0.54	0.48 ± 0.09	+++	0.61	0.49 ± 0.11	+++
	5	0.73	0.27 ± 0.14	++++	0.71	0.29 ± 0.03	++++
	10	0.89	0.16 ± 0.08	++++	0.76	0.26 ± 0.03	++++
Fludarabine	1	0.35	0.89 ± 0.29	+	0.44	1.06 ± 0.14	±
	2.5	0.37	0.93 ± 0.28	±	0.55	0.69 ± 0.14	+++
	5	0.51	0.69 ± 0.17	+++	0.61	0.56 ± 0.18	+++
	10	0.71	0.55 ± 0.13	+++	0.72	0.34 ± 0.07	+++
4-hydroperoxy-cyclophosphamide	0.25	0.40	0.75 ± 0.33	++	0.48	0.97 ± 0.30	±
	0.5	0.56	0.53 ± 0.26	+++	0.57	0.69 ± 0.28	+++
	1	0.73	0.36 ± 0.15	+++	0.68	0.42 ± 0.14	+++
	2	0.89	0.30 ± 0.07	++++	0.78	0.26 ± 0.10	++++
Bendamustine	10	0.24	1.08 ± 0.15	±	0.39	1.10 ± 0.08	±
	25	0.31	0.86 ± 0.15	+	0.49	0.89 ± 0.29	+
	50	0.40	0.66 ± 0.15	+++	0.52	0.76 ± 0.18	++
	100	0.65	0.34 ± 0.11	+++	0.66	0.41 ± 0.01	+++

++++, strong synergism; +++, synergism; ++, moderate synergism; +, slight synergism; ±, additive

Figure 4.20

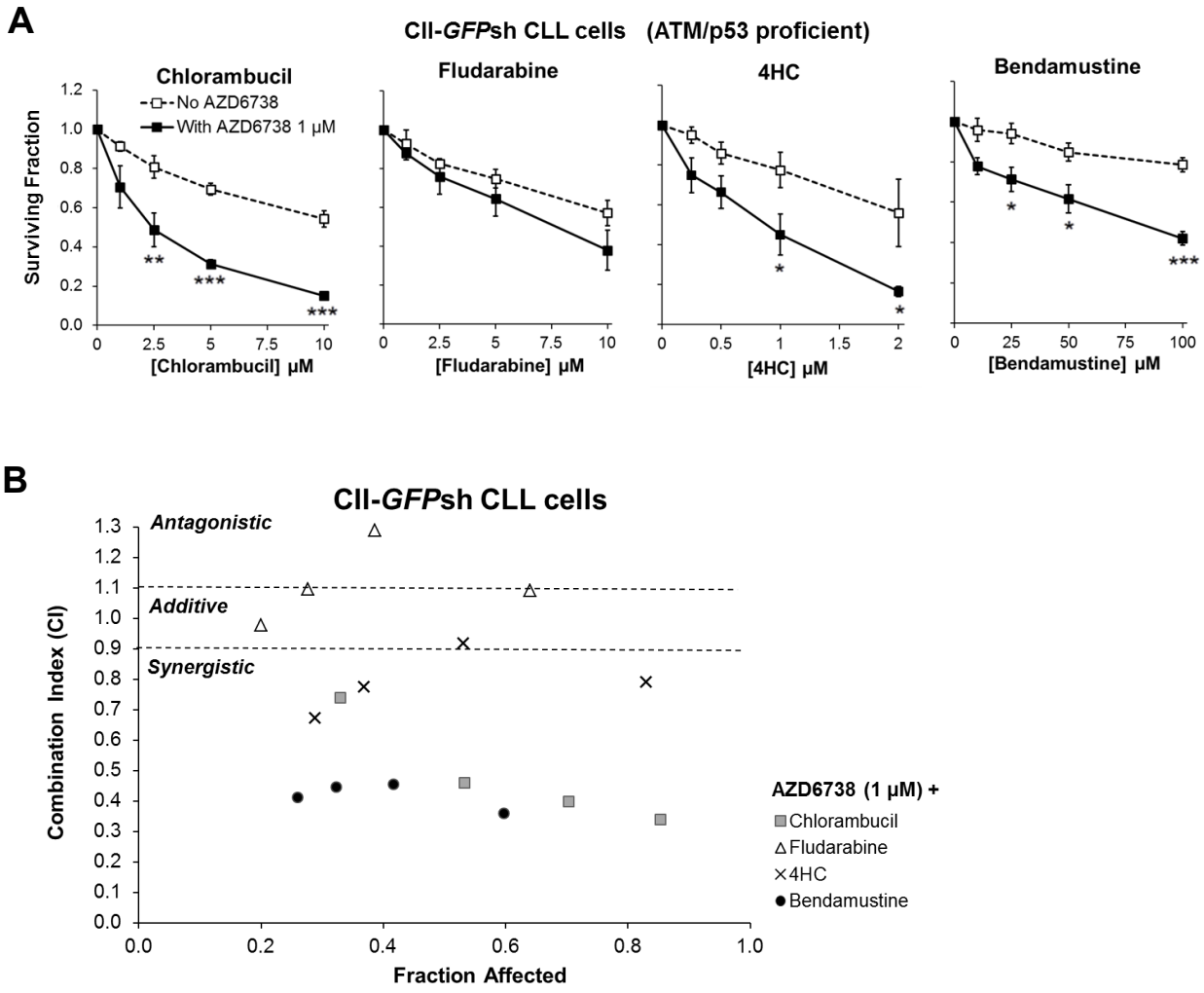

AZD6738 is synergistic with chlorambucil, 4-hydroperoxycyclophosphamide and bendamustine in CII-*GFP*sh CLL cells. (A) CII-sh*GFP* cells were treated with chlorambucil, fludarabine, 4-hydroperoxycyclophosphamide (4HC) or bendamustine with or without co-administration of AZD6738 (1 μM). Viability was assessed 96 hours later by the CellTiter-Glo assay. Surviving fraction is expressed relative to untreated controls for chemotherapy treatment alone (no AZD6738) and relative to 1 μM AZD6738 monotherapy for the co-treated samples. Addition of AZD6738 significantly enhanced the sensitivity of CII-sh*GFP* cells to cytotoxic chemotherapeutic agents. Data is displayed as mean ± SEM of triplicate experiments. Statistical significance was determined using two-way ANOVA with Bonferroni post-hoc analysis. Statistical significance vs no AZD6738 is indicated by *p<0.05, **p<0.01 and ***p<0.001. **(B)** AZD6738 is synergistic with chlorambucil, 4HC and bendamustine and mostly additive with fludarabine in CII-*GFP*sh cells. Combination indices (CI) were calculated using the median-effect method. Each point represents the mean CI value obtained from 3 independent experiments plotted against the corresponding affected fraction that is expressed relative to untreated controls. CI < 0.9 represents synergism, CI 0.9-1.1 represents additive effect, and CI > 1.1 represents antagonism. The actual values are presented in Table 4.3.

Table 4.3. Combination indices of AZD6738 (1 μM) with cytotoxic chemotherapy in CII-*GFP*sh cells

Drug combined with AZD6738	Dose, μM	Fraction Affected	Combination Index (mean ± SEM)	Synergism
Chlorambucil	1	0.33	0.74 ± 0.42	++
	2.5	0.53	0.46 ± 0.14	+++
	5	0.70	0.40 ± 0.03	+++
	10	0.85	0.34 ± 0.03	+++
Fludarabine	1	0.20	0.98 ± 0.24	±
	2.5	0.28	1.10 ± 0.27	±
	5	0.39	1.29 ± 0.36	−−
	10	0.64	1.09 ± 0.33	±
4-hydroperoxy-cyclophosphamide	0.25	0.29	0.67 ± 0.10	+++
	0.5	0.37	0.78 ± 0.10	++
	1	0.53	0.92 ± 0.22	±
	2	0.83	0.79 ± 0.04	++
Bendamustine	10	0.26	0.41 ± 0.09	+++
	25	0.32	0.45 ± 0.10	+++
	50	0.42	0.45 ± 0.10	+++
	100	0.60	0.36 ± 0.04	+++

−−, moderate antagonism. All other abbreviations are explained in Table 4.2.

Figure 4.21

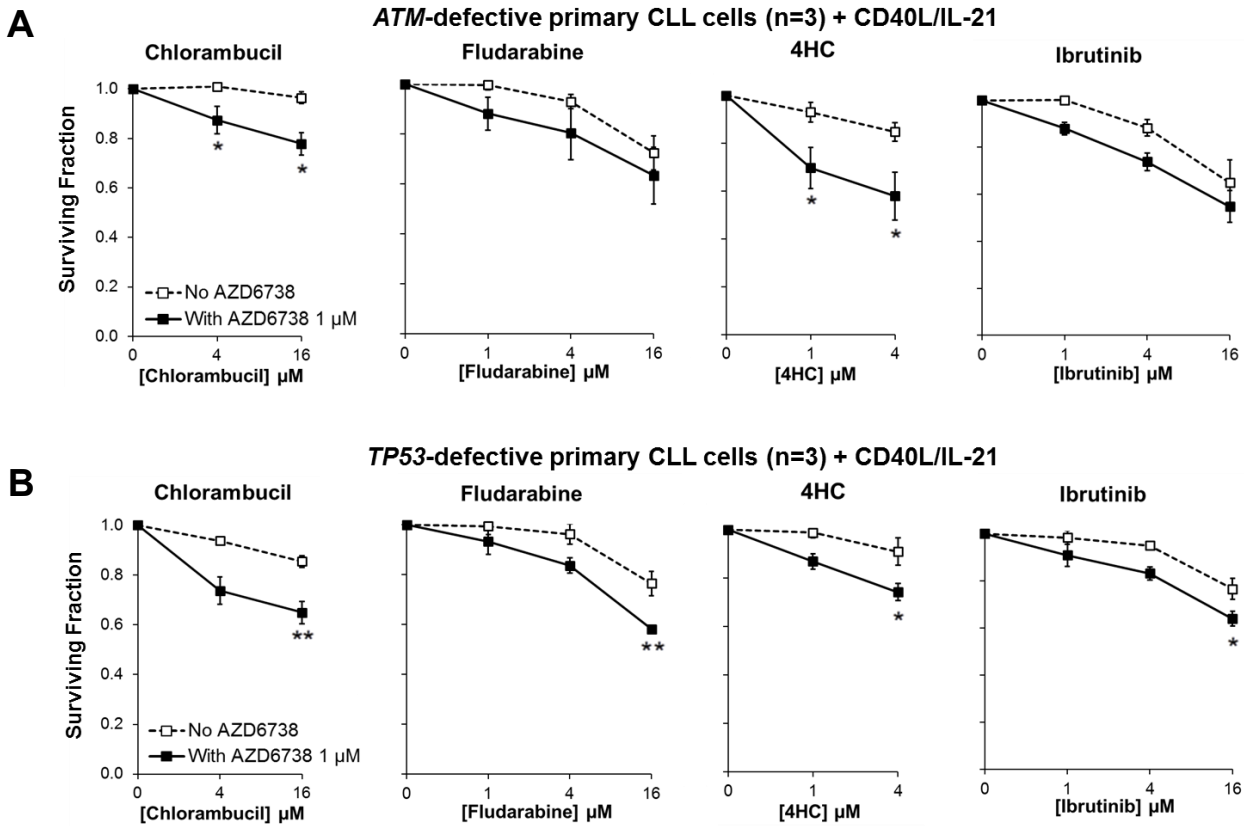

ATR inhibition sensitises both in *ATM*-defective and *TP53*-defective primary CLL cells to existing therapeutic agents. CFSE-labelled primary CLL cells with **(A)** *ATM* (CLL22, CLL23, CLL24) or **(B)** *TP53* defect (CLL29, CLL31, CLL32) co-cultured with CD40L/IL-21 were treated with chlorambucil, fludarabine, 4-hydroperoxycyclophosphamide (4HC) or ibrutinib with or without co-administration of AZD6738 (1 μM). Viability was assessed after 96 hours by propidium iodide exclusion of the proliferating cell population as identified by reduction in CFSE fluorescence intensity. Surviving fraction is expressed relative to untreated controls for chemotherapy treatment alone (no AZD6738) and relative to 1 μM AZD6738 monotherapy for the co-treated samples. Addition of AZD6738 significantly enhanced sensitivity of *ATM*-defective primary CLL samples to chlorambucil and 4HC, and *TP53*-defective primary CLL samples to these therapies and also to fludarabine and ibrutinib at ≥1 dose combination. Data is displayed as mean ± SEM. Statistical significance was determined using two-way ANOVA with Bonferroni post-hoc analysis. Statistical significance vs no AZD6738 is indicated by *p<0.05, **p<0.01 and ***p<0.001.

Figure 4.22

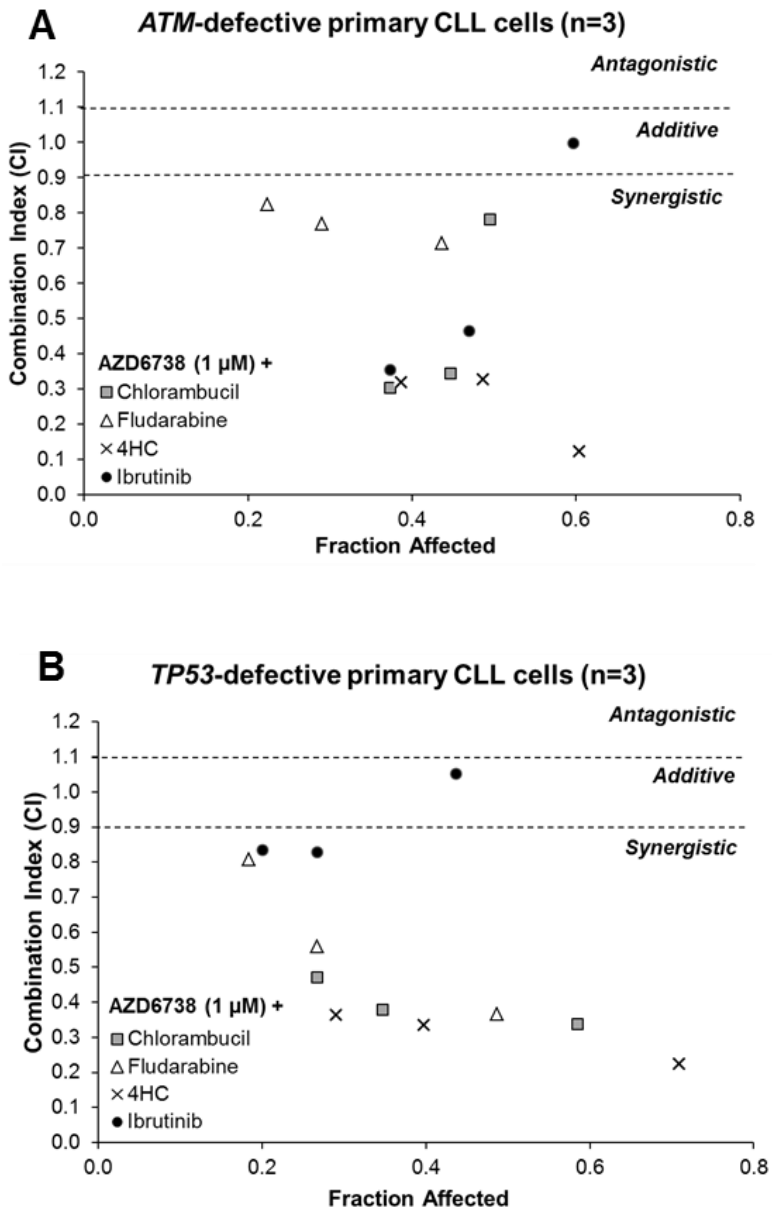

ATR inhibition synergises with existing therapeutic agents both in *ATM*-defective and *TP53*-defective primary CLL cells. AZD6738 is synergistic with chlorambucil, fludarabine, 4HC and ibrutinib in primary CLL samples with **(A)** *ATM* or **(B)** *TP53* defect across a range of effective drug doses. CI values were calculated using the median-effect method. Each point represents the mean CI value of 3 samples plotted against the corresponding mean affected fraction that is expressed relative to untreated controls. CI < 0.9 represents synergism, CI 0.9-1.1 represents additive effect and CI > 1.1 represents antagonism. The actual values are presented in Table 4.4.

Table 4.4. Combination indices of AZD6738 (1 or 3 μM) with cytotoxic chemotherapy or BCR signalling inhibitor in *ATM* or *TP53* defective primary CLL cells co-cultured with CD40L/IL-21

Drug combined with AZD6738		AZD6738 dose, μM	ATM-defective CLL (n=3)			*TP53*-defective CLL (n=3)		
Name	Dose, μM		Fraction Affected	Combination Index (mean ± SEM)	Synergism	Fraction Affected	Combination Index (mean ± SEM)	Synergism
Chlorambucil	4	1	0.37	0.30 ± 0.05	++++	0.27	0.47 ± 0.20	+++
	16	1	0.45	0.34 ± 0.04	+++	0.35	0.38 ± 0.17	+++
	16	3	0.50	0.78 ± 0.29	++	0.59	0.34 ± 0.08	+++
Fludarabine	1	1	0.22	0.83 ± 0.29	++	0.18	0.81 ± 0.24	++
	4	1	0.29	0.77 ± 0.27	++	0.27	0.56 ± 0.16	+++
	16	1	0.44	0.71 ± 0.21	++	0.49	0.37 ± 0.05	+++
4-hydroperoxy-cyclophosphamide	1	1	0.39	0.32 ± 0.11	+++	0.29	0.36 ± 0.11	+++
	4	1	0.49	0.33 ± 0.10	+++	0.40	0.34 ± 0.13	+++
	4	3	0.60	0.12 ± 0.02	++++	0.71	0.22 ± 0.07	++++
Ibrutinib	1	1	0.37	0.36 ± 0.00	+++	0.20	0.84 ± 0.27	++
	4	1	0.47	0.46 ± 0.04	+++	0.27	0.83 ± 0.20	++
	16	1	0.60	1.00 ± 0.13	±	0.44	1.05 ± 0.17	±

All abbreviations are explained in Table 4.2.

shown in **Figure 4.21**, **Figure 4.22** and **Table 4.4**. I addressed mechanisms behind the AZD6738-ibrutinib interaction. At higher doses, I postulated that this could be due to the off-target effects of ibrutinib on the ATR pathway, and, vice versa, to the off-target effects of AZD6738 on BCR signalling. I therefore assessed the impact of ibrutinib on Chk1 phosphorylation and the impact of AZD6738 on Erk and Syk phosphorylation in primary CLL cells. I found a dose-dependent reduction in HU-induced Chk1 phosphorylation with ibrutinib (**Figure 4.23A**), as well as a modest dose-dependent reduction in Erk and Syk phosphorylation with AZD6738 (**Figure 4.23B**). The former is supported by documented data showing 24% inhibition of Chk1 kinase activity with 0.1 μM ibrutinib (Medical Research Council International Centre for Kinase Profiling; Kinase Profiling Inhibitor Database http://www.kinase-screen.mrc.ac.uk/screening-compounds/349403). These findings are consistent with the above hypothesis, suggesting that the off-target effects of AZD6738 and ibrutinib may account for the potentiating effect at higher dose combinations involving 4 μM or 16 μM ibrutinib.

I also assessed whether distinct CLL populations were targeted by AZD6738 and ibrutinib respectively. I induced CFSE-labelled primary CLL cells to proliferate and treated them with AZD6738 or ibrutinib for 4 days prior to flow cytometric analysis. Viable (PI negative) CLL cells were gated and analysed for their CFSE content. I found that AZD6738 targeted primarily cycling CLL cells for killing, indicated by a dose-dependent reduction in the cycling population as a percentage of the remaining viable cells. Ibrutinib, on the other hand, targeted both the cycling and non-cycling populations as evidenced by minimal dose-dependent change in the composition of the viable population (**Figure 4.24**). Thus, the potentiating interaction between AZD6738 and ibrutinib at lower dose combinations involving 1 μM ibrutinib could possibly be accounted for by the limited overlap in the cellular populations targeted by these two agents.

Finally, the AZD6738-chlorambucil combination was assessed in a patient-derived CLL murine xenotransplantation model with del(11q) and *ATM* mutation p.I407T (CLL25). In

Figure 4.23

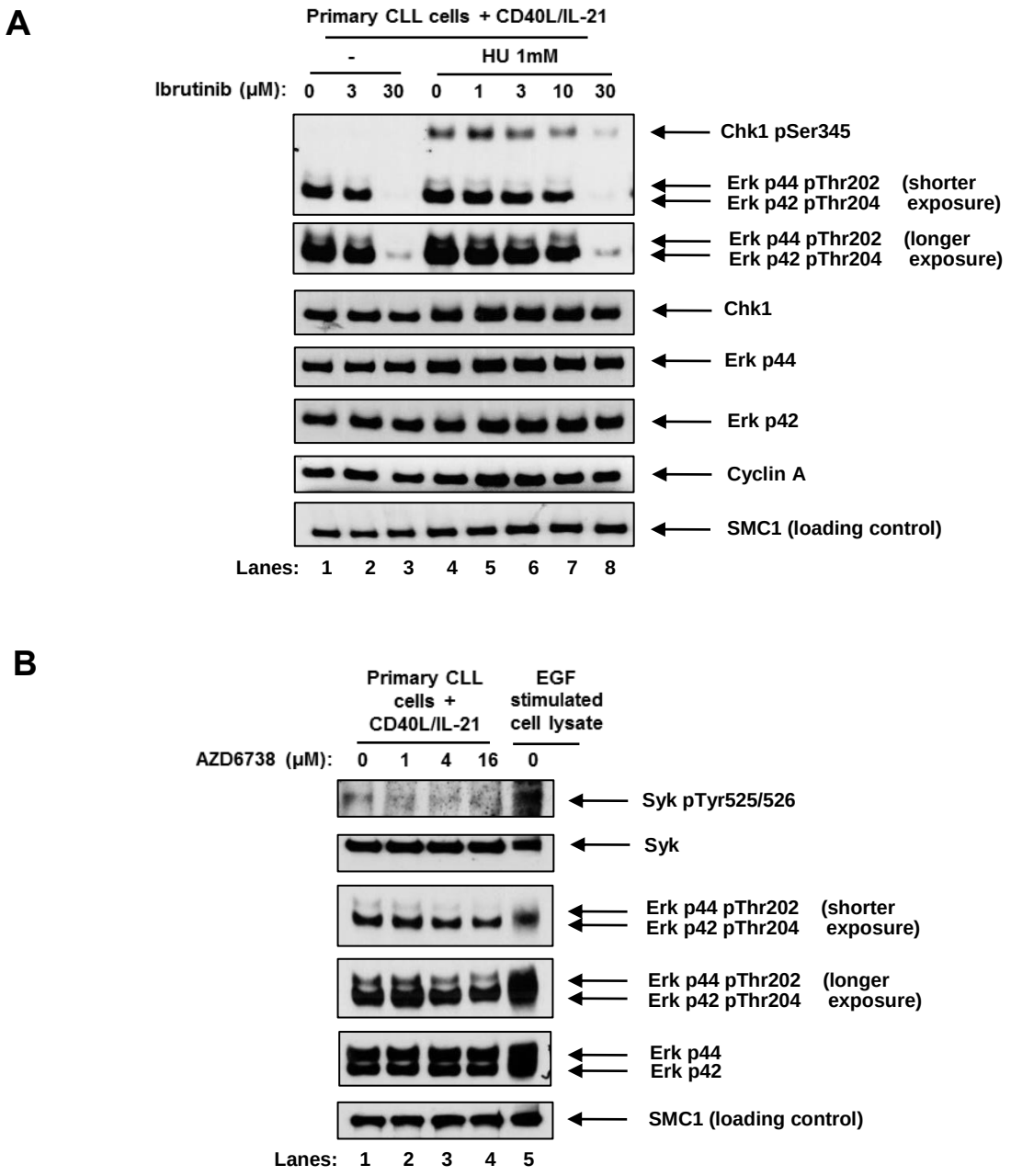

The additive to synergistic interaction between AZD6738 and ibrutinib at higher dose combinations may be attributable to the off-target effect of ibrutinib on the ATR pathway and to the off-target effect of AZD6738 on BCR signalling. (A) Primary CLL cells were pre-treated with escalating doses of ibrutinib for 1 hour before exposure to HU, and incubated for a further 5 hours prior to cell lysis and analysis using Western blotting. At ibrutinib doses >3 μM, there was a dose-dependent reduction in HU-induced Chk1 phosphorylation with ibrutinib. Cyclin A expression is a marker of proliferating cells. **(B)** Primary CLL cells were treated with escalating doses of AZD6738 for 5 hours prior to cell lysis. A small, dose-dependent reduction in Erk and Syk phosphorylation was seen with AZD6738. EGF; epidermal growth factor.

Figure 4.24

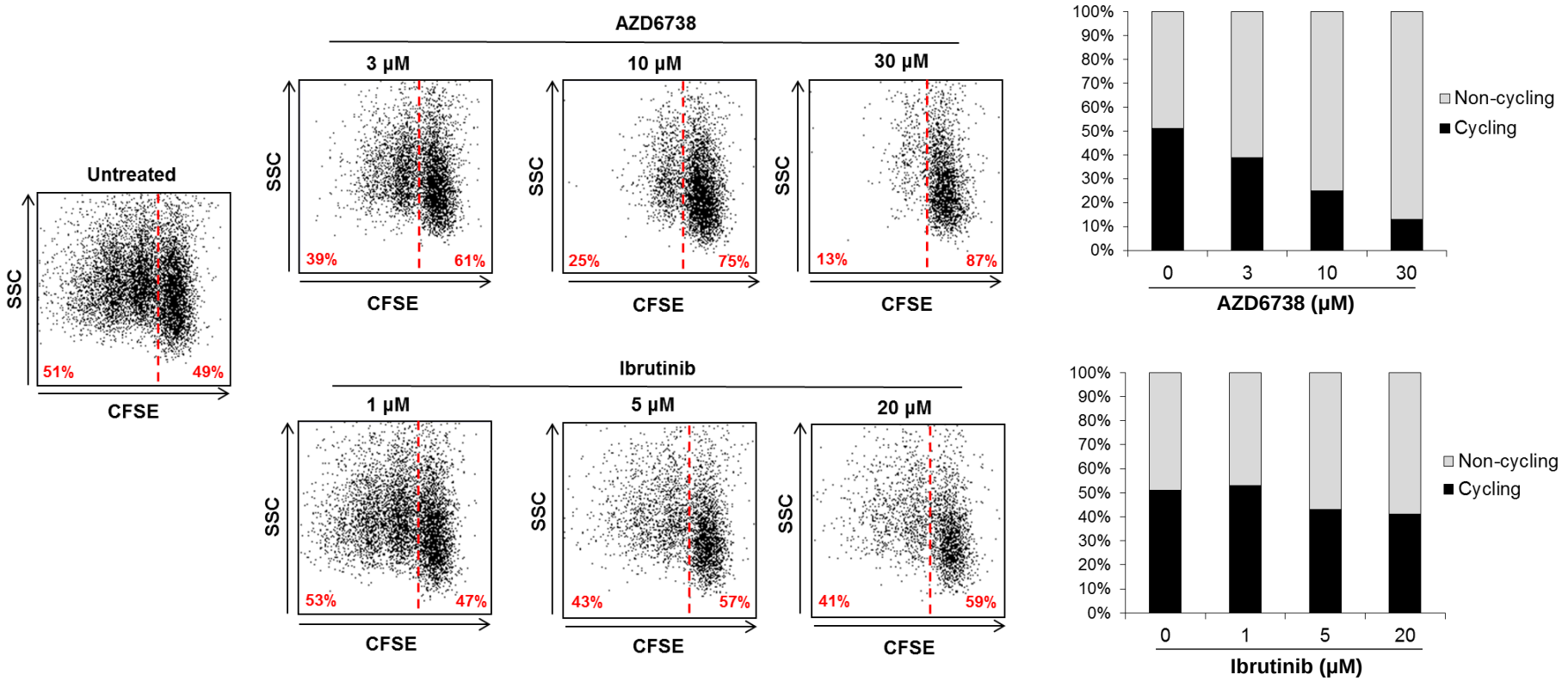

AZD6738 targets specifically cycling CLL cells while ibrutinib targets both cycling and non-cycling populations. CFSE-labelled primary CLL cells were induced to proliferate and treated with AZD6738 or ibrutinib for 96 hours prior to flow cytometric analysis. Viable (PI negative) cells were gated and analysed for their CFSE content. Results from a representative sample (CLL36) are displayed. On the flow cytometric plots, cells to the left of the dotted line represent the cycling population whereas those to the right were non-cycling. Relative ratios of cycling and non-cycling cells are provided at the bottom of the flow cytometric plots and summarized in stacked column graphs. AZD6738 targeted cycling CLL cells for killing, indicated by a dose-dependent reduction in the cycling population as a percentage of the remaining viable cells. Ibrutinib targeted both the cycling and non-cycling populations as evidenced by minimal dose-dependent change in the composition of the viable population. SSC, side scatter.

experiments carried out by Dr Nicholas Davies, twenty engrafted mice were randomised into 4 treatment arms: AZD6738, chlorambucil, the AZD6738-chlorambucil combination or vehicle (n=5 in each arm). AZD6738 monotherapy resulted in significant reduction in tumour load. Moreover, combination treatment yielded significantly greater reductions in tumour load than chlorambucil monotherapy (**Figure 4.25**). Collectively, these results support the combined use of ATR inhibitor with a range of existing therapeutic agents for CLL.

Figure 4.25

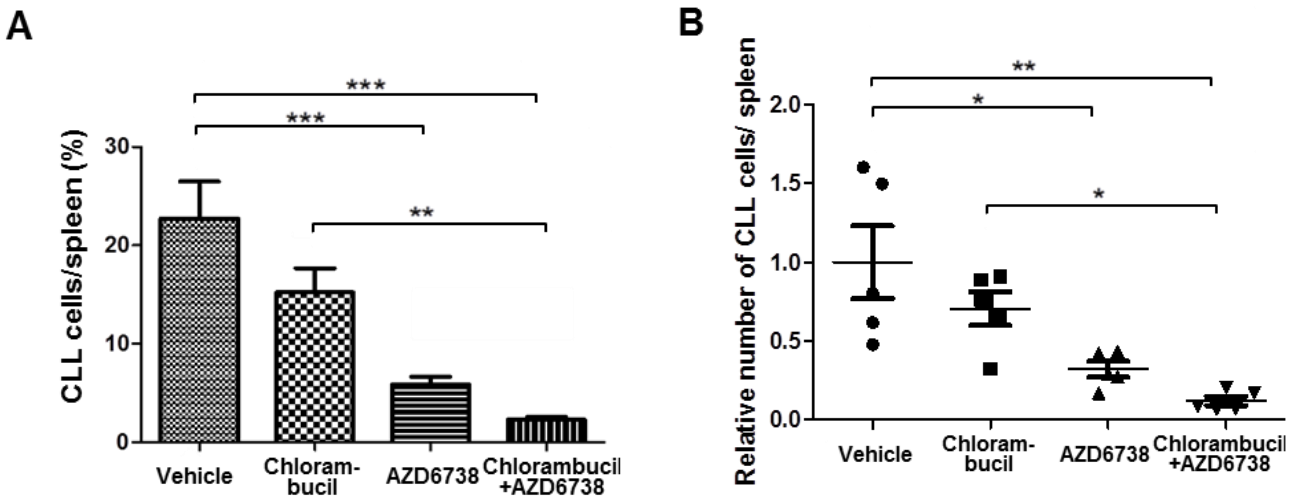

ATR inhibition potentiates chlorambucil in *ATM*-defective primary CLL xenograft models. A primary CLL xenograft (CLL25) with a biallelic *ATM* defect (del(11q) and 1407I>T *ATM* mutation) was randomised into four treatment arms (n=5 each): AZD6738, chlorambucil, AZD6738-chlorambucil co-treatment and vehicle. AZD6738 treatment alone or in combination with chlorambucil significantly reduced tumour load relative to vehicle, and the addition of AZD6738 to chlorambucil led to a significantly greater reduction in tumour load relative to chlorambucil monotherapy. The relative number of CLL cells in (B) was normalised to vehicle-treated controls. Data is displayed as mean ± SEM. Statistical significance was determined using two-way ANOVA with Bonferroni post-hoc analysis, and is indicated by *p<0.05, **p<0.01 and ***p<0.001.

4.2. Discussion

4.2.1. Cytotoxic mechanism underpinning ATR inhibition in CLL

As discussed earlier, cellular DDR is regulated by several pathways, involving proteins such as ATM, ATR and DNA-PK. Tumorigenesis is associated with a pervasive corruption of one or more of these pathways, often through mutation or deletion of key DNA repair or regulatory proteins, conferring on malignant cells a survival advantage, avoidance of apoptosis and chemoresistance (Jackson and Bartek, 2009). However, the subversion of normal DDR mechanisms can render tumour cells susceptible to further DNA insults, the accumulation of which may become incompatible with survival and results in mitotic catastrophe (Castedo et al., 2004; Vitale et al., 2011). Moreover, the disruption of a DNA repair pathway constrains tumour cells to rely on collateral repair pathways to maintain genome stability, thereby exposing them to a vulnerability that can be amenable to therapeutic targeting (O'Connor, 2015).

In this study, I produced experimental data demonstrating the pre-clinical efficacy of ATR inhibition in CLL with *TP53* or *ATM* defects. While a number of novel agents exhibit considerable activity against *TP53* defective CLL, ATR inhibition is unique in its ability to provide *specific* targeting of *TP53* defective and *ATM* defective CLL cells. Results detailed in the preceding section provide insight into the cytotoxic mechanism underpinning ATR inhibition in CLL, which is consistent with our current understanding of the role of ATR in resolving replication stress (**Figure 4.26A**; section 1.4.2). When ATR function is abolished, stalled replication forks with persistent ssDNA are susceptible to fork breakage and collapse resulting in the accumulation of partially replicated DNA fragments with double-stranded ends that have become disengaged from the replication template (**Figure 4.26B**). These DNA fragments require ATM-mediated HRR for repair and re-engagement with the

Figure 4.26

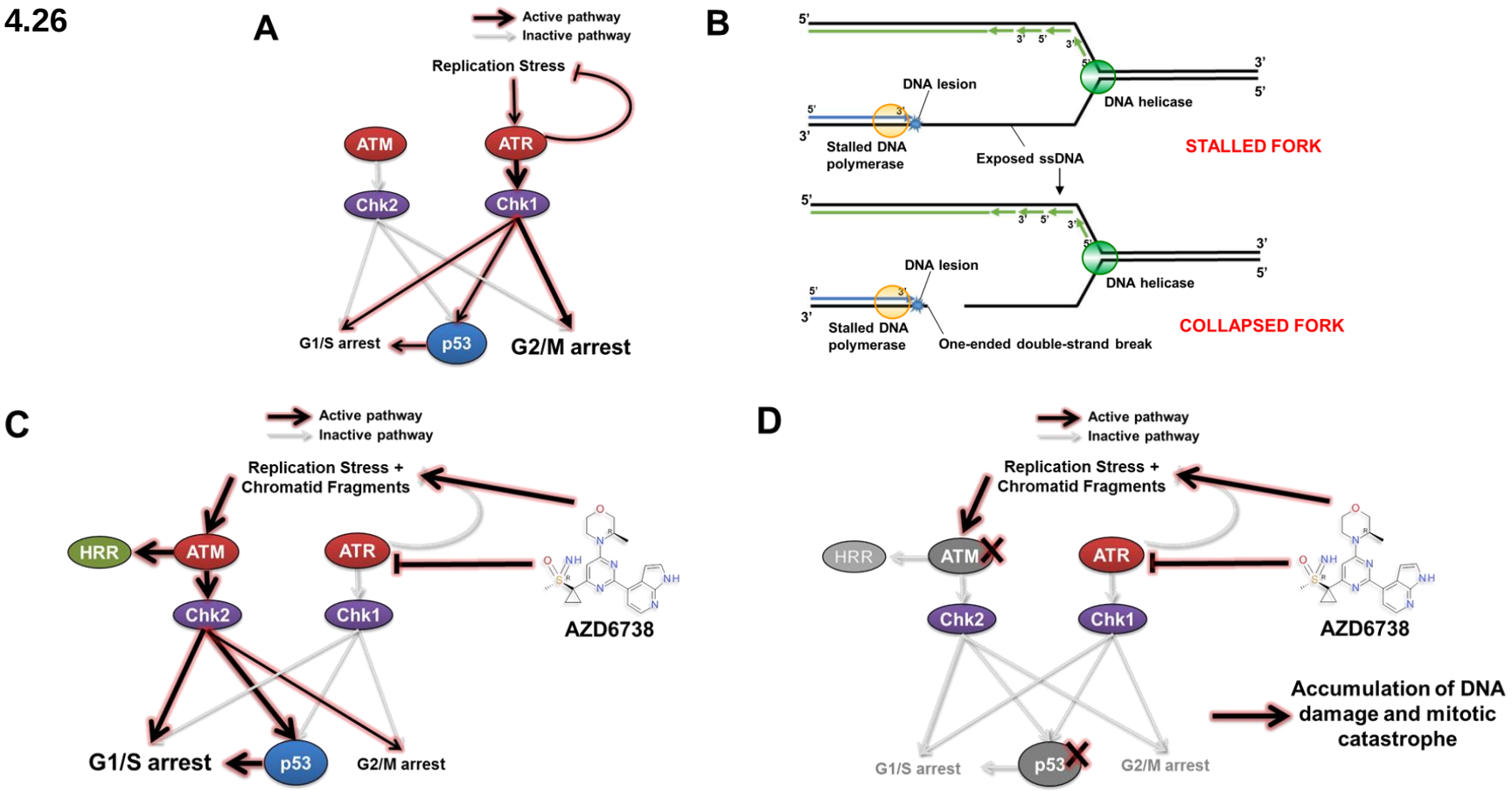

Figure 7. A model for synthetic lethality in CLL cells with ATM or p53 deficiency by inhibition of ATR. ATM and ATR are master regulators of DDR, with ATM being activated in response to DNA double-strand breaks, and ATR in response to replication stress. **(A)** Activation of the ATR pathway leads to cell cycle arrest mediated primarily through the G2/M checkpoint, and repair of stalled replication forks. This leads to the resolution of replication stress. **(B-C)** Inhibition of ATR by AZD6738 directly induces replication stress by slowing and stalling replication forks. The inability of CLL cells to resolve stalled forks as a result of suppressed ATR signalling leads to collapse of stalled replication forks into fragmented, partially-replicated sister chromatids with free DNA double-stranded ends (DSEs) that necessitate repair through the ATM/p53 pathway. This involves cell cycle arrest mediated primarily through the G1/S checkpoint and HRR. **(D)** In cells with defective ATM or p53, inhibition of ATR by AZD6738 results in an intolerable accumulation of unrepaired DNA damage. This arises from impaired HRR due to defective ATM and/or impaired cell cycle regulation resulting from combined loss of functional ATR and ATM/p53.

replication template. Additionally, because the G2/M checkpoint is lost as a consequence of ATR inhibition, functional p53 and ATM becomes required for G1/S cell cycle arrest to permit HRR-directed repair of collapsed forks (**Figure 4.26C**). In the absence of functional ATM, NHEJ mediated by DNA-PK can ligate the double-stranded ends of two DNA fragments. However, unlike HRR which is a high fidelity repair process, NHEJ is a low fidelity and error-prone repair mechanism. Therefore, in ATM defective CLL cells, NHEJ repair of collapsed forks occur at the expense of potential sequence deletions and aberrant chromosomal translocations that may arise during the repair process. Hence, CLL cells with defective p53 or ATM accumulate collapsed forks and damaged DNA, manifested by an accumulation of DNA proteins γH2AX and 53BP1 which appear as foci. The loss of both the G1/S and G2/M cell cycle checkpoints in turn permits subsequent unrestricted entry into mitosis, resulting in mitotic catastrophe (**Figure 4.26D**).

This mechanistic model accounts for the selective cytotoxicity of ATR inhibition for CLL cells with *TP53* or *ATM* defects. It is noteworthy to highlight the mechanistic difference between ATR inhibitor therapy and conventional chemotherapy. Both therapeutic modalities exert their cytotoxic effect through the induction of DNA damage, but ATR inhibition additionally inhibit the repair and regulatory processes that *TP53* and *ATM* defective cells are exceptionally dependent on, thus rendering these cells exquisitely sensitive to DNA damage.

4.2.2. Impact of ATR inhibition on proliferating vs quiescent CLL cells

Importantly, experimental results from this study show that ATR inhibition is capable of circumventing the protective effect of the microenvironment, which often hinders effective clearance of genomically unstable, proliferating CLL populations. This is evidenced by the ability of AZD6738 to overcome the pro-survival signals provided by the CD40L/IL-21 co-culture system that mimics interaction of CLL cells with T cells in proliferation centres

(**Figure 4.8**), and, in xenograft experiments, by the loss of tumour burden in murine spleens upon treatment with AZD6738 (**Figure 4.10**).

It is also important to note that ATR inhibition targets specifically the proliferating CLL population (**Figure 4.8**; **Figure 4.9**). At any one time only a fraction of CLL cells are proliferating *in vivo*. However, aggressive CLL associated with relapsed/refractory disease, for which the use of ATR inhibition is the most appropriate, are typically associated with higher proliferation rates. For instance, in relapsed/refractory cases up to 68% of CLL cells were found to be newly synthesised over an 84 day period within *in vivo* isotope labelling studies, equivalent to a proliferation rate of 1.76% per day (Messmer et al., 2005). Isotope labelling studies also showed that cell proliferation is ongoing in cells recently released into the circulation and as such they are also susceptible to ATR inhibition (Calissano et al., 2009). Furthermore, although only a proportion of CLL cells are proliferating at any given time, it is the proliferating CLL population that is the most genomically unstable, because new genomic changes arise during DNA replication. Expansion of novel, deleterious variants could result in clonal evolution. This argues for the need to target specifically the proliferating population, particularly given that this population is protected by the pro-survival microenvironmental signals as mentioned above. Finally, as studies with BCR signalling inhibitors have demonstrated, CLL cells that are driven out of proliferating centres contribute to a redistribution lymphocytosis of quiescent cells that is of no major clinical significance (Woyach et al., 2014b). CLL cells in peripheral circulation that re-enter the proliferative compartment would again be targetable by ATR inhibition.

4.2.3. Markers of sensitivity to ATR inhibitor in CLL

Interestingly, whereas *TP53* or *ATM* defective primary CLL PBMCs were uniformly and substantially more sensitive to ATR inhibition than healthy donor PBMCs, *TP53*/*ATM*-

wild-type primary CLL cells displayed variable sensitivity towards ATR inhibition (**Figure 4.8**). There are several potential explanations for this finding.

Firstly, the acquisition of alternative DDR defects that were unknown or not specifically characterised in this study could render some CLL patients sensitive to ATR inhibition even in the absence of defective *TP53* or *ATM*. For instance, cyclin E promotes G1/S cell cycle progression and hence contributes to a heighted level of cellular replication stress. Cyclin E is expressed at a higher level in CLL cells, particularly the ZAP-70 positive ones, compared to non-malignant B lymphocytes (Bogner et al., 2006; Decker et al., 2004). Its overexpression has been reported to exacerbate the effects of ATR inhibition (Toledo et al., 2011).

In addition, several studies have demonstrated synthetic lethality between ATR inhibition and other DDR defects. ATR inhibition was lethal in ovarian cancer cell lines with Breast cancer type 1 susceptibility protein (BRCA) or Rad51 deficiency, both of which are essential HRR proteins (Krajewska et al., 2015; Middleton et al., 2015; Yazinski et al., 2017). Deficiency in the DNA repair proteins XRCC1, ERCC1, POLD1, PRIM1 and the nucleosome remodelling protein AT-rich interaction domain 1A (ARID1A) has also been shown to enhance sensitivity to ATR inhibition (Hocke et al., 2016; Mohni et al., 2014; Sultana et al., 2013). XRCC1 is a protein involved in base excision repair and the single strand break repair pathway, whereas ERCC1 mediates the repair of several types of DNA lesions including bulky adducts, DSBs and inter-strand crosslinks, and facilitates the separation of sister chromatids during anaphase. POLD1 and PRIM1, on the other hand, are involved in DNA replication synthesis. Finally, ARID1A deficiency leads to disrupted topoisomerase localisation and cell cycle progression, thus imposing on cancer cells a dependence on the ATR signalling pathway (Williamson et al., 2016). Recurrent mutations in *ARID1A* have been reported in CLL, and loss of function mutations may lead to ARID1A deficiency (Puente et al., 2015). Although not recognised as CLL genomic drivers, mutations of all other

aforementioned genes have been reported in individual CLL cases (Landau et al., 2015; Puente et al., 2015).

Secondly, the variability in sensitivity to ATR inhibition could be due to different amounts of endogenous DNA damage in each sample, reflecting varying degrees of genomic instability. For instance, Myc, a major driver of replication stress (Cottini et al., 2015; Murga et al., 2011), is variably expressed in CLL, and higher levels correlate with progressive disease (Zhang et al., 2010). ATR inhibition may therefore potentially be most useful in heavily pre-treated relapsed/refractory patients, where higher levels of genomic instability could be due, in part, to enhanced replication stress. It remains to be established whether replication stress is associated with karyotypic and genomic complexity, as well as the emergence of subclonal driver mutations and clonal evolution in CLL.

Finally, Flynn *et al* has recently reported on the hypersensitivity to ATR inhibition of cancer cells that are reliant on a mechanism of telomere maintenance known as alternative lengthening of telomeres (ALT), whereby telomeres are elongated through recombination (Flynn et al., 2015). The absence of ATR leads to abrogation of ALT, compromising telomere stability in ALT-dependent cancer cells. This results in DNA damage, telomere loss as well as selective lethality of these cells. Alternative lengthening of telomeres has been reported in CLL cells (Damle et al., 2005), and could possibly provide an additional mechanism accounting for their sensitivity to ATR inhibition.

Further work is required to explore these hypotheses and identify markers of sensitivity to ATR inhibition in CLL other than *TP53* or *ATM* defects. With respect to *TP53* or *ATM* defects, the specificity of ATR inhibition for these lesions could allow alteration of the subclonal landscape in favour of less genomically unstable DDR-proficient subclones, which are less susceptible to clonal evolution, thus reducing the likelihood of therapeutic resistance or disease relapse. The specificity of ATR inhibition for *TP53*-defective CLL cells may possibly also reduce the likelihood of Richter's transformation, since *TP53* defects,

alongside Myc and *CDKN2A* abnormalities, as well as *NOTCH* mutations and trisomy 12, have been implicated in this process (Chigrinova et al., 2013; Fabbri et al., 2013; Rossi et al., 2011).

4.2.4. Potential toxicity and tolerability of ATR inhibition

Although the *in vivo* toxicity profile and long-term effects of AZD6738 remain to be established in a clinical setting, it is important to note the lack of detrimental effect on normal tissues reported in mice subjected to ATR suppression to 10% of its normal levels (Schoppy et al., 2012). Corroborating this report, the AZD6738 dose used in the current study to achieve effective tumour load reduction in *TP53*/*ATM*-defective xenografts was well tolerated. Indeed, considerable cytotoxic activity was observed in *TP53*/*ATM*-defective CLL cell lines and primary cells at AZD6738 doses below 3 μM which produce only partial inhibition of HU-induced Chk1 phosphorylation (**Figure 4.2**; **Figure 4.3**; **Figure 4.4**), suggesting that complete abolition of ATR activity may not necessarily be required to achieve therapeutic efficacy. In addition, the discrepancy between sensitivity of *TP53*/*ATM*-defective CLL cells and healthy donor PBMCs to AZD6738 argues for the existence of a substantial therapeutic window making it suitable for clinical use (**Figure 4.8**).

Nevertheless, the long-term effects and toxicity of ATR and Chk1 inhibition are unknown. Targeting a process of such importance to genome integrity can be potentially dangerous, if it also affects healthy cells. Moreover, sublethal targeting of tumour cells with ATR inhibitors can inadvertently promote tumorigenesis and clonal evolution, as these cells accumulate replication stress and DNA damage, but escape death (Gilad et al., 2010). It is therefore of paramount importance that patients are selected for ATR inhibitor treatment according to their CLL characteristics: whether they possess features that make them differentially sensitive to ATR inhibition. By selecting patients whose CLL is hypersensitive to these inhibitors, CLL killing can be maximised while minimising treatment duration, thereby

reducing both toxicity to healthy tissues and the risk of CLL evolution and therapeutic resistance. The experimental data from my work support the use of ATR inhibition specifically in CLL patients with *TP53* or *ATM* defects, where there is distinct reliance on ATR and sensitivity to ATR inhibition.

In the ongoing clinical trial of AZD6738 for relapsed/refractory solid tumours (PATRIOT; NCT02223923), the ATR inhibitor is given daily for an indefinite period, unless disease progression or toxicity occurs (Prof. Kevin Harrington, Institute of Cancer Research, London, personal communication). In the case of CLL, however, given its primary clinical utility will be for the treatment of patients with aggressive, relapsed/refractory disease with relatively high proliferation rates, and taking into account its potent cytotoxic effect on proliferating CLL cells with *TP53* or *ATM* defects, it is anticipated that prolonged treatment may not be necessary for the majority of patients with *TP53/ATM*-defective CLL. Daily administration of AZD6738 until the attainment of a maximum response can be envisaged, which could potentially be profound and achievable over weeks to months. This is especially the case if AZD6738 is used in combination with chemotherapy or other targeted therapies, as discussed below.

4.2.5. Combination of ATR inhibitor with chemotherapy and ibrutinib

Inhibitors of ATR such as AZD6738 could potentially augment current therapies for *TP53* or *ATM* defective CLL. This is likely to be due to potentiation by chemotherapeutic agents of AZD6738-induced replication stress to which *TP53* or *ATM* defective cells are distinctively susceptible (**Figure 4.18**; **Figure 4.21**). Combination of ATR inhibitor with cytotoxic chemotherapy could provide a realistic salvage option for *TP53* or *ATM* defective patients relapsing from BCR signalling inhibitors. The synergism of AZD6738 with chlorambucil and bendamustine (**Figure 4.19**; **Figure 4.22**; **Table 4.2**; **Table 4.4**) is

particularly attractive given their milder toxicity profiles, making these combinations potentially suitable for older or frailer CLL patients.

As expected, *TP53*/*ATM* wild-type CLL cells were substantially more sensitive to chemotherapeutic agents (chlorambucil, fludarabine, 4HC and bendamustine) compared to *TP53*/*ATM* defective CLL cells (**Figure 4.18**; **Figure 4.20**). Of note, similar to *TP53*/*ATM* defective cells, AZD6738 was highly synergistic with chemotherapeutic agents in *TP53*/*ATM* wild-type CLL cells, with the exception of fludarabine, where an additive effect was seen (**Figure 4.20; Table 4.3**). As with their DDR defective counterparts, the synergistic interaction between AZD6738 and chemotherapy in *TP53*/*ATM* wild-type cells may be due to the potentiation of AZD6738 induced replication stress by chemotherapeutic agents. In the presence of high levels of replication stress and DNA damage following combined treatment, the likely sequelae in these cells would be the induction of p53-mediated apoptosis rather than cell cycle arrest. All in all, the addition of AZD6738 renders ATM/p53 proficient and deficient cells equally sensitive to chemotherapeutic agents, as reflected by a similar fraction of cells affected (<10% difference among CII-*GFP*sh, CII-*ATM*sh and Mec1 cells) at the higher dose combinations (**Figure 4.18**; **Figure 4.20**).

Unexpectedly, I found, depending on the dose, additivity or synergism between AZD6738 and ibrutinib in *TP53*/*ATM* defective primary CLL cells (**Figure 4.22**; **Table 4.4**). The underlying mechanism of the potentiating interaction at higher dose combinations may involve off-target effects of AZD6738 and ibrutinib (**Figure 4.23**). At clinically relevant doses (with ≤ 1 μM ibrutinib), however, this is likely to be accounted for by the limited overlap in the cellular populations that are targeted by these two compounds (**Figure 4.24**). Should AZD6738 be used in combination with BCR signalling inhibitors, consideration needs to be given to the sequence of treatment, since signalling inhibitors, which evict CLL cells from proliferation centres, may render them quiescent and no longer sensitive to ATR inhibition (Byrd et al., 2013). Combination with chemotherapy or other targeted therapies would allow simultaneous targeting of both the proliferating and non-proliferating populations, and both

DDR proficient and deficient subclones. When combined with ibrutinib, AZD6738 should be initiated first, with ibrutinib added subsequently and dual therapy continued until maximum response is attained.

4.2.6. Potential mechanisms of resistance to ATR inhibition

A fundamental assumption underpinning models of synthetic lethality is that there are only two major pathways regulating a specific process. Therefore, if one pathway is defective, cellular demise is assured when the other pathway is blocked. However, this notion is inevitably an over-simplification of the myriad of collateral pathways regulating a cellular process, many of which are hitherto under-appreciated or unknown. When one collateral pathway is therapeutically inhibited, tumour cells may upregulate an alternative collateral pathway to mitigate the effects of the initial block, thereby resulting in therapeutic resistance.

As discussed previously, there have been reports pointing to a possible functional redundancy between ATR and DNA-PK in regulating downstream Chk1 activity (Lin et al., 2014). More recently, Buisson *et al* demonstrated the existence of a DNA-PK-Chk1 backup pathway that can mediate resistance to ATR inhibitors. In this model, ATR inhibition is cytotoxic to a proportion of tumour cells with the highest levels of replication stress, but those with moderate levels are protected through the backup pathway (Buisson et al., 2015). Although DNA-PK inhibition did not appear to have substantial impact on HU-induced Chk1 phosphorylation in CLL, such a DNA-PK-Chk1 backup pathway could still potentially mediate therapeutic resistance *in vivo*. Simultaneous targeting of ATR and Chk1 or DNA-PK could possibly overcome this. Indeed, a potentiating interaction between ATR and Chk1 inhibitors has been reported, suggesting that the combined use of these inhibitors could be more efficacious than either agent alone (Sanjiv et al., 2016). However, the potential toxicities and

adverse effects of any combined use of ATR and Chk1 inhibitors will need to be properly assessed.

Finally, both ATR and Chk1 inhibitors are kinase inhibitors. As observed from the small molecule kinase inhibitors currently in clinical use, point mutations in the target kinase can develop. This constitutes another potential source of therapeutic resistance that physicians and investigators will need to anticipate and overcome.

4.2.7. Clinical applicability of ATR inhibitors

In addition to CLL, *TP53* and *ATM* defects are poor prognostic markers in other haematological malignancies including mantle cell lymphoma (Schaffner et al., 2000), T-prolymphocytic leukaemia (Stilgenbauer et al., 1997; Stoppa-Lyonnet et al., 1998), acute myeloid leukaemia (Rucker et al., 2012; Seifert et al., 2009), myelodysplastic syndrome (Jadersten et al., 2011), multiple myeloma (Chng et al., 2007; Drach et al., 1998) and diffuse large B-cell lymphoma (Xu-Monette et al., 2012). The current work on CLL provides a model of how ATR inhibition could selectively target *TP53* or *ATM* defective cells, and its use in these malignancies could be explored in future studies.

The ATR kinase inhibitors AZD6738, as well as VX-970, have now entered Phase I/II clinical testing. However, most of these studies have been initiated recently, and no results have yet been reported. As of March 2017, 11 clinical trials on ATR inhibitors are ongoing for a range of solid tumours. These studies examine the use of the ATR inhibitor either alone or in combination with a range of conventional and novel therapeutic agents, including cisplatin, carboplatin, gemcitabine, etoposide, irinotecan, the PARP inhibitors olaparib and veliparib, and the anti-PD-L1 immune checkpoint inhibitor durvalumab. No clinical study of ATR inhibition has yet been initiated in haematological malignancies.

However, the pre-clinical data presented herein provides a basis for such investigations in refractory *TP53*/*ATM* defective CLL.

CHAPTER 5

LONG-TERM PROGNOSTIC SIGNIFICANCE OF MINIMAL RESIDUAL DISEASE IN CLL

This chapter has been published as:

Kwok M, et al. (2016). Minimal residual disease is an independent predictor for 10-year progression-free and overall survival in CLL. Blood. *128*, 2270-2273.

With the advent of chemoimmunotherapy and other novel therapeutic approaches, it has been possible, over the past two decades, to achieve MRD eradication in CLL to below 10^{-4}. As detailed in section 1.5, clinical trials that have incorporated MRD assessments have shown consistent correlation between post-treatment MRD level and therapeutic outcome (Abrisqueta et al., 2013; Bosch et al., 2008; Bottcher et al., 2012; Dreger et al., 2010; Fischer et al., 2012; Goede et al., 2014; Moreno et al., 2006; Moreton et al., 2005; Pettitt et al., 2012; Santacruz et al., 2014; Strati et al., 2014), with MRD status demonstrating independent prognostic significance in patients treated upfront with chemoimmunotherapy (Bottcher et al., 2012; Santacruz et al., 2014; Strati et al., 2014).. However, the independent prognostic relevance and long-term benefit of MRD negativity in other therapeutic settings and patient populations, such as with chemotherapy-free treatments and among relapsed/refractory patients, remain unclear. Moreover, a direct comparison of the clinical impact of MRD negativity between frontline and relapsed/refractory settings has not hitherto been undertaken.

For the past 20 years, MRD evaluation by flow cytometry has been an integral part of the response assessment for multiple UK CLL clinical trials led by Prof. Peter Hillmen. This resulted in the availability of patients at different disease stages and with different biological features, who have received various treatments. The MRD status of each individual following the end of treatment is known. Moreover, given that the clinical trials were initiated many years ago, the majority of these patients have extended follow-up. I therefore undertook a retrospective analysis of this historical cohort which addresses the long-term independent prognostic value of MRD status across different therapeutic settings and treatment modalities.

5.1. Results

5.1.1. Study criteria and cohort demographics

I retrospectively analysed all patients who completed treatment for CLL at St James's University Hospital in Leeds or associated regional hospitals in West and North Yorkshire during 1996 to 2007, achieved at least a partial response (PR), and received an MRD assessment from a bone marrow aspirate specimen taken within 6 months of treatment completion. These individuals were identified from computerised records at the HMDS laboratory in Leeds, where MRD analysis was undertaken. Patients who failed to respond or died before treatment completion were excluded, as were those who received allogeneic stem cell transplantation, because ongoing graft-versus-leukaemia effect can lead to continued depletion of residual disease. Also excluded were patients who subsequently received alemtuzumab for consolidation as part of the National Cancer Research Institute (NCRI) CLL207 trial, which prospectively evaluated the effect of MRD eradication in patients who remained MRD positive after chemotherapy (Varghese et al., 2017). For individuals who received multiple treatments, the first therapy completed between 1996 and 2007 was used for analysis.

Altogether 536 patients were assessed at the HMDS laboratory during the study period, of whom 173 received treatment in Leeds and other associated hospitals in the region. MRD assessments were carried out using multiparameter flow cytometry according to the international harmonised approach (Rawstron et al., 2013; Rawstron et al., 2016; Rawstron et al., 2007). Specifically, MRD was assessed using CD19 and CD20, in combination with CD5, CD79b, CD81 and CD43. Earlier MRD assessments, performed before 2003, did not necessarily contain all the reported markers. Indeed, MRD assays carried out during that period typically contained only four markers: CD19, CD20, CD5 and

CD79b. However, data was included only if it was ascertained from the pre-treatment material that a limit of detection of $\leq 10^{-4}$ CLL cells could be achieved with the available markers. MRD negativity was defined as the absence of detectable CLL cells using a detection threshold of 10^{-4} CLL cells.

Of these 173 patients, 23 were excluded due to a lack of CR/PR, 10 due to the assessment of blood rather than bone marrow MRD, 3 because of treatment with allogeneic stem cell transplantation and 4 as a result of subsequent enrolment into a consolidation trial (NCRI CLL207). Among the 133 who fulfilled the inclusion criteria, 67 received combination chemotherapy or chemoimmunotherapy, 31 received single-agent chemotherapy, 7 underwent autologous stem cell transplantation, and 28 were treated with chemotherapy-free regimens, mostly with monoclonal antibody therapy (**Figure 5.1A**). The median age of the cohort at the start of treatment was 62 (range, 38-83). One hundred and four patients (77%) were male. Fifty-seven (43%) received no previous CLL treatment, with the remainder having 1 to 7 prior therapies. The demographic details are summarised respectively in **Table 5.1**.

Clinical response assessments were made in accordance with the IWCLL response criteria. As explained in section 1.5.1, a CR requires the complete normalisation of blood counts and the complete disappearance of symptoms and signs associated with CLL. Patients with persistent cytopenias due to incomplete recovery of haematopoietic function following myelosuppressive treatments, but otherwise fulfil the criteria for a CR, were staged as CR with incomplete marrow recovery (CRi). On the other hand, those who otherwise fulfil the criteria for a CR, but have residual nodular aggregates in the bone marrow trephine composed of CLL cells as verified by immunohistochemistry, were staged as nodular PR (nPR). Patients not meeting the criteria for a CR, CRi or nPR, but achieved ≥50% reduction in lymphocytosis together with ≥50% regression of organomegaly, were considered as having had a PR. Lymphadenopathy and hepatosplenomegaly was evaluated in most cases

Figure 5.1

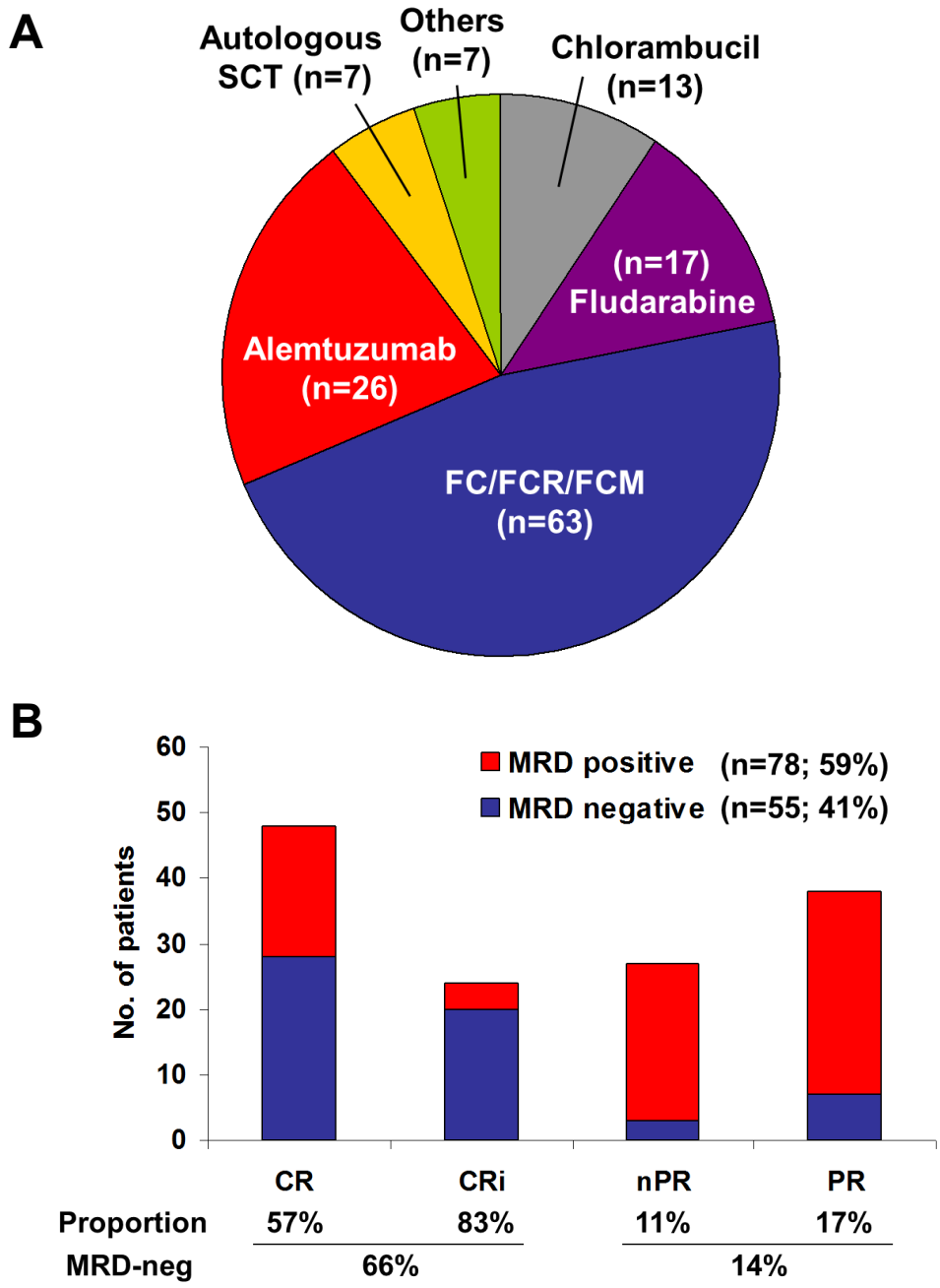

Treatment details (A) and IWCLL and MRD response (B) of patients enrolled in the current MRD study. In (B), the proportion patients with CR, CRi, nPR and PR who were also MRD-negative is displayed beneath the chart. A higher proportion of patients with CR/CRi were MRD-negative (66%) compared to patients with PR/nPR (14%).

Table 5.1. Pre-treatment characteristics of CLL patients by MRD status

Characteristics	Total no. of patient	MRD-negative (CLL < 0.01%)		MRD-positive (CLL 0.01-1%)		MRD-positive (CLL > 1%)	
		Number	%	Number	%	Number	%
Age, years							
< 60	51	27	52.9%	14	27.5%	10	19.6%
≥ 60	82	28	34.1%	21	25.6%	33	40.2%
Sex							
Female	29	11	37.9%	7	24.1%	11	37.9%
Male	104	44	42.3%	28	26.9%	32	30.8%
Binet stage							
A/B	70	33	47.1%	24	34.3%	13	18.6%
C	60	20	33.3%	10	16.7%	30	50.0%
Lymphadenopathy							
None	34	19	55.9%	4	11.8%	11	32.4%
Largest node < 5 cm	84	29	34.5%	29	34.5%	26	31.0%
Largest node ≥ 5cm	8	3	37.5%	1	12.5%	4	50.0%
Splenomegaly							
Absent	81	36	44.4%	21	25.9%	24	29.6%
Present	52	19	36.5%	14	26.9%	19	36.5%
Hepatomegaly							
Absent	128	53	41.4%	34	26.6%	41	32.0%
Present	5	2	40.0%	1	20.0%	2	40.0%
B-symptoms							
Absent	112	44	39.3%	28	25.0%	40	35.7%
Present	21	11	52.4%	7	33.3%	3	14.3%
White Cell Count							
< 30 x 10^9/L	58	31	53.4%	13	22.4%	14	24.1%
≥ 30 x 10^9/L	72	22	30.6%	21	29.2%	29	40.3%
Cytopenias							
Haemoglobin < 110 g/L	42	15	35.7%	10	23.8%	17	40.5%
Haemoglobin ≥ 110 g/L	88	38	43.2%	24	27.3%	26	29.5%
Platelet < 100 x 10^9/L	44	14	31.8%	10	22.7%	20	45.5%
Platelet ≥ 100 x 10^9/L	86	39	45.3%	24	27.9%	23	26.7%
Del(17p)							
Absent	84	36	42.9%	23	27.4%	26	30.1%
Present	9	3	33.3%	4	44.4%	2	22.2%
Del(11q)							
Absent	81	30	37.0%	24	29.6%	27	33.3%
Present	15	6	40.0%	4	26.7%	5	33.3%
Del(13q)							
Absent	45	20	44.4%	12	26.7%	13	28.9%
Present	56	18	32.1%	17	30.4%	21	37.5%
Trisomy 12							
Absent	87	36	41.4%	25	28.7%	26	29.9%
Present	18	4	22.2%	6	33.3%	8	44.4%
IGHV							
Mutated	26	18	69.2%	3	11.5%	5	19.2%
Unmutated	15	5	33.3%	4	26.7%	6	40.0%
Number of prior therapy							
0	57	24	42.1%	17	29.8%	16	28.1%
1	27	11	40.7%	5	18.5%	11	40.7%
2	24	12	50.0%	5	20.8%	7	29.2%
3	18	8	44.4%	3	16.7%	7	38.9%
≥ 4	7	2	28.6%	3	42.9%	2	28.6%
Prior Fludarabine							
No prior fludarabine	84	29	34.5%	23	27.4%	32	38.1%
Fludarabine responsive	30	17	56.7%	6	20.0%	7	23.3%
Fludarabine refractory	19	9	47.4%	6	31.6%	4	21.1%

(78%) by CT imaging. Of the 133 patients in the cohort, 46 achieved a CR, 24 achieved a CRi, 27 achieved an nPR and 36 achieved a PR.

Altogether 55 patients (41%) were MRD-negative post-treatment, including 46 with CR/CRi and 9 with PR/nPR (**Figure 5.1B**). A much greater proportion of patients with a CR or CRi were MRD-negative (67%) compared to those with a PR or nPR (16%). All patients with a MRD-negative PR had morphologically clear bone marrow but residual adenopathy. Among the 24 previously untreated individuals who attained MRD negativity following treatment, all received fludarabine-based combination therapy (FC: n=21 or FCR: n=1), with the exception of one individual who was treated with chlorambucil and one who received autologous stem cell transplantation. Of the 33 relapsed or refractory patients who became MRD negative, the majority received alemtuzumab (n=15) or fludarabine-based regimens (n=13). Of the 9 fludarabine-refractory patients who achieved MRD negativity, seven were treated with alemtuzumab and two with autologous stem cell transplantation. The proportion of patients achieving MRD negativity following each treatment type is shown in **Table 5.2**.

5.1.2. MRD negativity predicts for long-term PFS and OS independent of the type and line of therapy

To assess the impact of MRD status on clinical outcome, I performed Kaplan-Meier analysis, as well as univariate and multivariate statistical analyses, as described in section 2.12. Progression evaluations were made blinded to MRD status, and MRD status did not influence treatment duration, except for individuals receiving alemtuzumab who were treated until maximum IWCLL and MRD response was attained. For multivariate analyses, all prognostic variables that were routinely assessed and available for ≥70% of patients were included.

Table 5.2. MRD response according to the type of treatment given

Treatment Modality	Total no. of patients	MRD-negative (CLL < 0.01%)		MRD-positive (CLL 0.01-1%)		MRD-positive (CLL > 1%)	
		Number	%	Number	%	Number	%
Alemtuzumab	26	15	57.7%	8	30.8%	3	11.5%
Autologous SCT	7	5	71.4%	0	0.0%	2	28.6%
Chlorambucil	13	1	7.7%	2	15.4%	10	76.9%
CHOP + Rituximab	2	1	50.0%	1	50.0%	0	0.0%
Cyclophosphamide	1	0	0.0%	0	0.0%	1	100%
FC	57	26	45.6%	17	29.8%	14	24.6%
FCM	2	1	50.0%	0	0.0%	1	50.0%
FCR	4	3	75.0%	1	25.0%	0	0.0%
Fludarabine	17	2	11.8%	5	29.4%	10	58.8%
Fludarabine + Alemtuzumab	2	1	50.0%	1	50.0%	0	0.0%
Methylprednisolone	1	0	0.0%	0	0.0%	1	100%
Ofatumumab	1	0	0.0%	0	0.0%	1	100%

SCT: stem cell transplantation; CHOP: cyclophosphamide, doxorubicin, vincristine and prednisolone; FC: fludarabine and cyclophosphamide; FCM: fludarabine, cyclophosphamide and mitoxantrone; FCR: fludarabine, cyclophosphamide and rituximab.

With a median follow-up of 10.1 years (range 7.8-18.6) among surviving patients, the median PFS in MRD-negative (<0.01%) individuals was 7.6 years, compared to 3.3 and 2 years respectively in individuals with positive MRD at 0.01-1% and >1% (**Figure 5.2A**). The median OS was likewise prolonged in MRD-negative patients (10.6 years) compared to MRD-positive patients (5.3 and 3.6 years respectively for 0.01-1% and >1% MRD; **Figure 5.2B**).

When both IWCLL and MRD status were taken into account, the best PFS and OS outcomes were seen in patients with a CR/CRi who were MRD-negative (**Figure 5.3**). Among patients with a CR/CRi, there was a significant difference in both PFS and OS between the MRD-negative (n=46) and MRD-positive groups (n=24). Among the patients with a PR/nPR, there was a statistically significant difference in PFS between the MRD-negative (n=9) and positive groups (n=54), but not in OS. On the other hand, there was no statistically significant difference between CR and PR populations with the same MRD status (i.e. between MRD-negative CR vs MRD-negative PR, and between MRD-positive CR vs MRD-positive PR).

Patients with MRD-negative PR appeared to have outcomes intermediate between patients with MRD-negative CR and those with MRD-positive CR/PR (**Figure 5.3**). The nine patients with MRD-negative PR comprised six who were treated with chemotherapy-based combinations and two who were treated with single-agent alemtuzumab. These patients had residual disease in their lymph nodes and/or spleen, despite evidence of disease clearance from the bone marrow. This could potentially account for the inferior outcome, albeit not statistically significant, of the MRD-negative PR group relative to the MRD-negative CR group.

Finally, I considered MRD response in a multivariate analysis together with established prognostic factors including age, Binet stage, cytopenias (haemoglobin <110 g/L and platelet <100 x 10^9/L), prior treatment and adverse cytogenetics, either del(17p) or

Figure 5.2

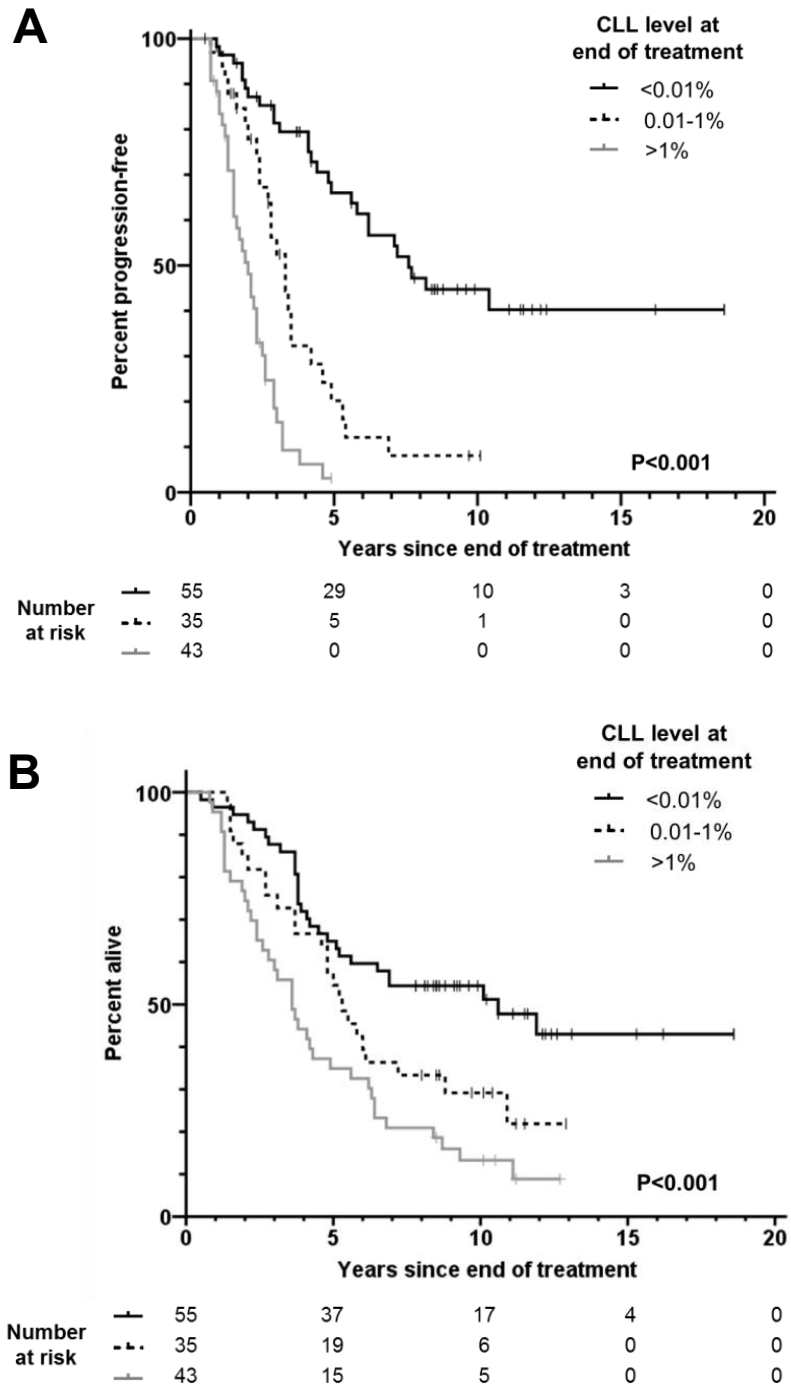

PFS (A) and OS (B) according to level of detectable disease at the end of treatment. Post-treatment MRD levels were obtained within 6 months following the end of treatment by multiparameter flow cytometry to a sensitivity of 10^{-4} (0.01%). A patient was considered MRD negative if the MRD level was below the level of detection (i.e. <0.01%). The log-rank p value is displayed, and $p<0.05$ is considered statistically significant. Presence of residual disease at the end of treatment predicts for long-term PFS and OS.

Figure 5.3

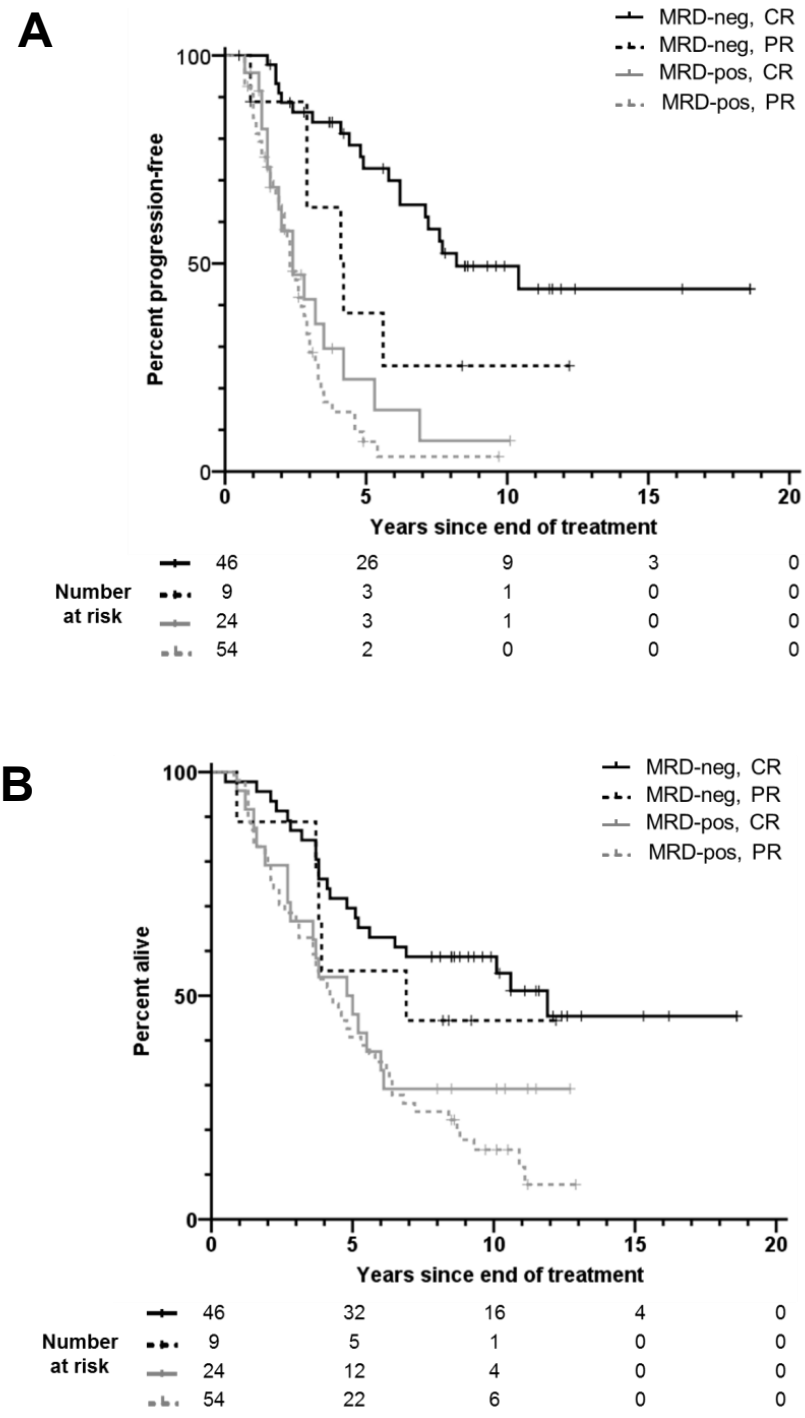

PFS (A) and OS (B) according to both the MRD and the IWCLL response status at the end of treatment. Among the patients with a CR, there was a statistically significant difference in both PFS and OS between the MRD-negative and MRD-positive groups. Among the patients with a PR, there was a statistically significant difference in PFS between the MRD-negative and MRD-positive groups, but not in OS. On the other hand, there was no statistically significant difference between CR and PR populations with the same MRD status. The PFS and OS curves for the MRD-negative PR group lie between that of the MRD-negative CR group and the MRD-positive CR/PR groups respectively.

del(11q), evaluated by metaphase FISH at the time of treatment, as well as treatment modality and IWCLL response. Only MRD response and adverse cytogenetics were significant for PFS, and only MRD response, age, stage and prior treatment were significant for OS on multivariate analysis (**Table 5.3**). IWCLL response was found not to be an independent predictor for either PFS or OS. *IGHV* mutational status, available in 41 patients (31%), was significant in univariate analysis for both PFS (p=0.016) and OS (p=0.014). However, due to the limited number of cases with *IGHV* data in this cohort, this parameter was not included in the multivariate analysis.

5.1.3. MRD negativity confers the greatest prognostic benefit when achieved in the frontline setting

Next, I analysed the treatment-naïve and previously treated patients separately, in order to compare the relative impact of MRD between frontline and relapsed/refractory settings. I found that patients receiving both frontline and subsequent treatments derived significant PFS and OS benefit from attaining MRD negativity (**Figure 5.4**). However, greater long-term benefit was seen when MRD negativity was achieved upfront, with 10-year PFS of 65% vs 10% and 10-year OS of 70% vs 30% for MRD-negative vs positive patients. In comparison, in the relapsed/refractory setting, the 10-year PFS was 30% vs 0% and the 10-year OS was 47% vs 11% for MRD-negative vs positive patients.

The PFS curve for the 23 patients who achieved MRD negativity upfront appears to plateau at 7.7 years, beyond which no clinical relapse was observed among the 12 (52%) who remained in remission (**Figure 5.4A**). This is similar to the PFS plateau previously reported in the *IGHV* mutated MRD-negative patients from the MD Anderson Cancer Center fludarabine, cyclophosphamide and rituximab (FCR) trial (Thompson et al., 2016). However, in the present cohort, 1 out of 9 patients with known *IGHV* mutational status in remission beyond 7.7 years had unmutated *IGHV*.

Table 5.3. Univariate and multivariate analysis of post-treatment MRD levels with other parameters of prognostic significance

Parameter	Progression-free Survival			Overall Survival		
	Univariate (Log-Rank) P Value	**Multivariate (Cox) P Value**	**Hazard Ratio (95% CI)**	**Univariate (Log-Rank) P Value**	**Multivariate (Cox) P Value**	**Hazard Ratio (95% CI)**
Age* (60 years)	0.513			**0.001**	**0.001**	**2.41 (1.45-4.00)**
Haemoglobin* (110 g/L)	0.957			0.058		
Platelet* (100 x 10^9/L)	**0.001**	0.983		**0.034**	0.168	
Binet stage* (A/B vs C)	**0.005**	0.870		**0.001**	**0.018**	**2.23 (1.14-4.33)**
Prior treatment (Y/N)	**0.003**	0.159		**0.003**	**<0.001**	**2.61 (1.61-4.23)**
Treatment type	**<0.001**	0.265		**0.004**	0.886	
IWCLL Response	**<0.001**	0.545		**0.001**	0.585	
MRD level (< 0.01 / 0.01-0.1 / 0.1-1 / > 1%)	**<0.001**	**<0.001**	**2.07 (1.59-2.69)**	**<0.001**	**0.002**	**1.39 (1.13-1.70)**
Adverse cytogenetics* (del 17p/11q)†	**0.024**	**0.013**	**2.00 (1.16-3.45)**	0.051		

* Age, haemoglobin and platelet count, Binet stage and cytogenetics were assessed at the time of treatment initiation.

† Cytogenetic aberrations [del(17p) and/or del(11q)] were evaluated by metaphase fluorescence in-situ hybridization (FISH).

Figure 5.4

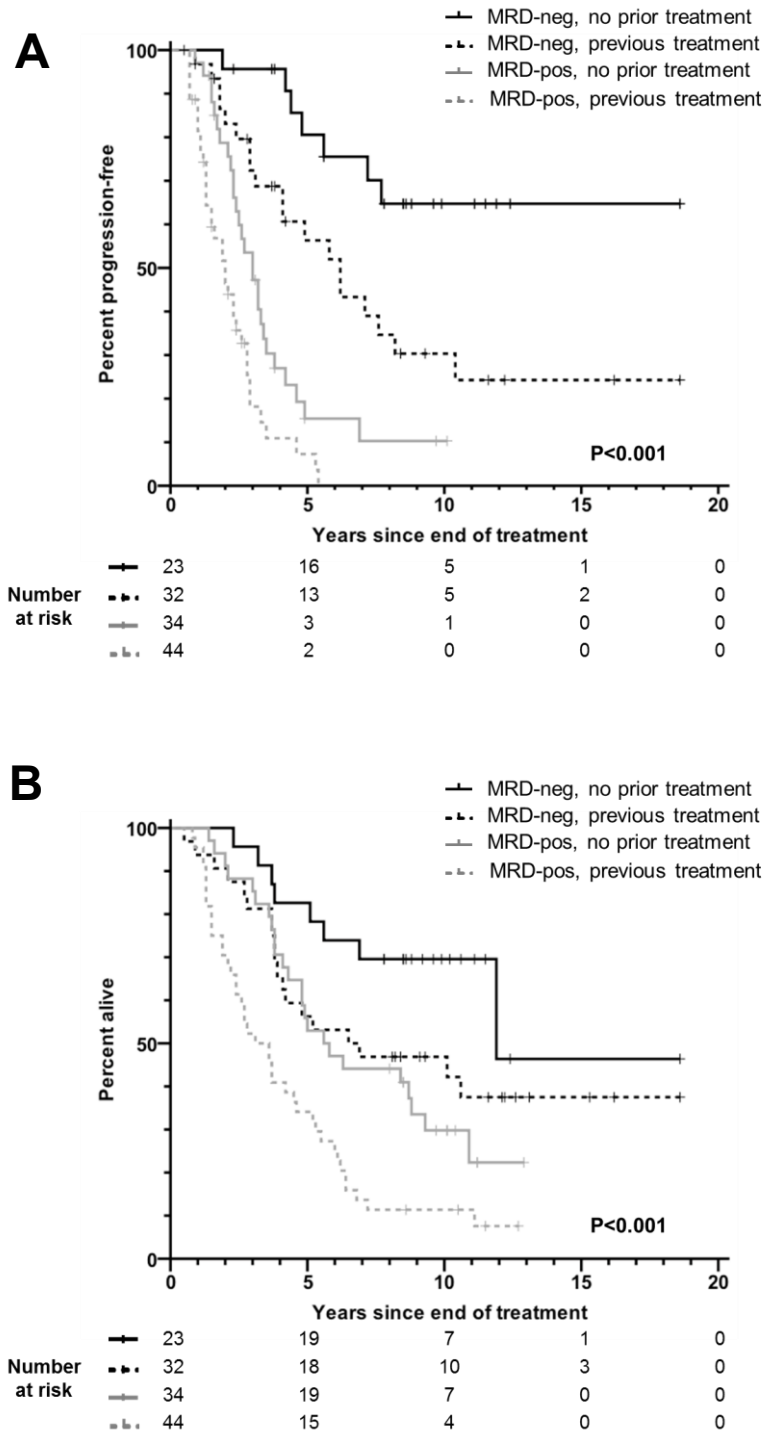

PFS (A) and OS (B) according to prior treatment and MRD status at the end of treatment. Presence of residual disease at the end of treatment predicts for long-term PFS and OS independent of prior treatment. MRD-neg, MRD-negative; MRD-pos, MRD-positive.

5.1.4. Attainment of MRD negativity partially overcomes the adverse prognostic impact of del(17p) and del(11q)

As mentioned in previous chapters, the adverse cytogenetic aberrations del(17p) and del(11q) are well-known prognostic factors in CLL. Furthermore, adverse cytogenetics, together with MRD status, are the two parameters found to possess independent prognostic significance for PFS in the present patient series. I therefore analysed PFS and OS according to both the presence of MRD and adverse cytogenetics (**Figure 5.5**). The best outcome was seen in MRD-negative patients without adverse cytogenetic features, whose median PFS was not reached and median OS was 10.1 years. In patients with del(17p) or del(11q), achievement of MRD negativity appeared to partially overcome the poor prognosis associated with their cytogenetic aberrations. Within this group of patients the median PFS and OS for MRD-negative vs MRD-positive subjects were significantly different: 4.9 vs 1.3 years for PFS (**Figure 5.5A**) and 6.5 vs 2.7 years for OS (**Figure 5.5B**). This suggests that achieving MRD negativity may potentially be of value in this group of CLL patients with deletion of *TP53* or *ATM*.

Figure 5.5

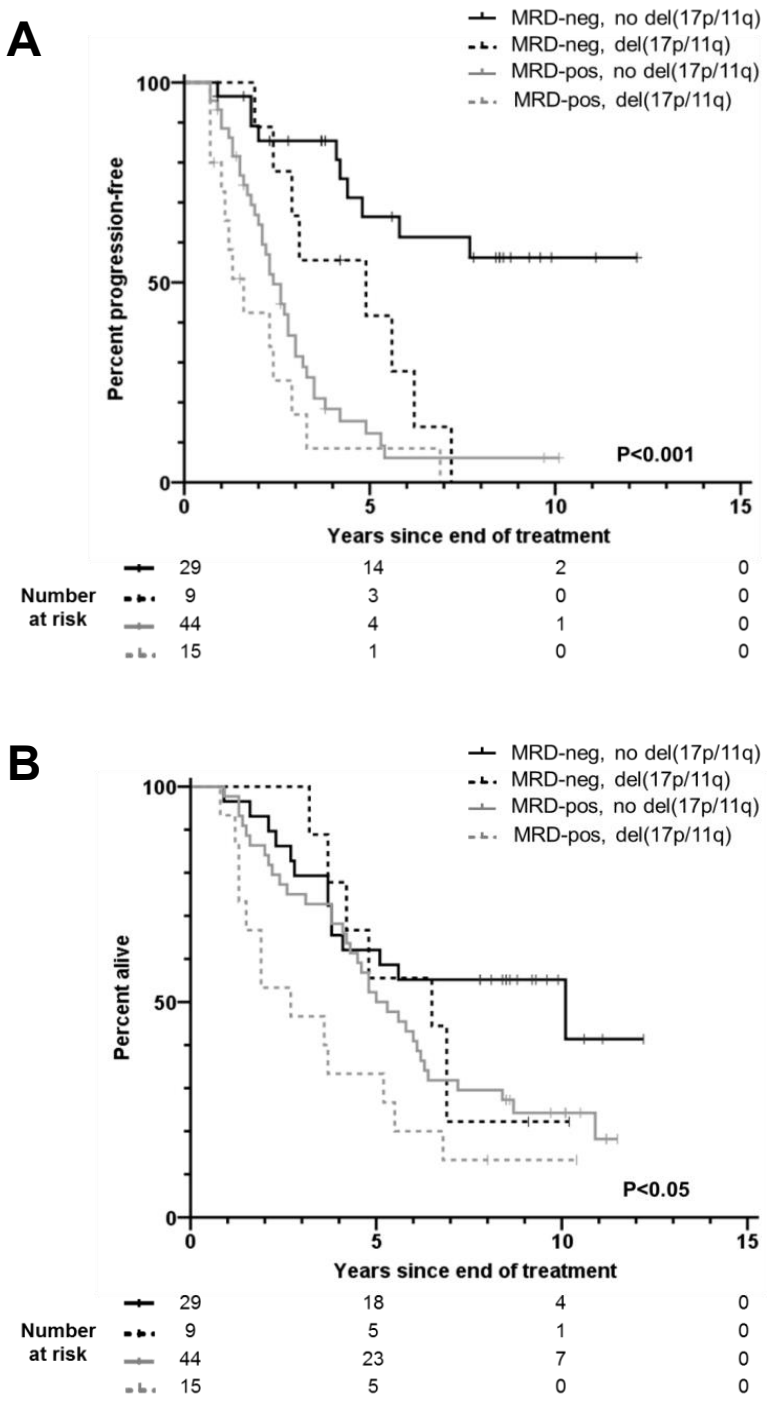

PFS (A) and OS (B) according to del(17p) or del(11q) and the MRD status at the end of treatment. Cytogenetic aberrations were evaluated by FISH. The balance of patients with del(17p) and del(11q) respectively was comparable between the MRD-negative and MRD-positive groups. In the MRD-negative del(17p/11q) group, 3/9 patients (33%) had del(17p) while 6/9 patients (67%) had del(11q). In the MRD-positive del(17p/11q) group, 6/15 patients (40%) had del(17p) while 9/15 patients (60%) had del(11q). Presence of residual disease at the end of treatment predicts for long-term PFS and OS independent of cytogenetics. MRD-neg, MRD-negative; MRD-pos, MRD-positive.

5.2. Discussion

5.2.1. Clinical significance of the findings from this study

As detailed in section 1.5.3.2, MRD has previously been shown to correlate with prognosis in a number of prospective clinical trials. However, the results I have generated from the current study provide several important additions to the existing literature on MRD as a prognostic variable in CLL.

Firstly, the duration of follow-up in most of the published CLL MRD studies has been relatively short. For instance, the median follow-up duration was 4.3 years within the published MRD study on the German CLL group CLL8 cohort (Bottcher et al., 2012). It is thus unclear whether MRD remains prognostically relevant with extended follow-up. In this present cohort, subjects were followed for a median of 10.1 years among surviving patients, and up to a maximum of 18.6 years. This has allowed confirmation of the 10-year prognostic impact of MRD status in CLL. Importantly, my results shows that the PFS and OS curves of the MRD-negative and MRD-positive groups do not converge for up to 18 years after the end of treatment.

Secondly, the independent prognostic importance of MRD in CLL has thus far been demonstrated only in patients treated upfront with chemotherapy-based combination therapeutic regimens. This is the first study to incorporate different treatment settings and therapeutic modalities into a single multivariable model to evaluate the clinical impact of post-treatment MRD status in CLL. Importantly, the results from this analysis confirm the independent predictive value of MRD not only in the frontline but also in the relapsed/refractory setting, and not only with chemoimmunotherapy but also with chemotherapy-free treatments (**Table 5.3**). Indeed, the median PFS of the MRD-negative and MRD-positive patients in this cohort treated with chemotherapy-free regimens was

significantly different at 4.9 and 1.3 years respectively (p=0.002). At present, MRD negativity is achieved predominantly through chemotherapy-containing regimens with considerable toxicity, such as FCR, thus precluding its use in frailer or older CLL patients, who are likely to be less tolerant to such therapies. Newer agents such as venetoclax can also produce MRD negativity in substantial proportions of CLL patients, including in individuals with del(17p) (Eichhorst et al., 2015; Ma et al., 2015). With the availability of new targeted therapies and therapeutic combinations for CLL, there will likely be a trend towards reduced reliance on chemotherapy, and therefore evidence to support the independent prognostic power of MRD status in the chemotherapy-free setting is of particular relevance.

Finally, the current study provides a direct comparison of the relative value of achieving MRD negativity in the first and subsequent treatments. My results highlight the distinct PFS benefit of attaining MRD negativity in the upfront setting (**Figure 5.4A**). An explanation for the importance of achieving MRD negativity upfront could be that poor survival is associated with the development of a resistant genotype (e.g. *TP53* mutation), which arises or is enriched within residual disease post-therapy. Indeed, the emergence and expansion of resistant subclones during and after treatment has been described in CLL patient series (Landau et al., 2015; Nadeu et al., 2016; Rossi et al., 2014) as well as in animal models (Davies et al., 2017). This is also the reason why the durability of remissions tends to decrease with each subsequent treatment, regardless of the therapeutic modality. In patients with profound remissions (i.e. MRD negativity) there will inevitably be a smaller pool of residual cells in which such resistance can occur. My findings therefore underscore the importance of achieving the best possible response with first-line therapy.

5.2.2. Limitations of this study and other considerations

Due to the historical nature of the cohort in this study, *IGHV* mutational status was available only in a proportion of CLL patients. Therefore, in the multivariate analysis, *IGHV*

mutational status was not included. Likewise, due to data unavailability, other established prognostic variables, such as CD38 and ZAP-70 positivity, as well as putative prognostic markers such as *NOTCH1* and *SF3B1* mutational status, were not incorporated into the multivariate analysis. Moreover, some therapies used in the current cohort, such as chlorambucil, single-agent fludarabine and FC, were historical and are no longer CLL treatments of choice except in the palliative setting. However, the significance of this study lies in the demonstration that the clinical benefit of MRD negativity was independent of the type or line of therapy through which this was achieved.

This study is also limited by its retrospective nature. One topic of particular interest in the area of CLL MRD assessment is whether MRD could be used as a surrogate marker for PFS, and therefore potentially replacing PFS as a primary endpoint in CLL clinical trials. Such an idea is attractive because the prolonged PFS with FCR-like therapy and novel agents such as venetoclax, especially in the frontline setting, means that clinical trials aiming to improve outcome are inevitably very prolonged and require a very large sample size to observe a significant PFS difference. This greatly restricts the development of novel drugs and drug combinations for patients with CLL. Therefore, using MRD as a clinical trial endpoint may accelerate clinical drug development in CLL.

However, the results from this study do not provide a definitive proof of surrogacy of MRD for PFS and OS because of the retrospective nature of this study. Although MRD was demonstrated to be an independent predictor for both PFS and OS in this cohort, it is unlikely that this was the only factor that influences PFS and OS. Other factors such as prior treatment and adverse cytogenetics might also independently affect PFS and OS, as shown in the multivariate analysis. As highlighted in an editorial accompanying the published manuscript of this study, in order to use MRD as a surrogate for PFS and OS, it is incumbent on investigators to prospectively compare, within randomised clinical trials, the impact of each individual treatment on MRD, and whether the magnitude of effect on MRD corresponds to the magnitude of effect on PFS or OS (Little and McShane, 2016). As such,

the clinical importance of MRD with each treatment needs to be prospectively validated in the context of randomised clinical trials.

In the current study, bone marrow rather than peripheral blood MRD was evaluated. While work is still ongoing internationally to determine the comparability between bone marrow and peripheral blood MRD assessments, previously published data shows that bone marrow is a more sensitive site for MRD detection than peripheral blood when assessed at three months after the end of treatment or earlier. This is particularly the case in patients treated with single-agent monoclonal antibodies such as rituximab or alemtuzumab, where clearance of peripheral blood CLL cells occurs earlier than the clearance of infiltrated bone marrow CLL cells. Therefore, there could be more than 10-fold discrepancy between residual disease levels in the bone marrow and peripheral blood while on treatment and early after treatment completion (Rawstron et al., 2007). For this reason, the standard practice at many institutions is to use bone marrow aspirate samples for MRD quantification at the time of response assessment, in line with recommendations from the IWCLL 2008 guidelines (Hallek et al., 2008).

Finally, it is of relevance to provide a discussion of MRD-negative PR. Recently, an analysis of the German CLL group CLL8 trial by both IWCLL and MRD response status shows that patients with MRD-negative PR had significantly superior PFS compared to both the MRD-positive CR and PR groups. On the other hand, compared to the MRD-negative CR group, MRD-negative PR patients with residual splenomegaly had equally good PFS, whereas patients MRD-negative PR with residual lymphadenopathy had inferior PFS (Kovacs et al., 2016). As explained in the results section of this chapter, patients with MRD-negative PR in the current study had outcomes intermediate between patients with MRD-negative CR and those with MRD-positive CR/PR (**Figure 5.3**), consistent with findings from the German CLL8 study. However, the lack of statistically significant difference between the MRD-negative PR group in relation to the MRD-negative or the MRD-positive CR groups might be due to the small number of patients in the current study with MRD-negative PR

(n=9), and to the fact that more patients had residual splenomegaly than residual lymphadenopathy.

5.2.3. MRD negativity as a therapeutic goal in CLL

In this study, I demonstrated that long-term treatment-free remissions are associated with MRD negativity, particularly when MRD negativity is attained upfront. Hence, my findings support MRD as a prognostic marker for long-term PFS. However, whether MRD negativity should be a therapeutic goal in CLL remains a subject of intense debate.

With the therapeutic options available at present, MRD negativity is an appropriate therapeutic goal for only a minority of CLL patients. Specifically, they are younger, physically fitter individuals who are more likely to tolerate an aggressive treatment approach involving combination chemoimmunotherapy, which is at present the only widely available treatment that can produce MRD negativity in substantial proportions of patients. As mentioned earlier, these treatments can be associated with significant toxicity, and are therefore unsuitable for many CLL patients who are at an advanced age, are frail or have multiple co-morbidities. It is therefore imperative that therapeutic approaches aiming at disease control or palliation are not dismissed in favour of MRD negativity. In CLL, new targeted therapies such as BCR signalling inhibitors have important clinical utility, despite the lack of deep remissions and MRD negativity. This is particularly the case for older and frailer patients, in the absence of other more efficacious and curative, but equally tolerable, treatments. Therefore, MRD evaluations should not be used to screen out novel therapies that do not yield MRD-negative responses.

With regards to the clinical deployment of novel therapies, a number of factors needs to be taken into consideration, such as toxicity and tolerability, in addition to efficacy. In the context of an early-phase trial, MRD negativity might be an indication of efficacy, and

could support further clinical investigation of the treatment, as exemplified by the case of venetoclax in CLL (Eichhorst et al., 2015; Ma et al., 2015). Moreover, there are ongoing studies to examine the role of consolidation therapy aiming to convert patients with residual disease at the end of treatment to MRD negativity. Results from UK CLL207 study, which assessed alemtuzumab consolidation in patients with MRD after chemotherapy, showed that subjects who were MRD-negative after consolidation had improved survival outcomes that were comparable with those who were MRD-negative after initial chemotherapy (Varghese et al., 2017).

At present, due to the limited number of well-tolerated treatments that can yield MRD negativity, MRD negativity is an appropriate therapeutic goal only for a subgroup of relatively young and fit CLL patients. However, MRD is clearly a powerful prognostic marker for long term clinical outcome, and its assessment can be incorporated into clinical trials. There is an ongoing effort by myself (Chapter 4) and others to develop new chemotherapy-free treatments that may produce deep, MRD-negative remissions. In future, chemotherapy-free combinations may potentially allow MRD eradication with minimal toxicity, making MRD negativity a feasible therapeutic goal, including for patients with adverse biological features such as del(17p) or *TP53*/*ATM* mutations.

CHAPTER 6

CONCLUSION

6.1. Novel insights into the clinical heterogeneity of CLL

This thesis sets out to generate novel insights into the clinical heterogeneity and treatment of CLL through a series of investigations that focus on three distinct groups of CLL patients: (1) patients who have undergone spontaneous disease regression; (2) patients with poor-risk CLL carrying *TP53* or *ATM* defects in need of novel therapies; and (3) patients who have achieved MRD negativity after treatment.

CLL is characterised by substantial clinical heterogeneity, and patients with CLL could have disparate clinical outcomes. While several biological processes have been found to influence disease heterogeneity in CLL, as outlined in section 1.2, and numerous prognostic biomarkers for disease progression and survival have been uncovered, there remains a knowledge gap in our understanding of the biological features of patients with spontaneous CLL regression and the potential mechanisms underpinning this process. Moreover, although MRD has been shown in multiple studies to have predictive value on the clinical outcome of patients after CLL treatment, it remains unclear whether MRD has independent prognostic value outside the frontline chemoimmunotherapy setting. It is also unclear whether MRD negativity confers long-term prognostic benefit.

Through analysis of 19 individuals with spontaneous CLL regression, both on residual circulating CLL cells, as well as on stored cells where available, I identified a range of novel features in this group of patients. CLL tumours that have undergone spontaneous disease regression express somatically mutated immunoglobulin genes, demonstrate short telomeres, and have a phenotype of B cell anergy with unresponsiveness to both IgM and IgD BCR stimulation. This phenotypic profile suggests a model in which the CLL clone undergoes an initial phase of proliferation which subsequently subside into a state of clonal anergy and low proliferation. In addition, other features such as reduced tumour expression

of CD49d and ROR1, and increased FasR expression, could potentially also contribute to spontaneous disease regression in CLL. Finally, through characterisation of the genomic landscape in these individuals, I found that in some cases spontaneous CLL regression occurred in the presence of known CLL genetic aberrations, including *TP53* mutations.

In addition, through analysis of 133 patients with CLL who have received a bone marrow MRD assessment after treatment, I identified MRD, as evaluated by standardised multiparameter flow cytometry, as an independent predictor for long-term PFS and OS. Moreover, while the prognostic benefit of achieving MRD negativity was independent of the type and line of treatment, with patients receiving both frontline and subsequent treatments deriving benefit from MRD negativity, a greater PFS and OS benefit with MRD negativity was seen in patients receiving their first CLL treatment.

These findings provide novel insights into the biological properties and potential mechanisms underpinning spontaneous CLL regression, as well as the long-term independent prognostic role of MRD in CLL. These results have implications for the treatment of CLL, as highlighted in subsequent sections.

6.2. Novel insights into the treatment of CLL

The treatment of CLL has historically relied upon cytotoxic chemotherapy, which has limited efficacy when used as a single therapeutic agent and is associated with substantial toxicity and side effects. Subsequently monoclonal antibodies targeting CLL surface antigens have become widely available, and more recently, small molecule inhibitors of the BCR signalling pathway and Bcl-2 have revolutionised the treatment of CLL. However, despite these therapeutic advances, there remains a need to develop novel therapeutic approaches and therapeutic combinations for CLL, because effective treatment options remain limited for multiply relapsed CLL, particularly in patients with poor-risk features such as *TP53* and *ATM* defects.

The unique phenotypic characteristics identified from the analysis of patients with spontaneous disease regression provide several insights into the treatment of CLL. Firstly, the finding that spontaneously regressed CLL tumours were unresponsive to BCR stimulation supports the use of BCR signalling inhibitors in CLL. Secondly, the findings from this study suggest that therapies that target ROR1, or those that upregulate FasR and downregulate CD49d and ROR1 expression in CLL cells may also have therapeutic potential.

Despite the therapeutic success of BCR signalling inhibitors in CLL, patients with poor-risk CLL, particularly those with *TP53* or *ATM* defects, can relapse from BCR signalling inhibitors. In addition, some may become intolerant to these agents. Only a proportion of patients with CLL relapsing from BCR signalling inhibitors respond to alternative kinase inhibitors, highlighting the need for novel therapeutic approaches (Jain et al., 2015; Mato et al., 2016). In the work presented in this thesis, I evaluated the pre-clinical efficacy and mechanism of ATR inhibition in CLL. Through the use of a novel and highly-specific ATR

inhibitor AZD6738, I demonstrated that ATR inhibition was selectively cytotoxic to CLL cells with *TP53* or *ATM* defects arising from deletions and/or mutations of these genes. This was accomplished through the suppression of the ATR pathway that is essential for the resolution of replication stress in CLL cells with compromised ATM/p53 function, resulting in the accumulation of DNA damage and mitotic catastrophe in these cells. The specificity of ATR inhibition for *TP53* and *ATM* defects allows selective targeting of genomically unstable DDR-defective CLL cells, therefore potentially helping to avert clonal evolution, a major cause of treatment refractoriness and disease relapse. Furthermore, ATR inhibitor was synergistic in combination with chemotherapeutic agents, and has a synergistic or additive effect in combination with the BCR signalling inhibitor ibrutinib.

The presence of residual disease provides a reservoir for eventual disease relapse, especially in DDR-defective CLL with high levels of genomic instability. In my study investigating the long-term impact of MRD on clinical outcome, I confirmed that the long-term survival benefit of achieving MRD negativity extends to poor-risk CLL patients with *TP53* or *ATM* deletions. Indeed, my findings suggest that the attainment of MRD negativity partially overcomes the poor prognosis associated with these DDR defects. Therefore, therapies eliciting deep remissions may provide enhanced benefit for del(17p) or del(11q) CLL.

At present, therapies capable of producing MRD negativity in *TP53* defective CLL are lacking. As evidenced from several patients within my MRD study cohort, alemtuzumab can occasionally yield MRD-negative responses. However, alemtuzumab is no longer routinely available for the treatment of CLL. More recently, venetoclax has been shown to be capable of producing MRD-negative remissions in up to 17% of patients *TP53* defective CLL (Eichhorst et al., 2015), which represents a small fraction of these patients. Given the potent cytotoxic effect of ATR inhibition against proliferating *TP53* defective CLL cells as demonstrated in my pre-clinical study, and the relatively high proliferation rate associated with these CLL cells, particularly in the context of clinically aggressive, relapsed/refractory

disease (Messmer et al., 2005), it is anticipated that depth of response to ATR inhibitor could be profound. However, this will require confirmation within well-designed clinical trials.

In summary, the phenotypic features evident from the analysis of patients with spontaneous disease regression support the use of BCR signalling inhibitors for the treatment of CLL. The findings from this thesis also provide demonstration of the pre-clinical efficacy of ATR inhibition against *TP53* or *ATM* defective CLL, and support the clinical evaluation of this therapeutic strategy.

6.3. A stratified approach for the treatment of CLL

The BCR signalling inhibitor ibrutinib is an example of a treatment that achieves disease control but not disease eradication. The direct cytotoxic effect of ibrutinib on CLL cells is modest at clinically achievable doses, as evidenced from the results of my drug combination experiments described section 4.1.4 and from other published studies (Herman et al., 2011). Moreover, detectable MRD remains in the vast majority of patients on ibrutinib monotherapy. Despite this, BCR signalling inhibitors have shown remarkable efficacy in CLL in improving clinical outcomes despite the lack of disease eradication. Moreover, the finding in this thesis of curtailed proliferation associated with clonal anergy in CLL cells from patients with spontaneous disease regression, including from three spontaneous regression cases with *TP53* defects, lends further support for such a therapeutic approach. On the other hand, it is widely recognised that MRD eradication leads to improved clinical outcome, and this is further supported by results from my study on the impact of MRD on long-term outcomes. How can this apparent contradiction be reconciled? Should the treatment strategy in CLL be that of disease control or disease eradication?

For many patients with CLL requiring treatment, a disease control approach could be sufficient to produce durable remissions. This is evidenced from studies that showed durable response (e.g. remissions > 3 years) in patients treated with ibrutinib, particularly among patients who were treated upfront and those without poor-risk features such as adverse cytogenetic aberrations and complex karyotype (Burger et al., 2015; Byrd et al., 2015). In this regard, spontaneous regressing CLL tumours all possessed mutated *IGHV* and most had low genomic complexity. Although three of the spontaneous regression cases in my study harboured *TP53* mutation, this may possibly be countered by features such as clonal anergy with unresponsiveness to both IgM and IgD BCR triggering, low CD49d and ROR1 expression, as well as high CD95/FasR expression that are uncommon in non-

regressing *TP53* mutant CLL. On the other hand, patients progressing on ibrutinib tend to be those with *TP53* or *ATM* aberrations or genomic complexity (Burger et al., 2016; Maddocks et al., 2015; Woyach et al., 2014a).

It is plausible, therefore, that this group of patients with relapsed/refractory disease who carry poor-risk features are the ones who are most likely to benefit from therapeutic approaches that are aimed at disease eradication rather than merely disease control. This is because, owing to their genomic instability, these tumours are prone to the acquisition of further genomic events that could lead to the development of resistance mechanisms (e.g. *BTK* or *PLCγ2* mutations in the case of ibrutinib) and clonal evolution. The outgrowth of resistant CLL clones in turn leads to disease relapse. Although well-tolerated therapies that can produce MRD-negative remissions in this group of poor-risk patients remain severely limited at present, combination of different targeted treatment approaches are likely to be of promise, and the pre-clinical and clinical investigation of various combinations of small molecule inhibitors is likely to be an important future research focus.

The progressive selection and accrual of resistant CLL subclones, which eventually become the dominant ones, is reflected in the observation that remission durations dwindle with increasing numbers of therapies given (Kutsch et al., 2014; Zenz et al., 2010b). This is perhaps the reason why some would advocate for empirical treatments against clonal targets (i.e. “trunk” lesions) rather than subclonal lesions (i.e. “branches”), as has been suggested in a recent review (Landau and Wu, 2013). However, one limitation with such an approach is it does not recognise that some subclones are inherently more genomically unstable and prone to the evolution of resistant mechanisms than others, the Darwinian selection of which may lead to the eventual emergence of a more aggressive disease. This could explain, for instance, why therapeutic resistance to ibrutinib remains more common in CLL patients with *TP53* aberrations or genomic complexity, as highlighted above. This is also why it might be more appropriate to adopt a “trunk-plus-branch” approach, where, in addition to reducing tumour burden with generic agents that target “trunk” lesions, there is

active effort made to target the most aggressive or genomically unstable ”branches”, in order to reduce the likelihood of treatment failure or disease relapse. In this regard, therapeutic strategies such as ATR inhibition that specifically target *TP53* or *ATM* defective CLL subclones are likely to be important in the treatment of patients with poor-risk CLL.

For all the above reasons, it is of relevance to consider a stratified treatment approach for CLL. So far, prognostic stratification based on *IGHV* mutational status and genomic lesions have not translated into therapeutic stratification, with the exception of patients with del(17q) or *TP53* mutations, who would be diverted away from chemotherapeutic agents to treatments that bypass p53-dependent apoptosis, such as BCR signalling inhibitors. With the development of novel therapies against different CLL lesions, such as γ-secretase inhibitors (*NOTCH1*) (Lopez-Guerra et al., 2015), spliceosome inhibitors (*SF3B1*) (Larrayoz et al., 2016), selective inhibitors of nuclear export (*XPO1*) (Lapalombella et al., 2012), PARP inhibitor (*ATM*) (Weston et al., 2010) and ATR inhibitor (*ATM* and *TP53*), it is likely that therapeutic stratification of CLL based on the biological properties of the CLL clone in individual patients would be achievable in the near future. Indeed, the forthcoming UK-wide phase III CLL trial (CLL11) currently being planned will involve the stratification of patients into different sub-trials based on the biological properties of their CLL determined at the time of trial entry by extended immunophenotyping and NGS.

Finally, in the assessment of new therapeutic agents it will be important to delineate how the novel agent impacts upon subclonal composition. *In vivo* models that reflect subclonal heterogeneity and could recapitulate subclonal dynamics, such as the CLL xenograft models developed by our group and used in my ATR inhibitor study, are particularly useful for this purpose (Davies et al., 2017). Likewise, sequential assessment of the CLL subclonal composition may be a useful component within future clinical trials.

6.4. Unanswered questions and future work

The findings described in this thesis generate several interesting questions which provide several ideas for future work.

Firstly, my analysis of the spontaneous regression CLL cohort show that spontaneous regression was associated with only partial recovery of normal T cell phenotype, with patients who have undergone spontaneous CLL regression still exhibiting features such as CD4:CD8 inversion and high T cell PD-1 expression compared to age-matched healthy controls. Likewise, although treatment with BCR signalling inhibitors such as ibrutinib result in improvement in T cell phenotype and function, most of the published studies do not include healthy controls as comparators (Long et al., 2017; Niemann et al., 2016), and therefore it cannot be ascertained whether this represents a complete or partial normalisation. It is likely that the persistence of T cell dysfunction could be related to the persistence of CLL MRD, given the direct effect CLL cells exert on autologous T cells (Gorgun et al., 2005; Ramsay et al., 2008). It will be of interest to determine whether the eradication of MRD leads to normalisation of T cell phenotype and function.

Secondly, results from the spontaneous CLL regression study suggest a model in which clonal anergy, reduced CLL cell trafficking and possibly also the extrinsic apoptotic pathway co-operates in mediating disease regression. Further functional analyses, highlighted in sections 3.2.3 and 3.2.5, will be required to confirm this model. In addition, there may be other, as yet unidentified, features and potential mechanisms underpinning spontaneous regression in CLL. The transcriptomic analysis, currently underway, can potentially identify other pathways or processes that may be implicated in spontaneous CLL regression. Alternatively, there may be differences between spontaneous regression and non-regressing CLL cases at an epigenetic level that could potentially be investigated.

Thirdly, *TP53*/*ATM* wild-type CLL exhibit variable sensitivity to ATR inhibition, with several cases displaying sensitivity levels that were similar to that of *TP53*/*ATM* defective CLL. It is likely that there are markers of sensitivity to ATR inhibition in CLL other than *TP53* or *ATM* defects. It will be of interest, for instance, to explore whether sensitivity of CLL cells to ATR inhibition correlate with the level of endogenous replication stress, as assessed by the level of 53BP1 bodies or by DNA fibre analysis, and whether this also correlate with the level of Myc expression. The effect of mutations such as those affecting *ARID1A* on sensitivity to ATR inhibition could also be explored. Moreover, the combination of ATR inhibition with other therapeutic modalities such as PARP inhibitor or venetoclax has not been investigated in the current study, and could be an important area for future work. Additionally, there are currently plans to initiate early-phase trials of AZD6738 on patients with *TP53* or *ATM* defective CLL. It will be important to incorporate correlative biological studies within these trials. For instance, the mutant allele frequency of *TP53* or *ATM* in these patients should be monitored during the course of AZD6738 treatment.

Finally, although my study confirmed the long-term independent prognostic significance of MRD in CLL, the significance of MRD with novel targeted therapies such as venetoclax is unclear. It will be of importance to assess the prognostic impact of MRD with each novel therapeutic agent, be it venetoclax or any other novel treatment that is being evaluated in CLL.

APPENDICES

Appendix 1: List of antibodies used for flow cytometry

Antibody	Clone	Source	Catalogue No	Vol per sample/µl
Bcl2	Bcl-2/100	BD Biosciences	563600	1
CD10	HI10a	BD Biosciences	332777	5
CD184/CXCR4	12G5	BD Biosciences	562448	1
CD185/CXCR5	RF8B2	BD Biosciences	563105	1
CD19	SJ25C1	BD Biosciences	332780	5
CD196/CCR6	11A9	BD Biosciences	562515	1
CD197/CCR7	3D12	BD Biosciences	563449	1
CD20	L27	BD Biosciences	641414	5
CD27	M-T271	BD Biosciences	560609	1
CD3	HIT3a	Biolegend	300330	3
CD305/LAIR1	DX26	BD Biosciences	550811	5
CD38	HB7	BD Biosciences	335825	1
CD4	SK3	BD Biosciences	332772	5
CD43	1G10	BD Biosciences	563377	1
CD45RA	HI100	BD Biosciences	562298	5
CD49d	44H6	Abd Serotec	MCA923F	5
CD5	L17F12	BD Biosciences	348810	1
CD62L	DREG-56	BD Biosciences	555544	5
CD79b	CB3-1	Coulter	IM1612	5
CD8	SK1	BD Biosciences	560179	5
CD81	JS-81	BD Biosciences	551108	5
CD95	DX2	BD Biosciences	562616	1
IgD	IA6-2	BD Biosciences	555779	5
IgG	G18-145	BD Biosciences	555786	5
IgM	G20-127	BD Biosciences	551062	7.5
Ki-67	B56	BD Biosciences	558616	5
Mcl-1	Y37	Abcam	AB197035	1
PD-1	EH12.2H7	Biolegend	329952	3
ROR1	2A2	Miltenyi Biotec	130-098-320	5
ZAP70	1E7.2	BD Biosciences	344635	20

Appendix 2: List of antibodies used for Western Blotting

Antibody	Source	Catalogue No	Animal	Dilution	Size/kDa
Actin	Sigma	A2228	Mouse	1:50000	42
ATM P-Ser1981	R&D	AF1655	Rabbit	1:250	350
ATM Total	Abcam	ab78	Mouse	1:1000	350
ATR Total	Santa Cruz	sc-1887	Goat	1:1000	250
Caspase 7	Cell Signaling	9494	Mouse	1:1000	35/30
Chk1 P-Ser345	Cell Signaling	2341	Rabbit	1:1000	56
Chk1 Total	Santa Cruz	sc-8408	Mouse	1:1000	56
Chk2 P-Thr68	Cell Signaling	2661	Rabbit	1:1000	56
Chk2 Total	Cell Signaling	sc-5278	Rabbit	1:1000	62
Cyclin A	Thermo Scientific	MS-1061	Mouse	1:1000	60
Erk P-Thr202/204	Cell Signaling	9101	Rabbit	1:1000	42/44
Erk Total	Cell Signaling	9102	Rabbit	1:1000	42/44
p53	In-house	n/a	Mouse	1:10	53
PARP	Cell Signaling	9532	Rabbit	1:1000	116/89
SMC1	Bethyl	A300-055A	Rabbit	1:1000	160
Syk P-Tyr525/526	Cell Signaling	2711	Rabbit	1:1000	72
Syk Total	Cell Signaling	2712	Rabbit	1:1000	72

Appendix 3: List of antibodies used for immunofluorescence microscopy

Antibody	Source	Catalogue No	Animal	Dilution
γH2AX	Millipore	05-636	Mouse	1:1000
53BP1	Santa-Cruz	sc-22760	Rabbit	1:1000
Cyclin A	Santa-Cruz	sc-596-G	Goat	1:50
Lamin B	Santa-Cruz	sc-6216	Goat	1:200
P-Histone H3 Ser-10	Cell Signaling	9701	Rabbit	1:100

REFERENCES

Abraham, R.T. (2001). Cell cycle checkpoint signaling through the ATM and ATR kinases. Genes Dev *15*, 2177-2196.

Abrisqueta, P., Villamor, N., Terol, M.J., Gonzalez-Barca, E., Gonzalez, M., Ferra, C., Abella, E., Delgado, J., Garcia-Marco, J.A., Gonzalez, Y.*, et al.* (2013). Rituximab maintenance after first-line therapy with rituximab, fludarabine, cyclophosphamide, and mitoxantrone (R-FCM) for chronic lymphocytic leukemia. Blood *122*, 3951-3959.

Adachi, T., Wienands, J., Wakabayashi, C., Yakura, H., Reth, M., and Tsubata, T. (2001). SHP-1 requires inhibitory co-receptors to down-modulate B cell antigen receptor-mediated phosphorylation of cellular substrates. J Biol Chem *276*, 26648-26655.

Agathangelidis, A., Darzentas, N., Hadzidimitriou, A., Brochet, X., Murray, F., Yan, X.J., Davis, Z., van Gastel-Mol, E.J., Tresoldi, C., Chu, C.C.*, et al.* (2012). Stereotyped B-cell receptors in one-third of chronic lymphocytic leukemia: a molecular classification with implications for targeted therapies. Blood *119*, 4467-4475.

Alexandrov, L.B., Nik-Zainal, S., Wedge, D.C., Aparicio, S.A., Behjati, S., Biankin, A.V., Bignell, G.R., Bolli, N., Borg, A., Borresen-Dale, A.L.*, et al.* (2013). Signatures of mutational processes in human cancer. Nature *500*, 415-421.

Almazi, J.G., Mactier, S., Best, O.G., Crossett, B., Mulligan, S.P., and Christopherson, R.I. (2012). Fludarabine nucleoside induces accumulations of p53, p63 and p73 in the nuclei of human B-lymphoid cell lines, with cytosolic and mitochondrial increases in p53. Proteomics Clin Appl *6*, 279-290.

Amaral, J.D., Xavier, J.M., Steer, C.J., and Rodrigues, C.M. (2010). The role of p53 in apoptosis. Discov Med *9*, 145-152.

Anderson, L.W., Chen, T.L., Colvin, O.M., Grochow, L.B., Collins, J.M., Kennedy, M.J., and Strong, J.M. (1996). Cyclophosphamide and 4-Hydroxycyclophosphamide/aldophosphamide kinetics in patients receiving high-dose cyclophosphamide chemotherapy. Clin Cancer Res *2*, 1481-1487.

Anderson, M.A., Tam, C., Lew, T.E., Juneja, S., Juneja, M., Westerman, D., Wall, M., Lade, S., Gorelik, A., Huang, D.C.S.*, et al.* (2017). Clinico-pathological features and outcomes of progression of CLL on the BCL2 inhibitor venetoclax. Blood.

Austen, B., Powell, J.E., Alvi, A., Edwards, I., Hooper, L., Starczynski, J., Taylor, A.M., Fegan, C., Moss, P., and Stankovic, T. (2005). Mutations in the ATM gene lead to impaired overall and treatment-free survival that is independent of IGVH mutation status in patients with B-CLL. Blood *106*, 3175-3182.

Austen, B., Skowronska, A., Baker, C., Powell, J.E., Gardiner, A., Oscier, D., Majid, A., Dyer, M., Siebert, R., Taylor, A.M.*, et al.* (2007). Mutation status of the residual ATM allele is an important determinant of the cellular response to chemotherapy and survival in patients with chronic lymphocytic leukemia containing an 11q deletion. J Clin Oncol *25*, 5448-5457.

Awan, F.T., Kay, N.E., Davis, M.E., Wu, W., Geyer, S.M., Leung, N., Jelinek, D.F., Tschumper, R.C., Secreto, C.R., Lin, T.S.*, et al.* (2009). Mcl-1 expression predicts progression-free survival in chronic lymphocytic leukemia patients treated with pentostatin, cyclophosphamide, and rituximab. Blood *113*, 535-537.

Awasthi, P., Foiani, M., and Kumar, A. (2016). ATM and ATR signaling at a glance. J Cell Sci *129*, 1285.

Bagnara, D., Kaufman, M.S., Calissano, C., Marsilio, S., Patten, P.E., Simone, R., Chum, P., Yan, X.J., Allen, S.L., Kolitz, J.E.*, et al.* (2011). A novel adoptive transfer model of chronic lymphocytic leukemia suggests a key role for T lymphocytes in the disease. Blood *117*, 5463-5472.

Balakrishnan, K., Peluso, M., Fu, M., Rosin, N.Y., Burger, J.A., Wierda, W.G., Keating, M.J., Faia, K., O'Brien, S., Kutok, J.L.*, et al.* (2015). The phosphoinositide-3-kinase (PI3K)-delta and gamma inhibitor, IPI-145 (Duvelisib), overcomes signals from the PI3K/AKT/S6 pathway and promotes apoptosis in CLL. Leukemia *29*, 1811-1822.

Baliakas, P., Hadzidimitriou, A., Sutton, L.A., Minga, E., Agathangelidis, A., Nichelatti, M., Tsanousa, A., Scarfo, L., Davis, Z., Yan, X.J.*, et al.* (2014). Clinical effect of stereotyped B-cell receptor immunoglobulins in chronic lymphocytic leukaemia: a retrospective multicentre study. Lancet Haematol *1*, e74-84.

Baliakas, P., Hadzidimitriou, A., Sutton, L.A., Rossi, D., Minga, E., Villamor, N., Larrayoz, M., Kminkova, J., Agathangelidis, A., Davis, Z.*, et al.* (2015). Recurrent mutations refine prognosis in chronic lymphocytic leukemia. Leukemia *29*, 329-336.

Barrio, S., Shanafelt, T.D., Ojha, J., Chaffee, K.G., Secreto, C., Kortum, K.M., Pathangey, S., Van-Dyke, D.L., Slager, S.L., Fonseca, R.*, et al.* (2017). Genomic characterization of high-count MBL cases indicates that early detection of driver mutations and subclonal expansion are predictors of adverse clinical outcome. Leukemia *31*, 170-176.

Bass, T.E., Luzwick, J.W., Kavanaugh, G., Carroll, C., Dungrawala, H., Glick, G.G., Feldkamp, M.D., Putney, R., Chazin, W.J., and Cortez, D. (2016). ETAA1 acts at stalled replication forks to maintain genome integrity. Nat Cell Biol *18*, 1185-1195.

Berti, M., and Vindigni, A. (2016). Replication stress: getting back on track. Nat Struct Mol Biol *23*, 103-109.

Bieging, K.T., Mello, S.S., and Attardi, L.D. (2014). Unravelling mechanisms of p53-mediated tumour suppression. Nat Rev Cancer *14*, 359-370.

Binet, J.L., Auquier, A., Dighiero, G., Chastang, C., Piguet, H., Goasguen, J., Vaugier, G., Potron, G., Colona, P., Oberling, F.*, et al.* (1981). A new prognostic classification of chronic lymphocytic leukemia derived from a multivariate survival analysis. Cancer *48*, 198-206.

Biton, S., Dar, I., Mittelman, L., Pereg, Y., Barzilai, A., and Shiloh, Y. (2006). Nuclear ataxia-telangiectasia mutated (ATM) mediates the cellular response to DNA double strand breaks in human neuron-like cells. J Biol Chem *281*, 17482-17491.

Blankenstein, T., Coulie, P.G., Gilboa, E., and Jaffee, E.M. (2012). The determinants of tumour immunogenicity. Nat Rev Cancer *12*, 307-313.

Bogner, C., Sandherr, M., Perker, M., Weick, K., Ringshausen, I., Peschel, C., and Decker, T. (2006). Cyclin E but not bcl-2, bax or mcl-1 is differentially expressed in ZAP 70-positive and ZAP 70-negative B-CLL cells. Ann Hematol *85*, 458-462.

Bosch, F., Ferrer, A., Villamor, N., Gonzalez, M., Briones, J., Gonzalez-Barca, E., Abella, E., Gardella, S., Escoda, L., Perez-Ceballos, E.*, et al.* (2008). Fludarabine, cyclophosphamide, and mitoxantrone as initial therapy of chronic lymphocytic leukemia: high response rate and disease eradication. Clin Cancer Res *14*, 155-161.

Bottcher, S., Ritgen, M., Fischer, K., Stilgenbauer, S., Busch, R.M., Fingerle-Rowson, G., Fink, A.M., Buhler, A., Zenz, T., Wenger, M.K.*, et al.* (2012). Minimal residual disease quantification is an independent predictor of progression-free and overall survival in chronic lymphocytic leukemia: a multivariate analysis from the randomized GCLLSG CLL8 trial. J Clin Oncol *30*, 980-988.

Brachtl, G., Pinon Hofbauer, J., Greil, R., and Hartmann, T.N. (2014). The pathogenic relevance of the prognostic markers CD38 and CD49d in chronic lymphocytic leukemia. Ann Hematol *93*, 361-374.

Brachtl, G., Sahakyan, K., Denk, U., Girbl, T., Alinger, B., Hofbauer, S.W., Neureiter, D., Hofbauer, J.P., Egle, A., Greil, R.*, et al.* (2011). Differential bone marrow homing capacity of VLA-4 and CD38 high expressing chronic lymphocytic leukemia cells. PLoS One *6*, e23758.

Bradford, M.M. (1976). A rapid and sensitive method for the quantitation of microgram quantities of protein utilizing the principle of protein-dye binding. Anal Biochem *72*, 248-254.

Brodeur, G.M., and Bagatell, R. (2014). Mechanisms of neuroblastoma regression. Nat Rev Clin Oncol *11*, 704-713.

Brown, E.J., and Baltimore, D. (2003). Essential and dispensable roles of ATR in cell cycle arrest and genome maintenance. Genes Dev *17*, 615-628.

Buisson, R., Boisvert, J.L., Benes, C.H., and Zou, L. (2015). Distinct but Concerted Roles of ATR, DNA-PK, and Chk1 in Countering Replication Stress during S Phase. Mol Cell *59*, 1011-1024.

Bulian, P., Shanafelt, T.D., Fegan, C., Zucchetto, A., Cro, L., Nuckel, H., Baldini, L., Kurtova, A.V., Ferrajoli, A., Burger, J.A.*, et al.* (2014). CD49d is the strongest flow cytometry-based predictor of overall survival in chronic lymphocytic leukemia. J Clin Oncol *32*, 897-904.

Burger, J.A. (2011). Nurture versus nature: the microenvironment in chronic lymphocytic leukemia. Hematology Am Soc Hematol Educ Program *2011*, 96-103.

Burger, J.A., Keating, M.J., Wierda, W.G., Hartmann, E., Hoellenriegel, J., Rosin, N.Y., de Weerdt, I., Jeyakumar, G., Ferrajoli, A., Cardenas-Turanzas, M.*, et al.* (2014). Safety and activity of ibrutinib plus rituximab for patients with high-risk chronic lymphocytic leukaemia: a single-arm, phase 2 study. Lancet Oncol *15*, 1090-1099.

Burger, J.A., Landau, D.A., Taylor-Weiner, A., Bozic, I., Zhang, H., Sarosiek, K., Wang, L., Stewart, C., Fan, J., Hoellenriegel, J.*, et al.* (2016). Clonal evolution in patients with chronic lymphocytic leukaemia developing resistance to BTK inhibition. Nat Commun *7*, 11589.

Burger, J.A., Tedeschi, A., Barr, P.M., Robak, T., Owen, C., Ghia, P., Bairey, O., Hillmen, P., Bartlett, N.L., Li, J.*, et al.* (2015). Ibrutinib as Initial Therapy for Patients with Chronic Lymphocytic Leukemia. N Engl J Med *373*, 2425-2437.

Burger, J.A., Tsukada, N., Burger, M., Zvaifler, N.J., Dell'Aquila, M., and Kipps, T.J. (2000). Blood-derived nurse-like cells protect chronic lymphocytic leukemia B cells from spontaneous apoptosis through stromal cell-derived factor-1. Blood *96*, 2655-2663.

Burgess, M., Gill, D., Singhania, R., Cheung, C., Chambers, L., Renyolds, B.A., Smith, L., Mollee, P., Saunders, N., and McMillan, N.A. (2013). CD62L as a therapeutic target in chronic lymphocytic leukemia. Clin Cancer Res *19*, 5675-5685.

Burkle, A., Niedermeier, M., Schmitt-Graff, A., Wierda, W.G., Keating, M.J., and Burger, J.A. (2007). Overexpression of the CXCR5 chemokine receptor, and its ligand, CXCL13 in B-cell chronic lymphocytic leukemia. Blood *110*, 3316-3325.

Byrd, J.C., Brown, J.R., O'Brien, S., Barrientos, J.C., Kay, N.E., Reddy, N.M., Coutre, S., Tam, C.S., Mulligan, S.P., Jaeger, U.*, et al.* (2014). Ibrutinib versus ofatumumab in previously treated chronic lymphoid leukemia. N Engl J Med *371*, 213-223.

Byrd, J.C., Furman, R.R., Coutre, S.E., Burger, J.A., Blum, K.A., Coleman, M., Wierda, W.G., Jones, J.A., Zhao, W., Heerema, N.A.*, et al.* (2015). Three-year follow-up of treatment-naive and previously treated patients with CLL and SLL receiving single-agent ibrutinib. Blood *125*, 2497-2506.

Byrd, J.C., Furman, R.R., Coutre, S.E., Flinn, I.W., Burger, J.A., Blum, K.A., Grant, B., Sharman, J.P., Coleman, M., Wierda, W.G.*, et al.* (2013). Targeting BTK with ibrutinib in relapsed chronic lymphocytic leukemia. N Engl J Med *369*, 32-42.

Byrd, J.C., Harrington, B., O'Brien, S., Jones, J.A., Schuh, A., Devereux, S., Chaves, J., Wierda, W.G., Awan, F.T., Brown, J.R.*, et al.* (2016). Acalabrutinib (ACP-196) in Relapsed Chronic Lymphocytic Leukemia. N Engl J Med *374*, 323-332.

Bystry, V., Agathangelidis, A., Bikos, V., Sutton, L.A., Baliakas, P., Hadzidimitriou, A., Stamatopoulos, K., Darzentas, N., and European Research Initiative on, C.L.L. (2015). ARResT/AssignSubsets: a novel application for robust subclassification of chronic lymphocytic leukemia based on B cell receptor IG stereotypy. Bioinformatics *31*, 3844-3846.

Cabezudo, E., Matutes, E., Ramrattan, M., Morilla, R., and Catovsky, D. (1997). Analysis of residual disease in chronic lymphocytic leukemia by flow cytometry. Leukemia *11*, 1909-1914.

Calin, G.A., Cimmino, A., Fabbri, M., Ferracin, M., Wojcik, S.E., Shimizu, M., Taccioli, C., Zanesi, N., Garzon, R., Aqeilan, R.I.*, et al.* (2008). MiR-15a and miR-16-1 cluster functions in human leukemia. Proc Natl Acad Sci U S A *105*, 5166-5171.

Calin, G.A., Dumitru, C.D., Shimizu, M., Bichi, R., Zupo, S., Noch, E., Aldler, H., Rattan, S., Keating, M., Rai, K.*, et al.* (2002). Frequent deletions and down-regulation of micro- RNA genes miR15 and miR16 at 13q14 in chronic lymphocytic leukemia. Proc Natl Acad Sci U S A *99*, 15524-15529.

Calin, G.A., Ferracin, M., Cimmino, A., Di Leva, G., Shimizu, M., Wojcik, S.E., Iorio, M.V., Visone, R., Sever, N.I., Fabbri, M.*, et al.* (2005). A MicroRNA signature associated with prognosis and progression in chronic lymphocytic leukemia. N Engl J Med *353*, 1793-1801.

Calissano, C., Damle, R.N., Hayes, G., Murphy, E.J., Hellerstein, M.K., Moreno, C., Sison, C., Kaufman, M.S., Kolitz, J.E., Allen, S.L.*, et al.* (2009). In vivo intraclonal and interclonal kinetic heterogeneity in B-cell chronic lymphocytic leukemia. Blood *114*, 4832-4842.

Calissano, C., Damle, R.N., Marsilio, S., Yan, X.J., Yancopoulos, S., Hayes, G., Emson, C., Murphy, E.J., Hellerstein, M.K., Sison, C.*, et al.* (2011). Intraclonal complexity in chronic lymphocytic leukemia: fractions enriched in recently born/divided and older/quiescent cells. Mol Med *17*, 1374-1382.

Cambier, J.C., Gauld, S.B., Merrell, K.T., and Vilen, B.J. (2007). B-cell anergy: from transgenic models to naturally occurring anergic B cells? Nat Rev Immunol *7*, 633-643.

Castedo, M., Perfettini, J.L., Roumier, T., Andreau, K., Medema, R., and Kroemer, G. (2004). Cell death by mitotic catastrophe: a molecular definition. Oncogene *23*, 2825-2837.

Catovsky, D., Richards, S., Matutes, E., Oscier, D., Dyer, M.J., Bezares, R.F., Pettitt, A.R., Hamblin, T., Milligan, D.W., Child, J.A.*, et al.* (2007). Assessment of fludarabine plus cyclophosphamide for patients with chronic lymphocytic leukaemia (the LRF CLL4 Trial): a randomised controlled trial. Lancet *370*, 230-239.

Chakraborty, M., Qiu, S.G., Vasudevan, K.M., and Rangnekar, V.M. (2001). Par-4 drives trafficking and activation of Fas and Fasl to induce prostate cancer cell apoptosis and tumor regression. Cancer Res *61*, 7255-7263.

Charrier, J.D., Durrant, S.J., Golec, J.M., Kay, D.P., Knegtel, R.M., MacCormick, S., Mortimore, M., O'Donnell, M.E., Pinder, J.L., Reaper, P.M.*, et al.* (2011). Discovery of potent and selective inhibitors of ataxia telangiectasia mutated and Rad3 related (ATR) protein kinase as potential anticancer agents. J Med Chem *54*, 2320-2330.

Chen, L., Apgar, J., Huynh, L., Dicker, F., Giago-McGahan, T., Rassenti, L., Weiss, A., and Kipps, T.J. (2005). ZAP-70 directly enhances IgM signaling in chronic lymphocytic leukemia. Blood *105*, 2036-2041.

Chen, L., Widhopf, G., Huynh, L., Rassenti, L., Rai, K.R., Weiss, A., and Kipps, T.J. (2002). Expression of ZAP-70 is associated with increased B-cell receptor signaling in chronic lymphocytic leukemia. Blood *100*, 4609-4614.

Chen, Y.H., Jones, M.J., Yin, Y., Crist, S.B., Colnaghi, L., Sims, R.J., 3rd, Rothenberg, E., Jallepalli, P.V., and Huang, T.T. (2015). ATR-mediated phosphorylation of FANCI regulates dormant origin firing in response to replication stress. Mol Cell *58*, 323-338.

Chigrinova, E., Rinaldi, A., Kwee, I., Rossi, D., Rancoita, P.M., Strefford, J.C., Oscier, D., Stamatopoulos, K., Papadaki, T., Berger, F.*, et al.* (2013). Two main genetic pathways lead to the transformation of chronic lymphocytic leukemia to Richter syndrome. Blood *122*, 2673-2682.

Chiorazzi, N., Rai, K.R., and Ferrarini, M. (2005). Chronic lymphocytic leukemia. N Engl J Med *352*, 804-815.

Chng, W.J., Price-Troska, T., Gonzalez-Paz, N., Van Wier, S., Jacobus, S., Blood, E., Henderson, K., Oken, M., Van Ness, B., Greipp, P.*, et al.* (2007). Clinical significance of TP53 mutation in myeloma. Leukemia *21*, 582-584.

Choi, J.W., Lee, J.S., Kim, S.W., and Yun, C.O. (2012). Evolution of oncolytic adenovirus for cancer treatment. Adv Drug Deliv Rev *64*, 720-729.

Chou, T.C., and Talalay, P. (1984). Quantitative analysis of dose-effect relationships: the combined effects of multiple drugs or enzyme inhibitors. Adv Enzyme Regul *22*, 27-55.

Christopoulos, P., Pfeifer, D., Bartholome, K., Follo, M., Timmer, J., Fisch, P., and Veelken, H. (2011). Definition and characterization of the systemic T-cell dysregulation in untreated indolent B-cell lymphoma and very early CLL. Blood *117*, 3836-3846.

Chu, P., Deforce, D., Pedersen, I.M., Kim, Y., Kitada, S., Reed, J.C., and Kipps, T.J. (2002). Latent sensitivity to Fas-mediated apoptosis after CD40 ligation may explain activity of CD154 gene therapy in chronic lymphocytic leukemia. Proc Natl Acad Sci U S A *99*, 3854-3859.

Ciccia, A., and Elledge, S.J. (2010). The DNA damage response: making it safe to play with knives. Mol Cell *40*, 179-204.

Cimmino, A., Calin, G.A., Fabbri, M., Iorio, M.V., Ferracin, M., Shimizu, M., Wojcik, S.E., Aqeilan, R.I., Zupo, S., Dono, M.*, et al.* (2005). miR-15 and miR-16 induce apoptosis by targeting BCL2. Proc Natl Acad Sci U S A *102*, 13944-13949.

Cimprich, K.A., and Cortez, D. (2008). ATR: an essential regulator of genome integrity. Nat Rev Mol Cell Biol *9*, 616-627.

Coelho, V., Krysov, S., Steele, A., Sanchez Hidalgo, M., Johnson, P.W., Chana, P.S., Packham, G., Stevenson, F.K., and Forconi, F. (2013). Identification in CLL of circulating intraclonal subgroups with varying B-cell receptor expression and function. Blood *122*, 2664-2672.

Compagno, M., Wang, Q., Pighi, C., Cheong, T.C., Meng, F.L., Poggio, T., Yeap, L.S., Karaca, E., Blasco, R.B., Langellotto, F.*, et al.* (2017). Phosphatidylinositol 3-kinase delta blockade increases genomic instability in B cells. Nature *542*, 489-493.

Cooper, M.D. (2015). The early history of B cells. Nat Rev Immunol *15*, 191-197.

Cotta-Ramusino, C., McDonald, E.R., 3rd, Hurov, K., Sowa, M.E., Harper, J.W., and Elledge, S.J. (2011). A DNA damage response screen identifies RHINO, a 9-1-1 and TopBP1 interacting protein required for ATR signaling. Science *332*, 1313-1317.

Cottini, F., Hideshima, T., Suzuki, R., Tai, Y.T., Bianchini, G., Richardson, P.G., Anderson, K.C., and Tonon, G. (2015). Synthetic Lethal Approaches Exploiting DNA Damage in Aggressive Myeloma. Cancer Discov *5*, 972-987.

Couch, F.B., Bansbach, C.E., Driscoll, R., Luzwick, J.W., Glick, G.G., Betous, R., Carroll, C.M., Jung, S.Y., Qin, J., Cimprich, K.A.*, et al.* (2013). ATR phosphorylates SMARCAL1 to prevent replication fork collapse. Genes Dev *27*, 1610-1623.

Cremona, C.A., and Behrens, A. (2014). ATM signalling and cancer. Oncogene *33*, 3351-3360.

Crespo, M., Bosch, F., Villamor, N., Bellosillo, B., Colomer, D., Rozman, M., Marce, S., Lopez-Guillermo, A., Campo, E., and Montserrat, E. (2003). ZAP-70 expression as a surrogate for immunoglobulin-variable-region mutations in chronic lymphocytic leukemia. N Engl J Med *348*, 1764-1775.

Cui, B., Ghia, E.M., Chen, L., Rassenti, L.Z., DeBoever, C., Widhopf, G.F., 2nd, Yu, J., Neuberg, D.S., Wierda, W.G., Rai, K.R.*, et al.* (2016). High-level ROR1 associates with accelerated disease progression in chronic lymphocytic leukemia. Blood *128*, 2931-2940.

D'Avola, A., Drennan, S., Tracy, I., Henderson, I., Chiecchio, L., Larrayoz, M., Rose-Zerilli, M., Strefford, J., Plass, C., Johnson, P.W.*, et al.* (2016). Surface IgM expression and function are associated with clinical behavior, genetic abnormalities, and DNA methylation in CLL. Blood *128*, 816-826.

Daccache, A., Kizhakekuttu, T., Siebert, J., and Veeder, M. (2007). Hematologic and cytogenetic spontaneous remission in acute monocytic leukemia (FAB M5b) with trisomy 8. J Clin Oncol *25*, 344-346.

Damle, R.N., Banapour, T., Sison, C., Allen, S.L., Rai, K.R., and Chiorazzi, N. (2005). Evidence for alternative lengthening of telomeres in chronic lymphocytic leukemia patients [abstract]. Blood *106*, Abstract 1179.

Damle, R.N., Batliwalla, F.M., Ghiotto, F., Valetto, A., Albesiano, E., Sison, C., Allen, S.L., Kolitz, J., Vinciguerra, V.P., Kudalkar, P.*, et al.* (2004). Telomere length and telomerase activity delineate distinctive replicative features of the B-CLL subgroups defined by immunoglobulin V gene mutations. Blood *103*, 375-382.

Damle, R.N., Temburni, S., Banapour, T., Paul, S., Mongini, P.K., Allen, S.L., Kolitz, J.E., Rai, K.R., and Chiorazzi, N. (2012). T-cell independent, B-cell receptor-mediated induction of telomerase activity differs among IGHV mutation-based subgroups of chronic lymphocytic leukemia patients. Blood *120*, 2438-2449.

Damle, R.N., Temburni, S., Calissano, C., Yancopoulos, S., Banapour, T., Sison, C., Allen, S.L., Rai, K.R., and Chiorazzi, N. (2007). CD38 expression labels an activated subset within chronic lymphocytic leukemia clones enriched in proliferating B cells. Blood *110*, 3352-3359.

Damle, R.N., Wasil, T., Fais, F., Ghiotto, F., Valetto, A., Allen, S.L., Buchbinder, A., Budman, D., Dittmar, K., Kolitz, J.*, et al.* (1999). Ig V gene mutation status and CD38 expression as novel prognostic indicators in chronic lymphocytic leukemia. Blood *94*, 1840-1847.

Damm, F., Mylonas, E., Cosson, A., Yoshida, K., Della Valle, V., Mouly, E., Diop, M., Scourzic, L., Shiraishi, Y., Chiba, K.*, et al.* (2014). Acquired initiating mutations in early hematopoietic cells of CLL patients. Cancer Discov *4*, 1088-1101.

Davies, N.J., Kwok, M., Gould, C., Oldreive, C.E., Mao, J., Parry, H., Smith, E., Agathanggelou, A., Pratt, G., Taylor, A.M.R.*, et al.* (2017). Dynamic changes in clonal cytogenetic architecture during progression of chronic lymphocytic leukemia in patients and patient-derived murine xenografts. Oncotarget.

de Gorter, D.J., Beuling, E.A., Kersseboom, R., Middendorp, S., van Gils, J.M., Hendriks, R.W., Pals, S.T., and Spaargaren, M. (2007). Bruton's tyrosine kinase and phospholipase Cgamma2 mediate chemokine-controlled B cell migration and homing. Immunity *26*, 93-104.

de Klein, A., Muijtjens, M., van Os, R., Verhoeven, Y., Smit, B., Carr, A.M., Lehmann, A.R., and Hoeijmakers, J.H. (2000). Targeted disruption of the cell-cycle checkpoint gene ATR leads to early embryonic lethality in mice. Curr Biol *10*, 479-482.

De Silva, N.S., and Klein, U. (2015). Dynamics of B cells in germinal centres. Nat Rev Immunol *15*, 137-148.

Decker, T., Hipp, S., Hahntow, I., Schneller, F., and Peschel, C. (2004). Expression of cyclin E in resting and activated B-chronic lymphocytic leukaemia cells: cyclin E/cdk2 as a potential therapeutic target. Br J Haematol *125*, 141-148.

Del Giudice, I., Chiaretti, S., Santangelo, S., Tavolaro, S., Peragine, N., Marinelli, M., Ilari, C., Raponi, S., Messina, M., Nanni, M.*, et al.* (2014). Stereotyped subset #1 chronic lymphocytic leukemia: a direct link between B-cell receptor structure, function, and patients' prognosis. Am J Hematol *89*, 74-82.

Del Giudice, I., Chiaretti, S., Tavolaro, S., De Propris, M.S., Maggio, R., Mancini, F., Peragine, N., Santangelo, S., Marinelli, M., Mauro, F.R.*, et al.* (2009). Spontaneous regression of chronic lymphocytic leukemia: clinical and biologic features of 9 cases. Blood *114*, 638-646.

Del Poeta, G., Maurillo, L., Venditti, A., Buccisano, F., Epiceno, A.M., Capelli, G., Tamburini, A., Suppo, G., Battaglia, A., Del Principe, M.I.*, et al.* (2001). Clinical significance of CD38 expression in chronic lymphocytic leukemia. Blood *98*, 2633-2639.

Dicker, F., Kater, A.P., Fukuda, T., and Kipps, T.J. (2005). Fas-ligand (CD178) and TRAIL synergistically induce apoptosis of CD40-activated chronic lymphocytic leukemia B cells. Blood *105*, 3193-3198.

Diede, S.J. (2014). Spontaneous regression of metastatic cancer: learning from neuroblastoma. Nat Rev Cancer *14*, 71-72.

Dimri, G.P., Lee, X., Basile, G., Acosta, M., Scott, G., Roskelley, C., Medrano, E.E., Linskens, M., Rubelj, I., Pereira-Smith, O.*, et al.* (1995). A biomarker that identifies senescent human cells in culture and in aging skin in vivo. Proc Natl Acad Sci U S A *92*, 9363-9367.

Dohner, H., Stilgenbauer, S., Benner, A., Leupolt, E., Krober, A., Bullinger, L., Dohner, K., Bentz, M., and Lichter, P. (2000). Genomic aberrations and survival in chronic lymphocytic leukemia. N Engl J Med *343*, 1910-1916.

Drach, J., Ackermann, J., Fritz, E., Kromer, E., Schuster, R., Gisslinger, H., DeSantis, M., Zojer, N., Fiegl, M., Roka, S.*, et al.* (1998). Presence of a p53 gene deletion in patients with multiple myeloma predicts for short survival after conventional-dose chemotherapy. Blood *92*, 802-809.

Dreger, P., Dohner, H., Ritgen, M., Bottcher, S., Busch, R., Dietrich, S., Bunjes, D., Cohen, S., Schubert, J., Hegenbart, U.*, et al.* (2010). Allogeneic stem cell transplantation provides durable disease control in poor-risk chronic lymphocytic leukemia: long-term clinical and MRD results of the German CLL Study Group CLL3X trial. Blood *116*, 2438-2447.

Duhren-von Minden, M., Ubelhart, R., Schneider, D., Wossning, T., Bach, M.P., Buchner, M., Hofmann, D., Surova, E., Follo, M., Kohler, F.*, et al.* (2012). Chronic lymphocytic leukaemia is driven by antigen-independent cell-autonomous signalling. Nature *489*, 309-312.

Durig, J., Schmucker, U., and Duhrsen, U. (2001). Differential expression of chemokine receptors in B cell malignancies. Leukemia *15*, 752-756.

Eichhorst, B.F., Schetelig, J., Coutre, S., Seymour, J.F., Munir, T., Puvvada, S.D., Wendtner, C.-M., Roberts, A.W., Jurczak, W., Mulligan, S.*, et al.* (2015). Venetoclax (ABT-199/GDC-0199) Monotherapy Induces Deep Remissions, Including Complete Remission and Undetectable MRD, in Ultra-High Risk Relapsed/Refractory Chronic Lymphocytic Leukemia with 17p Deletion: Results of the Pivotal International Phase 2 Study. Blood *126*, LBA-6-LBA-6.

Fabbri, G., and Dalla-Favera, R. (2016). The molecular pathogenesis of chronic lymphocytic leukaemia. Nat Rev Cancer *16*, 145-162.

Fabbri, G., Khiabanian, H., Holmes, A.B., Wang, J., Messina, M., Mullighan, C.G., Pasqualucci, L., Rabadan, R., and Dalla-Favera, R. (2013). Genetic lesions associated with chronic lymphocytic leukemia transformation to Richter syndrome. J Exp Med *210*, 2273-2288.

Faderl, S., Keating, M.J., Do, K.A., Liang, S.Y., Kantarjian, H.M., O'Brien, S., Garcia-Manero, G., Manshouri, T., and Albitar, M. (2002). Expression profile of 11 proteins and their prognostic significance in patients with chronic lymphocytic leukemia (CLL). Leukemia *16*, 1045-1052.

Fais, F., Ghiotto, F., Hashimoto, S., Sellars, B., Valetto, A., Allen, S.L., Schulman, P., Vinciguerra, V.P., Rai, K., Rassenti, L.Z.*, et al.* (1998). Chronic lymphocytic leukemia B cells express restricted sets of mutated and unmutated antigen receptors. J Clin Invest *102*, 1515-1525.

Fenwick, C., Na, S.Y., Voll, R.E., Zhong, H., Im, S.Y., Lee, J.W., and Ghosh, S. (2000). A subclass of Ras proteins that regulate the degradation of IkappaB. Science *287*, 869-873.

Fialkow, P.J., Najfeld, V., Reddy, A.L., Singer, J., and Steinmann, L. (1978). Chronic lymphocytic leukaemia: Clonal origin in a committed B-lymphocyte progenitor. Lancet *2*, 444-446.

Fischer, K., Cramer, P., Busch, R., Bottcher, S., Bahlo, J., Schubert, J., Pfluger, K.H., Schott, S., Goede, V., Isfort, S.*, et al.* (2012). Bendamustine in combination with rituximab for previously untreated patients with chronic lymphocytic leukemia: a multicenter phase II trial of the German Chronic Lymphocytic Leukemia Study Group. J Clin Oncol *30*, 3209-3216.

Flynn, R.L., Cox, K.E., Jeitany, M., Wakimoto, H., Bryll, A.R., Ganem, N.J., Bersani, F., Pineda, J.R., Suva, M.L., Benes, C.H.*, et al.* (2015). Alternative lengthening of telomeres renders cancer cells hypersensitive to ATR inhibitors. Science *347*, 273-277.

Foote, K.M., Blades, K., Cronin, A., Fillery, S., Guichard, S.S., Hassall, L., Hickson, I., Jacq, X., Jewsbury, P.J., McGuire, T.M.*, et al.* (2013). Discovery of 4-{4-[(3R)-3-Methylmorpholin-4-yl]-6-[1-(methylsulfonyl)cyclopropyl]pyrimidin-2-y l}-1H-indole (AZ20): a potent and selective inhibitor of ATR protein kinase with monotherapy in vivo antitumor activity. J Med Chem *56*, 2125-2138.

Foote, K.M., Lau, A., and Nissink, J.W. (2015). Drugging ATR: progress in the development of specific inhibitors for the treatment of cancer. Future Med Chem *7*, 873-891.

Foran, J.M., Oscier, D., Orchard, J., Johnson, S.A., Tighe, M., Cullen, M.H., de Takats, P.G., Kraus, C., Klein, M., and Lister, T.A. (1999). Pharmacokinetic study of single doses of oral fludarabine phosphate in patients with "low-grade" non-Hodgkin's lymphoma and B-cell chronic lymphocytic leukemia. J Clin Oncol *17*, 1574-1579.

Forconi, F., and Moss, P. (2015). Perturbation of the normal immune system in patients with CLL. Blood *126*, 573-581.

Fragkos, M., Ganier, O., Coulombe, P., and Mechali, M. (2015). DNA replication origin activation in space and time. Nat Rev Mol Cell Biol *16*, 360-374.

Frouin, I., Montecucco, A., Spadari, S., and Maga, G. (2003). DNA replication: a complex matter. EMBO Rep *4*, 666-670.

Fulci, V., Chiaretti, S., Goldoni, M., Azzalin, G., Carucci, N., Tavolaro, S., Castellano, L., Magrelli, A., Citarella, F., Messina, M.*, et al.* (2007). Quantitative technologies establish a novel microRNA profile of chronic lymphocytic leukemia. Blood *109*, 4944-4951.

Furman, R.R., Sharman, J.P., Coutre, S.E., Cheson, B.D., Pagel, J.M., Hillmen, P., Barrientos, J.C., Zelenetz, A.D., Kipps, T.J., Flinn, I.*, et al.* (2014). Idelalisib and rituximab in relapsed chronic lymphocytic leukemia. N Engl J Med *370*, 997-1007.

Gauld, S.B., Benschop, R.J., Merrell, K.T., and Cambier, J.C. (2005). Maintenance of B cell anergy requires constant antigen receptor occupancy and signaling. Nat Immunol *6*, 1160-1167.

Ge, X.Q., and Blow, J.J. (2010). Chk1 inhibits replication factory activation but allows dormant origin firing in existing factories. J Cell Biol *191*, 1285-1297.

Getahun, A., Beavers, N.A., Larson, S.R., Shlomchik, M.J., and Cambier, J.C. (2016). Continuous inhibitory signaling by both SHP-1 and SHIP-1 pathways is required to maintain unresponsiveness of anergic B cells. J Exp Med *213*, 751-769.

Gilad, O., Nabet, B.Y., Ragland, R.L., Schoppy, D.W., Smith, K.D., Durham, A.C., and Brown, E.J. (2010). Combining ATR suppression with oncogenic Ras synergistically increases genomic instability, causing synthetic lethality or tumorigenesis in a dosage-dependent manner. Cancer Res *70*, 9693-9702.

Goede, V., Fischer, K., Busch, R., Engelke, A., Eichhorst, B., Wendtner, C.M., Chagorova, T., de la Serna, J., Dilhuydy, M.S., Illmer, T.*, et al.* (2014). Obinutuzumab plus chlorambucil in patients with CLL and coexisting conditions. N Engl J Med *370*, 1101-1110.

Gorgun, G., Holderried, T.A., Zahrieh, D., Neuberg, D., and Gribben, J.G. (2005). Chronic lymphocytic leukemia cells induce changes in gene expression of CD4 and CD8 T cells. J Clin Invest *115*, 1797-1805.

Gounari, M., Ntoufa, S., Apollonio, B., Papakonstantinou, N., Ponzoni, M., Chu, C.C., Rossi, D., Gaidano, G., Chiorazzi, N., Stamatopoulos, K.*, et al.* (2015). Excessive antigen reactivity may underlie the clinical aggressiveness of chronic lymphocytic leukemia stereotyped subset #8. Blood *125*, 3580-3587.

Greaney, P., Nahimana, A., Lagopoulos, L., Etter, A.L., Aubry, D., Attinger, A., Beltraminelli, N., Huni, B., Bassi, I., Sordat, B.*, et al.* (2006). A Fas agonist induces high levels of apoptosis in haematological malignancies. Leuk Res *30*, 415-426.

Gu, B., Dao, L.P., and Wiley, J. (2001). Impaired transendothelial migration of B-CLL lymphocytes: a defect linked to low L-selectin expression. Leuk Lymphoma *42*, 5-12.

Guarini, A., Chiaretti, S., Tavolaro, S., Maggio, R., Peragine, N., Citarella, F., Ricciardi, M.R., Santangelo, S., Marinelli, M., De Propris, M.S.*, et al.* (2008). BCR ligation induced by IgM stimulation results in gene expression and functional changes only in IgV H unmutated chronic lymphocytic leukemia (CLL) cells. Blood *112*, 782-792.

Haahr, P., Hoffmann, S., Tollenaere, M.A., Ho, T., Toledo, L.I., Mann, M., Bekker-Jensen, S., Raschle, M., and Mailand, N. (2016). Activation of the ATR kinase by the RPA-binding protein ETAA1. Nat Cell Biol *18*, 1196-1207.

Hallek, M., Cheson, B.D., Catovsky, D., Caligaris-Cappio, F., Dighiero, G., Dohner, H., Hillmen, P., Keating, M.J., Montserrat, E., Rai, K.R.*, et al.* (2008). Guidelines for the diagnosis and treatment of chronic lymphocytic leukemia: a report from the International Workshop on Chronic Lymphocytic Leukemia updating the National Cancer Institute-Working Group 1996 guidelines. Blood *111*, 5446-5456.

Hallek, M., Fischer, K., Fingerle-Rowson, G., Fink, A.M., Busch, R., Mayer, J., Hensel, M., Hopfinger, G., Hess, G., von Grunhagen, U.*, et al.* (2010). Addition of rituximab to fludarabine and cyclophosphamide in patients with chronic lymphocytic leukaemia: a randomised, open-label, phase 3 trial. Lancet *376*, 1164-1174.

Hamblin, T.J., Davis, Z., Gardiner, A., Oscier, D.G., and Stevenson, F.K. (1999). Unmutated Ig V(H) genes are associated with a more aggressive form of chronic lymphocytic leukemia. Blood *94*, 1848-1854.

Hamblin, T.J., Orchard, J.A., Ibbotson, R.E., Davis, Z., Thomas, P.W., Stevenson, F.K., and Oscier, D.G. (2002). CD38 expression and immunoglobulin variable region mutations are independent prognostic variables in chronic lymphocytic leukemia, but CD38 expression may vary during the course of the disease. Blood *99*, 1023-1029.

Hanada, M., Delia, D., Aiello, A., Stadtmauer, E., and Reed, J.C. (1993). bcl-2 gene hypomethylation and high-level expression in B-cell chronic lymphocytic leukemia. Blood *82*, 1820-1828.

Hanahan, D., and Weinberg, R.A. (2011). Hallmarks of cancer: the next generation. Cell *144*, 646-674.

Harrigan, J.A., Belotserkovskaya, R., Coates, J., Dimitrova, D.S., Polo, S.E., Bradshaw, C.R., Fraser, P., and Jackson, S.P. (2011). Replication stress induces 53BP1-containing OPT domains in G1 cells. J Cell Biol *193*, 97-108.

Herishanu, Y., Perez-Galan, P., Liu, D., Biancotto, A., Pittaluga, S., Vire, B., Gibellini, F., Njuguna, N., Lee, E., Stennett, L.*, et al.* (2011). The lymph node microenvironment promotes B-cell receptor signaling, NF-kappaB activation, and tumor proliferation in chronic lymphocytic leukemia. Blood *117*, 563-574.

Herishanu, Y., Solar, I., Ben-Ezra, J., Cipok, M., Meirsdorf, S., Amariglio, N., Hoffman, S., Kay, S., Aharon, Z., Perry, C.*, et al.* (2012). Complete spontaneous regression of chronic lymphocytic leukemia. J Clin Oncol *30*, e254-256.

Herling, C.D., Klaumunzer, M., Rocha, C.K., Altmuller, J., Thiele, H., Bahlo, J., Kluth, S., Crispatzu, G., Herling, M., Schiller, J.*, et al.* (2016). Complex karyotypes and KRAS and POT1 mutations impact outcome in CLL after chlorambucil-based chemotherapy or chemoimmunotherapy. Blood *128*, 395-404.

Herman, S.E., Gordon, A.L., Hertlein, E., Ramanunni, A., Zhang, X., Jaglowski, S., Flynn, J., Jones, J., Blum, K.A., Buggy, J.J.*, et al.* (2011). Bruton tyrosine kinase represents a promising therapeutic target for treatment of chronic lymphocytic leukemia and is effectively targeted by PCI-32765. Blood *117*, 6287-6296.

Hills, S.A., and Diffley, J.F. (2014). DNA replication and oncogene-induced replicative stress. Curr Biol *24*, R435-444.

Hocke, S., Guo, Y., Job, A., Orth, M., Ziesch, A., Lauber, K., De Toni, E.N., Gress, T.M., Herbst, A., Goke, B.*, et al.* (2016). A synthetic lethal screen identifies ATR-inhibition as a novel therapeutic approach for POLD1-deficient cancers. Oncotarget *7*, 7080-7095.

Hofbauer, J.P., Heyder, C., Denk, U., Kocher, T., Holler, C., Trapin, D., Asslaber, D., Tinhofer, I., Greil, R., and Egle, A. (2011). Development of CLL in the TCL1 transgenic mouse model is associated with severe skewing of the T-cell compartment homologous to human CLL. Leukemia *25*, 1452-1458.

Hoogeboom, R., van Kessel, K.P., Hochstenbach, F., Wormhoudt, T.A., Reinten, R.J., Wagner, K., Kater, A.P., Guikema, J.E., Bende, R.J., and van Noesel, C.J. (2013). A mutated B cell chronic lymphocytic leukemia subset that recognizes and responds to fungi. J Exp Med *210*, 59-70.

Huang, X., Tran, T., Zhang, L., Hatcher, R., and Zhang, P. (2005). DNA damage-induced mitotic catastrophe is mediated by the Chk1-dependent mitotic exit DNA damage checkpoint. Proc Natl Acad Sci U S A *102*, 1065-1070.

Huergo-Zapico, L., Acebes-Huerta, A., Gonzalez-Rodriguez, A.P., Contesti, J., Gonzalez-Garcia, E., Payer, A.R., Villa-Alvarez, M., Fernandez-Guizan, A., Lopez-Soto, A., and Gonzalez, S. (2014). Expansion of NK cells and reduction of NKG2D expression in chronic lymphocytic leukemia. Correlation with progressive disease. PLoS One *9*, e108326.

Ibrahim, S., Keating, M., Do, K.A., O'Brien, S., Huh, Y.O., Jilani, I., Lerner, S., Kantarjian, H.M., and Albitar, M. (2001). CD38 expression as an important prognostic factor in B-cell chronic lymphocytic leukemia. Blood *98*, 181-186.

Ivey, A., Hills, R.K., Simpson, M.A., Jovanovic, J.V., Gilkes, A., Grech, A., Patel, Y., Bhudia, N., Farah, H., Mason, J.*, et al.* (2016). Assessment of Minimal Residual Disease in Standard-Risk AML. N Engl J Med *374*, 422-433.

Jackson, D.A., and Pombo, A. (1998). Replicon clusters are stable units of chromosome structure: evidence that nuclear organization contributes to the efficient activation and propagation of S phase in human cells. J Cell Biol *140*, 1285-1295.

Jackson, S.P., and Bartek, J. (2009). The DNA-damage response in human biology and disease. Nature *461*, 1071-1078.

Jadersten, M., Saft, L., Smith, A., Kulasekararaj, A., Pomplun, S., Gohring, G., Hedlund, A., Hast, R., Schlegelberger, B., Porwit, A.*, et al.* (2011). TP53 mutations in low-risk myelodysplastic syndromes with del(5q) predict disease progression. J Clin Oncol *29*, 1971-1979.

Jain, P., Keating, M., Wierda, W., Estrov, Z., Ferrajoli, A., Jain, N., George, B., James, D., Kantarjian, H., Burger, J.*, et al.* (2015). Outcomes of patients with chronic lymphocytic leukemia after discontinuing ibrutinib. Blood *125*, 2062-2067.

Jeromin, S., Weissmann, S., Haferlach, C., Dicker, F., Bayer, K., Grossmann, V., Alpermann, T., Roller, A., Kohlmann, A., Haferlach, T.*, et al.* (2014). SF3B1 mutations correlated to cytogenetics and mutations in NOTCH1, FBXW7, MYD88, XPO1 and TP53 in 1160 untreated CLL patients. Leukemia *28*, 108-117.

Jilani, I., O'Brien, S., Manshuri, T., Thomas, D.A., Thomazy, V.A., Imam, M., Naeem, S., Verstovsek, S., Kantarjian, H., Giles, F.*, et al.* (2003). Transient down-modulation of CD20 by rituximab in patients with chronic lymphocytic leukemia. Blood *102*, 3514-3520.

Jones, G.G., Reaper, P.M., Pettitt, A.R., and Sherrington, P.D. (2004). The ATR-p53 pathway is suppressed in noncycling normal and malignant lymphocytes. Oncogene *23*, 1911-1921.

Karande, A., Fialkow, P.J., Nilsson, K., Povey, S., Klein, G., Najfeld, V., and Penfold, G. (1980). Establishment of a lymphoid cell line from leukemic cells of a patient with chronic lymphocytic leukemia. Int J Cancer *26*, 551-556.

Karenko, L., Hahtola, S., Paivinen, S., Karhu, R., Syrja, S., Kahkonen, M., Nedoszytko, B., Kytola, S., Zhou, Y., Blazevic, V.*, et al.* (2005). Primary cutaneous T-cell lymphomas show a deletion or translocation affecting NAV3, the human UNC-53 homologue. Cancer Res *65*, 8101-8110.

Kasar, S., Kim, J., Improgo, R., Tiao, G., Polak, P., Haradhvala, N., Lawrence, M.S., Kiezun, A., Fernandes, S.M., Bahl, S.*, et al.* (2015). Whole-genome sequencing reveals activation-induced cytidine deaminase signatures during indolent chronic lymphocytic leukaemia evolution. Nat Commun *6*, 8866.

Kaufmann, Y., Many, A., Rechavi, G., Mor, O., Biniaminov, M., Rosenthal, E., Levanon, M., Davidsohn, J., Aizman, I., Mark, Z.*, et al.* (1995). Brief report: lymphoma with recurrent cycles of spontaneous remission and relapse--possible role of apoptosis. N Engl J Med *332*, 507-510.

Kikushige, Y., Ishikawa, F., Miyamoto, T., Shima, T., Urata, S., Yoshimoto, G., Mori, Y., Iino, T., Yamauchi, T., Eto, T.*, et al.* (2011). Self-renewing hematopoietic stem cell is the primary target in pathogenesis of human chronic lymphocytic leukemia. Cancer Cell *20*, 246-259.

Klein, U., Lia, M., Crespo, M., Siegel, R., Shen, Q., Mo, T., Ambesi-Impiombato, A., Califano, A., Migliazza, A., Bhagat, G.*, et al.* (2010). The DLEU2/miR-15a/16-1 cluster controls B cell proliferation and its deletion leads to chronic lymphocytic leukemia. Cancer Cell *17*, 28-40.

Klein, U., Tu, Y., Stolovitzky, G.A., Mattioli, M., Cattoretti, G., Husson, H., Freedman, A., Inghirami, G., Cro, L., Baldini, L.*, et al.* (2001). Gene expression profiling of B cell chronic lymphocytic leukemia reveals a homogeneous phenotype related to memory B cells. J Exp Med *194*, 1625-1638.

Kontoyiannis, D.P., Georgiadou, S.P., Wierda, W.G., Wright, S., Albert, N.D., Ferrajoli, A., Keating, M., and Lewis, R.E. (2013). Impaired bactericidal but not fungicidal activity of polymorphonuclear neutrophils in patients with chronic lymphocytic leukemia. Leuk Lymphoma *54*, 1730-1733.

Kovacs, G., Robrecht, S., Fink, A.M., Bahlo, J., Cramer, P., von Tresckow, J., Maurer, C., Langerbeins, P., Fingerle-Rowson, G., Ritgen, M.*, et al.* (2016). Minimal Residual Disease Assessment Improves Prediction of Outcome in Patients With Chronic Lymphocytic Leukemia (CLL) Who Achieve Partial Response: Comprehensive Analysis of Two Phase III Studies of the German CLL Study Group. J Clin Oncol.

Krajewska, M., Fehrmann, R.S., Schoonen, P.M., Labib, S., de Vries, E.G., Franke, L., and van Vugt, M.A. (2015). ATR inhibition preferentially targets homologous recombination-deficient tumor cells. Oncogene *34*, 3474-3481.

Krysov, S., Dias, S., Paterson, A., Mockridge, C.I., Potter, K.N., Smith, K.A., Ashton-Key, M., Stevenson, F.K., and Packham, G. (2012). Surface IgM stimulation induces MEK1/2-dependent MYC expression in chronic lymphocytic leukemia cells. Blood *119*, 170-179.

Krzysiek, R., Lefevre, E.A., Bernard, J., Foussat, A., Galanaud, P., Louache, F., and Richard, Y. (2000). Regulation of CCR6 chemokine receptor expression and responsiveness to macrophage inflammatory protein-3alpha/CCL20 in human B cells. Blood *96*, 2338-2345.

Kulis, M., Heath, S., Bibikova, M., Queiros, A.C., Navarro, A., Clot, G., Martinez-Trillos, A., Castellano, G., Brun-Heath, I., Pinyol, M.*, et al.* (2012). Epigenomic analysis detects widespread gene-body DNA hypomethylation in chronic lymphocytic leukemia. Nat Genet *44*, 1236-1242.

Kurosaki, T., Kometani, K., and Ise, W. (2015). Memory B cells. Nat Rev Immunol *15*, 149-159.

Kutsch, N., Hallek, M., and Eichhorst, B. (2014). Emerging therapies for refractory chronic lymphocytic leukemia. Leukemia & lymphoma, 1-8.

Lamanna, N., Jurcic, J.G., Noy, A., Maslak, P., Gencarelli, A.N., Panageas, K.S., Heaney, M.L., Brentjens, R.J., Golde, D.W., Scheinberg, D.A.*, et al.* (2009). Sequential therapy with fludarabine, high-dose cyclophosphamide, and rituximab in previously untreated patients with chronic lymphocytic leukemia produces high-quality responses: molecular remissions predict for durable complete responses. J Clin Oncol *27*, 491-497.

Lampson, B.L., Kasar, S.N., Matos, T.R., Morgan, E.A., Rassenti, L., Davids, M.S., Fisher, D.C., Freedman, A.S., Jacobson, C.A., Armand, P.*, et al.* (2016). Idelalisib given front-line for treatment of chronic lymphocytic leukemia causes frequent immune-mediated hepatotoxicity. Blood *128*, 195-203.

Landau, D.A., Carter, S.L., Stojanov, P., McKenna, A., Stevenson, K., Lawrence, M.S., Sougnez, C., Stewart, C., Sivachenko, A., Wang, L.*, et al.* (2013). Evolution and impact of subclonal mutations in chronic lymphocytic leukemia. Cell *152*, 714-726.

Landau, D.A., Tausch, E., Taylor-Weiner, A.N., Stewart, C., Reiter, J.G., Bahlo, J., Kluth, S., Bozic, I., Lawrence, M., Bottcher, S.*, et al.* (2015). Mutations driving CLL and their evolution in progression and relapse. Nature *526*, 525-530.

Landau, D.A., and Wu, C.J. (2013). Chronic lymphocytic leukemia: molecular heterogeneity revealed by high-throughput genomics. Genome medicine *5*, 47.

Landgren, O., Albitar, M., Ma, W., Abbasi, F., Hayes, R.B., Ghia, P., Marti, G.E., and Caporaso, N.E. (2009). B-cell clones as early markers for chronic lymphocytic leukemia. N Engl J Med *360*, 659-667.

Lanemo Myhrinder, A., Hellqvist, E., Bergh, A.C., Jansson, M., Nilsson, K., Hultman, P., Jonasson, J., Buhl, A.M., Bredo Pedersen, L., Jurlander, J.*, et al.* (2013). Molecular characterization of neoplastic and normal "sister" lymphoblastoid B-cell lines from chronic lymphocytic leukemia. Leuk Lymphoma *54*, 1769-1779.

Langerak, A.W., Groenen, P.J., Bruggemann, M., Beldjord, K., Bellan, C., Bonello, L., Boone, E., Carter, G.I., Catherwood, M., Davi, F.*, et al.* (2012). EuroClonality/BIOMED-2 guidelines for interpretation and reporting of Ig/TCR clonality testing in suspected lymphoproliferations. Leukemia *26*, 2159-2171.

Lanham, S., Hamblin, T., Oscier, D., Ibbotson, R., Stevenson, F., and Packham, G. (2003). Differential signaling via surface IgM is associated with VH gene mutational status and CD38 expression in chronic lymphocytic leukemia. Blood *101*, 1087-1093.

Lapalombella, R., Sun, Q., Williams, K., Tangeman, L., Jha, S., Zhong, Y., Goettl, V., Mahoney, E., Berglund, C., Gupta, S.*, et al.* (2012). Selective inhibitors of nuclear export show that CRM1/XPO1 is a target in chronic lymphocytic leukemia. Blood *120*, 4621-4634.

Larrayoz, M., Blakemore, S.J., Dobson, R.C., Blunt, M.D., Rose-Zerilli, M.J., Walewska, R., Duncombe, A., Oscier, D., Koide, K., Forconi, F.*, et al.* (2016). The SF3B1 inhibitor spliceostatin A (SSA) elicits apoptosis in chronic lymphocytic leukaemia cells through downregulation of Mcl-1. Leukemia *30*, 351-360.

Lazarian, G., Guieze, R., and Wu, C.J. (2017). Clinical Implications of Novel Genomic Discoveries in Chronic Lymphocytic Leukemia. J Clin Oncol *35*, 984-993.

Lia, M., Carette, A., Tang, H., Shen, Q., Mo, T., Bhagat, G., Dalla-Favera, R., and Klein, U. (2012). Functional dissection of the chromosome 13q14 tumor-suppressor locus using transgenic mouse lines. Blood *119*, 2981-2990.

Lin, T.T., Letsolo, B.T., Jones, R.E., Rowson, J., Pratt, G., Hewamana, S., Fegan, C., Pepper, C., and Baird, D.M. (2010). Telomere dysfunction and fusion during the progression of chronic lymphocytic leukemia: evidence for a telomere crisis. Blood *116*, 1899-1907.

Lin, Y.F., Shih, H.Y., Shang, Z., Matsunaga, S., and Chen, B.P. (2014). DNA-PKcs is required to maintain stability of Chk1 and Claspin for optimal replication stress response. Nucleic Acids Res *42*, 4463-4473.

Linsley, P.S., Schelter, J., Burchard, J., Kibukawa, M., Martin, M.M., Bartz, S.R., Johnson, J.M., Cummins, J.M., Raymond, C.K., Dai, H.*, et al.* (2007). Transcripts targeted by the microRNA-16 family cooperatively regulate cell cycle progression. Mol Cell Biol *27*, 2240-2252.

Little, R.F., and McShane, L.M. (2016). Measure for measure: minimal residual disease in CLL. Blood *128*, 2747-2748.

Liu, Y., Nielsen, C.F., Yao, Q., and Hickson, I.D. (2014). The origins and processing of ultra fine anaphase DNA bridges. Curr Opin Genet Dev *26*, 1-5.

Lobry, C., Oh, P., and Aifantis, I. (2011). Oncogenic and tumor suppressor functions of Notch in cancer: it's NOTCH what you think. J Exp Med *208*, 1931-1935.

Logan, A.C., Zhang, B., Narasimhan, B., Carlton, V., Zheng, J., Moorhead, M., Krampf, M.R., Jones, C.D., Waqar, A.N., Faham, M.*, et al.* (2013). Minimal residual disease quantification using consensus primers and high-throughput IGH sequencing predicts post-transplant relapse in chronic lymphocytic leukemia. Leukemia *27*, 1659-1665.

Long, M., Beckwith, K., Do, P., Mundy, B.L., Gordon, A., Lehman, A.M., Maddocks, K.J., Cheney, C., Jones, J.A., Flynn, J.M.*, et al.* (2017). Ibrutinib treatment improves T cell number and function in CLL patients. J Clin Invest.

Lopez-Guerra, M., Xargay-Torrent, S., Rosich, L., Montraveta, A., Roldan, J., Matas-Cespedes, A., Villamor, N., Aymerich, M., Lopez-Otin, C., Perez-Galan, P.*, et al.* (2015). The gamma-secretase inhibitor PF-03084014 combined with fludarabine antagonizes migration, invasion and angiogenesis in NOTCH1-mutated CLL cells. Leukemia *29*, 96-106.

Lukas, C., Savic, V., Bekker-Jensen, S., Doil, C., Neumann, B., Pedersen, R.S., Grofte, M., Chan, K.L., Hickson, I.D., Bartek, J.*, et al.* (2011). 53BP1 nuclear bodies form around DNA

lesions generated by mitotic transmission of chromosomes under replication stress. Nat Cell Biol *13*, 243-253.

Ma, C.X., Cai, S., Li, S., Ryan, C.E., Guo, Z., Schaiff, W.T., Lin, L., Hoog, J., Goiffon, R.J., Prat, A.*, et al.* (2012). Targeting Chk1 in p53-deficient triple-negative breast cancer is therapeutically beneficial in human-in-mouse tumor models. J Clin Invest *122*, 1541-1552.

Ma, S., Brander, D.M., Seymour, J.F., Kipps, T.J., Barrientos, J.C., Davids, M.S., Anderson, M.A., Choi, M.Y., Tam, C.S., Mason-Bright, T.*, et al.* (2015). Deep and Durable Responses Following Venetoclax (ABT-199 / GDC-0199) Combined with Rituximab in Patients with Relapsed/Refractory Chronic Lymphocytic Leukemia: Results from a Phase 1b Study. Blood *126*, 830-830.

Macheret, M., and Halazonetis, T.D. (2015). DNA replication stress as a hallmark of cancer. Annu Rev Pathol *10*, 425-448.

Maciejowski, J., and de Lange, T. (2017). Telomeres in cancer: tumour suppression and genome instability. Nat Rev Mol Cell Biol *18*, 175-186.

Maddocks, K.J., Ruppert, A.S., Lozanski, G., Heerema, N.A., Zhao, W., Abruzzo, L., Lozanski, A., Davis, M., Gordon, A., Smith, L.L.*, et al.* (2015). Etiology of Ibrutinib Therapy Discontinuation and Outcomes in Patients With Chronic Lymphocytic Leukemia. JAMA Oncol *1*, 80-87.

Mahon, F.-x., Richter, J., Guilhot, J., Hjorth-Hansen, H., Almeida, A., Janssen, J.J.W.M.J., Mayer, J., Porkka, K., Panayiotidis, P., Stromberg, U.*, et al.* (2016). Cessation of Tyrosine Kinase Inhibitors Treatment in Chronic Myeloid Leukemia Patients with Deep Molecular Response: Results of the Euro-Ski Trial. Blood *128*, 787-787.

Malcikova, J., Smardova, J., Rocnova, L., Tichy, B., Kuglik, P., Vranova, V., Cejkova, S., Svitakova, M., Skuhrova Francova, H., Brychtova, Y.*, et al.* (2009). Monoallelic and biallelic inactivation of TP53 gene in chronic lymphocytic leukemia: selection, impact on survival, and response to DNA damage. Blood *114*, 5307-5314.

Maloum, K., Settegrana, C., Chapiro, E., Cazin, B., Lepretre, S., Delmer, A., Leporrier, M., Dreyfus, B., Tournilhac, O., Mahe, B.*, et al.* (2009). IGHV gene mutational status and LPL/ADAM29 gene expression as clinical outcome predictors in CLL patients in remission following treatment with oral fludarabine plus cyclophosphamide. Ann Hematol *88*, 1215-1221.

Mankouri, H.W., Huttner, D., and Hickson, I.D. (2013). How unfinished business from S-phase affects mitosis and beyond. EMBO J *32*, 2661-2671.

Mansouri, L., Sutton, L.A., Ljungstrom, V., Bondza, S., Arngarden, L., Bhoi, S., Larsson, J., Cortese, D., Kalushkova, A., Plevova, K.*, et al.* (2015). Functional loss of IkappaBepsilon leads to NF-kappaB deregulation in aggressive chronic lymphocytic leukemia. J Exp Med *212*, 833-843.

Marechal, A., and Zou, L. (2013). DNA damage sensing by the ATM and ATR kinases. Cold Spring Harb Perspect Biol *5*.

Marechal, A., and Zou, L. (2015). RPA-coated single-stranded DNA as a platform for post-translational modifications in the DNA damage response. Cell Res *25*, 9-23.

Marinelli, M., Peragine, N., Di Maio, V., Chiaretti, S., De Propris, M.S., Raponi, S., Tavolaro, S., Mauro, F.R., Del Giudice, I., Guarini, A.*, et al.* (2013). Identification of molecular and functional patterns of p53 alterations in chronic lymphocytic leukemia patients in different phases of the disease. Haematologica *98*, 371-375.

Marklin, M., Heitmann, J.S., Fuchs, A.R., Truckenmuller, F.M., Gutknecht, M., Bugl, S., Saur, S.J., Lazarus, J., Kohlhofer, U., Quintanilla-Martinez, L.*, et al.* (2017). NFAT2 is a critical regulator of the anergic phenotype in chronic lymphocytic leukaemia. Nat Commun *8*, 755.

Mato, A.R., Nabhan, C., Barr, P.M., Ujjani, C.S., Hill, B.T., Lamanna, N., Skarbnik, A.P., Howlett, C., Pu, J.J., Sehgal, A.R.*, et al.* (2016). Outcomes of CLL patients treated with sequential kinase inhibitor therapy: a real world experience. Blood *128*, 2199-2205.

McLornan, D.P., List, A., and Mufti, G.J. (2014). Applying synthetic lethality for the selective targeting of cancer. N Engl J Med *371*, 1725-1735.

Melo, J.V., and Ross, D.M. (2011). Minimal residual disease and discontinuation of therapy in chronic myeloid leukemia: can we aim at a cure? Hematology Am Soc Hematol Educ Program *2011*, 136-142.

Messmer, B.T., Albesiano, E., Efremov, D.G., Ghiotto, F., Allen, S.L., Kolitz, J., Foa, R., Damle, R.N., Fais, F., Messmer, D.*, et al.* (2004). Multiple distinct sets of stereotyped antigen receptors indicate a role for antigen in promoting chronic lymphocytic leukemia. J Exp Med *200*, 519-525.

Messmer, B.T., Messmer, D., Allen, S.L., Kolitz, J.E., Kudalkar, P., Cesar, D., Murphy, E.J., Koduru, P., Ferrarini, M., Zupo, S.*, et al.* (2005). In vivo measurements document the dynamic cellular kinetics of chronic lymphocytic leukemia B cells. J Clin Invest *115*, 755-764.

Middleton, F.K., Patterson, M.J., Elstob, C.J., Fordham, S., Herriott, A., Wade, M.A., McCormick, A., Edmondson, R., May, F.E., Allan, J.M.*, et al.* (2015). Common cancer-associated imbalances in the DNA damage response confer sensitivity to single agent ATR inhibition. Oncotarget *6*, 32396-32409.

Mockridge, C.I., Potter, K.N., Wheatley, I., Neville, L.A., Packham, G., and Stevenson, F.K. (2007). Reversible anergy of sIgM-mediated signaling in the two subsets of CLL defined by VH-gene mutational status. Blood *109*, 4424-4431.

Mohle, R., Failenschmid, C., Bautz, F., and Kanz, L. (1999). Overexpression of the chemokine receptor CXCR4 in B cell chronic lymphocytic leukemia is associated with increased functional response to stromal cell-derived factor-1 (SDF-1). Leukemia *13*, 1954-1959.

Mohni, K.N., Kavanaugh, G.M., and Cortez, D. (2014). ATR pathway inhibition is synthetically lethal in cancer cells with ERCC1 deficiency. Cancer Res *74*, 2835-2845.

Morabito, F., Cutrona, G., Gentile, M., Fabbi, M., Matis, S., Colombo, M., Reverberi, D., Megna, M., Spriano, M., Callea, V.*, et al.* (2010). Prognostic relevance of in vitro response to cell stimulation via surface IgD in binet stage a CLL. Br J Haematol *149*, 160-163.

Moreno, C., Villamor, N., Colomer, D., Esteve, J., Gine, E., Muntanola, A., Campo, E., Bosch, F., and Montserrat, E. (2006). Clinical significance of minimal residual disease, as assessed by different techniques, after stem cell transplantation for chronic lymphocytic leukemia. Blood *107*, 4563-4569.

Moreton, P., Kennedy, B., Lucas, G., Leach, M., Rassam, S.M., Haynes, A., Tighe, J., Oscier, D., Fegan, C., Rawstron, A.*, et al.* (2005). Eradication of minimal residual disease in B-cell chronic lymphocytic leukemia after alemtuzumab therapy is associated with prolonged survival. J Clin Oncol *23*, 2971-2979.

Murga, M., Bunting, S., Montana, M.F., Soria, R., Mulero, F., Canamero, M., Lee, Y., McKinnon, P.J., Nussenzweig, A., and Fernandez-Capetillo, O. (2009). A mouse model of ATR-Seckel shows embryonic replicative stress and accelerated aging. Nat Genet *41*, 891-898.

Murga, M., Campaner, S., Lopez-Contreras, A.J., Toledo, L.I., Soria, R., Montana, M.F., D'Artista, L., Schleker, T., Guerra, C., Garcia, E.*, et al.* (2011). Exploiting oncogene-induced replicative stress for the selective killing of Myc-driven tumors. Nat Struct Mol Biol *18*, 1331-1335.

Murphy, E.J., Neuberg, D.S., Rassenti, L.Z., Hayes, G., Redd, R., Emson, C., Li, K., Brown, J.R., Wierda, W.G., Turner, S.*, et al.* (2017). Leukemia-cell proliferation and disease progression in patients with early stage chronic lymphocytic leukemia. Leukemia.

Murray, F., Darzentas, N., Hadzidimitriou, A., Tobin, G., Boudjogra, M., Scielzo, C., Laoutaris, N., Karlsson, K., Baran-Marzsak, F., Tsaftaris, A.*, et al.* (2008). Stereotyped patterns of somatic hypermutation in subsets of patients with chronic lymphocytic leukemia: implications for the role of antigen selection in leukemogenesis. Blood *111*, 1524-1533.

Musashi, M., Abe, S., Yamada, T., Tanaka, J., Gotohda, Y., Maeda, S., Sato, Y., Morioka, M., Sakurada, K., Minagawa, T.*, et al.* (1997). Spontaneous remission in a patient with chronic myelogenous leukemia. N Engl J Med *336*, 337-339.

Muzio, M., Apollonio, B., Scielzo, C., Frenquelli, M., Vandoni, I., Boussiotis, V., Caligaris-Cappio, F., and Ghia, P. (2008). Constitutive activation of distinct BCR-signaling pathways in a subset of CLL patients: a molecular signature of anergy. Blood *112*, 188-195.

Nadeu, F., Delgado, J., Royo, C., Baumann, T., Stankovic, T., Pinyol, M., Jares, P., Navarro, A., Martin-Garcia, D., Bea, S.*, et al.* (2016). Clinical impact of clonal and subclonal TP53, SF3B1, BIRC3, NOTCH1, and ATM mutations in chronic lymphocytic leukemia. Blood *127*, 2122-2130.

Nakhla, P.S., Butera, J.N., Treaba, D.O., Castillo, J.J., and Quesenberry, P.J. (2013). Spontaneous regression of chronic lymphocytic leukemia to a monoclonal B-lymphocytosis or to a normal phenotype. Leuk Lymphoma *54*, 1647-1651.

Neelsen, K.J., and Lopes, M. (2015). Replication fork reversal in eukaryotes: from dead end to dynamic response. Nat Rev Mol Cell Biol *16*, 207-220.

Nghiem, P., Park, P.K., Kim, Y., Vaziri, C., and Schreiber, S.L. (2001). ATR inhibition selectively sensitizes G1 checkpoint-deficient cells to lethal premature chromatin condensation. Proc Natl Acad Sci U S A *98*, 9092-9097.

Niemann, C.U., Herman, S.E., Maric, I., Gomez-Rodriguez, J., Biancotto, A., Chang, B.Y., Martyr, S., Stetler-Stevenson, M., Yuan, C.M., Calvo, K.R.*, et al.* (2016). Disruption of in vivo Chronic Lymphocytic Leukemia Tumor-Microenvironment Interactions by Ibrutinib--Findings from an Investigator-Initiated Phase II Study. Clin Cancer Res *22*, 1572-1582.

Nossal, G.J. (1996). Clonal anergy of B cells: a flexible, reversible, and quantitative concept. J Exp Med *183*, 1953-1956.

Nowak, D., Hofmann, W.K., and Koeffler, H.P. (2009). Genome-wide Mapping of Copy Number Variations Using SNP Arrays. Transfus Med Hemother *36*, 246-251.

Nunes, C., Wong, R., Mason, M., Fegan, C., Man, S., and Pepper, C. (2012). Expansion of a CD8(+)PD-1(+) replicative senescence phenotype in early stage CLL patients is associated with inverted CD4:CD8 ratios and disease progression. Clin Cancer Res *18*, 678-687.

O'Connor, M.J. (2015). Targeting the DNA Damage Response in Cancer. Mol Cell *60*, 547-560.

O'Driscoll, M., Ruiz-Perez, V.L., Woods, C.G., Jeggo, P.A., and Goodship, J.A. (2003). A splicing mutation affecting expression of ataxia-telangiectasia and Rad3-related protein (ATR) results in Seckel syndrome. Nat Genet *33*, 497-501.

Ogura, M., Ando, K., Taniwaki, M., Watanabe, T., Uchida, T., Ohmachi, K., Matsumoto, Y., Tobinai, K., and Japanese Bendamustine Lymphoma Study, G. (2011). Feasibility and pharmacokinetic study of bendamustine hydrochloride in combination with rituximab in relapsed or refractory aggressive B cell non-Hodgkin's lymphoma. Cancer Sci *102*, 1687-1692.

Os, A., Burgler, S., Ribes, A.P., Funderud, A., Wang, D., Thompson, K.M., Tjonnfjord, G.E., Bogen, B., and Munthe, L.A. (2013). Chronic lymphocytic leukemia cells are activated and proliferate in response to specific T helper cells. Cell Rep *4*, 566-577.

Ouillette, P., Collins, R., Shakhan, S., Li, J., Li, C., Shedden, K., and Malek, S.N. (2011). The prognostic significance of various 13q14 deletions in chronic lymphocytic leukemia. Clin Cancer Res *17*, 6778-6790.

Packham, G., Krysov, S., Allen, A., Savelyeva, N., Steele, A.J., Forconi, F., and Stevenson, F.K. (2014). The outcome of B-cell receptor signaling in chronic lymphocytic leukemia: proliferation or anergy. Haematologica *99*, 1138-1148.

Palamarchuk, A., Efanov, A., Nazaryan, N., Santanam, U., Alder, H., Rassenti, L., Kipps, T., Croce, C.M., and Pekarsky, Y. (2010). 13q14 deletions in CLL involve cooperating tumor suppressors. Blood *115*, 3916-3922.

Palma, M., Gentilcore, G., Heimersson, K., Mozaffari, F., Nasman-Glaser, B., Young, E., Rosenquist, R., Hansson, L., Osterborg, A., and Mellstedt, H. (2017). T cells in chronic lymphocytic leukemia display dysregulated expression of immune checkpoints and activation markers. Haematologica *102*, 562-572.

Panayiotidis, P., Ganeshaguru, K., Foroni, L., and Hoffbrand, A.V. (1995). Expression and function of the FAS antigen in B chronic lymphocytic leukemia and hairy cell leukemia. Leukemia *9*, 1227-1232.

Parikh, S.A., Kay, N.E., and Shanafelt, T.D. (2014). How we treat Richter syndrome. Blood *123*, 1647-1657.

Parker, H., Rose-Zerilli, M.J., Parker, A., Chaplin, T., Wade, R., Gardiner, A., Griffiths, M., Collins, A., Young, B.D., Oscier, D.G.*, et al.* (2011). 13q deletion anatomy and disease progression in patients with chronic lymphocytic leukemia. Leukemia *25*, 489-497.

Parry, H.M., Stevens, T., Oldreive, C., Zadran, B., McSkeane, T., Rudzki, Z., Paneesha, S., Chadwick, C., Stankovic, T., Pratt, G.*, et al.* (2016). NK cell function is markedly impaired in

patients with chronic lymphocytic leukaemia but is preserved in patients with small lymphocytic lymphoma. Oncotarget *7*, 68513-68526.

Pascutti, M.F., Jak, M., Tromp, J.M., Derks, I.A., Remmerswaal, E.B., Thijssen, R., van Attekum, M.H., van Bochove, G.G., Luijks, D.M., Pals, S.T.*, et al.* (2013). IL-21 and CD40L signals from autologous T cells can induce antigen-independent proliferation of CLL cells. Blood *122*, 3010-3019.

Patten, P.E., Chen, S.-S., Bagnara, D., Simone, R., Marsilio, S., Tong, T., Barrientos, J.C., Kolitz, J.E., Allen, S.L., Rai, K.R.*, et al.* (2011). Engraftment of CLL-derived T cells in NSG mice is feasible, can support CLL cell proliferation, and eliminates the need for third party antigen presenting cells [abstract]. Blood *118*, Abstract 975.

Patten, P.E., Chen, S.-S., Bagnara, D., Simone, R., Marsilio, S., Tong, T., Barrientos, J.C., Kolitz, J.E., Allen, S.L., Rai, K.R.*, et al.* (2015). Engraftment of CLL-Derived T Cells in NSG Mice Is Feasible, Can Support CLL Cell Proliferation, and Eliminates the Need for Third Party Antigen Presenting Cells. Blood *118*, 975-975.

Patten, P.E., Chu, C.C., Albesiano, E., Damle, R.N., Yan, X.J., Kim, D., Zhang, L., Magli, A.R., Barrientos, J., Kolitz, J.E.*, et al.* (2012). IGHV-unmutated and IGHV-mutated chronic lymphocytic leukemia cells produce activation-induced deaminase protein with a full range of biologic functions. Blood *120*, 4802-4811.

Paul, R., Remes, K., Lakkala, T., and Pelliniemi, T.T. (1994). Spontaneous remission in acute myeloid leukaemia. Br J Haematol *86*, 210-212.

Peng, C.Y., Graves, P.R., Thoma, R.S., Wu, Z., Shaw, A.S., and Piwnica-Worms, H. (1997). Mitotic and G2 checkpoint control: regulation of 14-3-3 protein binding by phosphorylation of Cdc25C on serine-216. Science *277*, 1501-1505.

Pepper, C., Lin, T.T., Pratt, G., Hewamana, S., Brennan, P., Hiller, L., Hills, R., Ward, R., Starczynski, J., Austen, B.*, et al.* (2008). Mcl-1 expression has in vitro and in vivo significance in chronic lymphocytic leukemia and is associated with other poor prognostic markers. Blood *112*, 3807-3817.

Perbellini, O., Falisi, E., Giaretta, I., Boscaro, E., Novella, E., Facco, M., Fortuna, S., Finotto, S., Amati, E., Maniscalco, F.*, et al.* (2014). Clinical significance of LAIR1 (CD305) as assessed by flow cytometry in a prospective series of patients with chronic lymphocytic leukemia. Haematologica *99*, 881-887.

Petermann, E., Woodcock, M., and Helleday, T. (2010). Chk1 promotes replication fork progression by controlling replication initiation. Proc Natl Acad Sci U S A *107*, 16090-16095.

Petlickovski, A., Laurenti, L., Li, X., Marietti, S., Chiusolo, P., Sica, S., Leone, G., and Efremov, D.G. (2005). Sustained signaling through the B-cell receptor induces Mcl-1 and promotes survival of chronic lymphocytic leukemia B cells. Blood *105*, 4820-4827.

Petrilli, R., Eloy, J.O., Marchetti, J.M., Lopez, R.F., and Lee, R.J. (2014). Targeted lipid nanoparticles for antisense oligonucleotide delivery. Curr Pharm Biotechnol *15*, 847-855.

Pettitt, A.R., Jackson, R., Carruthers, S., Dodd, J., Dodd, S., Oates, M., Johnson, G.G., Schuh, A., Matutes, E., Dearden, C.E.*, et al.* (2012). Alemtuzumab in combination with methylprednisolone is a highly effective induction regimen for patients with chronic lymphocytic leukemia and deletion of TP53: final results of the national cancer research institute CLL206 trial. J Clin Oncol *30*, 1647-1655.

Pfitzner, T., Engert, A., Wittor, H., Schinkothe, T., Oberhauser, F., Schulz, H., Diehl, V., and Barth, S. (2000). A real-time PCR assay for the quantification of residual malignant cells in B cell chronic lymphatic leukemia. Leukemia *14*, 754-766.

Pospisilova, S., Gonzalez, D., Malcikova, J., Trbusek, M., Rossi, D., Kater, A.P., Cymbalista, F., Eichhorst, B., Hallek, M., Dohner, H.*, et al.* (2012). ERIC recommendations on TP53 mutation analysis in chronic lymphocytic leukemia. Leukemia *26*, 1458-1461.

Potter, K.N., Mockridge, C.I., Neville, L., Wheatley, I., Schenk, M., Orchard, J., Duncombe, A.S., Packham, G., and Stevenson, F.K. (2006). Structural and functional features of the B-cell receptor in IgG-positive chronic lymphocytic leukemia. Clin Cancer Res *12*, 1672-1679.

Proto-Siqueira, R., Panepucci, R.A., Careta, F.P., Lee, A., Clear, A., Morris, K., Owen, C., Rizzatti, E.G., Silva, W.A., Jr., Falcao, R.P.*, et al.* (2008). SAGE analysis demonstrates increased expression of TOSO contributing to Fas-mediated resistance in CLL. Blood *112*, 394-397.

Puente, X.S., Bea, S., Valdes-Mas, R., Villamor, N., Gutierrez-Abril, J., Martin-Subero, J.I., Munar, M., Rubio-Perez, C., Jares, P., Aymerich, M.*, et al.* (2015). Non-coding recurrent mutations in chronic lymphocytic leukaemia. Nature *526*, 519-524.

Puig, N., Trudel, S., Keats, J.J., Li, Z.H., Braggio, E., Ahmann, G.J., Zeng, S., Fonseca, R., and Kukreti, V. (2009). Spontaneous remission in a patient with t(4;14) translocation multiple myeloma. J Clin Oncol *27*, e194-197.

Rai, K.R., Peterson, B.L., Appelbaum, F.R., Kolitz, J., Elias, L., Shepherd, L., Hines, J., Threatte, G.A., Larson, R.A., Cheson, B.D.*, et al.* (2000). Fludarabine compared with chlorambucil as primary therapy for chronic lymphocytic leukemia. N Engl J Med *343*, 1750-1757.

Rai, K.R., Sawitsky, A., Cronkite, E.P., Chanana, A.D., Levy, R.N., and Pasternack, B.S. (1975). Clinical staging of chronic lymphocytic leukemia. Blood *46*, 219-234.

Rampazzo, E., Bonaldi, L., Trentin, L., Visco, C., Keppel, S., Giunco, S., Frezzato, F., Facco, M., Novella, E., Giaretta, I.*, et al.* (2012). Telomere length and telomerase levels delineate subgroups of B-cell chronic lymphocytic leukemia with different biological characteristics and clinical outcomes. Haematologica *97*, 56-63.

Ramsay, A.G., Johnson, A.J., Lee, A.M., Gorgun, G., Le Dieu, R., Blum, W., Byrd, J.C., and Gribben, J.G. (2008). Chronic lymphocytic leukemia T cells show impaired immunological synapse formation that can be reversed with an immunomodulating drug. J Clin Invest *118*, 2427-2437.

Ramsay, A.J., Quesada, V., Foronda, M., Conde, L., Martinez-Trillos, A., Villamor, N., Rodriguez, D., Kwarciak, A., Garabaya, C., Gallardo, M.*, et al.* (2013). POT1 mutations cause telomere dysfunction in chronic lymphocytic leukemia. Nat Genet *45*, 526-530.

Rathmell, J.C., Cooke, M.P., Ho, W.Y., Grein, J., Townsend, S.E., Davis, M.M., and Goodnow, C.C. (1995). CD95 (Fas)-dependent elimination of self-reactive B cells upon interaction with CD4+ T cells. Nature *376*, 181-184.

Rawstron, A.C., Bennett, F.L., O'Connor, S.J., Kwok, M., Fenton, J.A., Plummer, M., de Tute, R., Owen, R.G., Richards, S.J., Jack, A.S.*, et al.* (2008). Monoclonal B-cell lymphocytosis and chronic lymphocytic leukemia. N Engl J Med *359*, 575-583.

Rawstron, A.C., Bottcher, S., Letestu, R., Villamor, N., Fazi, C., Kartsios, H., de Tute, R.M., Shingles, J., Ritgen, M., Moreno, C.*, et al.* (2013). Improving efficiency and sensitivity: European Research Initiative in CLL (ERIC) update on the international harmonised approach for flow cytometric residual disease monitoring in CLL. Leukemia *27*, 142-149.

Rawstron, A.C., Fazi, C., Agathangelidis, A., Villamor, N., Letestu, R., Nomdedeu, J., Palacio, C., Stehlikova, O., Kreuzer, K.A., Liptrot, S*., et al.* (2016). A complementary role of multiparameter flow cytometry and high-throughput sequencing for minimal residual disease detection in chronic lymphocytic leukemia: an European Research Initiative on CLL study. Leukemia *30*, 929-936.

Rawstron, A.C., Kennedy, B., Evans, P.A., Davies, F.E., Richards, S.J., Haynes, A.P., Russell, N.H., Hale, G., Morgan, G.J., Jack, A.S*., et al.* (2001). Quantitation of minimal disease levels in chronic lymphocytic leukemia using a sensitive flow cytometric assay improves the prediction of outcome and can be used to optimize therapy. Blood *98*, 29-35.

Rawstron, A.C., Kreuzer, K.A., Soosapilla, A., Spacek, M., Stehlikova, O., Gambell, P., McIver-Brown, N., Villamor, N., Psarra, K., Arroz, M*., et al.* (2017). Reproducible diagnosis of Chronic Lymphocytic Leukemia by flow cytometry: an European Research Initiative on CLL (ERIC) & European Society for Clinical Cell Analysis (ESCCA) harmonisation project. Cytometry B Clin Cytom.

Rawstron, A.C., Villamor, N., Ritgen, M., Bottcher, S., Ghia, P., Zehnder, J.L., Lozanski, G., Colomer, D., Moreno, C., Geuna, M*., et al.* (2007). International standardized approach for flow cytometric residual disease monitoring in chronic lymphocytic leukaemia. Leukemia *21*, 956-964.

Reaper, P.M., Griffiths, M.R., Long, J.M., Charrier, J.D., Maccormick, S., Charlton, P.A., Golec, J.M., and Pollard, J.R. (2011). Selective killing of ATM- or p53-deficient cancer cells through inhibition of ATR. Nat Chem Biol *7*, 428-430.

Rengarajan, J., Mittelstadt, P.R., Mages, H.W., Gerth, A.J., Kroczek, R.A., Ashwell, J.D., and Glimcher, L.H. (2000). Sequential involvement of NFAT and Egr transcription factors in FasL regulation. Immunity *12*, 293-300.

Riches, J.C., Davies, J.K., McClanahan, F., Fatah, R., Iqbal, S., Agrawal, S., Ramsay, A.G., and Gribben, J.G. (2013). T cells from CLL patients exhibit features of T-cell exhaustion but retain capacity for cytokine production. Blood *121*, 1612-1621.

Roberts, A.W., Davids, M.S., Pagel, J.M., Kahl, B.S., Puvvada, S.D., Gerecitano, J.F., Kipps, T.J., Anderson, M.A., Brown, J.R., Gressick, L*., et al.* (2016). Targeting BCL2 with Venetoclax in Relapsed Chronic Lymphocytic Leukemia. N Engl J Med *374*, 311-322.

Romano, C., Sellitto, A., Chiurazzi, F., Simeone, L., De Fanis, U., Raia, M., Del Vecchio, L., and Lucivero, G. (2015). Clinical and phenotypic features of CD5-negative B cell chronic lymphoproliferative disease resembling chronic lymphocytic leukemia. Int J Hematol *101*, 67-74.

Roos, G., Krober, A., Grabowski, P., Kienle, D., Buhler, A., Dohner, H., Rosenquist, R., and Stilgenbauer, S. (2008). Short telomeres are associated with genetic complexity, high-risk genomic aberrations, and short survival in chronic lymphocytic leukemia. Blood *111*, 2246-2252.

Rose-Zerilli, M.J., Forster, J., Parker, H., Parker, A., Rodriguez, A.E., Chaplin, T., Gardiner, A., Steele, A.J., Collins, A., Young, B.D*., et al.* (2014). ATM mutation rather than BIRC3

deletion and/or mutation predicts reduced survival in 11q-deleted chronic lymphocytic leukemia: data from the UK LRF CLL4 trial. Haematologica *99*, 736-742.

Rosen, A., Murray, F., Evaldsson, C., and Rosenquist, R. (2010). Antigens in chronic lymphocytic leukemia--implications for cell origin and leukemogenesis. Semin Cancer Biol *20*, 400-409.

Rosenquist, R., Ghia, P., Hadzidimitriou, A., Sutton, L.A., Agathangelidis, A., Baliakas, P., Darzentas, N., Giudicelli, V., Lefranc, M.P., Langerak, A.W.*, et al.* (2017). Immunoglobulin gene sequence analysis in chronic lymphocytic leukemia: updated ERIC recommendations. Leukemia.

Rosenwald, A., Alizadeh, A.A., Widhopf, G., Simon, R., Davis, R.E., Yu, X., Yang, L., Pickeral, O.K., Rassenti, L.Z., Powell, J.*, et al.* (2001). Relation of gene expression phenotype to immunoglobulin mutation genotype in B cell chronic lymphocytic leukemia. J Exp Med *194*, 1639-1647.

Rossi, D., Fangazio, M., Rasi, S., Vaisitti, T., Monti, S., Cresta, S., Chiaretti, S., Del Giudice, I., Fabbri, G., Bruscaggin, A.*, et al.* (2012a). Disruption of BIRC3 associates with fludarabine chemorefractoriness in TP53 wild-type chronic lymphocytic leukemia. Blood *119*, 2854-2862.

Rossi, D., Khiabanian, H., Spina, V., Ciardullo, C., Bruscaggin, A., Fama, R., Rasi, S., Monti, S., Deambrogi, C., De Paoli, L.*, et al.* (2014). Clinical impact of small TP53 mutated subclones in chronic lymphocytic leukemia. Blood *123*, 2139-2147.

Rossi, D., Rasi, S., Fabbri, G., Spina, V., Fangazio, M., Forconi, F., Marasca, R., Laurenti, L., Bruscaggin, A., Cerri, M.*, et al.* (2012b). Mutations of NOTCH1 are an independent predictor of survival in chronic lymphocytic leukemia. Blood *119*, 521-529.

Rossi, D., Rasi, S., Spina, V., Bruscaggin, A., Monti, S., Ciardullo, C., Deambrogi, C., Khiabanian, H., Serra, R., Bertoni, F.*, et al.* (2013). Integrated mutational and cytogenetic analysis identifies new prognostic subgroups in chronic lymphocytic leukemia. Blood *121*, 1403-1412.

Rossi, D., Spina, V., Deambrogi, C., Rasi, S., Laurenti, L., Stamatopoulos, K., Arcaini, L., Lucioni, M., Rocque, G.B., Xu-Monette, Z.Y.*, et al.* (2011). The genetics of Richter syndrome reveals disease heterogeneity and predicts survival after transformation. Blood *117*, 3391-3401.

Rossi, D.L., Vicari, A.P., Franz-Bacon, K., McClanahan, T.K., and Zlotnik, A. (1997). Identification through bioinformatics of two new macrophage proinflammatory human chemokines: MIP-3alpha and MIP-3beta. J Immunol *158*, 1033-1036.

Rothkamm, K., Barnard, S., Moquet, J., Ellender, M., Rana, Z., and Burdak-Rothkamm, S. (2015). DNA damage foci: Meaning and significance. Environ Mol Mutagen *56*, 491-504.

Rozman, C., Montserrat, E., and Vinolas, N. (1988). Serum immunoglobulins in B-chronic lymphocytic leukemia. Natural history and prognostic significance. Cancer *61*, 279-283.

Rucker, F.G., Schlenk, R.F., Bullinger, L., Kayser, S., Teleanu, V., Kett, H., Habdank, M., Kugler, C.M., Holzmann, K., Gaidzik, V.I.*, et al.* (2012). TP53 alterations in acute myeloid leukemia with complex karyotype correlate with specific copy number alterations, monosomal karyotype, and dismal outcome. Blood *119*, 2114-2121.

Ruzankina, Y., Pinzon-Guzman, C., Asare, A., Ong, T., Pontano, L., Cotsarelis, G., Zediak, V.P., Velez, M., Bhandoola, A., and Brown, E.J. (2007). Deletion of the developmentally essential gene ATR in adult mice leads to age-related phenotypes and stem cell loss. Cell Stem Cell *1*, 113-126.

Ruzankina, Y., Schoppy, D.W., Asare, A., Clark, C.E., Vonderheide, R.H., and Brown, E.J. (2009). Tissue regenerative delays and synthetic lethality in adult mice after combined deletion of Atr and Trp53. Nat Genet *41*, 1144-1149.

Saint-Georges, S., Quettier, M., Bouyaba, M., Le Coquil, S., Lauriente, V., Guittat, L., Levy, V., Ajchenbaum-Cymbalista, F., Varin-Blank, N., Le Roy, C.*, et al.* (2016). Protein kinase D-dependent CXCR4 down-regulation upon BCR triggering is linked to lymphadenopathy in chronic lymphocytic leukaemia. Oncotarget *7*, 41031-41046.

Sangster-Guity, N., Conrad, B.H., Papadopoulos, N., and Bunz, F. (2011). ATR mediates cisplatin resistance in a p53 genotype-specific manner. Oncogene *30*, 2526-2533.

Sanjiv, K., Hagenkort, A., Calderon-Montano, J.M., Koolmeister, T., Reaper, P.M., Mortusewicz, O., Jacques, S.A., Kuiper, R.V., Schultz, N., Scobie, M.*, et al.* (2016). Cancer-Specific Synthetic Lethality between ATR and CHK1 Kinase Activities. Cell Rep *17*, 3407-3416.

Santacruz, R., Villamor, N., Aymerich, M., Martinez-Trillos, A., Lopez, C., Navarro, A., Rozman, M., Bea, S., Royo, C., Cazorla, M.*, et al.* (2014). The prognostic impact of minimal residual disease in patients with chronic lymphocytic leukemia requiring first-line therapy. Haematologica *99*, 873-880.

Schaffner, C., Idler, I., Stilgenbauer, S., Dohner, H., and Lichter, P. (2000). Mantle cell lymphoma is characterized by inactivation of the ATM gene. Proc Natl Acad Sci U S A *97*, 2773-2778.

Schlesinger, M., Broman, I., and Lugassy, G. (1996). The complement system is defective in chronic lymphatic leukemia patients and in their healthy relatives. Leukemia *10*, 1509-1513.

Schmidt, H.H., Sill, H., Eibl, M., Beham-Schmid, C., Hofler, G., Haas, O.A., Krejs, G.J., and Linkesch, W. (1995). Hodgkin's disease developing after spontaneous remission of chronic lymphocytic leukemia. Ann Hematol *71*, 247-252.

Schoppy, D.W., Ragland, R.L., Gilad, O., Shastri, N., Peters, A.A., Murga, M., Fernandez-Capetillo, O., Diehl, J.A., and Brown, E.J. (2012). Oncogenic stress sensitizes murine cancers to hypomorphic suppression of ATR. J Clin Invest *122*, 241-252.

Seifert, H., Mohr, B., Thiede, C., Oelschlagel, U., Schakel, U., Illmer, T., Soucek, S., Ehninger, G., and Schaich, M. (2009). The prognostic impact of 17p (p53) deletion in 2272 adults with acute myeloid leukemia. Leukemia *23*, 656-663.

Seifert, M., Sellmann, L., Bloehdorn, J., Wein, F., Stilgenbauer, S., Durig, J., and Kuppers, R. (2012). Cellular origin and pathophysiology of chronic lymphocytic leukemia. J Exp Med *209*, 2183-2198.

Shaheen, M., Allen, C., Nickoloff, J.A., and Hromas, R. (2011). Synthetic lethality: exploiting the addiction of cancer to DNA repair. Blood *117*, 6074-6082.

Shiloh, Y., and Ziv, Y. (2013). The ATM protein kinase: regulating the cellular response to genotoxic stress, and more. Nat Rev Mol Cell Biol *14*, 197-210.

Silvennoinen, R., Malminiemi, K., Malminiemi, O., Seppala, E., and Vilpo, J. (2000). Pharmacokinetics of chlorambucil in patients with chronic lymphocytic leukaemia: comparison of different days, cycles and doses. Pharmacol Toxicol *87*, 223-228.

Skowronska, A., Parker, A., Ahmed, G., Oldreive, C., Davis, Z., Richards, S., Dyer, M., Matutes, E., Gonzalez, D., Taylor, A.M.*, et al.* (2012). Biallelic ATM inactivation significantly reduces survival in patients treated on the United Kingdom Leukemia Research Fund Chronic Lymphocytic Leukemia 4 trial. J Clin Oncol *30*, 4524-4532.

Slager, S.L., Caporaso, N.E., de Sanjose, S., and Goldin, L.R. (2013). Genetic susceptibility to chronic lymphocytic leukemia. Semin Hematol *50*, 296-302.

Sorensen, C.S., Syljuasen, R.G., Falck, J., Schroeder, T., Ronnstrand, L., Khanna, K.K., Zhou, B.B., Bartek, J., and Lukas, J. (2003). Chk1 regulates the S phase checkpoint by coupling the physiological turnover and ionizing radiation-induced accelerated proteolysis of Cdc25A. Cancer Cell *3*, 247-258.

Spaargaren, M., Beuling, E.A., Rurup, M.L., Meijer, H.P., Klok, M.D., Middendorp, S., Hendriks, R.W., and Pals, S.T. (2003). The B cell antigen receptor controls integrin activity through Btk and PLCgamma2. J Exp Med *198*, 1539-1550.

Stacchini, A., Aragno, M., Vallario, A., Alfarano, A., Circosta, P., Gottardi, D., Faldella, A., Rege-Cambrin, G., Thunberg, U., Nilsson, K.*, et al.* (1999). MEC1 and MEC2: two new cell lines derived from B-chronic lymphocytic leukaemia in prolymphocytoid transformation. Leuk Res *23*, 127-136.

Stamatopoulos, K., Agathangelidis, A., Rosenquist, R., and Ghia, P. (2017). Antigen receptor stereotypy in chronic lymphocytic leukemia. Leukemia *31*, 282-291.

Stankovic, T., and Skowronska, A. (2014). The role of ATM mutations and 11q deletions in disease progression in chronic lymphocytic leukemia. Leuk Lymphoma *55*, 1227-1239.

Steininger, C., Widhopf, G.F., 2nd, Ghia, E.M., Morello, C.S., Vanura, K., Sanders, R., Spector, D., Guiney, D., Jager, U., and Kipps, T.J. (2012). Recombinant antibodies encoded by IGHV1-69 react with pUL32, a phosphoprotein of cytomegalovirus and B-cell superantigen. Blood *119*, 2293-2301.

Stevenson, F.K., Krysov, S., Davies, A.J., Steele, A.J., and Packham, G. (2011). B-cell receptor signaling in chronic lymphocytic leukemia. Blood *118*, 4313-4320.

Stilgenbauer, S., Schaffner, C., Litterst, A., Liebisch, P., Gilad, S., Bar-Shira, A., James, M.R., Lichter, P., and Dohner, H. (1997). Biallelic mutations in the ATM gene in T-prolymphocytic leukemia. Nat Med *3*, 1155-1159.

Stilgenbauer, S., Schnaiter, A., Paschka, P., Zenz, T., Rossi, M., Dohner, K., Buhler, A., Bottcher, S., Ritgen, M., Kneba, M.*, et al.* (2014). Gene mutations and treatment outcome in chronic lymphocytic leukemia: results from the CLL8 trial. Blood *123*, 3247-3254.

Stoppa-Lyonnet, D., Soulier, J., Lauge, A., Dastot, H., Garand, R., Sigaux, F., and Stern, M.H. (1998). Inactivation of the ATM gene in T-cell prolymphocytic leukemias. Blood *91*, 3920-3926.

Strati, P., Keating, M.J., O'Brien, S.M., Burger, J., Ferrajoli, A., Jain, N., Tambaro, F.P., Estrov, Z., Jorgensen, J., Challagundla, P.*, et al.* (2014). Eradication of bone marrow

minimal residual disease may prompt early treatment discontinuation in CLL. Blood *123*, 3727-3732.

Strati, P., and Shanafelt, T.D. (2015). Monoclonal B-cell lymphocytosis and early-stage chronic lymphocytic leukemia: diagnosis, natural history, and risk stratification. Blood *126*, 454-462.

Strefford, J.C., Kadalayil, L., Forster, J., Rose-Zerilli, M.J., Parker, A., Lin, T.T., Heppel, N., Norris, K., Gardiner, A., Davies, Z.*, et al.* (2015). Telomere length predicts progression and overall survival in chronic lymphocytic leukemia: data from the UK LRF CLL4 trial. Leukemia *29*, 2411-2414.

Struck, R.F., Alberts, D.S., Horne, K., Phillips, J.G., Peng, Y.M., and Roe, D.J. (1987). Plasma pharmacokinetics of cyclophosphamide and its cytotoxic metabolites after intravenous versus oral administration in a randomized, crossover trial. Cancer Res *47*, 2723-2726.

Sultana, R., Abdel-Fatah, T., Perry, C., Moseley, P., Albarakti, N., Mohan, V., Seedhouse, C., Chan, S., and Madhusudan, S. (2013). Ataxia telangiectasia mutated and Rad3 related (ATR) protein kinase inhibition is synthetically lethal in XRCC1 deficient ovarian cancer cells. PLoS One *8*, e57098.

Syljuasen, R.G. (2007). Checkpoint adaptation in human cells. Oncogene *26*, 5833-5839.

Tam, C.S., O'Brien, S., Plunkett, W., Wierda, W., Ferrajoli, A., Wang, X., Do, K.A., Cortes, J., Khouri, I., Kantarjian, H.*, et al.* (2014). Long-term results of first salvage treatment in CLL patients treated initially with FCR (fludarabine, cyclophosphamide, rituximab). Blood *124*, 3059-3064.

Tam, C.S., O'Brien, S., Wierda, W., Kantarjian, H., Wen, S., Do, K.A., Thomas, D.A., Cortes, J., Lerner, S., and Keating, M.J. (2008). Long-term results of the fludarabine, cyclophosphamide, and rituximab regimen as initial therapy of chronic lymphocytic leukemia. Blood *112*, 975-980.

Taylor, R.C., Cullen, S.P., and Martin, S.J. (2008). Apoptosis: controlled demolition at the cellular level. Nat Rev Mol Cell Biol *9*, 231-241.

Te Raa, G.D., Derks, I.A., Navrkalova, V., Skowronska, A., Moerland, P.D., van Laar, J., Oldreive, C., Monsuur, H., Trbusek, M., Malcikova, J.*, et al.* (2015). The impact of SF3B1 mutations in CLL on the DNA-damage response. Leukemia *29*, 1133-1142.

Ten Hacken, E., Sivina, M., Kim, E., O'Brien, S., Wierda, W.G., Ferrajoli, A., Estrov, Z., Keating, M.J., Oellerich, T., Scielzo, C.*, et al.* (2016). Functional Differences between IgM and IgD Signaling in Chronic Lymphocytic Leukemia. J Immunol *197*, 2522-2531.

Terrin, L., Trentin, L., Degan, M., Corradini, I., Bertorelle, R., Carli, P., Maschio, N., Bo, M.D., Noventa, F., Gattei, V.*, et al.* (2007). Telomerase expression in B-cell chronic lymphocytic leukemia predicts survival and delineates subgroups of patients with the same igVH mutation status and different outcome. Leukemia *21*, 965-972.

Thomas, R., Ribeiro, I., Shepherd, P., Johnson, P., Cook, M., Lakhani, A., Kaczmarski, R., Carrington, P., and Catovsky, D. (2002). Spontaneous clinical regression in chronic lymphocytic leukaemia. Br J Haematol *116*, 341-345.

Thompson, P.A., O'Brien, S.M., Wierda, W.G., Ferrajoli, A., Stingo, F., Smith, S.C., Burger, J.A., Estrov, Z., Jain, N., Kantarjian, H.M.*, et al.* (2015). Complex karyotype is a stronger predictor than del(17p) for an inferior outcome in relapsed or refractory chronic lymphocytic leukemia patients treated with ibrutinib-based regimens. Cancer *121*, 3612-3621.

Thompson, P.A., Tam, C.S., O'Brien, S.M., Wierda, W.G., Stingo, F., Plunkett, W., Smith, S.C., Kantarjian, H.M., Freireich, E.J., and Keating, M.J. (2016). Fludarabine, cyclophosphamide, and rituximab treatment achieves long-term disease-free survival in IGHV-mutated chronic lymphocytic leukemia. Blood *127*, 303-309.

Till, K.J., Lin, K., Zuzel, M., and Cawley, J.C. (2002). The chemokine receptor CCR7 and alpha4 integrin are important for migration of chronic lymphocytic leukemia cells into lymph nodes. Blood *99*, 2977-2984.

Till, K.J., Spiller, D.G., Harris, R.J., Chen, H., Zuzel, M., and Cawley, J.C. (2005). CLL, but not normal, B cells are dependent on autocrine VEGF and alpha4beta1 integrin for chemokine-induced motility on and through endothelium. Blood *105*, 4813-4819.

Tinhofer, I., Weiss, L., Gassner, F., Rubenzer, G., Holler, C., and Greil, R. (2009). Difference in the relative distribution of CD4+ T-cell subsets in B-CLL with mutated and unmutated immunoglobulin (Ig) VH genes: implication for the course of disease. J Immunother *32*, 302-309.

Toledo, L.I., Altmeyer, M., Rask, M.B., Lukas, C., Larsen, D.H., Povlsen, L.K., Bekker-Jensen, S., Mailand, N., Bartek, J., and Lukas, J. (2013). ATR prohibits replication catastrophe by preventing global exhaustion of RPA. Cell *155*, 1088-1103.

Toledo, L.I., Murga, M., Zur, R., Soria, R., Rodriguez, A., Martinez, S., Oyarzabal, J., Pastor, J., Bischoff, J.R., and Fernandez-Capetillo, O. (2011). A cell-based screen identifies ATR inhibitors with synthetic lethal properties for cancer-associated mutations. Nat Struct Mol Biol *18*, 721-727.

Trbusek, M., Smardova, J., Malcikova, J., Sebejova, L., Dobes, P., Svitakova, M., Vranova, V., Mraz, M., Francova, H.S., Doubek, M.*, et al.* (2011). Missense mutations located in structural p53 DNA-binding motifs are associated with extremely poor survival in chronic lymphocytic leukemia. J Clin Oncol *29*, 2703-2708.

van Krieken, J.H., Langerak, A.W., Macintyre, E.A., Kneba, M., Hodges, E., Sanz, R.G., Morgan, G.J., Parreira, A., Molina, T.J., Cabecadas, J.*, et al.* (2007). Improved reliability of lymphoma diagnostics via PCR-based clonality testing: report of the BIOMED-2 Concerted Action BHM4-CT98-3936. Leukemia *21*, 201-206.

Vardi, A., Agathangelidis, A., Stalika, E., Karypidou, M., Siorenta, A., Anagnostopoulos, A., Rosenquist, R., Hadzidimitriou, A., Ghia, P., Sutton, L.A.*, et al.* (2016). Antigen Selection Shapes the T-cell Repertoire in Chronic Lymphocytic Leukemia. Clin Cancer Res *22*, 167-174.

Vardi, A., Vlachonikola, E., Karypidou, M., Stalika, E., Bikos, V., Gemenetzi, K., Maramis, C., Siorenta, A., Anagnostopoulos, A., Pospisilova, S.*, et al.* (2017). Restrictions in the T-cell repertoire of chronic lymphocytic leukemia: high-throughput immunoprofiling supports selection by shared antigenic elements. Leukemia.

Varghese, A.M., Howard, D.R., Pocock, C., Rawstron, A.C., Follows, G., McCarthy, H., Dearden, C., Fegan, C., Milligan, D., Smith, A.F.*, et al.* (2017). Eradication of minimal residual disease improves overall and progression-free survival in patients with chronic

lymphocytic leukaemia, evidence from NCRN CLL207: a phase II trial assessing alemtuzumab consolidation. Br J Haematol *176*, 573-582.

Vitale, I., Galluzzi, L., Castedo, M., and Kroemer, G. (2011). Mitotic catastrophe: a mechanism for avoiding genomic instability. Nat Rev Mol Cell Biol *12*, 385-392.

Vlad, A., Deglesne, P.A., Letestu, R., Saint-Georges, S., Chevallier, N., Baran-Marszak, F., Varin-Blank, N., Ajchenbaum-Cymbalista, F., and Ledoux, D. (2009). Down-regulation of CXCR4 and CD62L in chronic lymphocytic leukemia cells is triggered by B-cell receptor ligation and associated with progressive disease. Cancer Res *69*, 6387-6395.

Voena, C., Ladetto, M., Astolfi, M., Provan, D., Gribben, J.G., Boccadoro, M., Pileri, A., and Corradini, P. (1997). A novel nested-PCR strategy for the detection of rearranged immunoglobulin heavy-chain genes in B cell tumors. Leukemia *11*, 1793-1798.

Vora, A., Goulden, N., Mitchell, C., Hancock, J., Hough, R., Rowntree, C., Moorman, A.V., and Wade, R. (2014). Augmented post-remission therapy for a minimal residual disease-defined high-risk subgroup of children and young people with clinical standard-risk and intermediate-risk acute lymphoblastic leukaemia (UKALL 2003): a randomised controlled trial. Lancet Oncol *15*, 809-818.

Vora, A., Goulden, N., Wade, R., Mitchell, C., Hancock, J., Hough, R., Rowntree, C., and Richards, S. (2013). Treatment reduction for children and young adults with low-risk acute lymphoblastic leukaemia defined by minimal residual disease (UKALL 2003): a randomised controlled trial. Lancet Oncol *14*, 199-209.

Wagner, M., Oelsner, M., Moore, A., Gotte, F., Kuhn, P.H., Haferlach, T., Fiegl, M., Bogner, C., Baxter, E.J., Peschel, C.*, et al.* (2016). Integration of innate into adaptive immune responses in ZAP-70-positive chronic lymphocytic leukemia. Blood *127*, 436-448.

Walton, J.A., Lydyard, P.M., Nathwani, A., Emery, V., Akbar, A., Glennie, M.J., and Porakishvili, N. (2010). Patients with B cell chronic lymphocytic leukaemia have an expanded population of CD4 perforin expressing T cells enriched for human cytomegalovirus specificity and an effector-memory phenotype. Br J Haematol *148*, 274-284.

Wang, L., Brooks, A.N., Fan, J., Wan, Y., Gambe, R., Li, S., Hergert, S., Yin, S., Freeman, S.S., Levin, J.Z.*, et al.* (2016). Transcriptomic Characterization of SF3B1 Mutation Reveals Its Pleiotropic Effects in Chronic Lymphocytic Leukemia. Cancer Cell *30*, 750-763.

Wang, L., Lawrence, M.S., Wan, Y., Stojanov, P., Sougnez, C., Stevenson, K., Werner, L., Sivachenko, A., DeLuca, D.S., Zhang, L.*, et al.* (2011). SF3B1 and other novel cancer genes in chronic lymphocytic leukemia. N Engl J Med *365*, 2497-2506.

Weiner, G.J. (2010). Rituximab: mechanism of action. Semin Hematol *47*, 115-123.

Weston, V.J., Oldreive, C.E., Skowronska, A., Oscier, D.G., Pratt, G., Dyer, M.J., Smith, G., Powell, J.E., Rudzki, Z., Kearns, P.*, et al.* (2010). The PARP inhibitor olaparib induces significant killing of ATM-deficient lymphoid tumor cells in vitro and in vivo. Blood *116*, 4578-4587.

Widhopf, G.F., 2nd, Rassenti, L.Z., Toy, T.L., Gribben, J.G., Wierda, W.G., and Kipps, T.J. (2004). Chronic lymphocytic leukemia B cells of more than 1% of patients express virtually identical immunoglobulins. Blood *104*, 2499-2504.

Wierda, W., O'Brien, S., Wen, S., Faderl, S., Garcia-Manero, G., Thomas, D., Do, K.A., Cortes, J., Koller, C., Beran, M.*, et al.* (2005). Chemoimmunotherapy with fludarabine, cyclophosphamide, and rituximab for relapsed and refractory chronic lymphocytic leukemia. J Clin Oncol *23*, 4070-4078.

Williamson, C.T., Miller, R., Pemberton, H.N., Jones, S.E., Campbell, J., Konde, A., Badham, N., Rafiq, R., Brough, R., Gulati, A.*, et al.* (2016). ATR inhibitors as a synthetic lethal therapy for tumours deficient in ARID1A. Nat Commun *7*, 13837.

Woyach, J.A., Furman, R.R., Liu, T.M., Ozer, H.G., Zapatka, M., Ruppert, A.S., Xue, L., Li, D.H., Steggerda, S.M., Versele, M.*, et al.* (2014a). Resistance mechanisms for the Bruton's tyrosine kinase inhibitor ibrutinib. N Engl J Med *370*, 2286-2294.

Woyach, J.A., Johnson, A.J., and Byrd, J.C. (2012). The B-cell receptor signaling pathway as a therapeutic target in CLL. Blood *120*, 1175-1184.

Woyach, J.A., Smucker, K., Smith, L.L., Lozanski, A., Zhong, Y., Ruppert, A.S., Lucas, D., Williams, K., Zhao, W., Rassenti, L.*, et al.* (2014b). Prolonged lymphocytosis during ibrutinib therapy is associated with distinct molecular characteristics and does not indicate a suboptimal response to therapy. Blood *123*, 1810-1817.

Xu-Monette, Z.Y., Wu, L., Visco, C., Tai, Y.C., Tzankov, A., Liu, W.M., Montes-Moreno, S., Dybkaer, K., Chiu, A., Orazi, A.*, et al.* (2012). Mutational profile and prognostic significance of TP53 in diffuse large B-cell lymphoma patients treated with R-CHOP: report from an International DLBCL Rituximab-CHOP Consortium Program Study. Blood *120*, 3986-3996.

Yang, L., Han, Y., Suarez Saiz, F., and Minden, M.D. (2007). A tumor suppressor and oncogene: the WT1 story. Leukemia *21*, 868-876.

Yang, S.M., Li, J.Y., Gale, R.P., and Huang, X.J. (2015). The mystery of chronic lymphocytic leukemia (CLL): Why is it absent in Asians and what does this tell us about etiology, pathogenesis and biology? Blood Rev *29*, 205-213.

Yazinski, S.A., Comaills, V., Buisson, R., Genois, M.M., Nguyen, H.D., Ho, C.K., Todorova Kwan, T., Morris, R., Lauffer, S., Nussenzweig, A.*, et al.* (2017). ATR inhibition disrupts rewired homologous recombination and fork protection pathways in PARP inhibitor-resistant BRCA-deficient cancer cells. Genes Dev *31*, 318-332.

Yoo, H.Y., Kumagai, A., Shevchenko, A., and Dunphy, W.G. (2004). Adaptation of a DNA replication checkpoint response depends upon inactivation of Claspin by the Polo-like kinase. Cell *117*, 575-588.

Yu, J., Chen, L., Cui, B., Widhopf, G.F., 2nd, Shen, Z., Wu, R., Zhang, L., Zhang, S., Briggs, S.P., and Kipps, T.J. (2016). Wnt5a induces ROR1/ROR2 heterooligomerization to enhance leukemia chemotaxis and proliferation. J Clin Invest *126*, 585-598.

Zeman, M.K., and Cimprich, K.A. (2014). Causes and consequences of replication stress. Nat Cell Biol *16*, 2-9.

Zenz, T., Eichhorst, B., Busch, R., Denzel, T., Habe, S., Winkler, D., Buhler, A., Edelmann, J., Bergmann, M., Hopfinger, G.*, et al.* (2010a). TP53 mutation and survival in chronic lymphocytic leukemia. J Clin Oncol *28*, 4473-4479.

Zenz, T., Krober, A., Scherer, K., Habe, S., Buhler, A., Benner, A., Denzel, T., Winkler, D., Edelmann, J., Schwanen, C.*, et al.* (2008). Monoallelic TP53 inactivation is associated with

poor prognosis in chronic lymphocytic leukemia: results from a detailed genetic characterization with long-term follow-up. Blood *112*, 3322-3329.

Zenz, T., Mertens, D., Kuppers, R., Dohner, H., and Stilgenbauer, S. (2010b). From pathogenesis to treatment of chronic lymphocytic leukaemia. Nature reviews Cancer *10*, 37-50.

Zenz, T., Vollmer, D., Trbusek, M., Smardova, J., Benner, A., Soussi, T., Helfrich, H., Heuberger, M., Hoth, P., Fuge, M.*, et al.* (2010c). TP53 mutation profile in chronic lymphocytic leukemia: evidence for a disease specific profile from a comprehensive analysis of 268 mutations. Leukemia *24*, 2072-2079.

Zhang, W., Kater, A.P., Widhopf, G.F., 2nd, Chuang, H.Y., Enzler, T., James, D.F., Poustovoitov, M., Tseng, P.H., Janz, S., Hoh, C.*, et al.* (2010). B-cell activating factor and v-Myc myelocytomatosis viral oncogene homolog (c-Myc) influence progression of chronic lymphocytic leukemia. Proc Natl Acad Sci U S A *107*, 18956-18960.

Zighelboim, I., Schmidt, A.P., Gao, F., Thaker, P.H., Powell, M.A., Rader, J.S., Gibb, R.K., Mutch, D.G., and Goodfellow, P.J. (2009). ATR mutation in endometrioid endometrial cancer is associated with poor clinical outcomes. J Clin Oncol *27*, 3091-3096.

Zupo, S., Massara, R., Dono, M., Rossi, E., Malavasi, F., Cosulich, M.E., and Ferrarini, M. (2000). Apoptosis or plasma cell differentiation of CD38-positive B-chronic lymphocytic leukemia cells induced by cross-linking of surface IgM or IgD. Blood *95*, 1199-1206.

LYMPHOID NEOPLASIA

ATR inhibition induces synthetic lethality and overcomes chemoresistance in *TP53*- or *ATM*-defective chronic lymphocytic leukemia cells

Marwan Kwok,[1,2,*] Nicholas Davies,[1,*] Angelo Agathanggelou,[1] Edward Smith,[1] Ceri Oldreive,[1] Eva Petermann,[1] Grant Stewart,[1] Jeff Brown,[3] Alan Lau,[4] Guy Pratt,[1,5] Helen Parry,[1,2] Malcolm Taylor,[1] Paul Moss,[1,2] Peter Hillmen,[6] and Tatjana Stankovic[1,2]

[1]School of Cancer Sciences, University of Birmingham, Birmingham, United Kingdom; [2]Centre for Clinical Haematology, Queen Elizabeth Hospital Birmingham, Birmingham, United Kingdom; [3]Oncology iMed, AstraZeneca Pharmaceuticals, Waltham, MA; [4]R&D Oncology iMed, AstraZeneca Pharmaceuticals, Alderley Park, United Kingdom; [5]Birmingham Heartlands Hospital, Birmingham, United Kingdom; and [6]Section of Experimental Haematology, Leeds Institute of Cancer and Pathology, University of Leeds, Leeds, United Kingdom

Key Points

- ATR inhibition is synthetically lethal to *TP53*- or *ATM*-defective CLL cells.
- ATR targeting induces selective cytotoxicity and chemosensitization in *TP53*- or *ATM*-defective CLL cells in vitro and in vivo.

TP53 **and ataxia telangiectasia mutated (*ATM*) defects are associated with genomic instability, clonal evolution, and chemoresistance in chronic lymphocytic leukemia (CLL). Currently, therapies capable of providing durable remissions in relapsed/refractory *TP53*- or *ATM*-defective CLL are lacking. Ataxia telangiectasia and Rad3-related (ATR) mediates response to replication stress, the absence of which leads to collapse of stalled replication forks into chromatid fragments that require resolution through the ATM/p53 pathway. Here, using AZD6738, a novel ATR kinase inhibitor, we investigated ATR inhibition as a synthetically lethal strategy to target CLL cells with *TP53* or *ATM* defects. Irrespective of *TP53* or *ATM* status, induction of CLL cell proliferation upregulated ATR protein, which then became activated in response to replication stress. In *TP53*- or *ATM*-defective CLL cells, inhibition of ATR signaling by AZD6738 led to an accumulation of unrepaired DNA damage, which was carried through into mitosis because of defective cell cycle checkpoints, resulting in cell death by mitotic catastrophe. Consequently, AZD6738 was selectively cytotoxic to both *TP53*- and *ATM*-defective CLL cell lines and primary cells. This was confirmed in vivo using primary xenograft models of *TP53*- or *ATM*-defective CLL, where treatment with AZD6738 resulted in decreased tumor load and reduction in the proportion of CLL cells with such defects. Moreover, AZD6738 sensitized *TP53*- or *ATM*-defective primary CLL cells to chemotherapy and ibrutinib. Our findings suggest that ATR is a promising therapeutic target for *TP53*- or *ATM*-defective CLL that warrants clinical investigation. (*Blood*. 2016;127(5):582-595)**

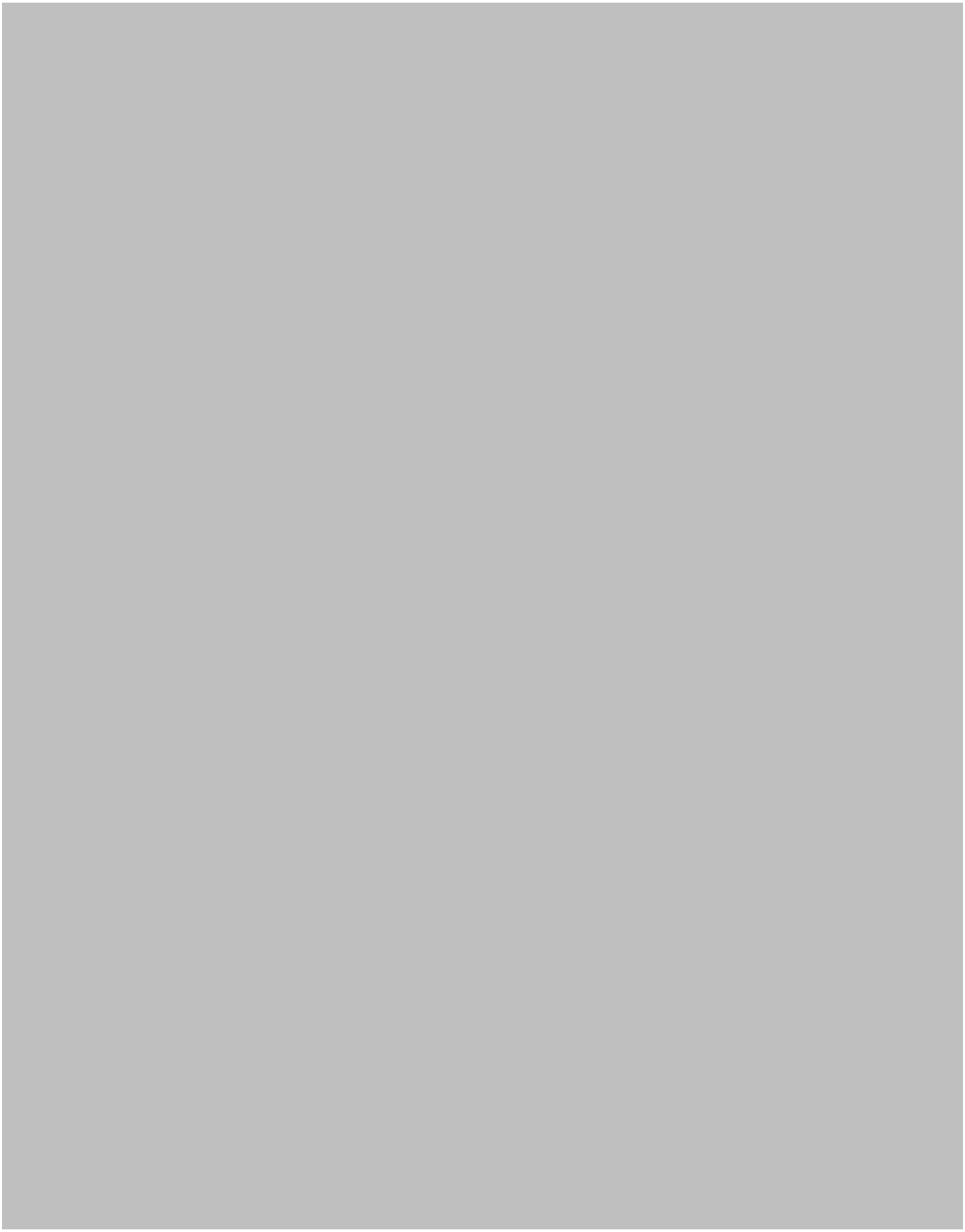

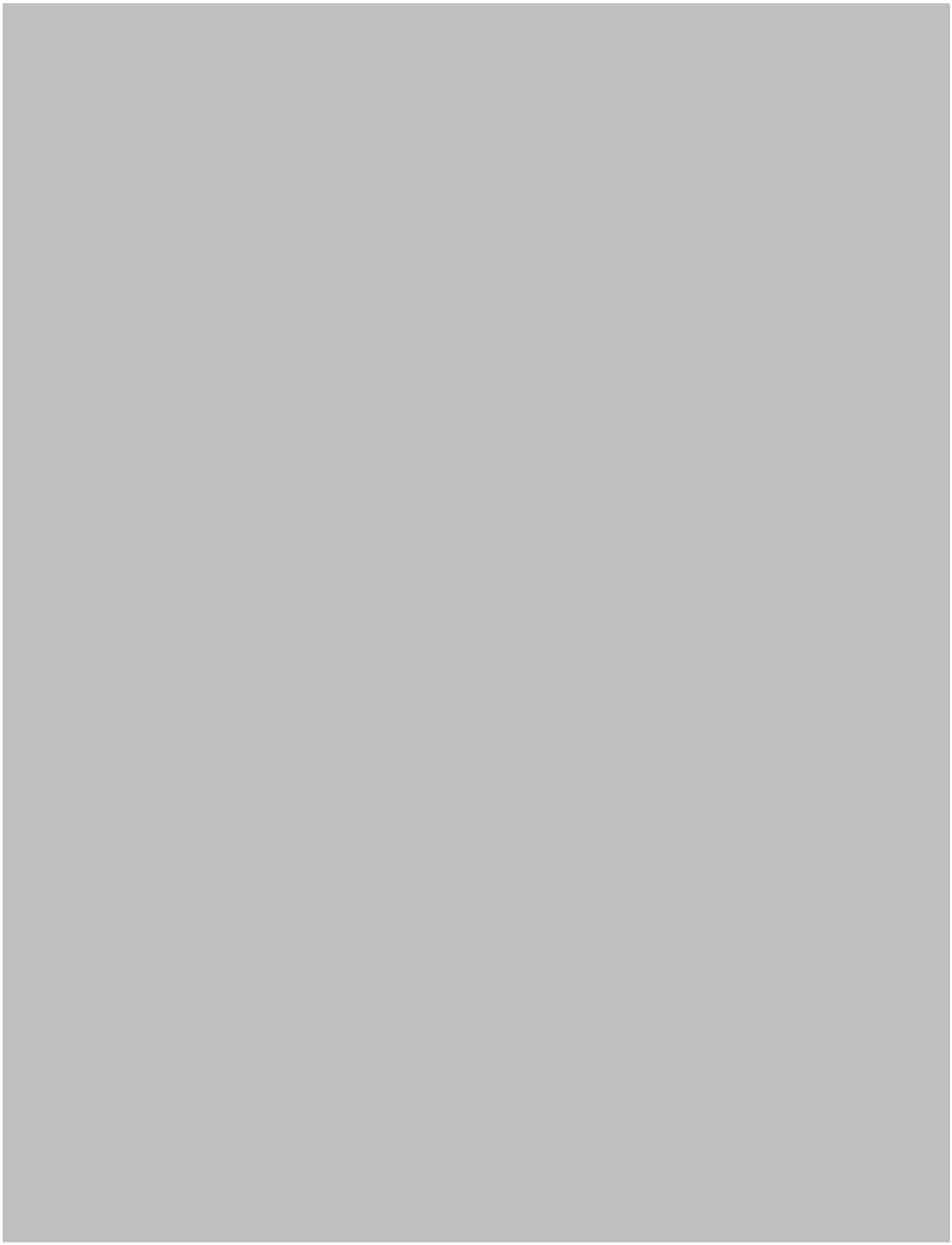

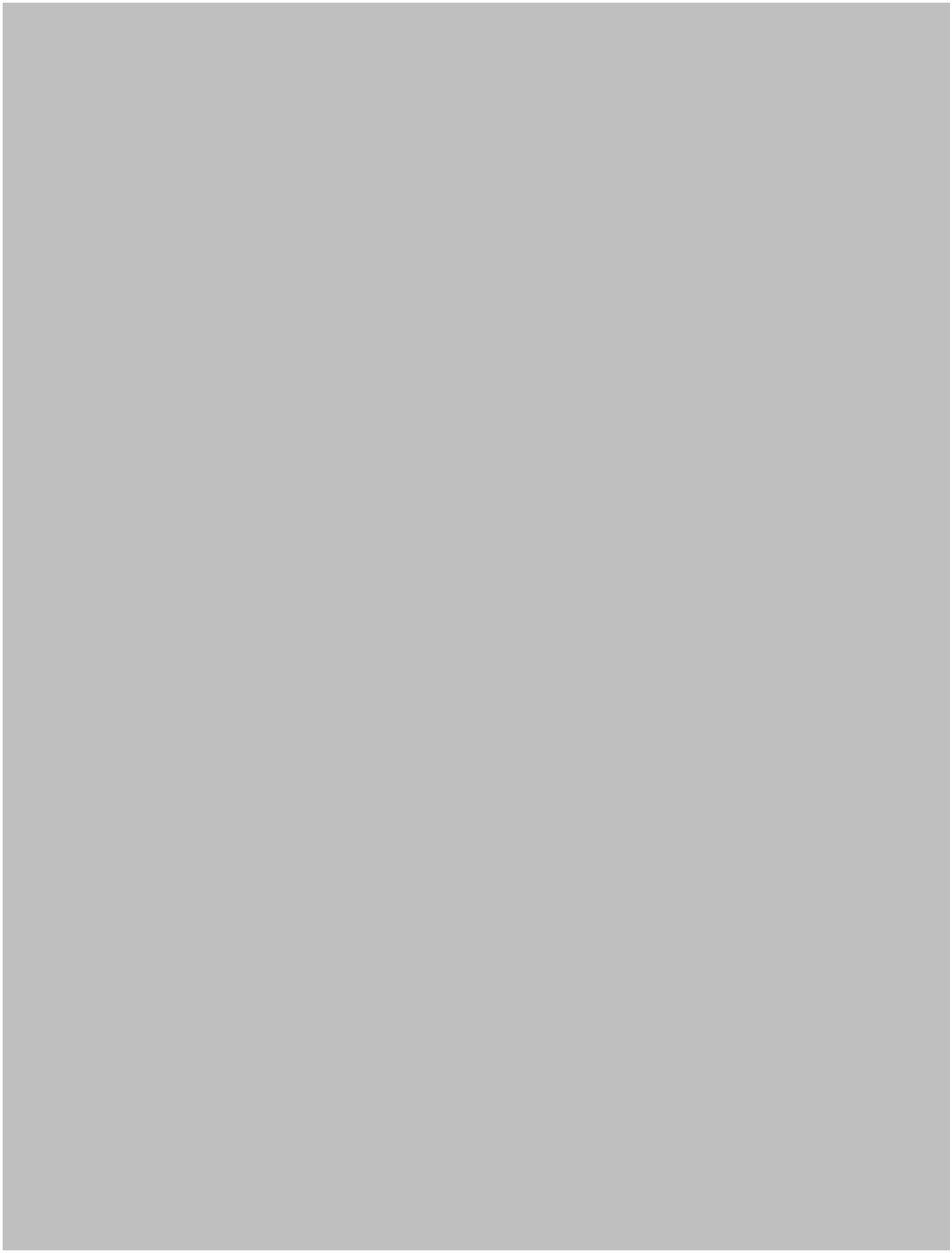

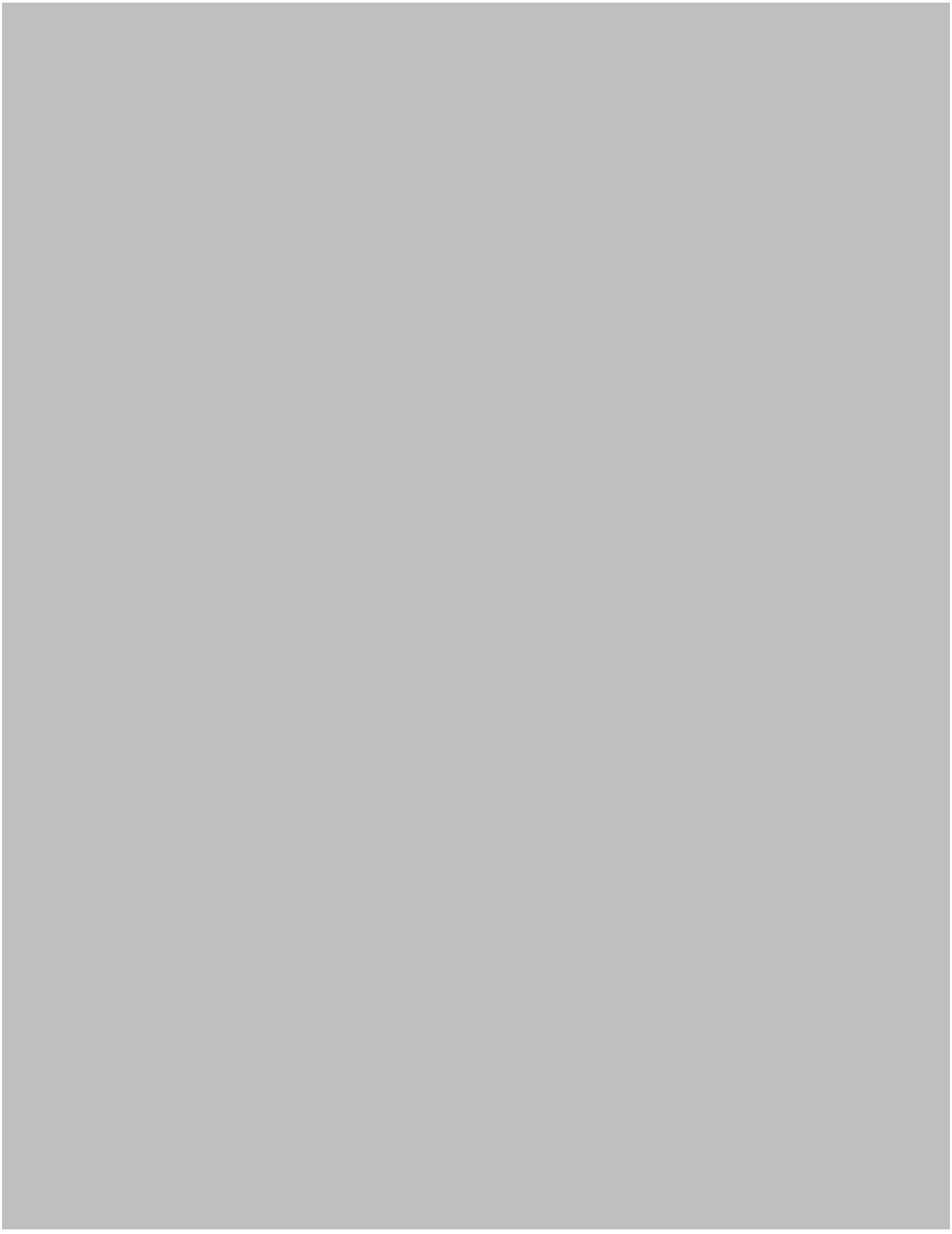

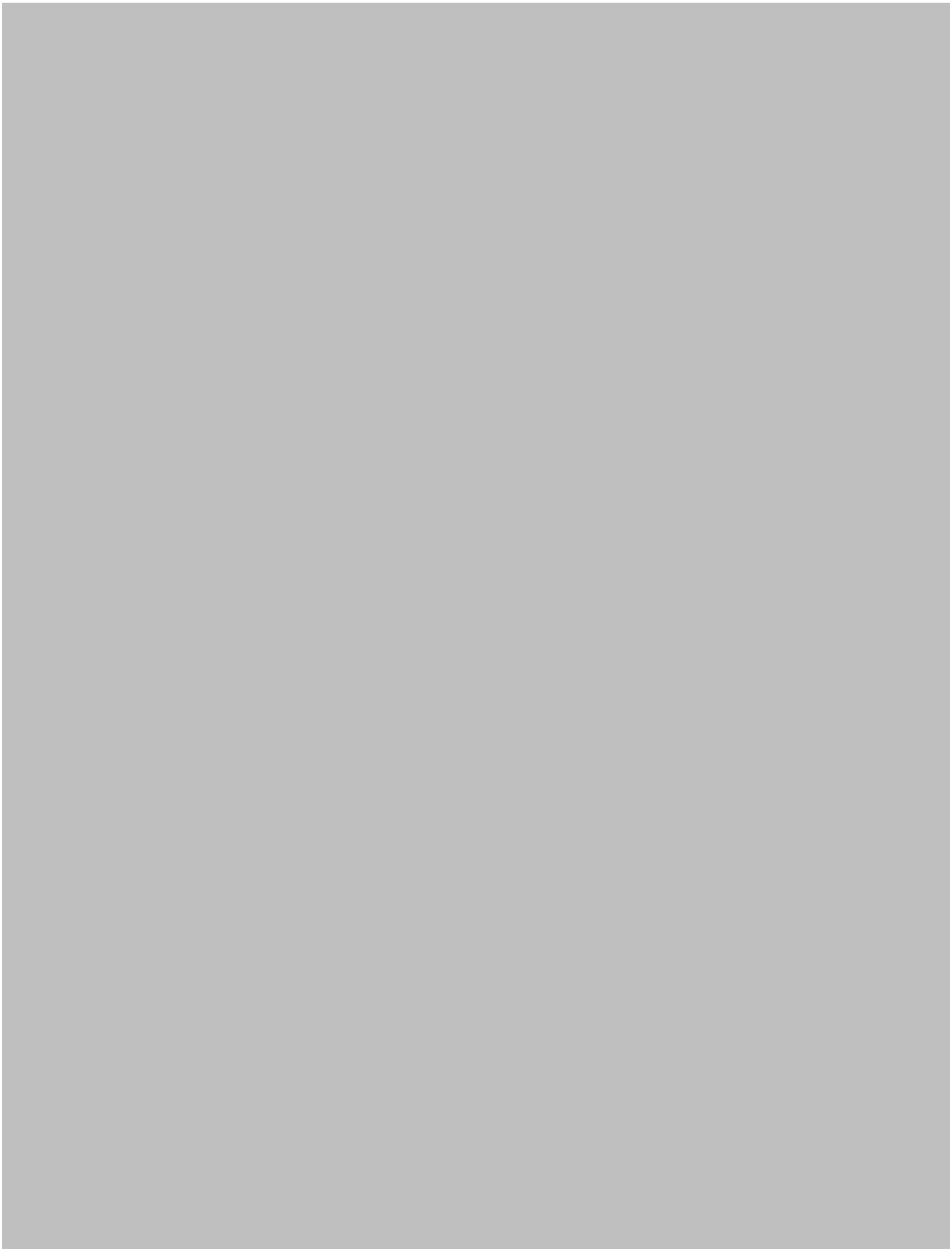

2016 127: 582-595
doi:10.1182/blood-2015-05-644872 originally published online November 12, 2015

ATR inhibition induces synthetic lethality and overcomes chemoresistance in *TP53*- or *ATM*-defective chronic lymphocytic leukemia cells

Marwan Kwok, Nicholas Davies, Angelo Agathanggelou, Edward Smith, Ceri Oldreive, Eva Petermann, Grant Stewart, Jeff Brown, Alan Lau, Guy Pratt, Helen Parry, Malcolm Taylor, Paul Moss, Peter Hillmen and Tatjana Stankovic

Blood (print ISSN 0006-4971, online ISSN 1528-0020), is published weekly by the American Society of Hematology, 2021 L St, NW, Suite 900, Washington DC 20036.

CLINICAL TRIALS AND OBSERVATIONS

Minimal residual disease is an independent predictor for 10-year survival in CLL

Marwan Kwok,[1,2,*] Andy C. Rawstron,[1,*] Abraham Varghese,[1] Paul A. S. Evans,[1] Sheila J. M. O'Connor,[1] Chi Doughty,[1] Darren J. Newton,[3] Paul Moreton,[1] and Peter Hillmen[3]

[1]Haematological Malignancy Diagnostic Service, Department of Haematology, St. James's University Hospital, Leeds, United Kingdom; [2]Centre for Clinical Haematology, Queen Elizabeth Hospital Birmingham, Birmingham, United Kingdom; and [3]Section of Experimental Haematology, Leeds Institute of Cancer and Pathology, University of Leeds, Leeds, United Kingdom

Key Points

- MRD negativity is a predictor for long-term progression-free and overall survival independent of the type and line of therapy.
- MRD negativity confers the greatest prognostic benefit when achieved in the frontline setting.

Minimal residual disease (MRD) negativity, defined as <1 chronic lymphocytic leukemia (CLL) cell detectable per 10 000 leukocytes, has been shown to independently predict for clinical outcome in patients receiving combination chemoimmunotherapy in the frontline setting. However, the long-term prognostic value of MRD status in other therapeutic settings remains unclear. Here, we retrospectively analyzed, with up to 18 years follow-up, all patients at our institution who achieved at least a partial response (PR) with various therapies between 1996 and 2007, and received a bone marrow MRD assessment at the end of treatment according to the international harmonized approach. MRD negativity correlated with both progression-free survival (PFS) and overall survival (OS) independent of the type and line of treatment, as well as known prognostic factors including adverse cytogenetics. The greatest impact of achieving MRD negativity was seen in patients receiving frontline treatment, with 10-year PFS of 65% vs 10% and 10-year OS of 70% vs 30% for MRD-negative vs MRD-positive patients, respectively. Our results demonstrate the long-term benefit of achieving MRD negativity, regardless of the therapeutic setting and treatment modality, and support its use as a prognostic marker for long-term PFS and as a potential therapeutic goal in CLL. (*Blood*. 2016;128(24):2770-2773)

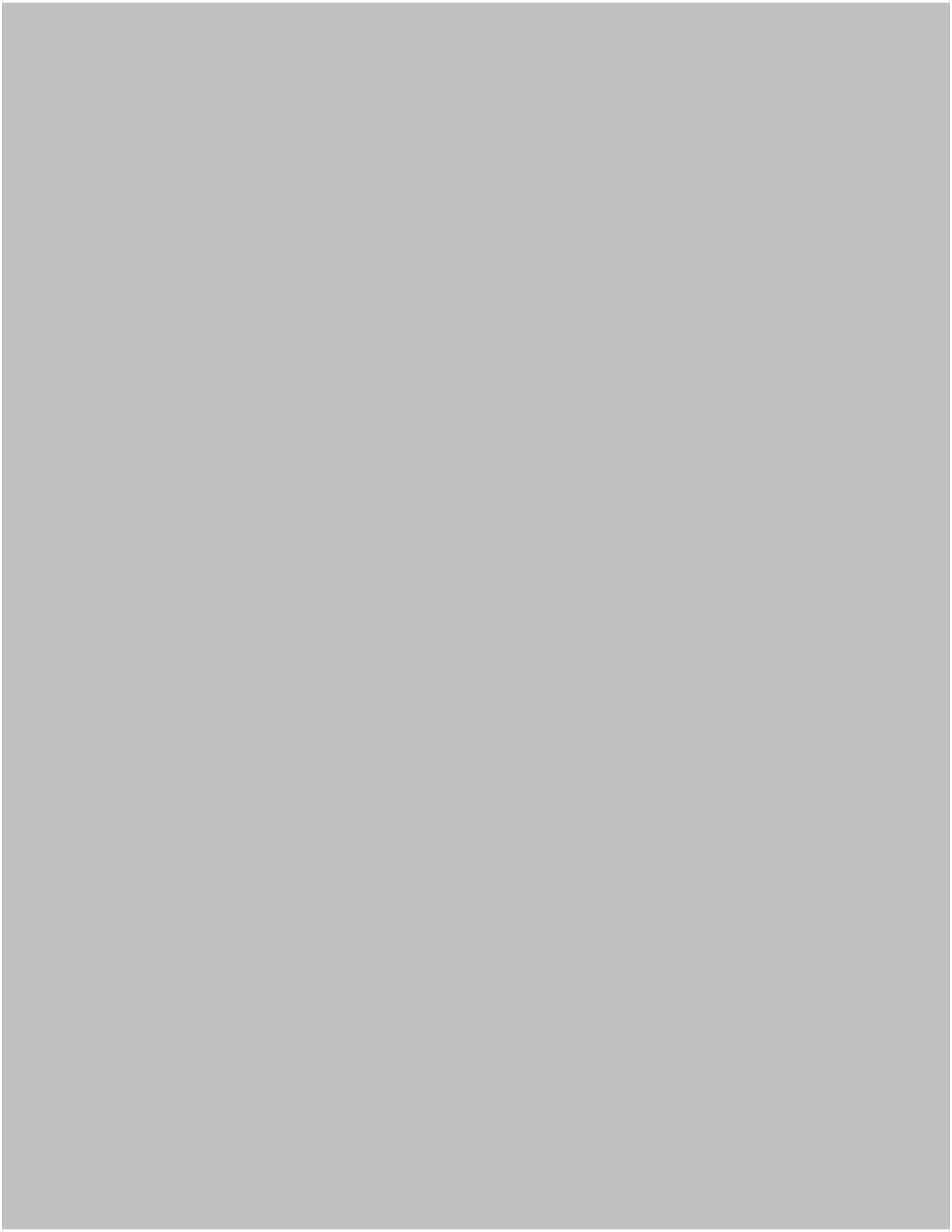

2016 128: 2770-2773
doi:10.1182/blood-2016-05-714162 originally published online October 3, 2016

Minimal residual disease is an independent predictor for 10-year survival in CLL

Marwan Kwok, Andy C. Rawstron, Abraham Varghese, Paul A. S. Evans, Sheila J. M. O'Connor, Chi Doughty, Darren J. Newton, Paul Moreton and Peter Hillmen

Blood (print ISSN 0006-4971, online ISSN 1528-0020), is published weekly by the American Society of Hematology, 2021 L St, NW, Suite 900, Washington DC 20036.

Regular Article

blood

LYMPHOID NEOPLASIA

USP7 inhibition alters homologous recombination repair and targets CLL cells independently of ATM/p53 functional status

Angelo Agathanggelou,[1,*] Edward Smith,[1,*] Nicholas J. Davies,[1] Marwan Kwok,[1,2] Anastasia Zlatanou,[1] Ceri E. Oldreive,[1] Jingwen Mao,[1] David Da Costa,[1] Sina Yadollahi,[1] Tracey Perry,[1] Pamela Kearns,[1] Anna Skowronska,[1] Elliot Yates,[1] Helen Parry,[1,2] Peter Hillmen,[3] Celine Reverdy,[4] Remi Delansorne,[4] Shankara Paneesha,[5] Guy Pratt,[1,2] Paul Moss,[1,2] A. Malcolm R. Taylor,[1] Grant S. Stewart,[1] and Tatjana Stankovic[1]

[1]Institute of Cancer and Genomic Sciences, College of Medical and Dental Sciences, University of Birmingham, Birmingham, United Kingdom; [2]Centre for Clinical Haematology, Queen Elizabeth Hospital Birmingham, Birmingham, United Kingdom; [3]Section of Experimental Haematology, Leeds Institute of Cancer and Pathology, University of Leeds, Leeds, United Kingdom; [4]Hybrigenics Services, Paris, France; and [5]Heartlands Hospital, Birmingham, United Kingdom

Key Points

- USP7 is overexpressed and regulates HRR in CLL cells.
- USP7 inhibition is selectively cytotoxic to CLL cells independently of ATM and p53 and synergizes with chemotherapy.

The role of deubiquitylase ubiquitin-specific protease 7 (USP7) in the regulation of the p53-dependent DNA damage response (DDR) pathway is well established. Whereas previous studies have mostly focused on the mechanisms underlying how USP7 directly controls p53 stability, we recently showed that USP7 modulates the stability of the DNA damage responsive E3 ubiquitin ligase RAD18. This suggests that targeting USP7 may have therapeutic potential even in tumors with defective p53 or ibrutinib resistance. To test this hypothesis, we studied the effect of USP7 inhibition in chronic lymphocytic leukemia (CLL) where the ataxia telangiectasia mutated (ATM)–p53 pathway is inactivated with relatively high frequency, leading to treatment resistance and poor clinical outcome. We demonstrate that USP7 is upregulated in CLL cells, and its loss or inhibition disrupts homologous recombination repair (HRR). Consequently, USP7 inhibition induces significant tumor-cell killing independently of ATM and p53 through the accumulation of genotoxic levels of DNA damage. Moreover, USP7 inhibition sensitized p53-defective, chemotherapy-resistant CLL cells to clinically achievable doses of HRR-inducing chemotherapeutic agents in vitro and in vivo in a murine xenograft model. Together, these results identify USP7 as a promising therapeutic target for the treatment of hematological malignancies with DDR defects, where ATM/p53-dependent apoptosis is compromised. (*Blood*. 2017;130(2):156-166)

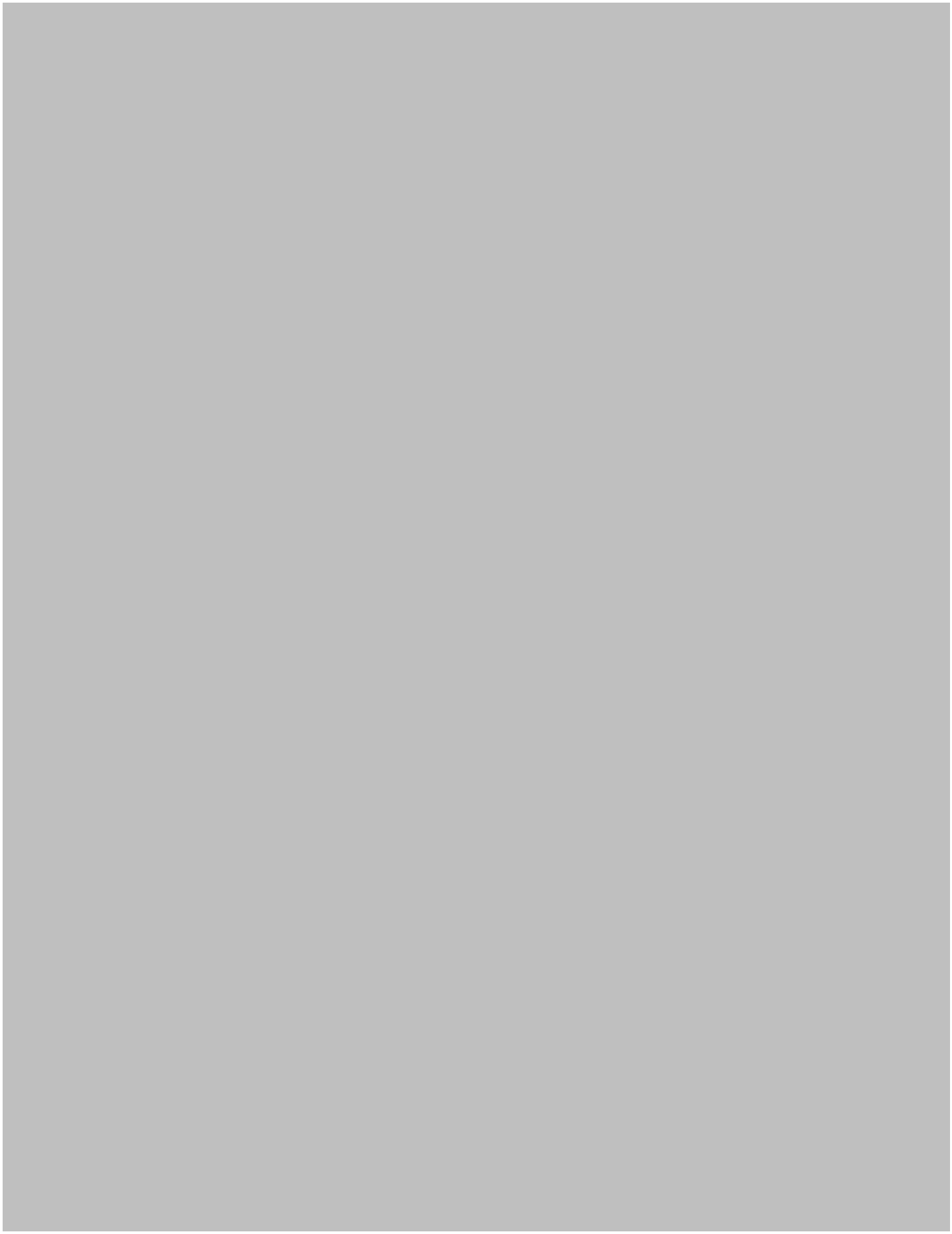

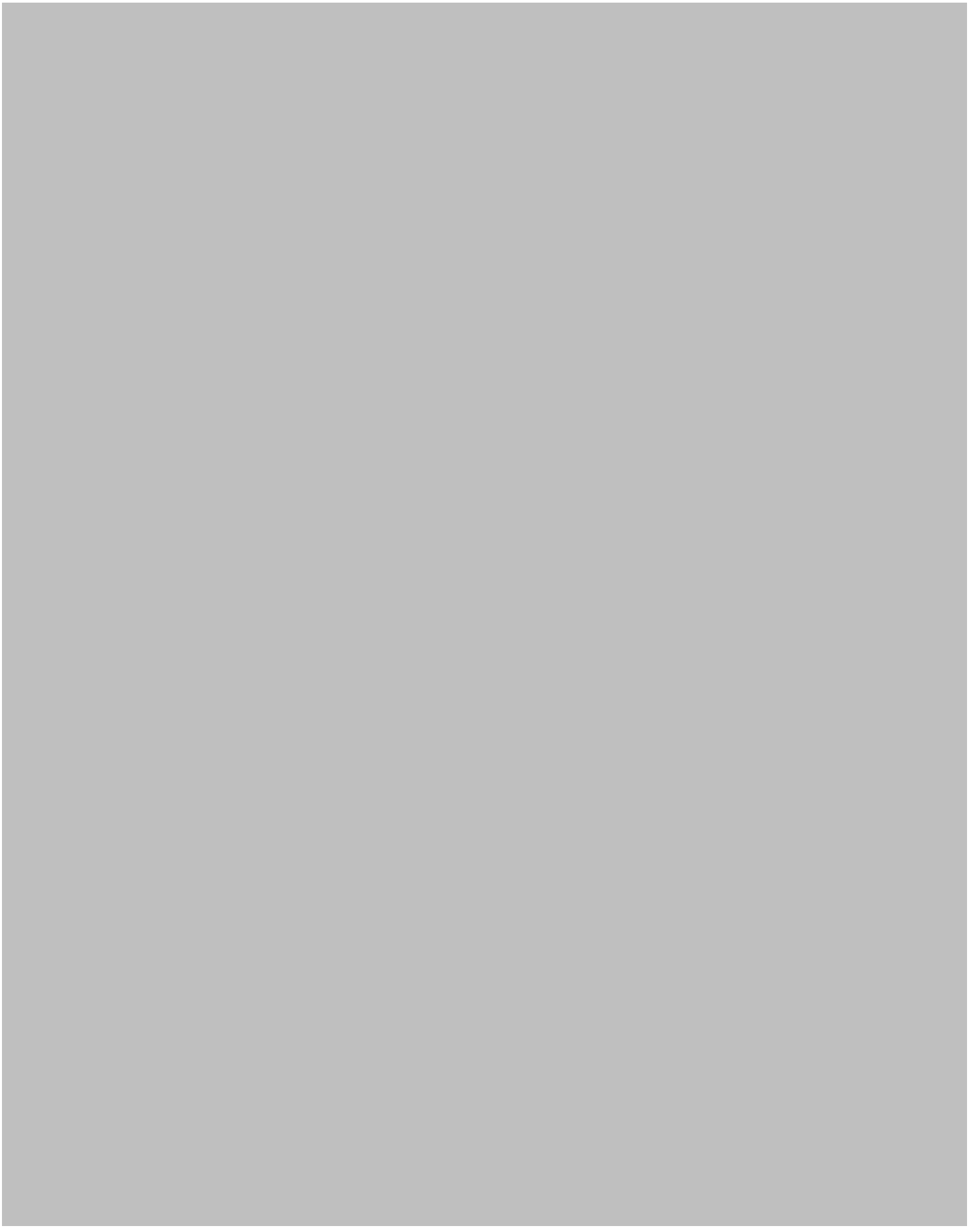

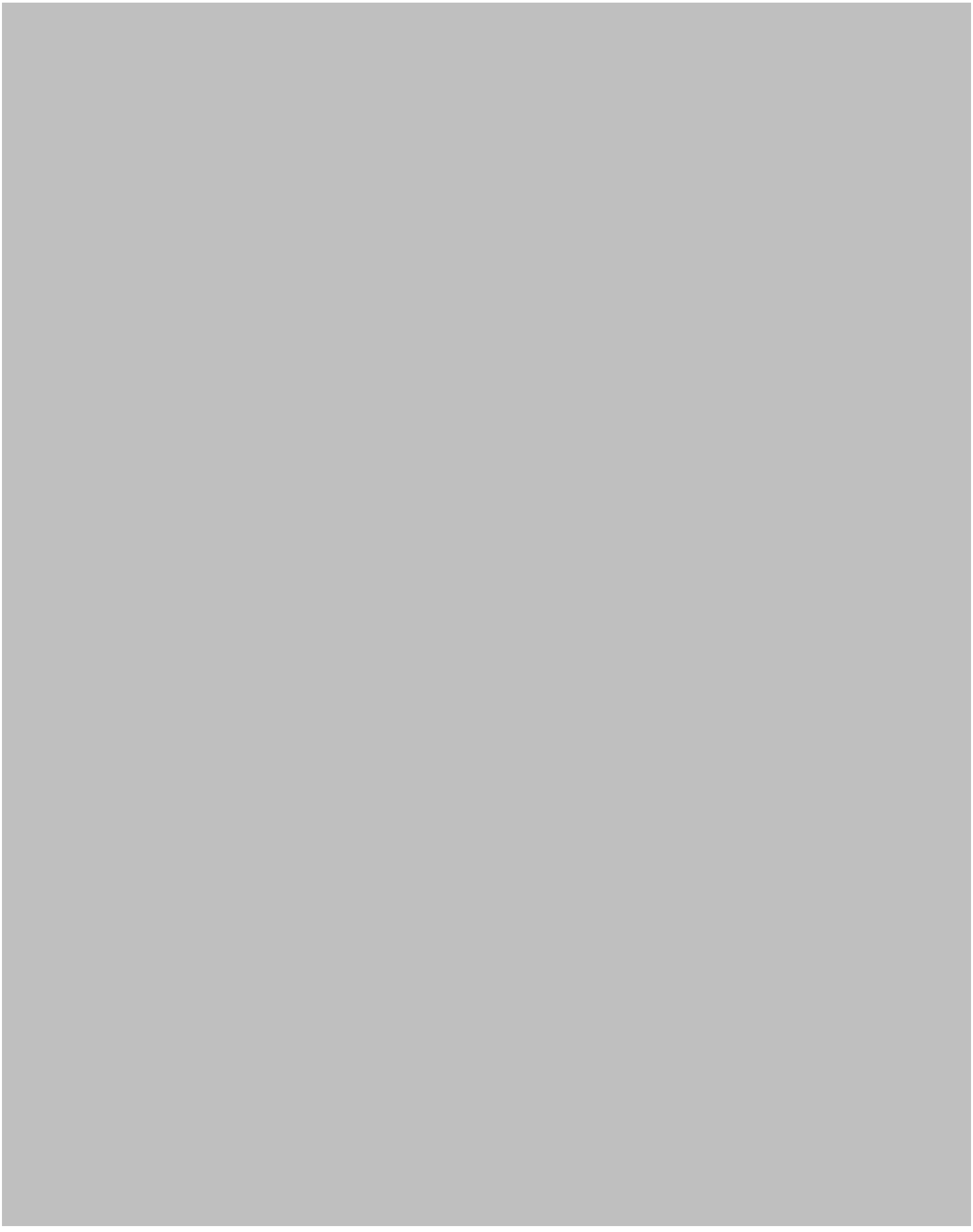

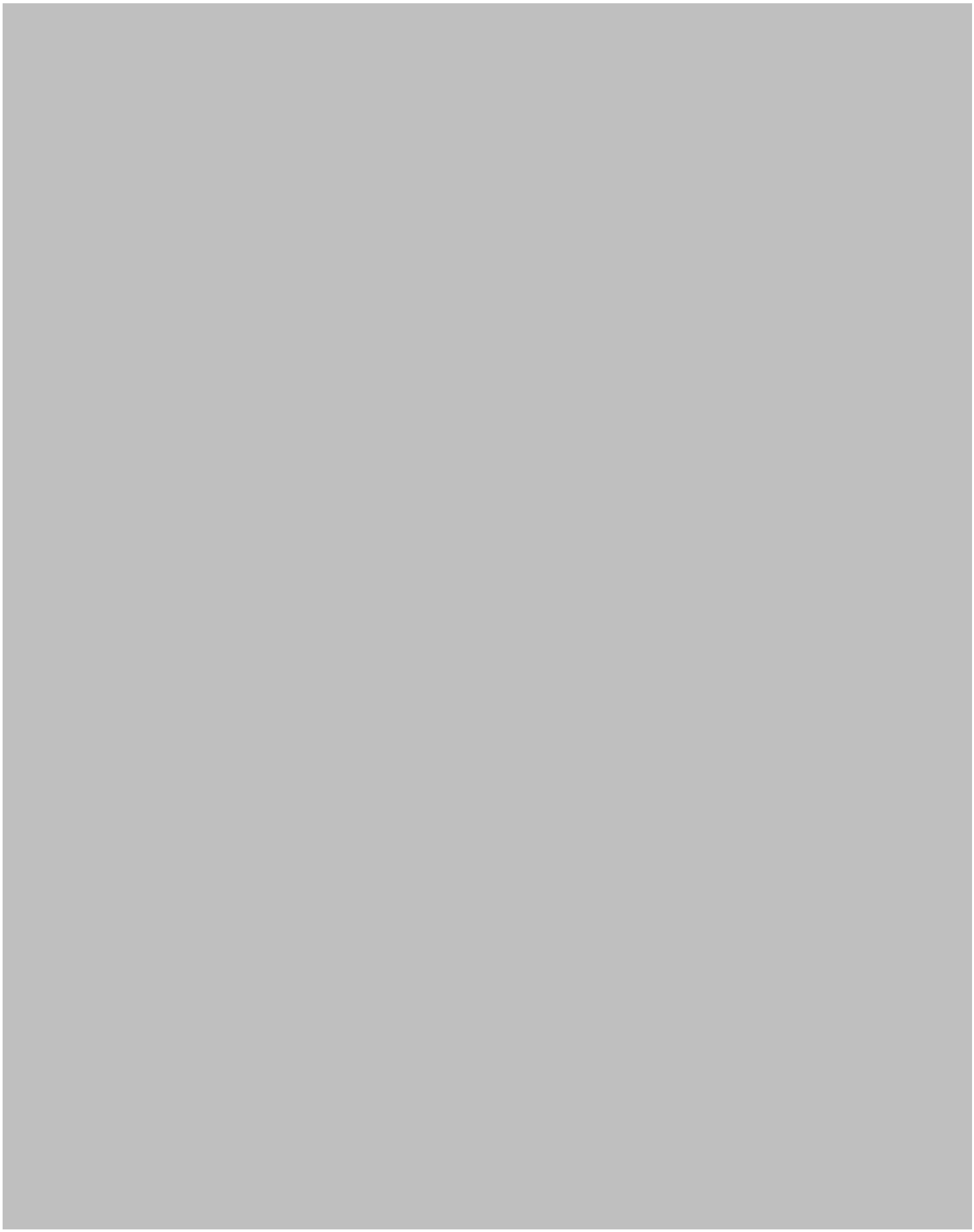

2017 130: 156-166
doi:10.1182/blood-2016-12-758219 originally published online May 11, 2017

USP7 inhibition alters homologous recombination repair and targets CLL cells independently of ATM/p53 functional status

Angelo Agathanggelou, Edward Smith, Nicholas J. Davies, Marwan Kwok, Anastasia Zlatanou, Ceri E. Oldreive, Jingwen Mao, David Da Costa, Sina Yadollahi, Tracey Perry, Pamela Kearns, Anna Skowronska, Elliot Yates, Helen Parry, Peter Hillmen, Celine Reverdy, Remi Delansorne, Shankara Paneesha, Guy Pratt, Paul Moss, A. Malcolm R. Taylor, Grant S. Stewart and Tatjana Stankovic

Blood (print ISSN 0006-4971, online ISSN 1528-0020), is published weekly by the American Society of Hematology, 2021 L St, NW, Suite 900, Washington DC 20036.

www.impactjournals.com/oncotarget/ Oncotarget, 2017, Vol. 8, (No. 27), pp: 44749-44760

Research Paper

Dynamic changes in clonal cytogenetic architecture during progression of chronic lymphocytic leukemia in patients and patient-derived murine xenografts

Nicholas J. Davies[1], Marwan Kwok[1], Clive Gould[2], Ceri E. Oldreive[1], Jingwen Mao[1], Helen Parry[3], Edward Smith[1], Angelo Agathanggelou[1], Guy Pratt[1], Alexander Malcolm R. Taylor[1], Paul Moss[3], Mike Griffiths[1,2] and Tatjana Stankovic[1]

[1]Institute of Cancer and Genomic Sciences, University of Birmingham, Birmingham, UK

[2]West Midlands Regional Genetics Laboratory, Birmingham Women's NHS Foundation Trust, Birmingham, UK

[3]Institute of Immunology and Immunotherapy, University of Birmingham, Birmingham, UK

Correspondence to: *Tatjana Stankovic,* ***email:*** *t.stankovic@bham.ac.uk*

Keywords: *chronic lymphocytic leukemia, xenograft, clonal evolution, multiplexed-FISH, cytogenetics*

Received: *March 15, 2017* ***Accepted:*** *March 29, 2017* ***Published:*** *April 26, 2017*

ABSTRACT

Subclonal heterogeneity and clonal selection influences disease progression in chronic lymphocytic leukemia (CLL). It is therefore important that therapeutic decisions are made based on an understanding of the CLL clonal architecture and its dynamics in individual patients. Identification of cytogenetic abnormalities by FISH remains the cornerstone of contemporary clinical practice and provides a simple means for prognostic stratification. Here, we demonstrate that multiplexed-FISH can enhance recognition of CLL subclonal repertoire and its dynamics during disease progression, both in patients and CLL patient-derived xenografts (PDX). We applied a combination of patient-specific FISH probes to 24 CLL cases before treatment and at relapse, and determined putative ancestral relationships between subpopulations with different cytogenetic features. We subsequently established 7 CLL PDX models in NOD/Shi-SCID/IL-2Rγc^{tm1sug}/Jic (NOG) mice. Application of multiplexed-FISH to these models demonstrated that all of the identified cytogenetic subpopulations had leukemia propagating activity and that changes in their representation during disease progression could be spontaneous, accelerated by treatment or treatment-induced. We conclude that multiplexed-FISH in combination with PDX models have the potential to distinguish between spontaneous and treatment-induced clonal selection, and therefore provide a valuable tool for the pre-clinical evaluation of novel therapies.